ESTABLISHMENT AND MAINTENANCE OF A NEW GEOSPATIAL FRAME FOR TANZANIA-TZRF10

JAMES DANIEL MTAMAKAYA

January 2009

ESTABLISHMENT AND MAINTENANCE OF A NEW GEOSPATIAL FRAME FOR TANZANIA-TZRF10

James Daniel Mtamakaya

Department of Geodesy and Geomatics Engineering
University of New Brunswick
P.O. Box 4400
Fredericton, N.B.
Canada
E3B 5A3

January 2009

PREFACE

This technical report is a reproduction of a thesis submitted in partial fulfillment of the requirements for the degree of Master of Science in Engineering in the Department of Geodesy and Geomatics Engineering, January 2009. The research was supervised by Dr. Marcelo Santos, and partial support was provided by the Canadian International Development Agency.

As with any copyrighted material, permission to reprint or quote extensively from this report must be received from the author. The citation to this work should appear as follows:

Mtamakaya, James Daniel (2009). *Establishment and Maintenance of a New Geospatial Frame for Tanzania-TZRF10.* M.Sc.E. thesis, Department of Geodesy and Geomatics Engineering Technical Report No. 266, University of New Brunswick, Fredericton, New Brunswick, Canada, 276 pp.

ABSTRACT

Tanzania like most of the African countries has an old and conventional Geodetic Network. This network was established and computed by the Directorate of Overseas Surveys (DOS) of Great Britain in the 1950's. The present network is based on the 30th arc-meridian of the Clarke 1880 modified ellipsoid with its origin at Buffelsfontein-Cape Town in the Republic of South Africa. The present network does not satisfy the overgrowing mapping requirements of the country as well as other Geo-related information requirements. They include homogeneous cross border mapping activities (most of the international boundaries have not been physically defined), smooth land regularization projects in new urban areas, production and update of large scale topographical maps in urban areas and homogenous spatial mapping as well as the studies of crustal dynamics as related to plate tectonics and natural hazards associated with seismic or volcanic activities.

The Survey and Mapping Division of Tanzania (SMD) has realized the values of high precision and geocentric dynamic spatial frame in facilitating the geodetic positioning (coordinates and velocities in the geocentric coordinate system), navigation and general purpose spatial referencing to date as the most versatile, accurate and economical way of addressing the above issues. In view of those values and strong capabilities of modern dynamic geodetic frames, Tanzania has been collaborating with other African countries to establish a unified African Geodetic

Reference Frame (AFREF). However, lack of appropriate expertise, proper awareness of the concept amongst most of the national mapping organizations and differences in economic levels in the African countries have always been the limiting factors.

In view those limitations, the primary objective of this thesis is to provide the basis for the establishment and maintenance of a 3-dimensional dynamic reference frame for Tanzania in the ITRF system with optimum accuracy requirement in an economic way. The new frame will be compatible to satellite position techniques and would consider the advancement in the communication technology and the increased capacity of the internet applications real time geodetic applications that has been illustrated by Weber [2002] and Weber et al. [2003].

To achieve the research objectives a conceptual plan to realize a new spatial framework in Tanzania (TZRF10) has been developed, using the least-squares covariance analysis technique as a tool to evaluate for its geometrical consistency. A case study on reference frame maintenance using the BerneseV5.0 scientific software; has been developed and evaluated for its performance based on NAD83 (CSRS) data from the Geodetic Survey Division of Natural Resources of Canada NRCan.

The present advancement in communication technologies and increased capacity of internet–based real time geodetic applications has been illustrated through implementation of a case study and evaluated for its performance using a developed matlab software code.

TABLE OF CONTENTS

vii

LIST OF TABLES

LIST OF FIGURES

CURRICULUM VITAE

ACKNOWLEDGMENTS

1. INTRODUCTION

In view of many mapping limitations associated with the present Tanzania conventional network, the primary objective of this research is to provide the basis for the establishment and maintenance of a 3-dimensional dynamic reference frame for Tanzania (TZRF10) in the ITRF system with optimum accuracy requirement in an economic way. The new geodetic frame will be compatible to satellite position techniques and the implementation strategy has considered the advancement in the communication technology with increased capacity of the internet for near real time geodetic applications as discussed by Weber [2002] and Weber et al. [2003].

The author realizes the problem of poor quantification of the economic value of a geodetic reference frame to most users in Tanzania despite of the high risks associated with wrong decision making on land related matters based on un-reliable geospatial frame. Risks have therefore been avoided in the implementation strategy by using the simulated least-squares covariance analysis as one of the available tools for planning a geometrically strong network as previously illustrated by Pullen and Parkinson [1995], Wolf and Ghilani [1997] and Raquet et al. [1998].

This chapter presents an overview of the current Tanzanian geodetic frame and its limitations as well as a brief summary of past and present initiatives to establish a unified African geodetic reference frame (AFREF). The concluding part of this chapter presents an overview and discusses the objectives of the new TZRF10 frame and the main contributions of this thesis.

1.1   Back ground information of Tanzanian geodetic network

Tanzania, like most African countries, has an old and conventional geodetic network based on the 1880 Clarke modified ellipsoid, with its datum at Buffelsfontein, near Port Elizabeth-Cape Town, in the Republic of South Africa. With reference to previous discussions by Zakiewicz [2005], two British Astronomers, Sir Thomas Maclear (1833 - 1870) and Sir David Gill (1879 - 1907), established the reference ellipsoid whose initial geodetic objectives were to verify the size and shape of the Earth in the Southern Hemisphere and provide geodetic control for topographic maps and navigation charts. The network was then extended to other countries in central Africa of Zimbabwe and Democratic Republic of Congo (Figure 1.1).

The current network was established and computed by the Directorate of Overseas (DOS) Surveys of Great Britain in the 1950's with the arc 30th meridian (Figure 1.2) of the Clarke 1880 modified ellipsoid as the base. The current Tanzanian 1950 arc datum control network was derived from the Republic of South Africa geodetic datum via Zimbabwe and since its establishment has never been validated to ascertain the extent of distortions. Like most of the conventional geodetic networks in other countries, the establishment and the densification methodology was done using traditional methods such as classical triangulation, trilateration and standard traversing.

Figure1.1 geodetic triangulation network in Southern Africa [Zakiewicz, 2005]
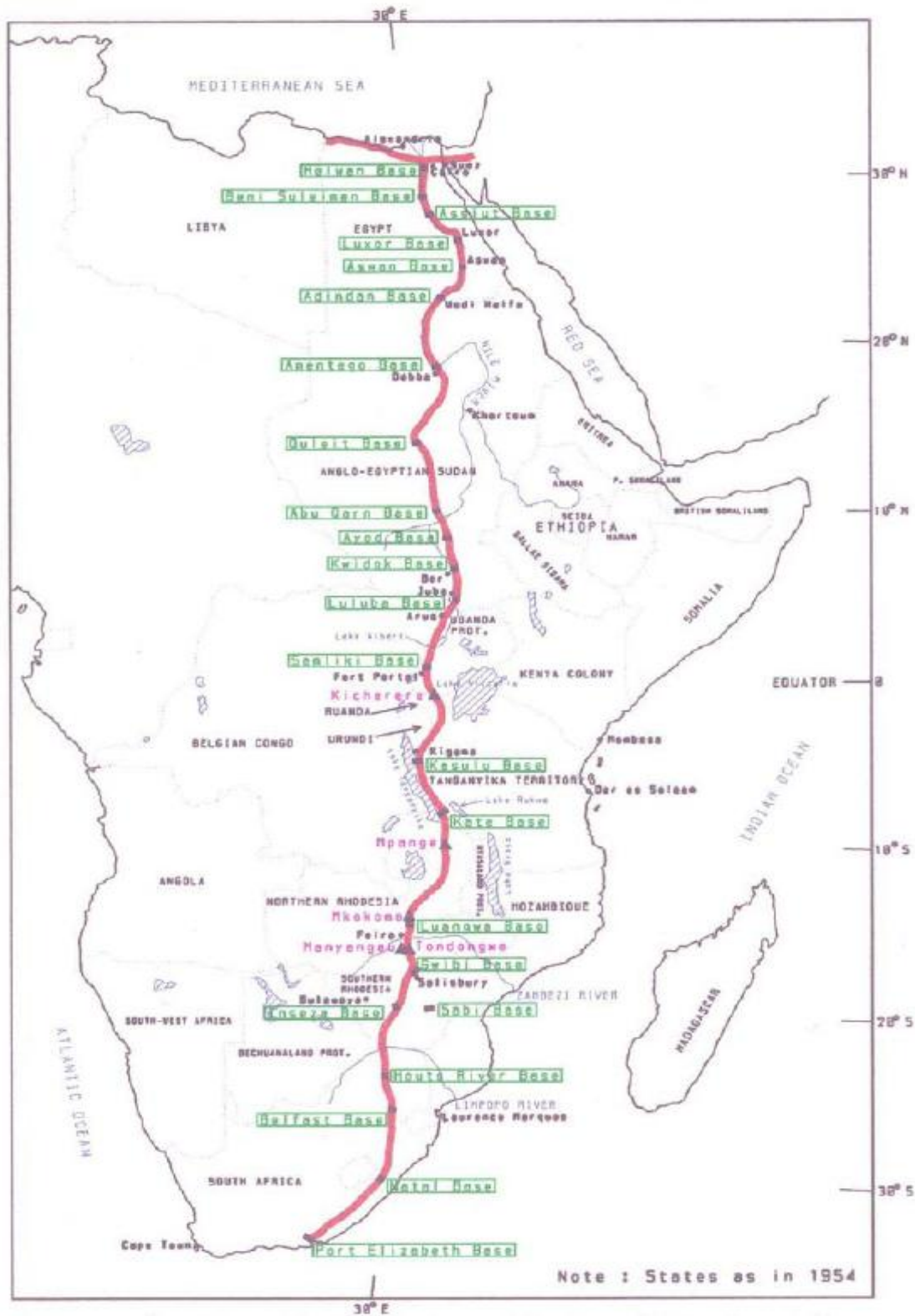
Figure 1.2 the 30th arc meridian [Zakiewicz, 2005]

The network was later improved by the addition of new points by tellurometer traversing between 1960 and 1965 and new computations were done. It also had a few Doppler control points that were incorporated during the African Doppler Survey project (ADOS) in the first attempt to have a unified reference frame for Africa (AFREF) [Wonnacott, 2005]. It also, has a few GPS controls that were established in the mid 1990s through the support of the Japanese International Cooperation Agency (JICA), the Danish International Development Agency (DANIDA) and the Directorate of civil aviations (DCA). Table 1.1 present the summary of the available horizontal controls in Tanzania.

Table 1.1- Summary of Tanzania horizontal controls

Category	Points	Spacing(km)	Period	Remarks
Triangulation	532	25 - 40	1950 -1965	Arc 1960 datum
Traverses	42	15 - 40	1960 - 1965	By Tellurometer
Doppler (ADOS)	9	Over 300	1980 - 1986	Redefined trig points
Aerodist	43	78-300	1973 -1974	
GPS Controls				
Mwanza–Geita	100	10-20	1992 -1993	JICA support
DCA Campaign	8	400-1100	1992-1992	
Usep Project	135	10-20	1993-1995	DANIDA support
Totals	**839**			

1.1.1 Limitations of the present Tanzanian geodetic network

The limitations of the present conventional geodetic network are many and they include the following:

1) It is not compatible with the current satellite positioning techniques, which are presently widely adopted to satisfy the overgrowing mapping requirements of the country and other geo-related information applications.

2) The present frame provides horizontal solutions only contrary to most positioning applications that require a 3D mapping reference frame.

3) The present mapping frame is not homogenous within itself and neighboring countries' mapping frames. This has resulted into mapping inconsistencies in cross border mapping activities, spatial mapping in urban areas as well as the production and update of large-scale topographical maps in urban areas.

4) The present frame cannot support the significant predictions as related to weather, rift valley dynamics, natural hazards mitigations and geophysical exploration surveys.

1.2 Overview of the African unified geodetic datum (AFREF)

The African Geodetic Reference Frame (AFREF) is conceived as a unified geodetic reference frame for Africa that shall be the fundamental basis for the national and regional three-dimensional reference networks fully consistent and homogeneous with the International Terrestrial Reference System (ITRS).

The concept of AFREF comes from some of the main obligations of the African Union (AU) and other international initiatives such as the World Summit on Sustainable Development, International Civil Aviation Organisation (ICAO) and UN Millennium Declaration. These forums require the member state countries to have joint political and economic activities such as New Partnership for African Development (NEPAD) for eradicating poverty in Africa and to place African countries, both individually and collectively, on a path of sustainable growth and development. AFREF would consist of a network of GPS stations established such that the distance between adjacent/successive stations, should not be more than 1000 km so as to allow users to have an easy and free access to GPS data and products from such stations. Its full implementation would include a unified vertical datum to support future efforts to establish a precise African Geoid and it will be such that:

1) It is the basic tool for effective planning and efficient implementation of joint projects that requires cross-border homogenous mapping.

2)   It provides reliable spatial framework for homogenous maps, Geomatics activities and natural hazard mitigation.

3)   It minimizes the increased misunderstandings, conflicts and difficulties of information sharing due to maps with mis-matched edges at the borders. These maps have been prepared from the conventional national mapping frameworks that exist in most African countries.

1.2.1 The initial attempt to create AFREF and its failure

The initial attempt to create a unified reference frame for Africa was first put into consideration between 1980 and 1986 when the African Doppler Survey (ADOS) project was being implemented. The International Association of Geodesy (IAG, 1981) in conjunction with the African Association of Cartography (AAC), the United Nations Economic Commission for Africa (UNECA) and the Regional Centre for Mapping of Resources for Development (RCMRD) did the main project planning with the following objectives:

- To provide zero-order control for future geodetic frameworks in Africa.
- To provide control for datum unification and strengthening; and,
- To provide an accurate geoid for Africa.

However, the ADOS project failed due to several factors that include:

- Difficulty in satisfying the simultaneous observations condition as required by the Doppler satellite technology used at the time.
- Lack of proper awareness and minimum participation in the project amongst the national mapping organizations of the African countries.
- No prior standards were set resulting into low quality observations.
- Bilateral relations with sister organizations did not always materialize.

1.2.2 The present status of AFREF and its objectives

In view of the strong requirements of sharing geo-information among African countries as a tool to eradicate poverty, the implementation of AFREF was accepted and declared in Windhoek, Namibia, during the AFREF annual technical meetings and workshops held in 2005 [Wonnacott, 2005] with the following objectives:

1) To define and establish a unified geodetic network that shall be in the same system as IERS and should be materialized based on the ITRF frame.

2) To define and establish a unified vertical datum that shall be the basis of establishing a more refined Geoid for Africa.

1.2.3 AFREF Management and operation structure

Management and operations of AFREF are under the Steering Committee (Figure 1.3) that is responsible for the overall management and coordination on the implementation of AFREF as described in its Terms of Reference.
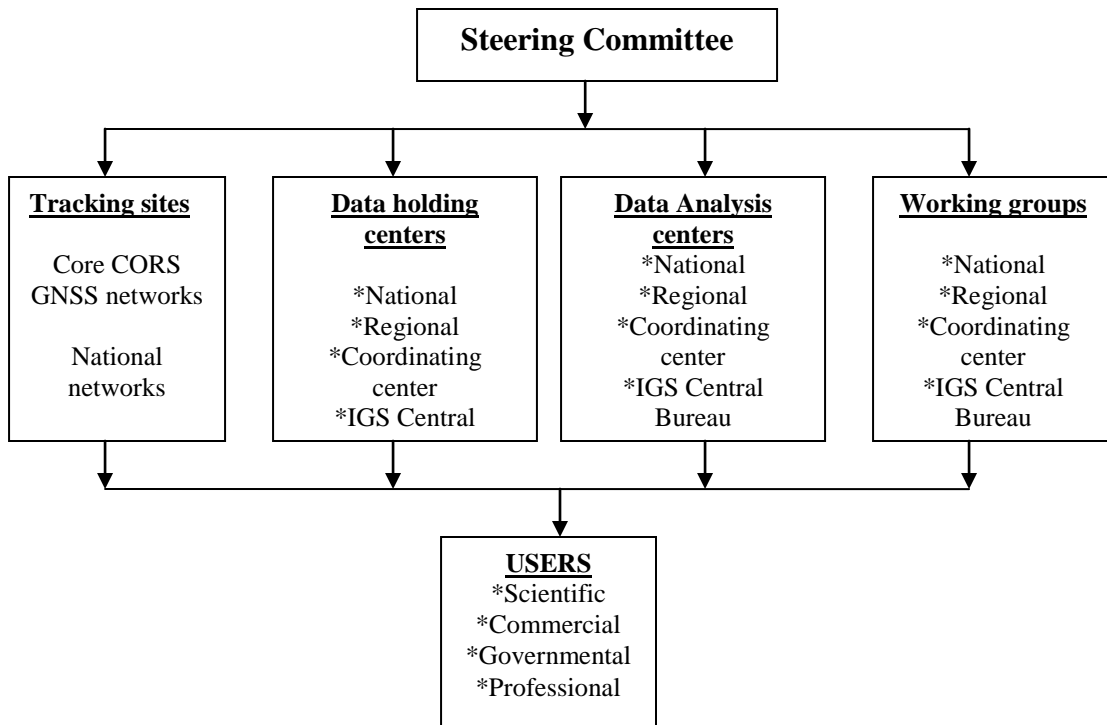
Figure 1.3 AFREF management and operation structure (Wonnacott [2005])

The Steering Committee has drawn its membership as follows:

1. IAG sub commission on Reference Frames, Africa (SC 1.3d) as the chairman.

2. AOCRS **-** African Organisation of Cartography and Remote Sensing in the Arabic speaking countries - Co chair.

3. Regional Centre for Mapping of Resources for Development in East Africa.

4. Regional Centre for Training in Aerospace Surveys in West Africa.

5. North African Countries Working Group (NAFREF) representative.

6. East African Countries Working Group (EAFREF) representative.

7. West African Countries Working Group (WAFREF) representative.

8. South African Countries Working Group (SAFREF) representative.

9. Central African Countries Working Group (CAFREF) representative.

1.2.4 Proposed action plan for AFREF implementation

In view of different levels of economic potential, professional expertise and awareness within African countries, it was agreed that the implementation strategy has to be divided into three main phases that are:

1) Each member state country should establish at least one permanent GPS station as part of continental network.

2) Densification of the network into permanent and semi-permanent base stations on country basis to relate the national frames into AFREF.

3) Development of more refined GEOID for Africa and definition of common vertical datum.

1.3 The new Tanzanian reference frame TZRF10

The new Tanzania frame is conceived as a three-dimensional modern geodetic reference network fully consistent and homogeneous with the International Terrestrial Reference Systems (ITRS). This frame shall consist of permanent and continuous GPS observing stations at a distance of about 500 km apart; and shall be the fundamental basis for the national and regional homogenous mapping supporting both post–mission and real time applications. The new reference frame TZRF10 shall be dynamic to facilitate the geodetic positioning, navigation and general purpose spatial referencing to date in the most versatile, accurate and economical way.

1.3.1 The objectives of TZRF10

The main objectives in the creation of this new frame are:

1) To define and establish a geocentric frame based on ITRS and materialize the same using the most recent realization of ITRF.

2) To define and establish a unique vertical datum based on ellipsoidal heights as basis of future establishment of the Tanzania refined geoid. However, this objective is beyond the scope of this thesis.

1.3.2 Relation between TZRF10 and AFREF

Basing on the basic objectives and activities of the Sub Commission 1.3d of IAG– Regional Reference - Africa, the AFREF implementation strategy requires that the regional working groups include national mapping organisations, academics and research institutions, transportation, communication and professional bodies to have a wide and active participation as much as it is possible in all respects. As part of these requirements, national mapping organisations (NMOs) of the member states are expected to spearhead the formation of national working groups (comparable with National Spatial Data Infrastructure). Through these working groups, member state countries have to establish their respective network control breakdown that shall be the densification of AFREF in the individual countries.

In view of those requirements, Tanzania can therefore be viewed as a sub-working group under the Sub Commission 1.3d (AFREF) such that, the new frame TZRF10 will be the densification of the of the unified African frame (AFREF) which is subject for official definition at a common epoch that shall be agreed. This will be through the integration of the country wide geocentric networks like TZRF10.

1.4 Contributions of this Thesis

The main contributions of this thesis are as follows:

1) To make the covariance analysis of the proposed Tanzanian geodetic network TZRF10 (that is establishing the conceptual overview of the new frame).

2) Develop a case study for modern geodetic reference frame maintenance as a basis for the maintenance of a modern geodetic frame in Tanzania.

3) Development of a case study for near real time positing as a basis of future Kinematic and DGPS survey for geodetic applications in Tanzania.

Some of the expected benefits upon the successful establishment and maintenance of TZRF10 include the following:

- Provide a basis of establishing IGS network stations in Tanzania in compliance with the IAG plans for Africa (Sub-commission 1.3d).

- Provide a homogenous framework for cross border mapping activities with minimized or no mis-matched edges at the borders. This will therefore support information sharing for regional economic and political activities and minimize misunderstandings and conflicts on boundary disputes.

- Establish the basis of geophysical explorations (such as crustal movements), potential atmospheric studies and related activities in the equatorial region.

1.5 The Structure of the Thesis

The thesis is organized into eight different chapters. Chapter one covers the general introduction including an overview of the present Tanzanian Geodetic horizontal frame and its limitations. It also presents a general overview of AFREF and its present status along with its objectives as well as broad implementation plan followed by the discussion of the new proposed frame for Tanzania (TZRF10) and the relation between them. The discussions of the main contributions and the expected benefits upon successful TZRF10 implementations are also in this chapter.

Chapter two reviews the economic value of investing in modern reference frame through a discussion of common misconceptions on technical investments that have been made along with the review of several impacts associated with adopting of a new mapping frame. The discussion uses the experience of Brazil in adopting the SIRGAS and that of Canada in adopting NAD83 to address the expected impacts of such a fundamental change of the reference frame to public and private communities.

Chapter three covers discussion of Tanzania Rift Valley geodynamics. The discussions covers what information is presently known regarding the related kinematics as well as the present and future initiatives to have a better understanding of the geodynamics of the Tanzania rift system. The concluding part of this chapter, discusses the importance of establishing and maintaining a modern dynamic spatial reference frame (the TZRF10) as a basis of quantifying the amplitude of the temporal and spatial deformations with millimeter level positional accuracy.

Chapter four covers the review on two different frame realization approaches that are commonly adopted in frame transformations. They are the rigorous and fiducially marked approaches and for elaborations purposes there are respective discussions of the Canadian Spatial Reference System (NAD83 CSRS) and the Geocentric Reference System for the Americas (SIRGAS). The discussions in this chapter also covers the advantages and disadvantages of each approach as the basis of the selection of the best approach that suits Tanzania's working capability in relation to the available resources and data. Some of the addressed aspects include the following:

- The general procedure adopted in the transformation.

- Handling of distortions in the transformed networks.

- Integration between the older and the new geodetic networks.

Chapter five covers the discussion on the frame implementation, mathematical maintenance and delivery. The first part covers the physical implementation of the system in accordance to the requirements of the IGS Central Bureau whereas the second part of this chapter, presents the discussions on the mathematical maintenance procedures of the frame as a way to control the time variations of the frame with respect to new realizations of the International Terrestrial Reference Frames. Section three covers the different types of data, products that the system will provide the user. They include observations in RINEX for post processing and near real time

applications and DGPS corrections. In concluding the chapter, the summary of the data transfer protocols to being used in the proposed network has been discussed.

Chapter six covers the discussion on the reference frame case studies. The first part of the chapter presents the discussions on the covariance analysis as the basic tool of the conceptual overview of the new frame. With this tool, design tradeoffs of the factors affecting the network performance has been done as a basis of planning and selecting geometrically strong network out of infinity available possibilities. The second part covers the discussions on the case study on reference frame maintenance using the Bernese software v5.0 as one of the available scientific software with the NAD83 (CSRS) as a case study area. Other scientific softwares for frame maintenance that are presently available are GAMIT and GIPSY. The last part of this chapter covers the discussion on a case study on real time GPS positioning using the Network Transfer Protocol of RTCM data via internet (NTRIP).

Chapter seven presents the results and analysis of different case studies. The first section contains the results of the covariance analysis in terms of plots of the error ellipses of the adjusted network points. Error ellipses provide a graphical means of viewing the results of a network adjustment in terms of orientation and scale. Section two presents the results and analysis of the reference frame maintenance from the Bernese software v5.0 and the third section of this chapter give the discussion on the results and the assessment of the case study on near real time GPS positioning.

Chapter eight of this thesis provides concluding remarks and other observations for possible future work.

2. ECONOMIC VALUE OF A MODERN GEODETIC FRAME AND ITS IMPACT

This chapter reviews the economic value of investing on a new geodetic frame and its impact to users. The discussion is divided into two main parts. The first part gives a review of the economic value of a modern geocentric mapping frame in the ITRF system. These are the justifications and benefits to be expected by establishing and using a modern frame. The second part discusses the social and economic impact to different users in adopting a new frame in relation to mapping (cadastral and topographic), land reforms, gender equality and other related issues.

2.1 Background Information

Financial resources are always scarce and a major limiting factor in achieving the required project goals in most government institutions in Tanzania and the Survey and Mapping Division of Tanzania (SMD) is not an exception. Consequently, there is a general trend for the decision makers and politicians to allocate the economic resources based on the economic efficiency of the investment.

From the theory of demand and supply it is evident that, it would appear to be logical and more sensible if more investment is done to projects that would bring immediate returns such that, various users and consumers would have strong

preference to make expenditures than otherwise. Unfortunately, there is often a poor quantification of the value of a geodetic reference frame to most users of the information system despite of the high risk associated with wrong decision making on land related matters as a consequence of an un-reliable geo spatial frame and therefore not a preference [Epstein, 1984].

2.2 Economic value of a new frame

In view of the interaction between the cost of investment and the demand of the resulting products to various system users as well as the misconceptions associated with technical investments related to survey and mapping, this section provides a review of the economic value (justification and benefits) of establishing and utilizing a new mapping frame. The discussions on the first part of this section, gives the summary of the concept of a geodetic reference frame and the second part reviews the most common misconception associated with investment in the survey and mapping projects. The last part of this section gives the modern perspective of a geodetic frame through the evaluation of the economic values of various products that are secondary and tertiary outputs of the geodetic reference frame. These are also are attributes of the economic inputs of a universal and compatible information delivery system as per illustrations by Epstein, [1984].

2.2.1 Concept of a geodetic frame and the use of its products

With reference to Santos [2007], a coordinate system can be broadly defined as a set of rules that gives the concept to define points in space of interest. It requires the information of four main parameters that are, origin of the system, orientation of the axes, parameters that position the point and the units of measure along the coordinate axes. The physical realization of the coordinate system to a defined scale is referred to as a frame and is usually associated with a number of related things such as collection of permanently marked points as per the specifications and coverage of an extensive area. Other related aspects include spatial relationship with known positional accuracy, the mathematical relationship with other frames and the universal availability of geodetic information for other applications.

A reference frame is usually associated with delivery of primary, secondary and tertiary products to different users under different scenarios. As detailed in section 5.3.2 of this thesis, examples of primary products include station coordinates and velocities, precise orbits, clock estimates, ionosphere and troposphere maps, meteorological data for weather and climate predictions. Secondary products include cadastral maps, topographic maps, utility maps, engineering maps, land use maps, valuation maps and navigation charts. Tertiary products include databases for different applications such as short and long-term land use applications, property owners, land tax revenue information, information on regional and international boundaries, environmental management information and urban development trends.

2.2.2 Misconceptions on investment on a geodetic frame

In the context of the traditional perspective, the geodetic coordinate frame was viewed as a self-contained entity rather than an input with an economic value in planning and decision making processes on land related issues. It was perceived as a set of ground controls to serve a certain primary application such as construction or geophysical exploration. In that perspective, the secondary and tertiary user requirements of integrated information from two or more such primary applications were exclusively looked at as not part of the geodetic reference frame.

With reference to previous studies by Duane [1977], Philip [1972] and Epstein [1984], a common traditional way to assess the economic value of a geodetic framework relied in terms of the number of days spent in establishing the new control system for a particular project rather than its universal compatibility. That is, the values of resulting information which is an economic input in other applications that have no direct relation to the frame were excluded in the benefits evaluation process. The traditional way to analyze economic values failed to distinguish the most important sources of inputs and outputs (supply and demand elements) and consequently, failed to identify the most important sources of benefits (secondary and tertiary users) as attributes of the global frame. As for that, they failed to focus on the magnitude of the benefits resulting from the utilization of geodetic frame and therefore, the investment on the establishment and maintenance a geodetic frame was always perceived negatively as a sunk cost.

2.2.3 Modern perspective on the value of a geodetic frame

The modern perspective in assessing the economic value of a global frame has changed from the traditional inclination of point-fix focus, which depends on the demand of its output to a wide scope of being focused as fixed points within an economic system. In this context, the economic value of a geodetic reference frame is evaluated from the overall demand of its respective geo-referenced information of physical features within the coverage of interest such as land surface, water bodies and atmosphere. Depending on the extent and scale of the required applications, the final information is usually available in many forms of maps (thematic, cadastral, topographic, etc) that provide universal compatibility as illustrated in Table 2.1.

Table 2.1- Example of universal compatibility in decision-making

Decision making involving land-related issues

Construction Activities	Geophysical research	land valuation/ research inventory	National defense
$C_1, \ldots, C_{10}$	$GR_1, \ldots, GR_{10}$	$LV_1, \ldots, LV_{10}$	$ND_1, \ldots, ND_{10}$
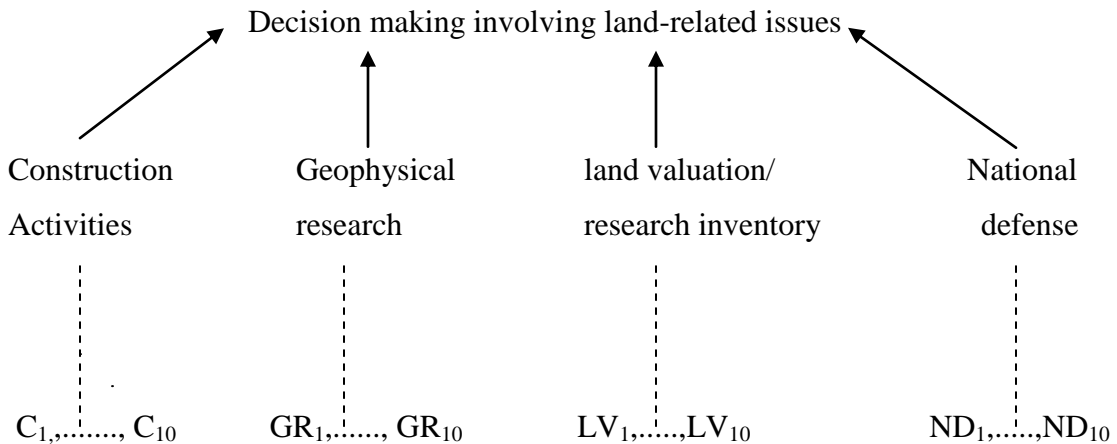
Such compatibility, allows secondary and tertiary users to combine information from individual and totally unrelated primary activities based on modern national geospatial framework based on satellite positioning technology to assist the process of making appropriate planning and decisions involving other land-related issues with minimum risk and conflicts [Epstein, 1984]. Several examples of the economic value of a modern geodetic frame through its secondary and tertiary universal compatible products as economic inputs in planning and decision-making activities include aspects discussed in the following subsections.

2.2.3.1 Integration of development activities

Most current development projects are interdependent for better and efficient implementation. As an example, the proper update of the geological and census data bases requires the availability and therefore integration of information from other national geospatial data bases such as accurate topographic maps which are secondary and tertiary products of a modern geodetic frame based on satellite positioning technology.

2.2.3.2 Border security and military operations

Border security and military operation are global in nature and require appropriate geo-information of the area in question for proper planning and accurate operations. Such applications become more complex in areas that require the definition of a Maritime Boundary Delineation (MBD) with neighboring states. This is due to the fact that apart from the essential need for national security, offshore development as well as development states with sizeable Exclusive Economic Zone (EEZ) are accurately required. Therefore, inability of a particular country to achieve acceptable maritime boundaries with her neighboring country is always hampering national security and offshore economic development to the full extent, especially in energy (oil/gas) and food (fish, etc).

Advanced planning and the deployment of such activities, require the knowledge of positions, navigation techniques and other inputs with reasonable accuracy, all of which are attributes of a reliable and modern dynamic geodetic frame.

2.2.3.3 Land management for Urban and Land use planning

Land is a vital asset that is always scarce in many parts of the case study area to match with the need of the nation wide overgrowing population. Because of that, users of land information are willing to pay for the service in terms of land acquisition, land rent, house rent, property taxes, utility information/thematic maps, site plans, etc. It is therefore important to have a short and long term land use plan to avoid unwanted confrontation.

The proper planning and management of land with minimum risk especially in urban areas requires accurate information of the location and extent of the available land and its relation to the present and future available spatial information with respect to other applications as per master plan requirements. These types of information can be made available through the use of a modern spatial reference frame capable of integrating the spatial information at no additional cost.

2.2.3.4 Cross border mapping activities

Globalization and free market economy necessitate economic partnerships that involves cross border mapping activities in many ways. These result in improved management and monitoring of natural resources including mineral exploration,

forest regeneration, agriculture crop yields, and studies on the impact of climate and soil on vegetative growth. However, this becomes a problem in situations of vital discoveries of economic potential (oil, gas and minerals etc) along border areas like what is happening in Lake Albert along the border between the neighboring countries of Uganda and Democratic Republic of Congo. In such situations, an appropriate geodetic mapping frame would always provide a proper solution.

2.2.3.5 Engineering and construction activities

The value of the geodetic frame in the construction of a new industry or any engineering activity is not limited to control extension and setting out activities as perceived in the traditional way. It has the obligation of observing other applications pertained to land for proper planning and decisions with minimum risk as per the requirement of the master plan in a most economic way. Examples include utility services, road reserves, property boundaries, security implications, impact on the environment and other land use applications.

From a modern perspective, the above land use applications are attributes of a spatial frame and therefore system users should be capable of having such information related to the engineering activity available with reliable accuracy for appropriate decision making with minimum risk.

2.3 Social economic impact of a new frame to users

With reference to previous discussions by Boal and Henderson [1988], Junkins [1988] and Azevedo et al. [2006] the impacts caused by the adoption of a new national geospatial framework are many. They affect both the government agencies and private companies associated with land issues. They include the technical issues, social impacts dealing with individual rights to land and related information, improvements in environmental management and natural resource development, gender equity and native rights, equal access to information for all citizens, improved services as well as good governance.

It is therefore necessary that the new geospatial frame (TZRF10) management should establish and maintain good communications for effective interfacing with the impacted user community while addressing and monitoring the impacts. Examples of communication tools include a web site, printed promotional material, update seminars, opinion polls, as well as the development of education seminars. These tools have to address the impacts of the new datum and the efficient use of the software application packages to support the conversions between the conventional and new systems while using experience from other countries like that of Brazil and Canada to make sure that users are provided with better access of the geo-referenced information.

Example of the impacts of adopting the new system includes aspects discussed in the following subsections.

2.3.1 Impact on coordinate conversions and visualization

The basic and the most important part of the implementation of a modern geodetic frame is the establishment of the GPS network for long-term sustainability whose the primary products are provided in the ITRF system. Unfortunately, most of the current mapping in Tanzania has been done under various coordinate systems currently in use (UTM and local coordinates).

Parallel efforts should therefore be made to address the question of data conversions and data visualization between the new and old systems. Suggestions and recommendations have to be made on software development (like NTv2 in Canada), to facilitate easy conversion between the systems with minimum possible distortions.

2.3.2 Impact on operational effectiveness

One of the main issues that need to be looked at closely is the operational effectiveness of the new system. This can be achieved through the establishment of strong communication links between the system management and the user community regarding the efficiency and the availability of the spatial data. In turn, this assists in the establishing the actual economic value of using the new frame and a better understanding of the impacts caused by its adoption.

2.3.3 Impact on topographical mapping

Topographic mapping in Tanzania is largely done at scales of 1:2,500 in urban areas and 1:50,000 in rural areas. These will be subject to major changes through the adoption of a new frame TZRF10. The changes will be first felt at the institutional level through policy changes to ensure that the delivered products are corrected such that the depiction of all features on the maps and charts are correctly placed according to the new national datum. Physically this mean, each map feature should move to a new position on the map by certain amount such that, in some cases the new maps will contain the same features as the old ones in narrow strips along the neat lines of the new map (overlaps), and in other cases features will be lost (a gap). Generally speaking, the change in position of map features (that is the impact) will be greatest on very large scale topographic maps such as those used in urban areas for land ownership descriptions at a scale of 1:2,500 and least for small scale maps at the scales of 1:50,000 and smaller.

These overlaps and gaps will be problematic and eventually they will have an impact on private citizens such that methods will be needed to deal with them through technical sessions and seminars to responsible agencies as well as public meetings and presentations to end-users of topographic maps.

2.3.4 Impact on cadastral mapping

The basic objectives of cadastral mapping in Tanzania is to provide cartographic representation of land parcels in urban areas, by defining the limits of public or private land in a given coordinate system preferably at a scale of 1:1,000. Adherence to a new reference frame TZRF10 would necessitate all agencies involved with cadastral mapping to implement their services using it so as have to consistency in the description of cadastral parcels and to provide better service to all public and private clients.

However, this brings serious consequences at the legal level because the coordinates are part of the land title under the present system in Tanzania. Therefore a change in the coordinate system will correspond to a change in the legal land title. Also, there will be map irregularities including overlaps and gaps between adjacent integrated maps and hence properties due to different amounts of errors on previous networks. Consequently, there may be disputes between property owners as well as the misidentification of property corners on the ground as the land surveyors attempt to find previously described corners using a different coordinate system than was shown on the original title and survey plans.

Strategies need to be developed on how to deal with such problems through technical sessions and seminars between the reference frame management and responsible cadastral agencies as well as public meetings and presentations to end-users of cadastral maps.

2.3.5 Impact on land reforms

Like many other third world countries, Tanzania is challenged by two main problems as related to land issues. The first is the massive migration of the young generation to urban areas. This results in the increasing inability of municipalities to provide services resulting in large urban informal settlements with unplanned development in the sub-urban areas. Most people in these settlements are poor and lack legal ownership making it difficult to access to bank credit, and impede land use planning, services, and general property improvement. The second problem is the inequities in the land allocation procedures due to tradition backgrounds that are still strong (e.g. inheritance and family roles) and new socioeconomic realities such as labour migration, education, and divorce.

These problems have made the issue of access to land and housing a big problem due to the growing number of female headed households in rural and urban areas. Unfortunately, with the present land recording system, no nation wide analysis has been made to assess the equity in registration procedures as well as access to credit, housing, and other services specifically for the women led households. Moreover, no proper assessment of landless and poor people has been done in urban and rural areas to evaluate what would be the best way to solve these problems. One of the main reasons of these problems is the lack of appropriate national geo referenced information infrastructure that can be used in the analysis and to plan possible land reforms in a most efficient way.

The adoption of a new geospatial frame will impact property rights boundaries (e.g., due to gaps, overlaps, and encroachments) and consequently will be able to identify and address the problem of inequity in landownership and the need of new land reforms policy for providing solutions. To solve these impacts, the government will have to change its governance policy and address them through technical and public meeting in collaboration with the private sector and other stakeholders. This will result in appropriate mechanisms to resolve the technical and legal issues that will aid each stakeholder to better understand and appreciate the roles of others. Governance will also be promoted by the ability of all of the stakeholders to access, exchange, and use better quality geospatial information to empower landholders when in negotiation with public authorities.

Consequently, the development of a new land registration and reallocation process can be made in a way that will pay special attention to the members of poor societies such as poor women, landless people and some indigenous people in surrounding urban areas as the basis (security) of access to loans. Secure land tenure and information on the location and extent of those rights are the basis of equitable and efficient property taxation that will also improve government revenues.

2.2.6 Impact on utilities

Utility related services such as construction and maintenance of roads, services lines for electricity, gas pipelines, telecommunications services lines and sewage systems are part of the land surveying industry in Tanzania. Some of the utility infrastructures is buried underground and its management (through GPS, GIS and paper maps) is very complex especially in urban environment with more than one reference mapping frame.

With the adoption of a new frame, these activities will have to be tied to it for data consistency and enhancement of good governance as well as efficient delivery of these products to the public. This adoption will impact institutional policy to assure confidence and consistency with the modern framework and eventually to private citizens due to improvements in public service delivery coupled with improved information access. Utility maps will have to be corrected such that the depiction of all features on the map or drawing is correctly placed according to the new national datum and hence overlaps and gaps will be created. These will be problematic to users in many ways and may destroy the integrity of these products and trust between the public institution that prepared the map and the individual making decisions based on the map information depicted on it. As a parallel activity, methods should therefore be developed to solve and address such impacts to the general public through technical and public meeting as well as communication tools.

2.2.7 Impact on environment

Environmental concerns have arisen throughout the urban and rural areas in Tanzania as the country attempts to meet the needs of her growing population in respect to settlements, food energy and water resources. Environmental scientists have been continuously advocating serious concern on severe changes of weather, continued depletion of rainforests, coastal pollution and threat to many species as some of the major impacts due to the lack of proper environmental management for the benefit of future generations.

Proper environmental management requires extensive and properly referenced geospatial information to enable the responsible institutions to have a broader understanding of the geographic areas they are dealing with and their impacts. This common understanding can be obtained through maps and information gathered electronically by Global Positioning System tools and satellite imagery and later on; analyzed, displayed, and printed with the use of Geographic Information Systems to enhance the basis of good governance, good order, national development and sound environmental management for the public interest.

Such an improved environmental management through the adoption of a new geospatial infrastructure will result into policy changes at the government institutional level to improve its governance and service delivery to the public and to related companies based on long-term benefits. Methods should therefore be developed to solve and address such impacts to the public.

2.2.8 Impact on natural disasters management

Tanzania falls within The East African Rift (EAR) which is an example of a modern archetype for rifting and continental breakup over its entire length of about 6,000 km with approximate North-South alignment with approximate width of about 48 – 64 km. The EAR has two main branches and both of them are still active with approximate area of about 637,593 km^2 out of which 153, 800 km^2 (24.1 percent) are in Tanzania. They are characterized by deep valleys, sheer escarpments, chain of lakes, and voluminous amounts of volcanic activities with great impact to the environment and the community living around those places.

However, as has been explained in section 3.4, both past and present-day kinematic studies have not been able to obtain significant and precise quantification of them as a basis of disaster management due to the lack of modern dynamic geodetic networks. With the adoption of a modern geospatial frame, the related geodynamics and kinematics will be precisely quantified and ultimately the expected impact. Consequently, we can have a planned displacement of settlement on the surrounding community as a measure of disaster monitoring as well as planned geological and archeological explorations researches.

3. THE TANZANIA RIFT VALLEY GEODYNAMICS

This chapter reviews the present available information on the Tanzania rift valley geodynamics. It also reviews past and present initiatives to understand them in collaboration with international organizations and the need for a modern dynamic frame to improve and update the information. This chapter ends with a discussion on how TZRF10 can contribute to a better understanding of the rift valley system

3.1 Background Information

The Rift is a feature among others, of plate tectonics in which large portions of the earth's upper mantle and crust have moved slowly apart (about 5 cm per year) but persistently through geological time helping to form the shapes of the continents, oceans, and mountains as we know them today.

The East African Rift (EAR) is often cited as a modern archetype for rifting and continental breakup over its entire length of about 6,000 km with approximate North-South alignment and approximate width of about 48 – 64 km.   The East African Rift has two main branches (the Eastern and the Western branches) and both of them are still active (Figure 3.1 and Figure 3.2) with approximate area of about 637,593 km^2 out of which 153, 800 km^2 (24.1 percent) are in Tanzania and is

characterized by deep valleys, sheer escarpments, a chain of lakes and voluminous amounts of volcanic activities.
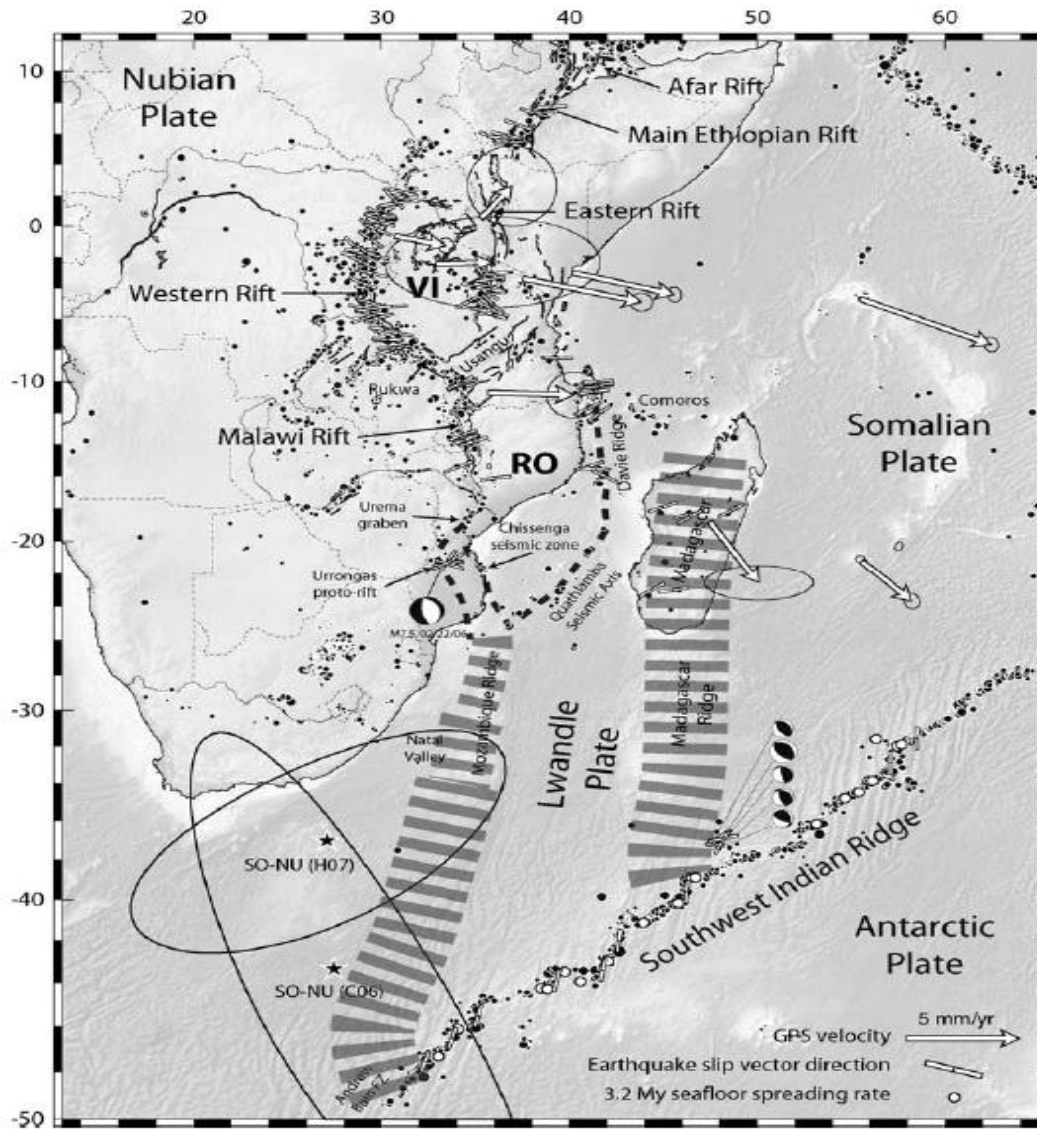
Figure 3.1- Topography and major active faults in the EAR (Stamps et al. [2007])

In Figure 3.1, the solid black lines show major active faults [Skobelev et al., 2004], and small back circles show seismicity (NEIC catalog). Dashed lines indicate

inferred plate boundary trace and the hatched area over Madagascar and the Madagascar ridge show the possibly diffuse Lwandle-Somalia plate boundary. Black stars indicate Nubia-Somalia rotation pole from Calais et al. [2006] and Horner-Johnson et al. [2007].
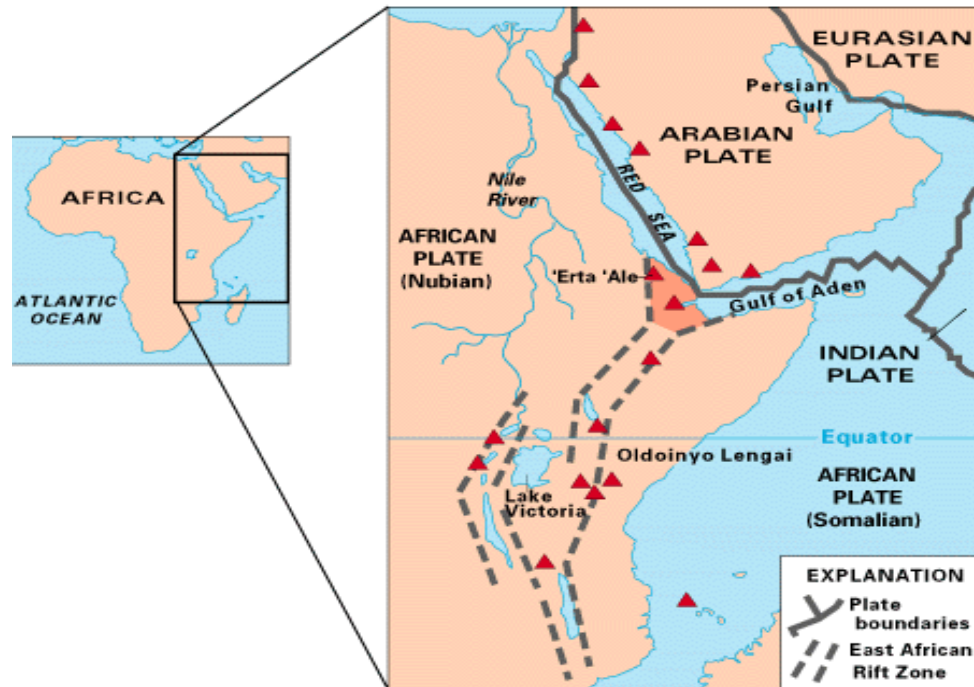
Figure 3.2 The East Africa rift (Klous and Tilling [1996])

In Figure 3.2, the red triangles are active volcanoes and the Afar Triangle (also known as triple junction) is shaded area at the center of the Arabian plate, African plate (Nubian) and the Somalia plate. The three plates are pulling apart from one another at the Afar triangle.

3.2 The EAR Eastern branch

The eastern branch of the East African Rift is about 5,000 kilometers long with series of fault-bounded depressions (steep gorges) passing through the central part of Tanzania and Kenya and going as far as Jordan in the Middle East with approximate north-south alignment marking the divergent boundary between two major tectonic plates of Somalia and Nubia. It is localized with geological features comprising of tall volcanic mountains such as Kilimanjaro, Kenya and Ol Doinyo Lengai, deep lakes such as Victoria and Albert, shallow soda Lake Natron with its thousands of flamingoes and pelicans. The East African Rift System is a great source of archaeological and anthropological discovery, particularly evident at Olduvai Gorge in the eastern Serengeti and is a central part of tourism industry in East Africa.

The EAR has tensional stresses due to the divergence of about 10-15 km between the two plates but appears to be too small to explain the uplift of the East African Plateau by crustal thinning or explain the voluminous volcanism, as observed by McKenzie and Bickle [1988] and Ebinger [1989]. It is believed that the continuous diversion of the plates by an un-quantified amount, may probably split off Eastern Africa to form a new land mass in a few million years to come. Some geologists (Stamps et al., 2007) have the opinion that this spreading processes whose focal point is Afar Triangle where the Red Sea meets the Gulf of Aden have already torn Saudi Arabia away from the rest of the African continent, forming the Red Sea.

3.3 The EAR Western Branch (Tanzania-Rukwa-Malawi rift-TRM)

The western branch of the EAR has active tectonic processes from Malawi to Lake Tanganyika through the southern highlands areas of Tanzania in the Rungwe volcanic province along Usangu basin and Buhoro flats. It has a wide variety of tectonism including active faulting, uplift and subsidence, volcanism, seismicity, erosion and sedimentation. With reference to Delvaux et al. [2001], the structures of the rift basins of Lakes Tanganyika, Rukwa and Nyassa have been developed through progressive interaction of half-graben building blocks.

Previous discussions by Van der Beeck [1998] and Dambon et al. [998], shows that the TRM volcanic province have been under investigation for the past 15 years using a wide range of approaches, such as seismology, fault kinematic and seismotectonics so as to understand the evolution basis of the rift basins and the related dynamic processes. A study by Ferdinand and Arvidsson [2002] indicated that, the 1992-1993 local seismic network recording has revealed that the focal mechanisms of minor earthquakes are presently dominant in the Mbeya area in the southern highlands of Tanzania. Rasskazov et al., [2003] confirmed that, rifting was already active during the first half of the Cainozoic and there is also a weak and very complex stress pattern trend of the TRM rift basin southwards prolongation to Zambia, south west of Congo and up to the Okavango delta in Botswana. However, these few findings are not enough to make exact quantification of the related dynamics of the evolution process as well as the most recent manifestations of rifting.

3.4 Available information about of the EAR Kinematics

East African rift system (EAR) is often cited as the archetype due to its models of continental rifting and breakup. However, both past kinematic studies by Jestin et al. [1994], Chu and Gordon [1999], Lemaux et al. [2002] and Horner-Johnson et al. [2005], or present-day GPS measurements studies by Sella et al. [2002], Prawirodirdjo and Bock [2004] and Fernandes et al. [2004] have not obtained significant and precise quantification of them. This lack of proper knowledge of the geodynamics is largely caused by the improper expertise and lack of modern dynamic geodetic networks that are capable of addressing some of the fundamental questions that are related to those geodynamics. Examples of the basic questions include the following:

- What is the origin of the magma in the Western rift system?
- What is the linkage of the kinematics between the Western and Eastern rift systems?
- Are the continental plate tectonics broadly distributed or localized within narrow zones?
- What are the cause and magnitude of the stresses that drive rifting (e.g., tensional stresses generated by far-field plate motions, pressure gradients induced by asthenospheric upwelling, and/or tractions at the base of the lithosphere produced by the convecting asthenosphere)?

- What is the deformational mechanisms of extension (e.g., symmetrical deformation by pure shear or asymmetrical by simple shear, strain distribution during rifting).

With reference to the most recent studies by Calais et al. [2006] and Horner-Johnson et al. [2007], the only significant finding is the consistent agreement between the sparse GPS data and earthquake slip vectors regarding the plate motions. That is, they all have approximate East West direction with different spatial variation as a function of the plates involved (Figure 3.3) such that:

- The Nubia-Somalia Euler pole is located between the southern tip of Africa and the Southwest Indian ridge.

- There exist two distinct micro plates as illustrated in Figure 3.3. They are the Victoria micro plate which is between the Eastern and Western rifts which is rotating counter-clockwise with respect to Nubia pole and the Rovuma micro plate. The later lies between the Malawi rift and the Davie ridge and it is possibly rotating clockwise with respect to Nubia-Somalia Euler pole.
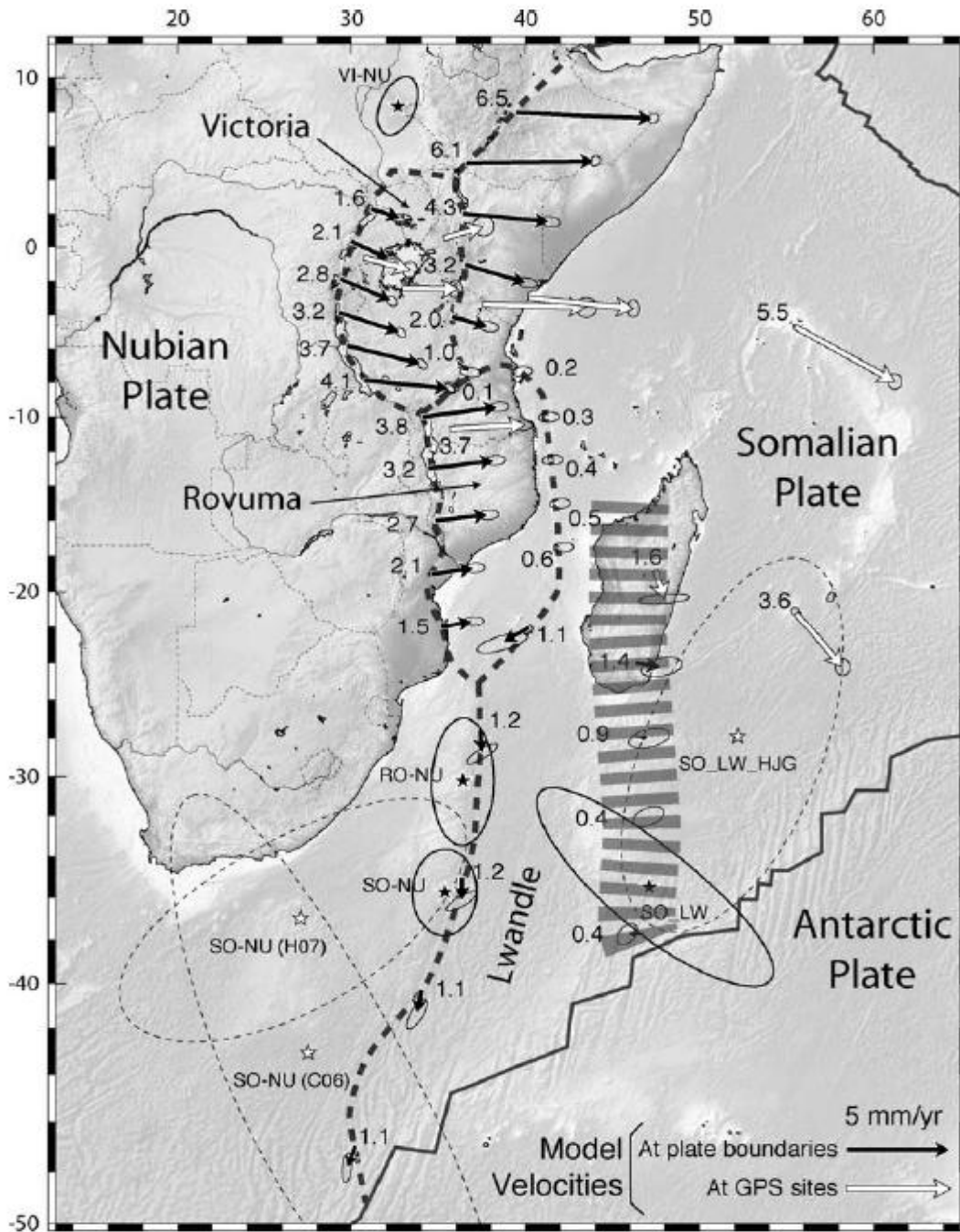
Figure 3.3: Plates relative motions within the East African Rift from the available continuous GPS sites earthquake slip vectors (Stamps et al. [2007])

3.5 Present initiatives to understand the EAR geodynamics

Presently there have been efforts to understand the Tanzania rift valley geodynamics using GPS technology. One of the most recent efforts (August 2006) was a joint endeavor involving the Survey and Mapping Division of Tanzania (SMD), Department of Geology (University of Dar Es Salaam), Department of Geomatics (University College of Lands and Architectural Studies, Dar Es Salaam-UCLAS), Purdue University (West Lafayette, IN, USA), University of Rochester (Rochester, NJ, USA) and the Royal Museum for Central Africa (Tervuren, Belgium).

With the technical support of the University NAVSTAR Consortium (UNAVCO), the first in a series of 3 GPS the campaigns was done in August 2006 aimed at quantifying the present-day kinematics of the East African Rift in Tanzania. The campaign, funded by the National Science Foundation had three main objectives:

- Installation and survey of 32 campaign GPS sites across Tanzania (Figure 3.4) to quantify the kinematics of the East African Rift. The points may as well serve as part of the proposed new Tanzanian geodetic network (TZRF10).
- Install one continuous GPS station in Dar es Salaam (UCLAS campus), in support of a NASA/JPL project.

- Reconnaissance for two continuous GPS stations collocated with seismic stations (Dodoma and Mbeya), to be installed by 2007. However, this activity has not been accomplished and the points are part of the proposed TZRF10.
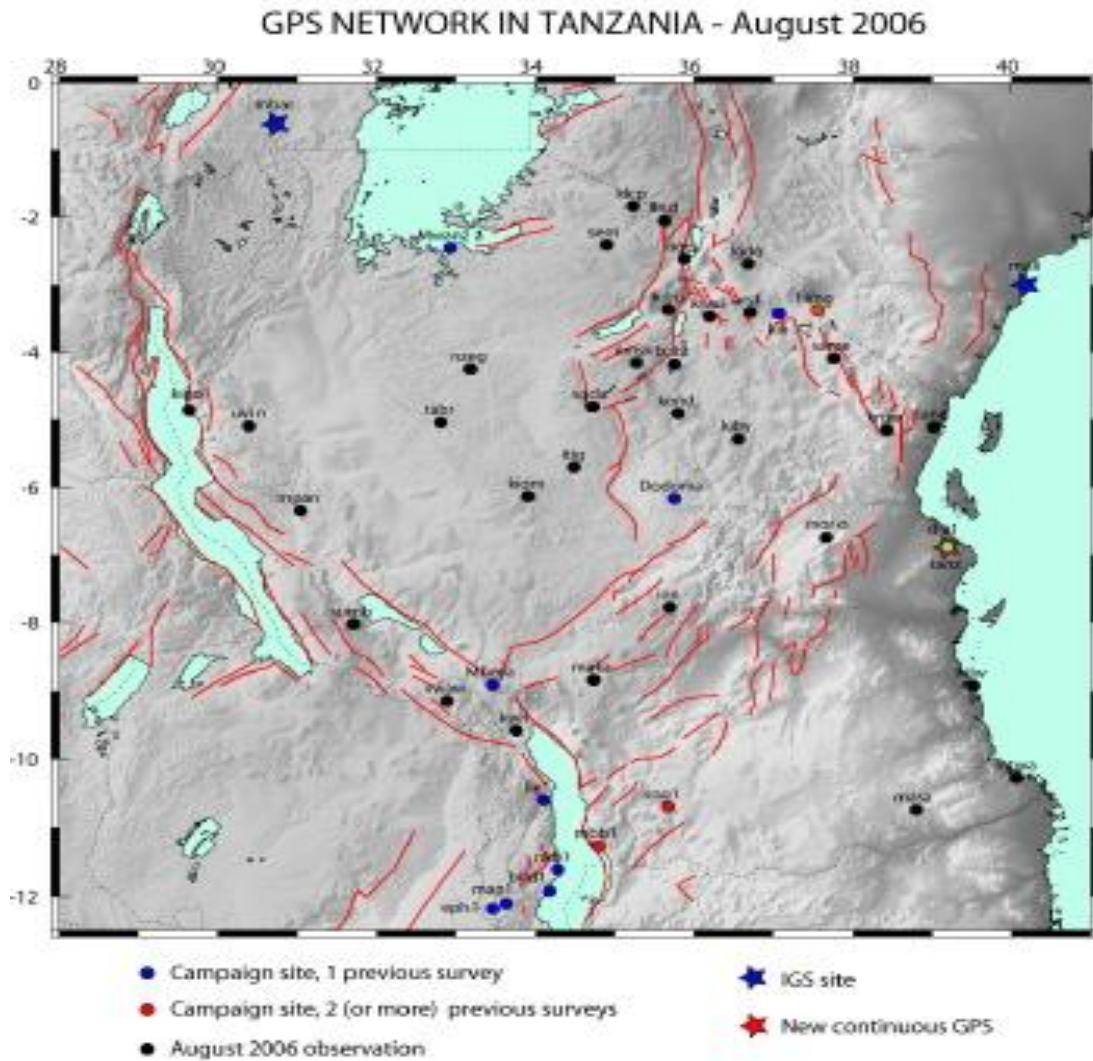
Figure 3.4 Map of GPS geodynamics network in Tanzania (http://web.ics.purdue.edu/~ecalais/projects/ear/tanz/tz06/index.html).

Figure 3.4 shows the map with the proposed GPS network points to be established for monitoring the kinematics of the East African Rift in Tanzania and the red lines show the approximate trace of major active faults. A few of the existing geodetic benchmarks and the triangulation pillars forms part of this network.

The second campaign was scheduled to be undertaken in 2008 whereas the third and the campaign in this series is planned to be done in 2010 in order to establish the first impression of the reliable site displacements. However, the second campaign was not accomplished and no details have been provided so far.

3.6 The TZRF10 frame and the EAR geodynamics

The Tanzania EAR deforms continuously at various temporal and spatial scales because of natural processes (plate motions, earthquakes etc.) that cannot be ignored as the relative positions of points keep changing as well as the reference frame. It is therefore necessary to quantify the amplitude of the deformations with millimeter level positional accuracy through precise measurement approaches. This can be achieved through the establishment and maintenance of a modern dynamic spatial reference frame (such as the TZRF10) that uses space geodetic techniques.

This new high precision and dynamic spatial frame TZRF10 shall facilitate the geodetic positioning (coordinates and velocities in the geocentric coordinate system), navigation and general purpose spatial referencing to date in the most

versatile, accurate and economical way. The new active control network that will realize the TZRF10 will provide continuous coverage over the country and consequently, it will be a basis for geodynamics studies in Tanzania. It will be capable to help addressing the questions that have been put forward in 3.4 above as related to the earth tectonic plate motion and their driving forces within the Tanzania Rift with better understanding at a cm level accuracy. They include the following:

- Extent of the divergence of the Somali and Nubian plate.

- Extent of the amplitudes of the global deformations and climate change.

- Mechanics of earthquakes, faults slip rates and earthquake hazard.

- Measure changes of shape (deformation) from global to local scales.

- Investigate all spatial and temporal.

4. GEODETIC FRAMES TRANSFORMATION STRATEGIES

This chapter gives a summary of two different methodologies commonly used to transform traditional frames into modern geodetic frames compatible with satellite positioning systems. They are rigorous and fiducially marked transformation approaches. For illustration purposes, two different frames transformation procedures have been discussed. They are the NAD83 (CSRS) frame maintained by the Geodetic Survey Division of Natural Resources Canada and the Geocentric Reference System for the Americas (SIRGAS) maintained by the South American countries. In concluding the discussion, the advantages and the limitations of each approach has been presented as the basis of selecting the transformation approach best suited for the Tanzania environment.

4.1 The Canadian Spatial Reference System -NAD83 (CSRS)

The present Canadian frame, NAD83 (CSRS) was realized from its predecessor, the conventional NAD27 frame, using rigorous transformation and readjustment. A rigorous transformation approach makes use of the original observations and requires the availability of sophisticated computing facilities to handle the computation procedures of a large network.

4.1.1 Background of the Canadian Mapping Frame

With reference to previous discussions in Boal and Henderson [1988], Mclintock et al. [1989], Craymer [2006] and Santos [2007], the mapping history in Canada goes back to 1927 when the first Geodetic Datum was established along with her close neighbor, the United States of America. This Datum, which is still considered legal, is referred to as the NAD27 and is based on the 1886 Clarke ellipsoid with its origin at Meades Ranch in Kansas in the USA. The NAD27 was realized by the use of conventional procedures of surveying and mapping that included triangulation, trilateration, standard traverses and classical astronomical observations. The realization of this reference system consisted of a network of thousands of geodetic control monuments (physical makers in the ground) spaced about 20 to 100 km apart at locations chosen for inter-visibility but which were usually inconvenient to access. The densification of the reference frame was performed in a piece-wise fashion by holding existing control points fixed to their published values. The NAD27 had only the horizontal network which accumulated considerable amount of systematic errors resulting into widespread distortions throughout the network of up to 40 m over long baselines. These errors were revealed by the evolution of electronic distance measurements (EDM), and later on by Doppler satellite positioning as illustrated by Junkins and Garrard [1998].

4.1.2 Realization of NAD83

Improvement in space positioning technology in parallel with the advent and increase use in computer technology led to a redefinition of a new global reference system to map the earth with reasonable accuracy in 1980, referred to as GRS80. GRS80 was adopted as the global Geodetic Reference System at the XVII General Assembly of the IUGG in Canberra, by means of resolution No.7 [Moritz, 1979]. It was positioned to be earth-centered with its rotation axis on the direction of the Conventional International Origin for the Polar Motion (CIO), and the zero meridian as defined by the Bureau International de l'Heure (BIH) Terrestrial System of 1984 (BTS-84).

The adoption of GRS80 led to the establishment of the new 2D geodetic datum NAD83 of 1986 - NAD83 'original' to map Canada, USA, Mexico and Denmark (Greenland). In Canada, this was done through long and short-term strategies of rigorous transformation and readjustment of the conventional NAD27 using GHOST software starting with the primary control network (about 8,000 stations). To facilitate this procedure, a relatively dense framework of new Doppler stations was established across the continent, and then the NAD83 (original) reference frame was brought into alignment with BTS84 using an internationally adopted transformation between BTS84 and the Doppler reference frame NWL 9D, as illustrated by Boal and Henderson [1988]. The VLBI stations in Canada and the USA were included in the transformation procedures to provide a connection to the

celestial reference frame and link the NAD83 to the later realization of the ITRF frames. This early realization of the NAD83 in Canada is referred to as the NAD83 (ITRF86) [Crymer, 2006]. The NAD83 (ITRF86) was the first step towards the full implementation of the NAD83 (original) in Canada, discussed in the following section.

4.1.3 Densification of NAD83 (1986)

With reference to the previous discussions by Parent [1988] and Craymer, [2006], the densification and updating of the NAD83 (1986) was done by the secondary integration of the low order networks into the primary network and the implementation was through the provisional agencies of the Canadian Geodetic Reference System Committee (CGRSC) over several years.

The first integration was done in 1989 covering the Eastern part of Canada including 374 primary provincial network stations from Ontario eastward. It is referred to as the Eastern Secondary Integration Helmert Block Adjustment (ESHIBA). The second integration completed in 1990 covered the provincial networks from Ontario westwards. It is referred to as the Western Secondary Integration Helmert Block Adjustment (WSHIBA). The two integrations were followed by a provisional GPS campaign to densify and adjust the entire western provisional networks and the northern territories. In attempt to avoid confusion by

adopting WSHIBA results and subsequently updating the western adjustment was recomputed with the new data in a campaign that was completed and made public in 1993. This campaign was referred to as Network Maintenances Integration project of 1993 (NMIP93). In parallel to these integrations, the NAD83 was officially accepted as the national datum and the federal government produced a official transformation and distortion model from NAD27 to NAD83 referred to as the National Transformation (NTv2), as illustrated by Junkins and Gerrard [1988] and by Junkins and Gerrard [1990]. The new frame is referred to as the NAD83 (original).

4.1.4 3D Realization of NAD83 (CSRS)

The increase in GPS technology in mid 90's led to a change in the global realization of reference frames and positioning accuracies. The International Global Navigation Satellite System (GNSS) service (IGS) with the participation of the the Geodetic Survey Division of NRCan (GSD) and other world wide geodetic institutions , was capable of producing more precise orbits than the broadcast ones for determining positions to a centimetre level. The continuous GPS solutions of global scale helped to determine that the initial realization of the BTS84 and the successive frames like NAD83 and WGS84 were not geocentric as intended to be but rather, they were offset, in case of NAD83 by 2 metres as illustrated by Beutler et al. [1999] and Duval et al. [1997]. It was also realized that the non-dynamic horizontal (2D)

solutions provided by the NAD83 (original) frame were contrary to many GPS application that requires 3D dynamic reference frame and furthermore had significant accumulation of errors of up to 1m in the northern parts of many provinces. In view of these limitations along with the need of having an accurate geoid for other mapping applications, a new 3D framework was realized in 1996 epoch 1997.0 referred to as NAD83 (CSRS96).

Following IERS recommendations, it was necessary to refine the NAD83 (CSRS 96) in 1998 for having continental consistency within North America. The most current IERS values and the NNR-NUVEL-1A plate motion model were adopted for transforming positions to and from the NAD83 (original) and NAD83 (ITRF96) at any arbitrary epoch as illustrated by DeMets et al. [1994], McCarthy [1996], and Larson et al. [1997]. This new realization of NAD83 was denoted as the NAD83 (CSRS).

The widely distributed VLBI points within Canada and USA (Figure 4.1) were included in the transformations and they act as both ITRF as well as NAD83 (CSRS) datum points. They therefore enable more accurate, convenient and direct integration of user data with high accuracy networks.

Figure 4.1 VLBI stations included in NAD83 (Original) and used in the ITRF96 transformation (Craymer [2006])

4.1.5 The structure and Hierarchy of the NAD83 (CSRS)

The present Canadian Spatial Reference framework is comprised of an active component and passive component. The active component of the network has about sixty(60) continuously observing GNSS stations referred to as Canadian Active Control System and VLBI stations. The GNSS observables in the active component are recorded in both 30-second intervals for post processing and 1-second intervals for real time applications. The active part is further subdivided into the federally maintained CACS and the collocated VLBI stations that forms part of the global ITRF reference frame and therefore responsible in relating the NAD83 (CSRS) to different realizations of ITRF without significant loss of accuracy.

The second part of the active component consists of all groups of continuously observing GNSS stations as maintained by regions and provinces and they are usually referred to as regional/provisional ACP and they are also considered as the densification of the ITRF and IGS global networks. These points have been established and maintained by respective groups to support local and regional projects such as monitoring crustal movement and sea level rises. An example of these projects includes the Western Arctic Deformation Network (WARDEN) and the Western Canada Deformation Array (WCDA). The CACS networks as operated by some provinces such as British Columbia, Quebec and New Brunswick, are also supplying DGPS corrections.

The passive component of the network is made up of three sub parts that are the Canadian Base Network (CBN), the Provisional High Precision Network and the Provisional, Municipal and Regional Networks. The CBN, consist of a sparse network of about 160 highly stable and forced centering pillars distributed all over the country whose main intended use was to relate the older networks into the NAD83 CSRS. Currently, the CBN are also used to establish long and short-term scientific studies of the land mass movement as well as reference frame maintenance.

The High Precision Networks (HPN) which are the densifications of the CBN and the Provincial, Municipal and Regional densification networks, most of which were established in parallel to the CBN. Their basic function is to integrate the NAD83 original and the local horizontal and vertical framework, into the NAD83 (CSRS) and the federal government provided a program called NTv2 for that purpose. Through these networks, about 8,000 points have been integrated.
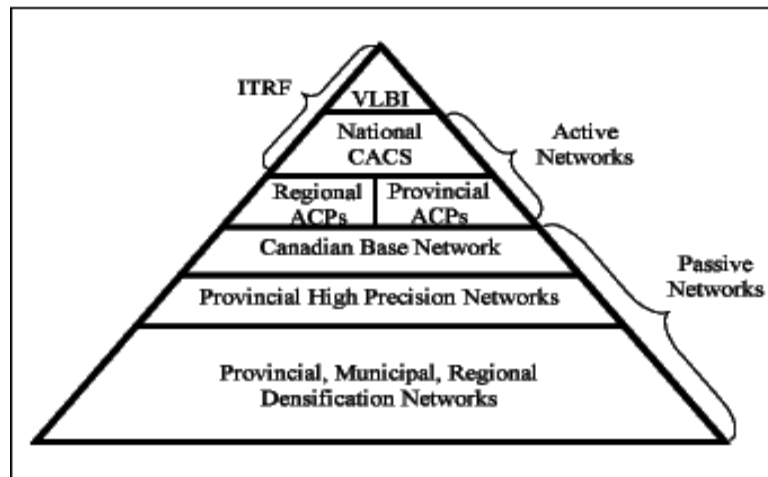
Fig4.2 Hierarchy of NAD83CSRS reference frame [Craymer, 2006]

4.1.6 Station velocities in NAD83 (CSRS)

With reference to the recommendations by the International Earth Rotational Services, as discussed by McCarthy [1996] and illustrations by Larson et al. [1997], NAD83 (CSRS) adopts the NNR-NUVEL-1A plate motion to account for tectonic motion. Velocities estimates from GPS measurements showed that the uncertainties of the horizontal velocity components range from 1.2 to 5.0 mm/yr with respect to the predictions of the NNR-NUVEL-1A, by DeMets et al. [1994] within the 95 percent confidence level for most of the sites in North America.

However, it is worth mentioning that, based on present density of space geodetic measurements in North America, it has been realized that there exist a small bias in the present North American plate which can be considered as additional rotations to the present NAD83 (CSRS) frame when considering the most accurate applications. With reference to previous discussions by Sella et al. [2002], Sella et al. [2004], Sella et al. [2006] and Snay et al. [2006], the available continuously recording GPS sites, has identified uplift in areas where significant present-day glacial isostatic adjustment (GIA) is expected due to ice mass unloading during deglaciation.

4.1.7 Maintenance of the NAD83 (CSRS)

Geodetic reference frames are subject to regular maintenance for a number of reasons including the networks' densification (addition of new points), the correction of survey blunders, unstable or disturbed monumentation, geodynamical effects such as plate tectonics and effects of crustal motion both locally and regionally, and to keep pace with ever increasing accuracy requirements.

With reference to the discussions by Sella et al. [2006] and Snay et al. [2006], the realization of NAD83 (CSRS) is known to be subjected to crustal motions that are significant along the west coast, central and eastern parts of the country. The NAD83 (CSRS) has been found to have vertical movements up to 2 cm/year due to post-glacial and the NNR-NUVEL-1A plate motion used in the defining ITRF-NAD83 transformation is presently known to be in error by the same amount, therefore, degrading the position fixes for high accuracy and scientific applications. Maintenance of the NAD83 (CSRS) frame is, therefore an inevitable necessity so that it is updated on a periodic basis so to maintain high accuracy as well as matching with the successive realizations of the ITRF. There exist two different approaches of frame maintenance which are the dynamic and the semi dynamic approaches. In the former, positions are assumed to be dynamic and are valid only for a specific epoch whereas in the latter, positions are valid within the entire period between successive releases of the global reference frame ITRF. The NAD83 (CSRS) frame is updated using the semi-dynamic approach and will be discussed in chapter five (5).

4.1.8 Advantages of the Canadian Approach

The advantages of a rigorous transformation and adjustment approach adopted in Canada for transforming conventional frames include the following:

- A network can be nearly-optimally adjusted by different adjustment methods to provide accurate position estimates depending on the accuracy of the original network while preserving the network geometry and strength.

- With the advances in the field of GPS positioning and the global densification of permanent GPS tracking stations, it is possible to determine the transformation parameters with the highest level of accuracy. In addition, the rates of change of the similarity transformation parameters between frames can also be computed to refine the transformations.

- Rigorous network adjustment has the advantage of highest possible geometrical accuracy for given input data because most traditional error parameters are statistically uncorrelated or are simply correlated.

- Lower operational costs because the method is highly stable and requires less external data such as additional ground control points.

4.1.9 Limitations of the Canadian Approach

The limitations of the Canadian approach include the following:

- Rigorous transformations of a 2D traditional network, results into horizontal (2D) non dynamic solutions. Such solutions limit many GPS application that requires 3D reference frame that are dynamic in nature.

- It requires the availability of a sophisticated computing mechanism, well trained and qualified personnel as well as the original observations.

- Limitations in the accuracy of the traditional horizontal control networks add significant distortion in the transformed network (new system) especially in the periphery of the network.

- The transformation model is mathematically complex, needing sophisticated software that requires considerable knowledge of the correlation of error parameters on both traditional and modern network so as to accommodate distortion as well as the conformal component of the transformation.

4.2 Geocentric Reference System for the Americas (SIRGAS)

SIRGAS is the dynamic reference frame for the South American countries that was realized through the adoption of the fiducially marks approach. These marks are such that they have known coordinates in traditional system to be transformed and the modern network to be realized (SRGAS in this case) in order to facilitate the computation of the transformation parameters between them.

4.2.1 Background of the South American Mapping

The mapping history of most of the South American counties goes way back to 1908 when there was a serious attempt to map the coastlines and common borders using classical approaches. Since then, there have been a number of improvements leading to the adoption of the South American Datum of 1969 (SAD69) as an official reference frame in 1974. The SAD69 origin is in Brazil at station Chuá where the reference latitude is 19° 45' 41.6527" South, reference Longitude is 48° 06' 04.0639" West of Greenwich and the defining azimuth from Chuá to Uberaba is 271° 30' 04.05". The orthometric elevation is 763.28 m, the components of the deflection of the vertical are 0.31" and -3.52" and ellipsoid height $h_o = 0$ m. The ellipsoid of reference is the International 1967 ellipsoid where $a = 6,378,160$ m and $1/f = 298.25$.

4.2.2 Initial realization of SIRGAS (SIRGAS95)

Developments in space positioning techniques in the early 90s revealed that most of the then conventional systems (including SAD69) had significant distortions despite of number of periodic changes and adjustments to improve them. As a result of these distortions, mapping inconsistencies and the incompatibility with satellite positioning techniques was very significant. It was therefore necessary to have a modern mapping frame and in that respect the South American countries agreed to establish the Geocentric Reference System for the Americas (SIRGAS) during a joint meeting held on 4-7 October, 1993, in Asuncion, Paraguay, under the sponsorship of the International Association of Geodesy (IAG), PanAmerican Institute of Geography and History and Nation Imagery and Mapping Agency [Brunner, 1998].

4.2.2.1 Objectives of SIRGAS

The objectives of establishing SIRGAS are as follows:

1) To define a geocentric reference system for South America in the IERS system and materialize the same using an International Terrestrial Reference Frame as a basis. The ITRF1993 was chosen for the initial realization.

(2) To establish and to maintain a geocentric reference datum with the GRS80 as the reference ellipsoid.

4.2.3 SIRGAS realization strategy

The realization strategy of SIRGAS was the result of work done through three different working groups using the operation structure illustrated in Figure 4.3 so as to maximize efficiency.
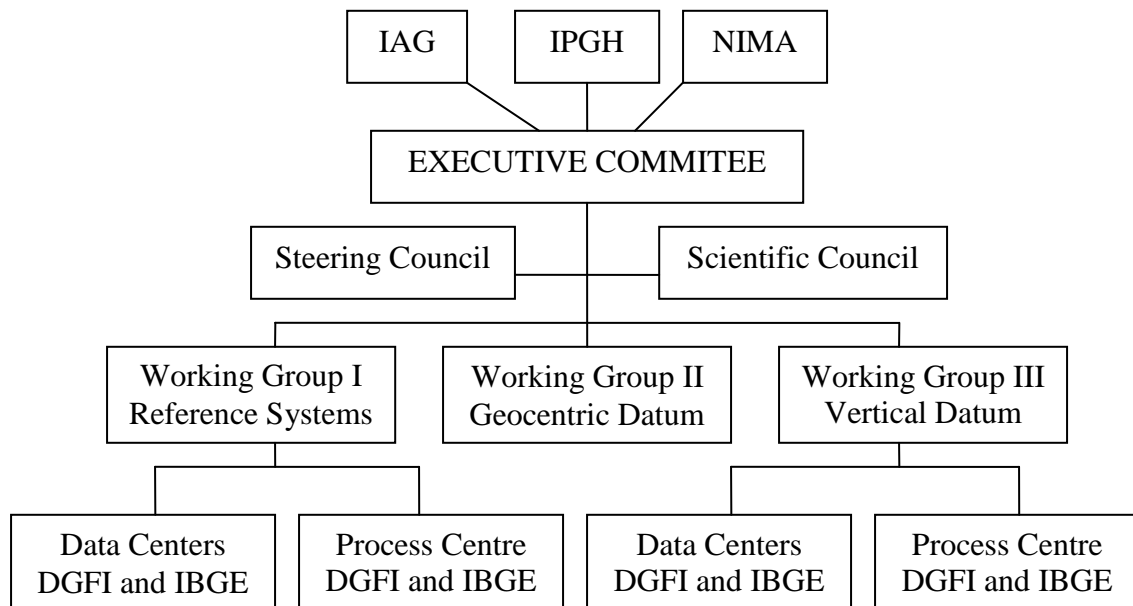
Figure 4.3 SIRGAS project structure
(http://www1.ibge.gov.br/home/geociencias/geodesia/sirgasing/estr_ingles.html)

In Figure 4.3, the Working Groups I and II had the responsibility of realizing the horizontal datum whereas the Working Group III was responsible to realize the vertical datum. The summary of different activities that were accomplished by different working groups to achieve the required objectives is as follows.

4.2.3.1 Station Selection and Establishment (WGI)

A continental GNSS network was established with a total of 58 stations over 11 countries by considering a number of technical related aspects. The first station selection criteria was the inclusion of the then existing LASER, VLBI, DORIS and GPS observation stations within the South American countries so as to coordinate the new network with the required strength as well as facilitate the transformation of the existing regional geodetic networks. The second criterion was the station suitability to GPS measurements with regards to technical requirements through the consideration of related factors such as accessibility, multipath, homogenous continental distribution and strong network geometry. The last consideration in the selection was the extent of overlap of the new system with conventional national geodetic networks to create homogenous mapping between border state countries.

4.2.3.2 Establishment of the GPS Antennas compatibility (WGI)

Different GPS antennas have different locations of phase centre. The relative locations of the phase centre between different GPS antennas need to be known during the data processing to make proper reduction of the coordinates to the station marker. By the time of the establishment of the SIRGAS, the phase centre corrections were not having a unique way of correction that was acceptable internationally (currently IGS recommendations are available). It was therefore necessary to establish them using local tie measurements by co-locating different receiver types at several stations.

4.2.3.3   GPS observations and data processing (WGII)

The network was continuously observed for 10 days from 26th May to 4th June 1995. This campaign, as well as the resulting, frame is usually referred to as the SIRGAS95. To establish consistency data processing was independently done by the DGFI and NIMA whereby the first unconstrained solutions were based on Terrestrial Reference Frame (ITRF93) epoch 1995.4. DGFI adopted IGS precise combined orbits and clock offsets to process data using the Bernese software v 3.4 with slight modifications relevant to SIRGAS. The NIMA used JPL orbits and clock parameters to process data by the use of the GIPSY-OASIS II software. The two solutions were

compared using the seven-parameter similarity transformations and the root mean square error (RMS) between the two solutions were found to be ±1.0 cm in X, ±1.4 cm in Y and ±0.7 cm in Z. The network was re-observed in 2000 for the purpose of obtaining the station velocities with time. The GPS campaign, as well as the resulting frame is referred to as the SIRGAS2000.

4.2.3.4 Realization of the vertical datum (WGIII)

With reference to previous discussions by Drewes et al. [2001], the WGIII became active in 1997 during the IAG Scientific Assembly in Rio de Janeiro with the basic intention of having a unified and unique vertical datum for the existing and future height systems in all South American countries. The main activities were:

- To define a unique vertical reference system for all South America in ellipsoidal heights and geopotential numbers systems.

- To realize the vertical reference system by a set of stations, with leveled heights, gravimetric measurements, and coordinates in the SIRGAS system, including those tide gauges as defined by the classical vertical datum.

With respect to the above, a network of 184 stations was established and observed by GPS. The network included all points in SIRGAS95, the primary tide gauges and other relevant tide gauges that provide additional information about the geographical variations of the sea level. With reference to Costa et al. [2001], Kaniuth et al. [2001] and Drewes and Heidback [2003], the border stations between neighboring countries with known heights in both systems were also included to harmonize the leveled heights due to differences in mean sea levels at the primary tide gauges during the epoch of definition as well as leveling and gravimetric correction errors.

4.2.4 Integration of the country networks into SIRGAS

Prior to SIRGAS, the South American countries had a variety of conventional geodetic networks with different datum and levels of distortions. With the establishment of SIRGAS, the traditional networks of each country were integrated into the new system by adopting different approachs depending on different technical and administrative reasons using the existing SIRGAS stations in the countries (fiducially marks). Countries like Argentina, related their system (POSGAR) by re-computing them using the same processing software as SIRGAS (Bernese V3.4) for establishing the transformation parameters between the two systems. Venezuela installed a completely new system (SAGECAN) and tied it to SIRGAS.

Other countries like Brazil used the approach of numerical partitioning with respect to regional aspects and type of network observation as a basis of rigorous fusion of triangulation networks and other geodetic systems into SIRGAS. The main reason of doing so was to facilitate the application of the GHOST software in the integration. With reference to Brunner [1998, pp. 190-191], the entire network was divided into eight (8) blocks based on a minimum number of junctions and stations between them. Each block was separately adjusted in three different phases of validation of the classical network as performed by the Helmert blocking adjustment, adjustment of GPS data and combined adjustment of the classical and the GPS data.

4.2.5 Advantages of the SIRGAS Approach

The advantages of the SIRGAS approach include the following:

1) It is easy to work with and a very straightforward operation. The only condition to be observed is the availability of common points in the conventional network and the new modern frame.

2) Aerial geometric distortions in scale and azimuth as realized by different networks are constrained in their respective adjustment blocks.

3) The original observations in the conventional networks are not required in the new computations.

4.2.6 Limitation of the SIRGAS Approach

The main disadvantage of this approach is that it results into heterogeneous coordinates. That is, two frames from two different coordinate systems with different computational and adjustment procedures cannot be strictly brought into coincidence, as illustrated by Seeber [2003].

Moreover, the approach is comparatively costly as it evolves the establishment of controls in a new system to affect the transformation procedures.

4.3   The best approach for Tanzania

The situation with the present Tanzania geodetic network is such that:

- Most of the original observations of the present network are missing.

- The distortions with the present Tanzania geodetic network are unknown as it has never been validated to establish their extent since it was realized.

- Tanzania lacks sophisticated computing facilities as well as experts to quantify and model distortions on different parts of the network so as to develop appropriate transformation software like NTv2.

- The present Tanzania conventional network is based on a 2D non dynamic, frame. Rigorous transformation will therefore result into another 2D system which is not favorable for most GPS applications.

Based on the present situation, Tanzania would not be in a position to deploy the rigorous approach as adopted by the Canadians with success. The fiducially mark approach as adopted by the SIRGAS community will therefore have to be adopted for the implementation of a modern frame TZRF10 allowing it to establish a relationship with the conventional geodetic network.

5. FRAME IMPLEMENTATION, MATHEMATICAL MAINTENANCE AND DELIVERY

This chapter discusses implementation, maintenance and delivery strategies of the new frame and the discussion are in main sections. Section one covers physical implementation whereby the technical requirements of the sites to be selected for permanent stations in the satisfaction of the IGS requirements have been reviewed with reference to the guidelines provided by the IGS Central Bureau.

The second section covers the discussion on the mathematical maintenance of frame, which is necessary in order to control the time variation of the frame. In the discussion, the general mathematical procedures of updating modern geodetic reference frames due to the addition of new points in the network, due to geophysical phenomena (such as tectonic motions, crustal deformations, postglacial rebound) and due to correction of survey errors and blunders has been reviewed.

The final section of this chapter covers the frame delivery, including the different products of the frame and the discussion is in two parts. The first part deals with data transmission protocols in TZRF10 to suit the real time applications and the summary of the NTRIP and the RTIGS data transfer protocols. The second part of entails discussion on the various products that the system will provide to the user. They include observations for post processing and real time applications, station coordinates and meteorological data for weather forecast.

5.1 Physical Implementation of the Frame

Physical implementation of the system has to consider several factors that the new sites have to satisfy in compliance with the requirement of the IGS central Bureau and the IGS Reference Frame Coordinator [Moore, 2006]. We take the IGS model as the reference since it is the international model followed by several national geodetic services as discussed below.

5.1.1 Station physical requirements

The new sites have to meet the following requirements:

1)   The sites have to be easily maintainable, accessible and well documented. Ideally, they should be on a stable regional crustal block, away from active faults or other sources of deformation and subsidence. The site location should not be located on soil that might slump, slide, heave, or vary in elevation (e.g. because of subsurface liquid variations etc).

2)   Materialization of the permanent stations using a forced centering device set up in a stable pillar or stable structure.

3)   The site locations should not have significant changes to the surroundings that result into any kind of interference to the GPS signals.

4)   The stations shall have no sky obstructions at all or at least no sky obstruction greater than 5 degrees above the horizon and should be restricted with public access to avoid man made surface vibrations.

5)   Provision of auxiliary stable monuments for local geodetic control, reference, azimuth for the replacement of antennas and recovery in the event that the primary monument is destroyed.

6)   Provide a physical marker, to allow the assignment of an M-type IERS DOME number.

7)   No successive radio frequency (RF) reflective surfaces (fences, walls, etc) close to the GPS antennas that are sources of signal multipath. In addition, there should be no electromagnetic sources in the range of the GPS frequencies (1.2 to 1.6 GHZ), or closer harmonics.

8)   The sites should have continuous power supply, telecommunication facility for data transmission as well as physical site security.

Examples of possible sites that satisfy these requirements in Tanzania include government buildings such as regional office headquarters and military barracks.

5.1.2 Equipment requirements to be satisfied

The implementation of the new frame will adopt the IGS guidelines [Moore, 2006]. They include the following items.

5.1.2.1 Permanence of equipment

The GNSS equipment, and its surroundings, must not be disturbed or changed unless a clear benefit outweighs the potential for discontinuities in the time series. Examples include equipment failure, planned replacement of obsolete equipment and vendor-recommended firmware updates. The GNSS equipment must be approximately oriented to true north using the north reference mark and/or antenna radio frequency (RF) connector.

5.1.2.2 GNSS antenna

The GPS antenna must be geodetic standard with well-defined phase (and gain) pattern to allow mixing with other standard antennas with negligible error and should have very low response to multipath. Antenna gain patterns must be reproducible (i.e. identical phase patterns). Absolute phase center stability must be

within +/- 2mm in the horizontal and +/- 4mm in the vertical relative. Therefore, the implementation would adopt the use of choke ring antenna to achieve high stability, improved low noise as well as reducing the strength of most multipath signals in the observables. The IGS provides the accurate phase center variations of the standard antennas (i.e. the Dorne Margolin choke ring) in the IGS phase center variation file (IGS05.atx) and for that reason, they do not need independent calibration.

5.1.2.3 Antenna eccentricities

The eccentricities (easting, northing, height) from the primary marker to the antenna reference point must be surveyed and reported in site logs and RINEX headers with an accuracy of 1 mm or less. It is required that, each eccentricity component must be less than 5 m.

5.1.2.4   Receiver types

The GPS receivers ought to be of high geodetic quality with appropriate software capable of matching with the present development trends as discussed by Jovancevic et al. [2001] and Todd et al. [2008]. Modern geodetic receivers should be digital with modules that are easily configurable through the internet with a user-friendly graphical interface for downloading, converting and sampling of the new

GPS signals. They should have software capability to track and process all possible open signal samples from healthy GNSS satellites in real time and store them for further processing. Other qualities include internal cycle slip mitigation and detection capabilities as well as compliance with the latest RINEX standards and low cost.

5.1.2.5 GNSS receiver recording capability

They GNSS receiver must be capable of collecting pseudo range and carrier phase observations in L1, L2, L2C and L5 frequencies under non anti-spoofing and record data from all GNSS satellites in view, simultaneously at a cutoff angle of 10 degrees above the horizon. They should be able to synchronize the actual observation instant with true GPS time to within +/- one (1) millisecond of the full second epoch.

5.1.2.6 Radomes

The implementation should avoid the use of radomes unless required operationally, for instance due to weather conditions, antenna security, wildlife concerns, etc. The strategy should also avoid the use of non-hemispherical radomes especially when the shape is not required by site characteristics.

5.1.2.7 Data transmission to data centre

The present plan is to establish a Tanzania data centre at the Surveys and Mapping headquarters in Tanzania for our national and continental users and to the IGS global community. The transmission of data to the data centre (DC) must be automated and has to be verified to be uncorrupted using TEQC and then compressed prior to their transmission to data centre in RINEX format. Usually, we do data verification for the site name, number of observations, epoch, equipment types, interval, and eccentricities. The minimum requirement for data submission should be hourly files with a 30-second sampling interval for post-processing and real time positioning data with 1-second sampling rate. The hourly files should be in such a way that they can be concatenated into the daily files (24 hour navigation message file) containing all messages with TOC/TOE (time of clock, time of ephemeris) at and between 00:00 and 23:59 GPS time of the respective day.

5.2   Frame maintenance

Geodetic reference frames are subject to regular maintenance due to addition of new points, tectonic motions, crustal deformations, volcanic uplifts, postglacial rebound, correction of survey errors and blunders. Usually, the maintenance and updating of modern frames uses a semi-dynamic approach, which periodically updates the coordinates with the new release of the ITRF versions. This approach uses scientific software such as Bernese v5.0, GAMIT and GPSY OASIS II.

With reference to Craymer et al. [2000], Santos [2007] and Dach et al.[2007, pp. 187-188], the mathematical maintenance of the modern geodetic reference frames at any required epoch t uses the generalized Helmet transformation model to account for the rotation factor of the plate motion as follows:

$$
\begin{bmatrix} X_{NAD}(t) \\ Y_{NAD}(t) \\ Z_{NAD}(t) \end{bmatrix} = \begin{bmatrix} T_X(t) \\ T_Y(t) \\ T_Z(t) \end{bmatrix} + \begin{bmatrix} 1+DS(t) & -R_Z(t) & R_Y(t) \\ R_Z(t) & 1+DS(t) & -R_X(t) \\ -R_Y(t) & R_X(t) & 1+DS(t) \end{bmatrix} \begin{bmatrix} X_{ITRF}(t) \\ Y_{ITRF}(t) \\ Z_{ITRF}(t) \end{bmatrix}, \qquad (5.1)
$$

where:

$X_{NAD}(t), Y_{NAD}(t), Z_{NAD}(t)$ are the geocentric Cartesian coordinates in reference frame.

$X_{ITRF}(t), Y_{ITRF}(t), Z_{ITRF}(t)$ are the geocentric Cartesian coordinates in ITRF frame.

$DS(t)$ is the scaling factor in the reference frame.

$R_X(t), R_Y(t), R_Z(t)$ are respective reference frame rotational factors in X, Y and Z.

$T_X(t), T_Y(t), T_Z(t)$ are respective reference frame translation factors in X, Y and Z.

The general procedure is to establish the Rotational factors (R_X, R_Y, R_Z), their respective rate of changes (dR_X, dR_Y and dR_z), the translation factors (T_X, T_Y, T_Z) and the scaling factor DS at the reference epoch t_o. Coordinate computations at any desired epoch t of interest, should involve computations of the values of the rotations and scaling factors at that particular epoch as follows:

$\Delta t = (t - t_o)$.

$k = 4.84813681 \times 10^{-9} \ rad/mas$ is the conversion factor from milliarc to seconds.

$T_X(t) = T_X + dT_X * \Delta t$.

$T_Y(t) = T_Y + dT_Y * \Delta t$.

$T_Z(t) = T_Z + dT_Z * \Delta t$.

$R_X(t) = [R_X + dR_X * \Delta t] * k$.

$R_Y(t) = [R_Y + dR_Y * \Delta t] * k$.

$R_Z(t) = [R_Z + dR_Z * \Delta t] * k$.

$DS(t) = DS + dDS * \Delta t$.

The parameters- T_X, T_Y, T_Z, $T_X(t), T_Y(t)$, $T_Z(t), dT_X, dT_Y$ and dT_Z are in meters, $R_X, R_Y, R_Z, R_X(t), R_Y(t), R_Z(t), dR_X, dR_Y$ and dR_Z are in radians and $DS, DS(t)$ and dDS are in parts per billion. The rotations in these expressions are positive in a clockwise direction.

5.2.1 Coordinates computations within a frame

Adopting the standard transformation model given in equation 5.1 above using transformation parameters in three (3) steps as follows:

1) Propagate coordinates of the point P from reference epoch (t_o) to epoch t using the velocity vector V_P :

$$X_P(t) = X_P(t_0) + V_P(t - t_0) \ .$$
(5.2)

2) Compute coordinates of new stations N from point P at epoch t using the observations and the propagated coordinates $X_P(t)$.

3) Transform back the coordinates of points N to reference frame epoch:

$$X_N(t_o) = X_N(t) - V_N(t - t_o) .$$
(5.3)

In the preceding equations 5.2 and 5.3, $X_P(t)$ are the geocentric Cartesian coordinates of point P in ITRF at epoch t where as $X_P(t_0)$ represents the geocentric Cartesian coordinates of point P in ITRF at reference epoch t_0 . V_P is the coordinate velocities vector of point P and V_N is the velocity vector of the new point N. Usually, the velocities of the new stations have to be derived from the crustal deformation models (rigid plate motions/continuous deformation) available.

5.3 Delivery of the frame

This section covers the discussion of the data transfer protocols that will suit real time application in the case study area along with the different types of GNSS products, which the system will provide the users.

5.3.1 Real time data transmission with TZRF10

The present availability of World Wide Web supports the dissemination of GNSS data streams (such as observations in RINEX and BINEX, DGPS corrections in the RTCM format, EGNOS and WAAS corrections in RTCA as well as SP3 orbits and clocks) to stationary or mobile users of GNSS data in an economical way. The implementation strategy of TZRF10 has earmarked this facility by allowing different users have access to the data streams by use of Personal Computers, Laptop, Personal Digital Assistants, GPS receiver and Mobile IP Networks like GSM, GPRS, EDGE, UMTS or other future technologies.

Presently, the Network Transfer of RTCM data over Internet Protocol (NTRIP) as developed by the Federal Agency for Cartography and Geodesy of Germany is the only available service on commercial basis for that purpose. However, it is worth mentioning that, efforts are underway to develop a data transfer protocol for public use by the Real Time IGS Working Group.

5.3.1.1 Networked Transport of RTCM via Internet Protocol

NTRIP is commercial service as provided by the BKG (the Germany Federal Agency of Cartography and Geodesy) and has been available since September 2004. In collaboration with the German Activities in Monitoring of Water Vapor with GPS (GFZ), it has developed software tools to suite the near Real Time (RT) GPS applications that allows registered users to transmit or receive GNSS data stream. The NTRIP service requires the applications of three system software components that are NTRIP Clients, NTRIP Servers and NTRIP Broadcasters (Figure 5.1).
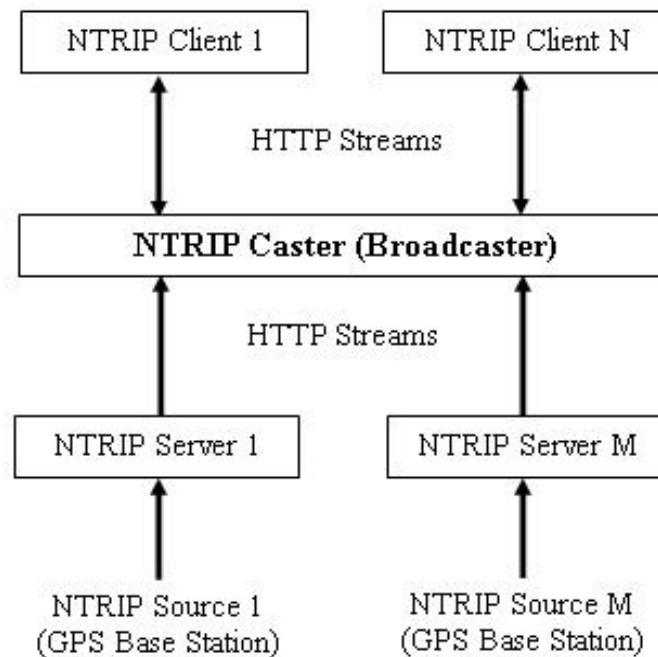
Figure 5.1 NTRIP Components [Thilantha et al., 2007]

Figure 5.1, shows the main components of the NTRIP protocol. With reference to it, GPS stations (also referred to as Mountpoints in NTRIP perspective) collects the GNSS data streams and store them in the NTRIP Server before transferring to the NTRIP Broadcaster using a TCP/IP connection. The NTRIP Broadcaster (also referred to as NTRIP Caster in NTRIP perspective) receive GNSS data streams from the collections centers and distribute them to several thousand simultaneously listening NTRIP clients without alteration. The NTRIP Broadcaster has to verify data from the NTRIP server before authorizing the transmission to several thousand simultaneously listening NTRIP clients of a particular domain (Table 5.1). One domain can have many interlinked NTRIP broadcasters.

Table 5.1 NTRIP Broadcasters

NTRIP Broadcaster (Domain)	Application area
EUREF-IP	Distributes data streams form the EUREF Permanent Network (EPN) and other European resources.
IGS-IP NTRIP	Distributes data streams form the International GNSS Service (IGS) and data from other global sources.
EGNOS-IP	Distributes data streams converted from (EGNOS) observations in the European Continent.

The NTRIP broadcaster also has an alarm system that generates Notice Advisories to Broadcaster Users (NABU) if the data streams are not available for

several minutes. NTRIP Clients needs authority of the NTRIP Broadcaster to receive GNSS data streams using user ID, password and additional information on Mountpoint (source) from which he want to receive data.

5.3.1.2 The RTIGS protocol

The RTIGS protocol is a new system that is still under development by the IGS to transmit and receive data and products on real time using internet in the form of messages. The RT-IGS protocol is under pilot implementation since February 2008 and The RTIGS Working Group believes that, the latency associated with data transmission will be highly minimized upon its successful completion.

5.3.1.3 The RTIGS software tools

The IGS Real-Time Working Group (RTWG) in collaboration with the Geodetic Survey Division of the Natural Resources Canada, Geosciences Department of Australia and other IGS agencies are developing software tools for IGS real time positioning applications [Caissy, 2006; Caissy, 2008]. The software tools (Table 5.2), will be capable of gathering, distributing, archiving and processing real-time data with minimum latency.

Table 5.2: RTIGS application toolset and their deployment

Application	Purpose	Deployments
RTGNSSR (Real-Time GNSS Reader)	1) Reads and validates the GNSS data in real-time from the receiver serial port. 2) Archives, native format GNSS messages in user defined file sizes. 3) Convert the GNSS data into the RTIGS format. 4) Transmit the RT-IGS data to a specified IP address (UDP). 5) Log the performance and error messages in daily log files.	NRCan, GA
RTIGSUDPR (Real-Time IGS UDPRelay)	Routes data and products to analysis centres, global data centers and end users.	JPL, GFZ, NRCan, ESA, GA, IEN, COSMIC
RTIGSA (RT-IGS Archival Software)	Creates files based on RTIGS observation data.	NRCan, CDDIS, BKG, UCAT, NOAA Space Environment Center, TUV, KASI, GOPE

Table 5.2: RTIGS application toolset and their deployment (continued)		
Application	**Purpose**	**Deployments**
RTIGSMR (RT-IGS Multicast Receive Software)	Reads and decodes RTIGS data messages and provides a frame work for real-time application development	TUV (facilitated interface between RTIGS data streams and custom application for IGU quality assurance)
RTIGSAR (RT- IGS Ashtech, Benchmark, Javad/Topcon Readers)	It configures, read and translate raw receiver data into RTIGS data messages. Optional scripts perform complete station level data management.	IEN, NGS, NRL, ROB, ESA

5.3.2 Delivery of the frame

By delivery of frame, we mean the different types of GNSS data and products that the new frame, TZRF10, shall deliver to different users in accordance with specification inspired on those of the IGS Central Bureau. The delivery shall be through the internet facilities and other convenient ways as recommended by the management as discussed in the following subsections.

5.3.2.1 GPS observation files in RINEX

The system will be providing users with GPS data in RINEX at no cost. These data can be used for phase differential baseline post-processing by combining with the GPS raw data from a rover receiver to compute a 3D baseline ($\Delta X, \Delta Y, \Delta Z$) difference to fix new positions.
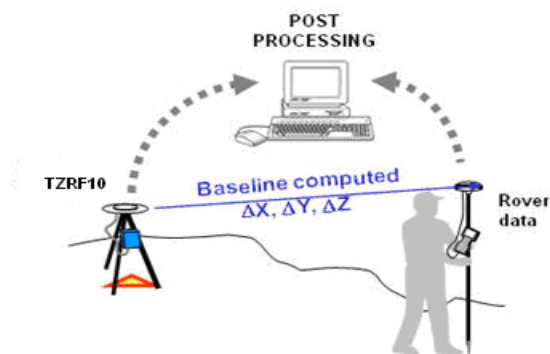
Figure 5.2 Phase differential baseline post-processing

The raw data shall be prepared and distributed in the RINEX format, version 2.2 or greater and then compacted into Hatanaka format with names that are in compliance with the requirements of the IGS central bureau conventions prior to their exchange or transfer to data centre as detailed in section 5.1.2.7.

5.3.2.2 Station coordinates and velocities (in SINEX format)

Station coordinates and velocities are other products that shall be deliverables of the frame. The computations will be on a daily basis using scientific software such as the Bernese v5.0, constrained to the IGS orbits of date and then combined to have weekly solutions that shall be for official use only as the basis of computation of new station coordinates with respect to new and old ITRF realizations. Potential users such as research institutions can have accesses to this information on daily solutions on request based on the special arrangements with the management.

5.3.2.3 DGPS corrections for Real Time positioning

Differential GPS corrections to facilitate the real time positioning shall be another product of the new frame. The present perspective is such that, each of the permanent stations should be capable of computing and transmiting corrections over internet to different GNSS users, using the most reliable and economical data transmission protocol available by then with minimum latency.

However, future considerations to match with the on going global technological advancements in the GPS positioning are not off the table. Presently, the IGS is working on a global model to allow GPS positioning independent of on baselines with reasonable accuracy as compared to the DGPS approach [Caissy, 2008]. Under this approach, the orbit corrections are determined from orbit predictions based on several daily global solutions and the statistics of the IGS combination to exclude problematic orbit data from the prediction process. Then after, the smoothed ionosphere-free and carrier-phase observations from dual frequency tracking data collected in real-time are combined with latest satellite orbit predictions in a least-squares adjustment to determine satellite and station clock corrections. Finally, the approach uses the Hopfield model and standard or measured meteorological parameters to estimate the troposphere delay corrections. The User Datagram Protocol (UDP) and the RTIGS software tools, which are under development, will transmit the overall correction model over internet.

5.3.2.4 Data streams for real time positioning

Data streams at one (1) second sampling will be one of the deliverables of the new TZRF10 frame. Mobile and stationary users can access them over internet using the most economical real time data streaming protocol that will be available by then upon their completion of the appropriate registration procedures. The present available protocols are the NTRIP and RTIGS that is still under development.

5.3.2.5 Meteorological data for weather forecast

The GPS observables are sensitive to variations in atmospheric variables, since the zenith total delay and the refractivity vary as function of height, temperature, pressure and humidity. Within reasonable accuracy, the GPS observations can extract the information of the integrated water vapor (IWV) in near real-time with a typical delay of one hour and assimilate them into numerical weather prediction (NWP) models to provide reliable information on weather forecast. The meteorological data shall therefore be one of the frame products, for the future benefit of the Tanzania Meteorological Department, which is one of the potential investors with potential sites for the permanent stations.

6. THE REFERENCE FRAME CASE STUDIES

This chapter reviews the practical aspects dealing with the implementation strategy of the new frame and the discussions are done in three sections.

Section one contains the discussion on the covariance analysis of the proposed network. This is basically the concept of design tradeoffs of the factors affecting the network performance as a basis of planning and selecting a geometrically strong network out of infinitely available possibilities.

Section two covers the case study in reference frame maintenance using the Bernese software v5.0 and the NAD83 (CSRS) that has been used as the case study area. In principle, reference frame maintenance is an update of the frame as a result of the factors that tend to degrade the accuracy of the frame products with time. They include crustal motions, errors of the previous networks, post glacial rebounds as well as the introduction of the new points in the system. The frame update can be done in many ways but the most commonly adopted approach is the semi-dynamic approach whereby coordinates are periodically updated as new versions of the ITRF are released and they are valid within that period of successive release.

Section three covers a case study on real time GPS positioning. Real time GPS positioning is the concept that deploys the use of real time differential corrections or observations in its application, through some sort of data link (internet, VHF radio, cellular telephone, satellite). Depending on the approach adopted, the real time GPS positioning can be referred to as Differential GPS (DGPS) or Real-Time

Kinematic (RTK). In this case study, the Network Transfer Protocol of RTCM data via internet (NTRIP) has been used. Efforts were taken to implement the case study using the RTIGS data transmission protocol though discussions with the RTIGS Working Group but it was not possible as the protocol is still under development.

6.1 The covariance analysis of the TZRF10

With reference to previous illustrations by Pullen and Parkinson [1995], [Raquet et al., 1998] and [Wolf and Ghilani, 1997], different designs of GPS networks of the same area produce different solutions with different quality of information which usually are never really known until the survey work has been completed, the data processed and then adjusted. These variations are caused by a number of factors that include the geometry of the receivers, the number and geometry of visible satellites, the possible position of user relative to the reference receivers, the magnitude and the correlation of the ionosphere and troposphere error, satellite position errors and characteristic of receiver multipath and receiver noise, as elaborated by Pullen et al. [1995].

Presently, there are available tools such as GeoLab simulation software and simulated least square covariance analysis for planning geometrically strong networks by making design trade offs of the factors affecting the network performance. These tools can give a reasonable projection of whether or not the design would, in theory

meet the overall project goals. This thesis adopts the least square covariance analysis technique based on double differential algorithm that minimizes the differential error variances to assess the performance of the proposed network (TZRF10) as implemented using Matlab software code developed by the author of this thesis. Sometimes the approach is also referred to as the net adjust method.

6.1.1 The concept of covariance analysis technique

Estimation of positional error of an adjusted point is done by establishing two parameters. With reference to the illustration on Figure 6.1, the two parameters are the orientation angle 't' which the axes 'u, v' of the error ellipse make with positioning axes 'x, y' and the lengths of the semi axes S_u and S_v of the error ellipse at that particular point.
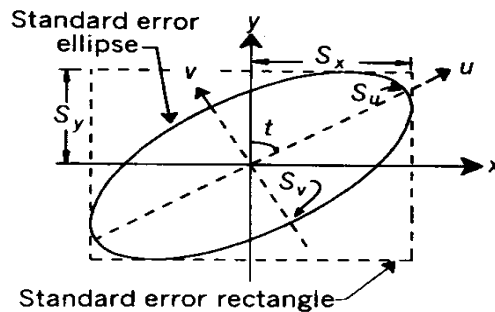
Figure 6.1 Graphical presentation of the standard error ellipse (Wolf and Ghilani [1997, pp.359])
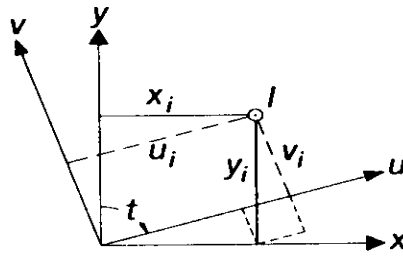
Figure 6.2 Two dimensional axes rotation (from Wolf and Ghilani, [1997, pp.359])

With reference to Figure 6.2, based on an illustration by Wolf and Ghilani [1997], such point 'I' in the (u, v) system of the error ellipse can be represented with respect to the positioning system (x, y) using the following mathematical relationship:

$$u_i = x_i \sin(t) + y_i \cos(t) \ .$$

$$v_i = -x_i \cos(t) + y_i \sin(t) . \qquad (6.1)$$

In matrix form, equation 5.1 can be re-written as follows:

$$\begin{bmatrix} u_i \\ v_i \end{bmatrix} = \begin{bmatrix} \sin(t) & \cos(t) \\ -\cos(t) & \sin(t) \end{bmatrix} \begin{bmatrix} x_i \\ y_i \end{bmatrix} . \qquad (6.2)$$

In simplified matrix form, equation 6.2 can be re-written as:

$$Z = RX . \qquad (6.3)$$

Assuming that, in the adjustment of point 'I' we have a covariance matrix Σ_{XY} in the (x, y) system, such that:

$$\Sigma_{XY} = \begin{bmatrix} q_{xx} & q_{xy} \\ q_{yx} & q_{yy} \end{bmatrix}.$$

(6.3a)

Then, its equivalent covariance matrix in the (u, v) system (Σ_{UV}) can be written as follows:

$$\Sigma_{UV} = \begin{bmatrix} q_{uu} & q_{uv} \\ q_{vu} & q_{vv} \end{bmatrix}.$$

(6.3b)

Σ_{UV} can be developed using the law of propagation of the covariance matrix as follows:

$$\Sigma_{UV} = R\Sigma_{XY} R^T.$$

(6.4)

where:

$$R = \begin{bmatrix} \sin(t) & \cos(t) \\ -\cos(t) & \sin(t) \end{bmatrix}.$$

Expanding equation 6.4 we have:

$$q_{uu} = \sin^2(t)q_{xx} + 2\cos(t)\sin(t)q_{xy} + \cos^2(t)q_{yy}.$$

(6.5)

Making use of the following trigonometric functions:

$$\sin(2t) = 2\sin(t)\cos(t), \cos(2t) = \cos^2(t) - \sin^2(t), \qquad \cos^2(t) + \sin^2(t) = 1 \qquad \text{and}$$

substituting the first function in equation 6.5, gives:

$$q_{uu} = \sin^2(t)q_{xx} + \cos^2(t)q_{yy} + 2\frac{\sin(2t)}{2}q_{xy}.$$

(6.6)

Equation 6.6 can be re-arranged and simplified using the last two trigonometric functions as follows:

$$q_{uu} = \frac{q_{xx} + q_{yy}}{2} + \frac{q_{yy} - q_{xx}}{2}\cos(2t) + q_{xy}\sin(2t). \tag{6.7}$$

To find the value of 't' that minimizes q_{uu}, we have to differentiate equation 6.7:

$$\frac{dq_{uu}}{dt} = \frac{q_{yy} - q_{xx}}{2}2[-\sin(2t)] + q_{xy}2\cos(2t) = 0 \tag{6.8}$$

Reducing and dividing equation 6.8 we have the final equation of 't' as follows:

$$\frac{\sin(2t)}{\cos(2t)} = \frac{2q_{xy}}{q_{yy} - q_{xx}} = \tan(2t), \tag{6.9a}$$

$$2t = \tan^{-1}\left[\frac{2q_{xy}}{q_{yy} - q_{xx}}\right], \tag{6.9b}$$

$$q_{uu} = q_{xx}\sin^2(t) + 2q_{xy}\cos(t)\sin(t) + q_{yy}\cos^2(t), \tag{6.10}$$

$$q_{vv} = q_{xx}\cos^2(t) - 2q_{xy}\cos(t)\sin(t) + q_{yy}\sin^2(t). \tag{6.11}$$

The solution of Equation 6.9b, gives the value of the orientation angle 't' which the axes 'u, v' of the error ellipse make with positioning axes 'x, y' and the solution of Equations 6.10 and 6.11 gives the respective numerical values of the variances q_{xx} and q_{yy}. The square root of the product of the variances and the reference variance S_0^2 gives the values of the semi major axis (S_U) and semi minor axis (S_V) of the error ellipse using Equation 6.12 as follows:

$$S_u = S_0 \sqrt{q_{uu}} \,,$$

$$S_v = S_0 \sqrt{q_{vv}} \,.$$ 6.12)

Equations 6.12 can be further used to determine standard confidence ellipse at any confidence using different approaches. When the a-priori variance factor is unknown, the computations use the Fischer statistic with 2 numerator degrees of freedom and the degrees of freedom for the adjustment in the denominator as follows:

$$S_{u\%} = S_u \sqrt{2F_{(\alpha,2,dof)}} = S_u c \,,$$

$$S_{v\%} = S_v \sqrt{2F_{(\alpha,2,dof)}} = S_v c \,.$$ (6.13a)

where: 'dof' represents the degrees of freedom.

With reference to illustration by Santos [2007], the main disadvantage of this approach (F statistic) is that the test leads to higher confidence limits due to uncertainty. However, when the a-priori variance is known, the above uncertainty can be minimized by using the χ^2 test with the expansion factor that corresponds to u degrees of freedom and α significant level as follows:

$$S_{u\%} = S_u \sqrt{\xi_{\chi_u^2}, 1-\alpha} \,,$$

$$S_{v\%} = S_v \sqrt{\xi_{\chi_v^2}, 1-\alpha} \,.$$ (13b)

This case study has adopted the latter for implementation.

6.1.2 The covariance analysis case study

A case study has been developed through simulation of the new network and then adjusted using a Matlab code developed by the author of this thesis. The code uses the covariance matrix of the adjusted parameters to compute the parameters of the error ellipses reflecting the positional errors of the adjusted positions in terms of the size of the error ellipses and orientation. A summary of the steps adopted in the covariance analysis case study is presented in this section.

6.1.2.1 Simulation of the TZRF10 network

The first step in the covariance analysis case study was the simulation of the network points to be adjusted so as to determine the size and orientation of the error ellipses in the adjusted network. With reference to Table 6.1, ten (10) different points within the case study area (Tanzania) have been simulated by the author of this thesis for the covariance analysis.

Table 6.1 Simulated network points

Location	Site- ID	Latitude			Longitude			height
		deg	min	sec	deg	min	sec	(m)
DSM	MCS	-6	48	56.40	39	17	46.26	49.592
Kidatu	PS1	-7	42	36.00	36	57	36.00	294.000
Mtwara	PS2	-10	20	21.00	40	10	54.00	113.081
Songea	PS3	-10	40	48.00	35	38	60.00	1182.927
Mbeya	PS4	-8	53	24.00	33	25	48.00	1758.004
Dodoma	PS5	-6	10	12.00	35	44	24.00	1148.789
Arusha	PS6	-3	21	36.00	36	40	12.00	1140.005
Tabora	PS7	-5	0	36.00	32	49	12.00	1200.008
Kigoma	PS8	-4	52	48.00	29	36	36.00	762.055
Mwanza	PS9	-2	31	12.00	32	53	24.00	1380.001

From the simulated points, three different networks herein after refereed to as TZRF10 SCENARIO 1, TZRF10 SCENARIO 2 and TZRF10 SCENARIO 3 have been designed by the author of this thesis out of infinity of possibilities available. The simulation of the above possible network points were based on four different main criteria as follows:

6.1.2.1.1 Geographical locations

Tanzania mainland is made up of about 24 administrative regions. Based on the geographical location of the regions, the Survey and Mapping Division of Tanzania has grouped them into four (4) different computing zones comprised of about six regions for better management of the land survey activities. The first criterion on the selection of the new sites in the simulated networks has therefore been based on the existing computing zones for better management of the new sites.

6.1.2.1.2 Security of the GPS sites

A lot of investment will have to be made in terms of finance, personnel and time to make the new frame operational to the required efficiency. The aspect of security for new sites is therefore vital and has been taken care of in the simulation of the new network such that, the selected sites are within the most secured place in the perspective of the case study area. They include the Tanzania government buildings such as regional office headquarters and places where the postal telecommunication towers have been built as well as military barracks.

6.1.2.1.3 Power and communication

Proper implementation of the concept of a real time geodetic network depends on the availability of adequate power supply and communication facilities such as internet and mobile telephone service amongst the GPS sites and the master control station. The network sites have been selected such that they do satisfy this requirement for successive implementation.

6.1.2.1.4 Special requirements

In additional to the above aspects, other sites have been included in the network depending on geophysical and political factors. These include regions that are often subject to earthquakes such as Rukwa and Mbeya regions on the southern highland along the western branch of the Tanzanian rift valley. Such sites will therefore be vital for geophysical exploration survey as well as risk management activities. Also in this criterion of special consideration, the author has included sites on the sensitive border regions such as Kagera and Kigoma on the north western part of Tanzania to facilitate precise border surveys for cross border mappings that are vital aspects for information sharing activities especially in joint projects.

6.1.2.2 Simulation of the GPS observations (code ranges)

Having simulated the location of the new sites, the second step in the covariance analysis was the simulation of the GPS observations for positioning and adjustment procedures. To do so, precise satellite ephemerides were obtained from the CDDIS site [ftp://cddis.gsfc.nasa.gov/pub/gps/products/1465/] for the date of interest which is February, 8, 2008 (GPS week 1465, day five). Then after, the visible satellites within the study area were found with the aid of developed excel program for three different epochs and Table 6.2 illustrates the results from master control station (MCS) at the Surveys and Mapping Division headquarters for epoch 8.30am.

From the known visible satellites, distances to a set of the selected satellites for the analysis were computed and simulated as P_1 code ranges and then after, P_2 codes were simulated by adding random numbers to the former as illustrated in Table 6.3. The simulated results for the remaining sites are in appendix III.

Table 6.2 Visible satellites at MCS on 8, February, 2008 epoch 8:30

Satellite-ID	Distance (m)	Elevation			Azimuth		
PRN		deg	min	sec	deg	min	sec
1	24670086.4548	8	28	46.718	145	42	29.683
5	22052755.4411	42	27	8.436	149	43	53.371
6	22763658.8871	31	30	37.843	161	12	10.009
9	25706669.8334	4	4	34.906	132	42	1.501
12	23001829.1500	27	3	28.062	145	52	40.791
14	22870430.6319	28	14	11.838	169	4	0.630
15	25231758.5406	5	6	3.613	113	14	52.207
16	25371552.2884	4	37	18.572	144	41	34.592
18	20923833.1020	63	26	57.767	165	37	7.032
21	23928878.8467	19	49	6.033	178	15	9.481
22	20546016.6515	67	9	10.825	121	1	50.938
24	25740068.6162	2	1	16.433	148	16	14.644
29	22753044.5455	31	6	58.575	129	44	9.608
30	20984311.9315	61	14	32.054	151	11	27.686
31	23270058.5647	24	18	37.354	108	26	35.050
32	21422243.9152	44	10	34.147	138	34	34.148

Table 6.3 Simulated code ranges for the point MCP

		Master control station point MCS at SMD head quarters			
		Date: 2008 8-February Epoch :8:30 am			
Sat_{ID}	$X_{sat}(km)$	$Y_{sat}(km)$	$Z_{sat}(km)$	$P_1(m)$	$P_2(m)$
6	11770.4250	17713.1344	16078.2701	22763536.581	22763539.587
18	18644.6977	18260.1565	6022.4328	20923701.626	20923703.923
22	23402.1366	10318.7188	-7082.2109	20545934.258	20545935.961
30	15143.5491	18679.6927	-11718.7348	20984252.528	20984252.808
		Date: 2008 8-February Epoch :9:00 am			
6	11454.2236	20908.4789	11865.0257	22082624.576	22082627.985
18	16755.6390	17678.1592	11169.8119	21666426.333	21666429.045
22	23974.1589	11352.7119	-1558.2962	20452823.276	20452824.780
30	12196.2337	17668.6603	-16032.7673	21754251.005	21754252.023
		Date: 2008 8-February Epoch :9:30 am			
6	11262.3383	23099.4041	6844.9803	21506563.167	21506566.071
18	13842.4192	16846.5436	15571.4066	22608311.029	22608313.387
22	23500.7892	11787.0612	4072.5367	20728615.844	20728617.771
30	8373.4683	16668.2500	-19276.4304	18415377.347	18415377.682

6.1.2.3 Mitigation of ionosphere bias

As per previous illustrations by Klobuchar [1991], [Rizos, 1997], [Teunissen and Kleusberg, 1998], [Hofmann-Wellenhof et al. 2001], [Leick, 2004] and Santos [2007], the ionosphere effects the code and phase measurements differently. Mitigation of the ionospheric biases is therefore necessary for any precise GPS measurements to have the most accurate position fixes possible through a number of approaches. In this case study, the ionosphere-free code combination approach was adopted using Equation 6.14 for each of the simulated GPS observations:

$$p_3 = \frac{p_1 f_1^2 - p_2 f_2^2}{f_1^2 - f_2^2},$$

(6.14)

where:

- p_3 - is the ionosphere free observation.

- p_1 *and* p_2 - are the measured/simulated code ranges as shown in Table 6.3.

- f_1 - is the GPS broadcasting frequency L_1 = 1575.42 MHz.

- f_2 - is the GPS broadcasting frequency L_2 = 1227.60 MHz.

The computed ionosphere free observables for the ten (10) simulated points for epoch 8:30 am of 8, February 2008 are illustrated in Table 6:4. The ionosphere free observables for other epochs are in appendix III.

Table 6.4 Ionosphere free observations from permanent stations

	P3 observables for epoch 8:30 am of 8 February, 2008			
Sat_{ID}	$P3_{MCS}(m)$	$P3_{PS1}(m)$	$P3_{PS2}(m)$	$P3_{PS3}(m)$
6	22763654.7443	22918915.1818	23059642.8031	23235324.9988
18	20923829.6345	21002345.1180	21096199.4135	21183440.1394
22	20546012.4133	20447277.4219	20515880.0915	20358914.0734
30	20984308.7162	21008928.9740	20811840.2720	20926829.6799

Sat_{ID}	$P3_{PS4}(m)$	$P3_{PS5}(m)$	$P3_{PS6}(m)$	$P3_{PS7}(m)$
6	23154364.8502	22824663.9583	22549151.2953	22837414.1221
18	21138052.4055	20951237.6525	20811665.5576	20970014.3255
22	20327710.4587	20443290.5639	20546573.9735	20398424.1481
30	21077200.1996	21118412.0028	21231657.6884	21280787.6236

Sat_{ID}	$P3_{PS8}(m)$	$P3_{PS9}(m)$
6	22967202.1207	22624576.8233
18	21065653.8948	20866736.1474
22	20344551.7955	20472704.2369
30	21423204.5235	21409453.6689

6.1.2.4 Mitigation of troposphere bias

The troposphere causes significant delay to the propagated GPS signals that is caused by neutral (none ionized) parts of the atmosphere and are usually decomposed into a dry or hydrostatic component and a wet or non-hydrostatic component. The hydrostatic component forms 90 percent of the total delay and is comparatively easy to model. The wet delay forms 10 percent of the total delay caused by water vapor, temperature and partial pressure that are extremely difficult to be modeled accurately.

The troposphere delay is a function of elevation and altitude of the receiver, and for that reasons it is not frequency-dependent and therefore its mitigation cannot be done through linear combinations of L1 and L2 observations like the ionosphere delays. As illustrated in Santos [2007], the modeling of atmospheric bias is done using a troposphere model and mapping functions that are commonly known by the name of the authors. This case study, has adopted the Hopfield troposphere model [Hopfield, 1969] using Equation 6.15 from Vanicek and Krakiwsky [1986, p.316].

$$d_{trop} = \frac{K_{dry}}{\sin\sqrt{v^2 + \theta_{dry}^2}} + \frac{K_{wet}}{\sin\sqrt{v^2 + \theta_{wet}^2}}, \tag{6.15}$$

where:

- $\theta_{dry} = 2.5^o$ and $\theta_{wet} = 1.5^o$ are the corrections to the elevation angle 'v'.

- $K_{dry} = 2.310$m and $K_{wet} = 0.200$m

Table 6.5a-6.5d gives the computed troposphere biases for TZRF10 SCENARIO 1.

Table 6.5a Troposphere delays TZRF10 SCENARIO1A epoch 8:30am

Computed delays (m) from MCS epoch 8:30am						
Satellite	deg	min	sec	Dry delay	Wet delay	Total delay
6	31	30	37.8428	4.4073	0.3823	4.7896
18	63	26	57.7671	2.5812	0.2235	2.8048
22	19	49	6.0331	6.7620	0.5883	7.3503
30	61	14	32.0541	2.6337	0.2281	2.8618
Computed delays (m) from PS1 epoch 8:30am						
Satellite	deg	min	sec	Dry delay	Wet delay	Total delay
6	29	39	10.1066	4.6541	0.4038	5.0579
18	61	30	0.6177	2.6273	0.2275	2.8548
22	70	18	7.7229	2.4529	0.2124	2.6653
30	60	39	55.6405	2.6484	0.2294	2.8778
Computed delays (m) from PS2 epoch 8:30am						
Satellite	deg	min	sec	Dry delay	Wet delay	Total delay
6	36	49	57.5445	3.8458	0.3334	4.1791
18	44	45	44.6170	3.2764	0.2839	3.5603
22	68	42	42.6024	2.4784	0.2146	2.6930
30	51	44	41.5266	2.9393	0.2546	3.1939

Table 6.5b Troposphere delays TZRF10 SCENARIO1B epoch 8:30am

Computed delays (m) from PS3 epoch 8:30am						
Satellite	deg	min	sec	Dry delay	Wet delay	Total delay
6	25	59	58.6533	5.2471	0.4555	5.7026
18	57	25	41.6171	2.7395	0.2373	2.9767
22	73	36	7.6122	2.4074	0.2085	2.6159
30	62	37	45.3222	2.6000	0.2252	2.8252
Computed delays (m) from PS4 epoch 8:30am						
Satellite	deg	min	sec	Dry delay	Wet delay	Total delay
6	26	55	4.3017	5.0823	0.4411	5.5235
18	58	23	27.3745	2.7108	0.2348	2.9456
22	74	55	0.8509	2.3920	0.2071	2.5991
30	59	5	54.4993	2.6907	0.2330	2.9237
Computed delays (m) from PS5 epoch 8:30am						
Satellite	deg	min	sec	Dry delay	Wet delay	Total delay
6	30	46	20.6993	4.5016	0.3905	4.8921
18	62	44	7.8593	2.5976	0.2250	2.8225
22	70	24	19.3575	2.4513	0.2123	2.6636
30	58	12	5.5299	2.7164	0.2353	2.9516

Table 6.5c Troposphere delays TZRF10 SCENARIO1C epoch 8:30am

Computed delays (m) from PS6 epoch 8:30am						
Satellite	deg	min	sec	Dry delay	Wet delay	Total delay
6	34	9	56.5709	4.1037	0.3558	4.4595
18	66	28	59.8395	2.5183	0.2181	2.7364
22	67	5	28.7742	2.5069	0.2171	2.7240
30	55	50	41.6998	2.7896	0.2416	3.0313
Computed delays (m) from PS7 epoch 8:30am						
Satellite	deg	min	sec	Dry delay	Wet delay	Total delay
6	30	37	36.5671	4.5208	0.3922	4.9129
18	62	16	37.7568	2.6084	0.2259	2.8343
22	72	1	10.1021	2.4280	0.2103	2.6383
30	54	53	5.4492	2.8220	0.2444	3.0664
Computed delays (m) from PS8 epoch 8:30am						
Satellite	deg	min	sec	Dry delay	Wet delay	Total delay
6	29	6	1.6654	4.7338	0.4107	5.1446
18	60	2	0.7408	2.6651	0.2308	2.8959
22	74	12	1.2911	2.4002	0.2078	2.6080
30	52	13	14.9554	2.9203	0.2530	3.1733

Table 6.5d Troposphere delays TZRF10 SCENARIO1D epoch 8:30am

Computed delays (m) from PS9 epoch 8:30am						
Satellite	deg	min	sec	Dry delay	Wet delay	Total delay
6	33	13	36.6490	4.2052	0.3647	4.5698
18	64	56	36.9893	2.5490	0.2207	2.7697
22	69	23	11.0020	2.4673	0.2137	2.6809
30	52	26	54.2869	2.9114	0.2522	3.1636

6.1.2.5 Double difference (DD) ionosphere free observables

GPS observations are also corrupted with other sources of error such as clock errors and orbital errors. These errors have to be minimized for accurate positioning and one way of doing it is through double differencing of the GPS observables. For this reason, different satellite pairs were selected as a basis of forming double differences ionosphere free observables between the control stations constrained to known coordinates and the stations to be adjusted. Table 6.6a through Table 6.6d illustrates results for the selected satellite pairs 6-18, 6-30, 30-18 and 22-30 between the master control station and the rest simulated points for TZRF10 SCENARIO1.

Table 6.6a Double difference (DD) ionosphere free observables for satellite pair 6-18

Epoch	$DDI_{MCP-PS1}$	$DDI_{MCP-PS2}$	$DDI_{MCP-PS3}$	$DDI_{MCP-PS4}$	$DDI_{MCP-PS5}$
8:30 am	-76744.954	-123618.280	-212059.750	-176487.335	-33601.196
9:00 am	-67372.916	23509.595	-103291.113	-164325.800	-101072.321
9:30 am	-45786.066	163095.402	21760.104	-122255.741	-148187.141
	$DDI_{MCP-PS6}$	$DDI_{MCP-PS7}$	$DDI_{MCP-PS8}$	$DDI_{MCP-PS9}$	
8:30 am	102339.372	-27574.687	-61723.116	81984.434	
9:00 am	-72067.355	-180830.544	-265389.053	-176887.127	
9:30 am	-228900.547	-296592.890	-414290.975	-396098.072	

Table 6.6b Double difference (DD) ionosphere free observables for satellite pair 6-30

Epoch	$DDI_{MCP-PS1}$	$DDI_{MCP-PS2}$	$DDI_{MCP-PS3}$	$DDI_{MCP-PS4}$	$DDI_{MCP-PS5}$
8:30 am	-130640.180	-468456.503	-529149.291	-297818.623	73094.073
9:00 am	-159001.222	-481760.810	-590228.014	-373157.014	38401.082
9:30 am	-162210.901	-455255.133	-581365.344	-388116.124	16651.416
	$DDI_{MCP-PS6}$	$DDI_{MCP-PS7}$	$DDI_{MCP-PS8}$	$DDI_{MCP-PS9}$	
8:30 am	461852.421	222719.530	235348.431	564222.874	
9:00 am	446009.286	156229.137	125231.552	503534.665	
9:30 am	402059.273	105582.520	48430.828	427411.736	

Table 6.6c Double difference ionosphere free observables for satellite pair 30-18

Epoch	$DDI_{MCP-PS1}$	$DDI_{MCP-PS2}$	$DDI_{MCP-PS3}$	$DDI_{MCP-PS4}$	$DDI_{MCP-PS5}$
8:30 am	53895.226	344838.223	317089.541	121331.288	-106695.269
9:00 am	91628.307	505270.406	486936.901	208831.214	-139473.404
9:30 am	116424.835	618350.535	603125.449	265860.383	-164838.557
	$DDI_{MCP-PS6}$	$DDI_{MCP-PS7}$	$DDI_{MCP-PS8}$	$DDI_{MCP-PS9}$	
8:30 am	-359513.049	-250294.216	-297071.547	-482238.440	
9:00 am	-518076.641	-337059.681	-390620.605	-680421.792	
9:30 am	-630959.820	-402175.330	-462721.802	-823509.809	

Table 6.6d Double difference ionosphere free observables for satellite pair 22-30

Epoch	$DDI_{MCP-PS1}$	$DDI_{MCP-PS2}$	$DDI_{MCP-PS3}$	$DDI_{MCP-PS4}$	$DDI_{MCP-PS5}$
8:30 am	123355.249	-142336.122	129619.304	311193.438	236825.136
9:00 am	80873.600	-331079.849	-69550.833	208280.149	276198.446
9:30 am	46702.400	-492366.270	-235398.755	126188.660	313046.859
	$DDI_{MCP-PS6}$	$DDI_{MCP-PS7}$	$DDI_{MCP-PS8}$	$DDI_{MCP-PS9}$	
8:30 am	246787.412	444067.173	640356.425	498453.129	
9:00 am	428987.863	543456.908	741884.553	723918.762	
9:30 am	587753.917	634679.609	838560.493	923771.201	

6.1.2.6 Double difference (DD) troposphere free observables

Using the same satellite pairs as in 6.1.2.5, a double difference of the observations free of the troposphere delay has been done. Results for the selected satellite pairs between the master control station and the permanent stations for TZRF10 SCENARIO1 have been illustrated in Table 6.7a through Table 6.7d where as the rest of the results are in appendix III.

Table 6.7a Double difference troposphere free observables Satellite pair 6-18

Epoch	$DDT_{MCP-PS1}$	$DDT_{MCP-PS2}$	$DDT_{MCP-PS3}$	$DDT_{MCP-PS4}$	$DDT_{MCP-PS5}$
8:30 am	-0.2182	-0.4261	-0.7410	-0.5930	-0.0848
9:00 am	-0.1130	-0.0471	-0.2620	-0.3130	-0.1250
9:30 am	0.0287	0.3309	0.2904	0.0691	-0.1198

	$DDT_{MCP-PS6}$	$DDT_{MCP-PS7}$	$DDT_{MCP-PS8}$	$DDT_{MCP-PS9}$	
8:30 am	0.26172	-0.09386	-0.26386	0.18473	
9:00 am	-0.02597	-0.22203	-0.37718	-0.15526	
9:30 am	-0.29754	-0.26940	-0.35688	-0.43616	

Table 6.7b Double difference troposphere free observables Satellite pair 6-30

Epoch	$DDT_{MCP-PS1}$	$DDT_{MCP-PS2}$	$DDT_{MCP-PS3}$	$DDT_{MCP-PS4}$	$DDT_{MCP-PS5}$
8:30 am	-0.2523	-0.6462	-0.9496	-0.6720	-0.0127
9:00 am	-0.1929	-0.4857	-0.7046	-0.5038	0.0044
9:30 am	-0.1387	-0.5375	-0.6252	-0.3432	0.1324
	$DDT_{MCP-PS6}$	$DDT_{MCP-PS7}$	$DDT_{MCP-PS8}$	$DDT_{MCP-PS9}$	
8:30 am	0.4995	0.0813	-0.0435	0.5215	
9:00 am	0.4439	0.1048	0.0286	0.5050	
9:30 am	0.6452	0.3878	0.4726	0.9201	

Table 6.7c Double difference troposphere free observables Satellite pair 30-18

Epoch	$DDT_{MCP-PS1}$	$DDT_{MCP-PS2}$	$DDT_{MCP-PS3}$	$DDT_{MCP-PS4}$	$DDT_{MCP-PS5}$
8:30 am	0.03403	0.22016	0.20858	0.07897	-0.07209
9:00 am	0.07988	0.43856	0.44260	0.19084	-0.12940
9:30 am	0.16739	0.86840	0.91565	0.41231	-0.25222
	$DDT_{MCP-PS6}$	$DDT_{MCP-PS7}$	$DDT_{MCP-PS8}$	$DDT_{MCP-PS9}$	
8:30 am	-0.2378	-0.1751	-0.2203	-0.3368	
9:00 am	-0.4698	-0.3268	-0.4058	-0.6603	
9:30 am	-0.9428	-0.6572	-0.8295	-1.3562	

Table 6.7d Double difference troposphere free observables Satellite pair 22-30

Epoch	$DDT_{MCP-PS1}$	$DDT_{MCP-PS2}$	$DDT_{MCP-PS3}$	$DDT_{MCP-PS4}$	$DDT_{MCP-PS5}$
8:30 am	0.0735	-0.0903	0.0703	0.1856	0.1490
9:00 am	0.0498	-0.2569	-0.0782	0.1380	0.2121
9:30 am	0.0412	-0.5266	-0.2719	0.1347	0.3646
	$DDT_{MCP-PS6}$	$DDT_{MCP-PS7}$	$DDT_{MCP-PS8}$	$DDT_{MCP-PS9}$	
8:30 am	0.1682	0.2892	0.4262	0.3436	
9:00 am	0.3717	0.4458	0.6345	0.6440	
9:30 am	0.7548	0.8085	1.1503	1.2768	

6.1.2.7 Least square network adjustment

This case study, has adopted the least squares parametric approach for network adjustment using Matlab software code. With reference to illustrations by Hofmann-Wellenhof et al. [2001] and Santos [2007], the adjustment has based on the generalized GPS observation given by Equation 6.16, where the observations are expressed as a function of the unknown parameters, as generalized in Equation 6.17:

$$P_A^j = \sqrt{\left((X_A - Xj(t_o))^2 + (Y_A - Yj(t_o))^2 + (Z_A - Zj(t_o))^2\right)} + c\delta t + \varepsilon_\rho^j, \qquad (6.16)$$

$$\ell = Ax, \qquad (6.17)$$

where:

$X_j(t_o), Y_j(t_o) \ and \ Z_j(t_o)$ - is the position of satellite 'j' at epoch t_o.

$X_A, Y_A \ and \ Z_A$ - is the initial approximate position to be adjusted.

$c\delta t$ - are the clock errors and ε_ρ^j are the residual errors.

x - is the vector of unknowns to be found in the adjustment process.

ℓ - is the vector of the observations P_A^J and A - is the design matrix.

The design matrix 'A' is comprised of 'n' rows equal to the number of the observations and 'u' columns equal to the number of unknown such that; $n > u$.

Assuming that σ_o^2 is the a-priori variance factor and Σ_l is the covariance matrix of the observations, then the cofactor matrix of the observations is as follows:

$$Q_l = \frac{1}{\sigma_o^2} \Sigma_l.$$ (6.18)

The resulting weight matrix P of the observations is as follows:

$$P = \Sigma_l^{-1} .$$ (6.19)

By least square principles, a unique solution of the Equation 6.17 is obtained by forming normal equations as follows:

$$(A^T PA)x = A^T P\ell .$$ (6.20)

This leads to a unique solution vector as follows:

$$x(\Delta x, \Delta y, \Delta z) \quad = \quad (A^T PA)^{-1} A^T P\ell.$$ (6.21)

Where; $\Delta x, \Delta y \ and \ \Delta z$ - are the respective differences in coordinate components between iterative adjustment process within the specified THRESHOLD such that:

$$\sqrt{\Delta x^2 + \Delta y^2 + \Delta z^2} \leq THRESHOLD.$$ (6.22)

The final adjusted coordinates (appendix III) are computed as follows:

$$\hat{X}_A = X_A + \Delta x ; \hat{Y}_A = Y_A + \Delta y \quad and \quad \hat{Z}_A = Z_A + \Delta z$$ (6.22a)

Computation of the parameters of the error ellipses has been done using the parameters of the covariance matrix that has been obtained using the law of propagation to determine the cofactor matrix of the solution as follows:

$$Q_{XY} = [(APA^T)^{-1} P]Q_l [(APA^T)^{-1} A^T P]^T .$$ (6.23)

Substituting Equation 6.19, the above equation can be reduced as follows:

$$Q_{XY} = (A^T PA)^{-1}.$$ (6.24)

The covariance matrix of the adjusted coordinates with respect to the positioning axes can be obtained as follows:

$$\Sigma_{XY} = \begin{bmatrix} q_{xx} & q_{xy} \\ q_{yx} & q_{yy} \end{bmatrix} = \sigma_0^2 Q_{XY}.$$

(6.25)

This covariance matrix is used to deduce the inclination angle t with which the axes U, V of the error ellipses of the adjusted positions makes with respect to the positioning axes X, Y using Equations 6.9a and 6.9b. In addition, the semi major and minor axes of the error ellipse are computed from the same matrix using Equations 6.10 and 6.11 respectively.

6.2 Case study on frame maintenance

A case study for reference frame maintenance of a modern reference frame has been done for the GPS week 1368 (26 March to 1 April 2006) using the present NAD83 (CSRS) as the case study area. GPS observations have been processed and compared to the official published results from the GSD that are also part of the solutions used for establishing the new reference frame for the North American countries (NAREF) and the computed results have been discussed in section 7.2.

The processing has been done using the Bernese v5.0, which is available in ten different updates as one of the available scientific software for reference frame maintenance. Other scientific software packages capable of similar tasks include the GAMIT and the GIPSY-OASIS II. In the context of geodetic reference frames, scientific software should be capable of managing the reference frame maintenance to the required geodetic standards. They require a deep understanding of GPS signals and error behavior associated with their propagation from the GPS satellites to the receiving GPS receivers. As a general overview, scientific software has three components each of which is embedded with a number of programs in them to handle a particular error associated with the GPS signal propagation. They are the pre-processing part, the main processing part and post processing part. The different programs that are embedded in them need appropriate configuration which is usually referred to as a processing strategy in order to achieve the desired deliverables as per the required geodetic specifications.

6.2.1 Overview of the Bernese v5.0 software

The Bernese v5.0 GPS Software is a sophisticated tool capable of meeting quality specifications of geodetic applications using Global Navigation Satellite Systems (GPS and GLONASS). Its program structure (Figure 6.3) allows the processing of information related to kinematic and reduced-dynamic precise orbit determination for low earth orbiters (LEO) as well as Satellite Laser Ranging measurements (SLR) to GNSS satellites.
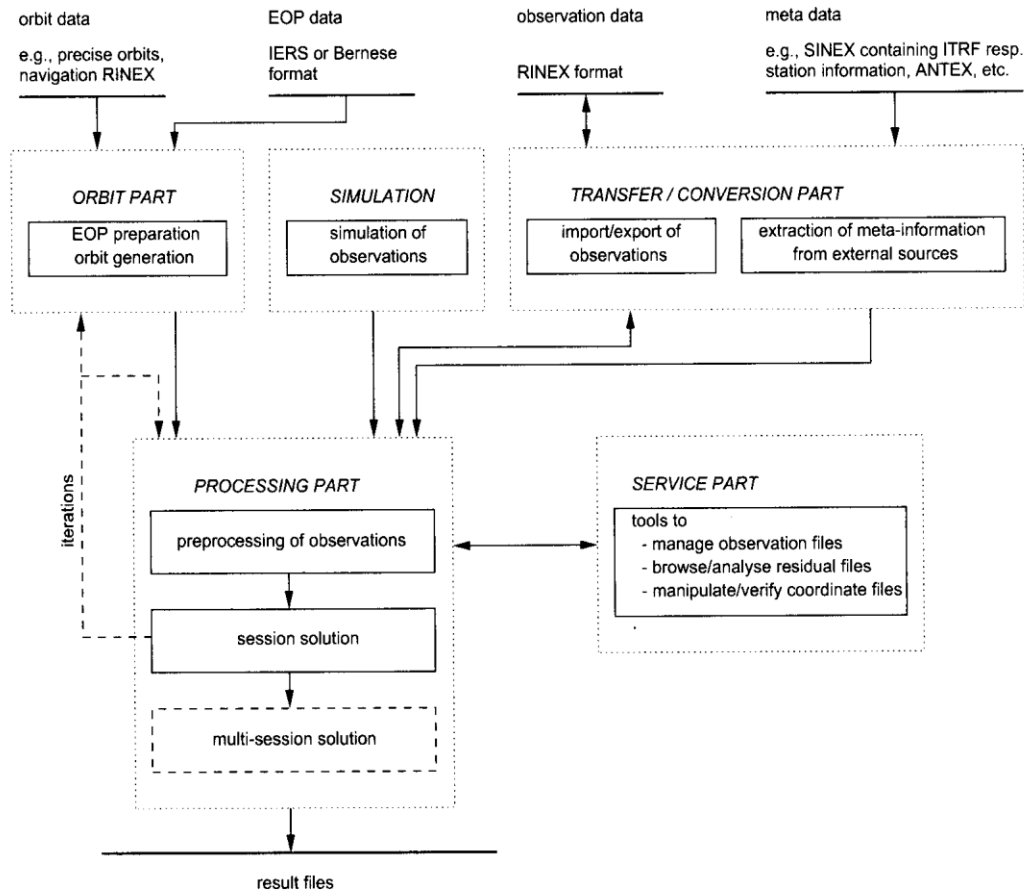
Figure 6.3 Functional flow diagram of standard processing in Bernese v5.0 GPS Software (Dach at al., [2007, pp. 7])

In Figure 6.3, the program inputs orbit data, EOP data and meta data and simulate them into Bernese processing format prior to their transfer to the Bernese processing engine. The processing part includes the code processing for the receiver and clock synchronization, phase pre-processing , parameter estimation based on GPS and/or GLONASS observations (program GPSEST) and on the superposition of normal equation systems (program ADDNEQ2). The final results are managed using the service part that consist of a collection of useful tools to edit/browse/manipulate binary data files, compare coordinate sets, display residuals, etc. Further details can be refereed from Dach at al. [2007, pp. 7 and pp.465-475]).

6.2.2 The pre-processing activities

The Bernese pre- processing activity includes the setting up of a new Bernese campaign as explained by Dach at al. [2007, pp. 43]. The new campaign will have nine subdirectories whereby seven of them require different data inputs to affect the processing and the results are stored into the remaining two directories as follows:

- ATM   - location of campaign specific atmosphere files (e.g., ION, TRP)
- BPE   - area for output from BPE runs
- OBS   - location of Bernese observation files

- ORB - location of orbit related files (orbit files, ERP-files, satellite clock files, DCB, etc.)

- ORX - original RINEX files

- OUT - output files

- RAW - RINEX files ready to import into the processing

- SOL - solution files (e.g., normal equations, SINEX)

- STA - campaign specific station files (STA, FIX, CRD, etc.), the campaign's session table (SES).

The input files are available in four different sites which are http://igscb.jpl.nasa.gov/components/dcnav/cddis_products_wwww.html (EOP and atmosphere files), ftp://ftp.unibe.ch/aiub/CODE (code differential files, IGS station information and FIX files), ftp://cddis.gsfc.nasa.gov/pub/gps/products/ (SP3 files) and http://sopac.ucsd.edu/pub/rinex (observation files). These files are zipped with files extension that are different from the ones used in the Bernese processing engine and the downloading process is cumbersome when working with more than two stations. Therefore, a matlab code (please refer appendix III) has been developed and used to easy the downloading procedure, unzipping the files and renaming them with Bernese extension format before copying them to the appropriate subdirectories that have created in the campaign creation.

6.2.3 The adopted Bernese V5.0 processing strategy

The Bernese processing engine is made up of five processing control files (BASTST.PCF, CLKDET.PCF, PPP.PCF, RNX2SNX.PCF and SUPERBPE.PCF) and each has a number of other programs embedded in it. Geodetic GPS processing requires the application of the PPP.PCF program for the approximate positioning and then after the RNX2SNX.PCF for the ambiguity resolution, final adjustment and the combination of the normal equations to provide the weekly solutions. They both have seventy two (72) programs embedded in them that have to be properly configured in appropriate processing strategies to meet the desired outputs. Table 6.1 summarizes the Bernese processing strategy adopted in this case study.

Table 6.8: The summary of the Bernese v5.0 processing strategy

1. Measurement models	
Basic observables	1) Carrier phase observations were used for processing. Code measurements used for receiver clock synchronization. 2) Elevation angle cutoff of 10 degrees. 3) Sampling rate of 180 seconds for 1-day solution.
Modeled observables	1) Double differences 2) Ionosphere-free linear combinations
RHC phase rotation correction	Phase polarization effects were applied.
Ground antenna	1) IGS absolute phase center corrections are applied to

phase centre calibration	model the differences between different antenna types.
Troposphere	1) Dry Niell was used as a prior model 2) Zenith delay every 2hrs for each daily solution 3) Wet Niell mapping function was used 4) Gradient tilting of 1 per session per site was adopted.
Ionosphere	1) Global ionosphere model used in ambiguity resolution 2) Ionosphere free combination used in final solution.
Tidal displacements	FES2004 model have been adopted
Satellite phase centre calibration	IGS phase centre corrections
2. Estimated parameters (a priori values and sigma)	
Adjustment	1) Weighted least squares 2) Outlier are being identified during preprocessing using criteria for L3 of 0.03 m. L3 is an abbreviation used to represent a quasi ionosphere free (QIF) linear combination frequency that are ambiguity free and 0.03m is the standard deviation. The Bernese v5.0 solves ambiguities using a narrow- lane approach. 3) Stations were constrained to the IGS precise orbits of the computation date based on ITRF05 frame.
Station coordinates	Constrained to IGS core sites coordinates which are constrained to the IGS weekly solution of date.

Orbital parameters	IGS final orbits were used

Troposphere	1) Zenith delay every 2hrs for each daily solution
	2) A priori sigma with respect to the applied model
	    ▪ First parameters ±5m absolute
	    ▪ Following parameters ±5m absolute
	Troposphere gradient (tilt of zenith) estimated for each
	    station.

Ionospheric corrections	1) Global ionosphere model used in ambiguity resolution 2) Ionosphere free combination used in final solution.
Ambiguity resolution strategy	Quasi Ionosphere Free (QIF) strategy was used to resolve ambiguities in baseline processing mode.
Clock bias	1) Satellite clock biases are eliminated by forming double-differences. Receiver clock corrections are estimated during the preprocessing using code measurements and later eliminated in phase processing by forming double differences.
Other parameters	1) The normal equations are later used in the weekly solution combination.
	3. Reference frame
	IGS05 through the use of IGS final orbits and constrained to Core sites (ALGO, DRAO, YELL, CHUR and SCH2).

6.3 Real time GPS positioning

Real time GPS positioning is the concept that deploys the use of real time differential corrections or observations in its application, through some sort of data link (internet, VHF radio, cellular telephone, satellite). Depending on the approach adopted the Real time GPS positioning can be refered to as Differential GPS (DGPS) or Real Time Kinematic (RTK). The basic concept under the DGPS positioning technique is that the position of the reference stations is accurately known and used to compute the transmit corrections to calibrate the fixed position. Under DGPS positing there exist a variety of different approaches such as the Wide area Augmentation System (WAAS) and Local Area Augmentation System (LAAS).

The Real Time Kinematics approach is more accurate than the DGPS approach as it can produce a positional fix of up to centimeter level using different ambiguity resolution approaches such as the wide-lane and the narrow.

However, for the purpose of this case study for real time positioning applications in Tanzania, much effort has been made to work with the Differential GPS position as it can be easily accommodated based on the present available communication infrastructure and the country economic position. The summary of the concept of real time positioning procedures is discussed in the following sections.

6.3.1 Differential GPS positioning (DGPS)

This is a real time differential positioning that utilize pseudorange differential corrections (pseudorange errors) for any GPS, GLONASS and future Galileo to achieve meter-level accuracy in its application. The DGPS corrections need to be refreshed every few seconds to keep up with atmospheric changes.

The underlying principle is such that, the position of each reference (base) station is accurately known, so that its measurements act as a calibration for other nearby receivers. The base station computes, formats, and transmits the pseudo range corrections (PRC) and the range rate of corrections (RRC) in RTCM-104 format through the data link to a roving unit. The DGPS positioning accuracy degrades as the distance between user and reference receivers increases, so for some applications, information from multiple reference stations is desirable.

6.3.1.1 The concept of DGPS using code ranges

The general mathematical principle underlying the differential GPS positioning, as illustrated by Hofmann et al. [2000, pp. 188-190], is such that, the code range $P_A^j(t_o)$ from the base station A to a satellite j at the initial epoch t_o can be expressed as follows:

$$P_A^j(t_o) = \rho_A^j(t_o) + \Delta\rho_A^j(t_o) + \Delta\rho^j(t_o) + \Delta\rho_A(t_o), \tag{6.26}$$

where:

- $\rho_A^j(t_o)$ is the geometric range

- $\Delta\rho_A^j(t_o)$ is the range biases depending on the terrestrial base position A and satellite position (such as radial errors, ionosphere and troposphere bias)

- $\Delta\rho^j(t_o)$ are satellite dependent bias such as satellite clock errors

- $\Delta\rho_A(t_o)$ are receiver dependent bias(receiver clock errors and multipath)

Since the geocentric coordinates of point A are known, the range to the satellite can be computed using:

$$P_A^j = \sqrt{\left((X_A - Xj(t_o))^2 + (Y_A - Yj(t_o))^2 + (Z_A - Zj(t_o))^2\right)}. \tag{6.27}$$

The observed range $P_A^j(t_o)$ can then be compared to evaluate the pseudorange correction $PRC^j(t_o)$ for satellite j at epoch-t_o:

$$PRC^j(t_o) = \rho_A^j(t_o) - P_A^j(t_o) = -\Delta\rho_A^j(t_o) - \Delta\rho^j(t_o) - \Delta\rho_A(t_o). \tag{6.28}$$

The time derivative of the corrections $RRC^j(t_o)$ can be determined as a function of time differences between the receiver station and the satellite j at the initial epoch t_o. The pseudorange correction PRC and the range rate correction RRC at the base station at the initial epoch are then transmitted in real time to the roving station B. The rover will compute the correction to be applied at epoch t *as* follows:

$$PRC^j(t) = PRC^j(t_o) + RRC^j(t_o) * (t - t_o) \quad . \tag{6.29}$$

When the time difference $\Delta t = t - t_o$ and the variation in the pseudorange correction are small, it implies that the accuracy of the real time positioning is high.

Adapting equation 6.26 to the roving station B we have the following relation:

$$P_B^j(t) = \rho_B^j(t) + \Delta\rho_B^j(t) + \Delta\rho^j(t) + \Delta\rho_B(t) \quad . \tag{6.30}$$

Applying the predicted corrections in $PRC^j(t)$ from equation (6.29) we have the corrected pseudo range at roving station B as follows:

$$P_B^j(t)_{corr} = P_B^j(t) + PRC^j(t) . \tag{6.31}$$

Substituting equations (6.27) and (6.29) in equation (6.31) we have:

$$P_B^j(t)_{corr} = P_B^j(t) + [\Delta\rho_B^j - \Delta\rho_A^j] + [\Delta\rho_B(t) - \Delta\rho_A(t)]. \tag{6.32}$$

Studies have revealed that error mitigation associated DGPS for moderate distances between the base and the rover changes slowly with time. Therefore, they are highly correlated both spatially and temporarily [Misra and Enge, 2006, pp. 49]. In that view, the influence of radial orbital errors and signal refraction are highly reduced and can be neglected; and equation (6.32) can be simplified to equation (6.33):

$$P_B^j(t)_{corr} = P_B^j(t) + \Delta\rho_A(t) - \Delta\rho_B(t) . \tag{6.33}$$

If the effect of multipath is also neglected, the differential correction becomes dependent on the receiver clocks bias as scaled to the range distances between the base and the rover as illustrated by Hofmann et al. [2000, pp. 188]:

$$\Delta\rho_{AB}(t) = c\delta_B(t) - c\delta_A(t) . \tag{6.34}$$

6.3.1.2 The concept of DGPS using phase ranges

With reference to Hofmann et al. [2000, pp. 188], it is possible to deploy the carrier phase measurements and compute the respective carrier phase pseudoranges and their respective correction in a similar approach as described in 6.3.1.1. That is the phase pseudo range from base station A to satellite j at the initial epoch t_0 can be modeled as follows:

$$\lambda \Phi_A^j(t_0) = \rho_A^j(t_0) + \Delta\rho_A^j(t_0) + \Delta\rho^j(t_0) + \Delta\rho_A(t_0) + \lambda N_A^j \ , \qquad (6.35)$$

where:

- $\lambda \Phi_A^j(t_0)$ is the phase pseudorange at the reference station epoch t_0

- $\rho_A^j(t_o)$ is the geometric range

- $\Delta\rho_A^j(t_o)$ is the range biases depending on the terrestrial base position A and satellite position (such as radial errors, ionosphere and troposphere biases)

- $\Delta\rho^j(t_o)$ represent satellite dependent biases such as satellite clock errors

- $\Delta\rho_A(t_o)$ represents receiver dependent biases such as clock errors and multipath

- N_A^j is the phase ambiguity

Similar to equation (6.29) above, the phase correction at the reference epoch t_0 can be given as follows:

$$PRC^j(t_0) = \rho_A^j(t_0) - \lambda\Phi_A^j(t_0)$$

$$= -\Delta\rho_A^j(t_0) - \Delta\rho^j(t_0) - \Delta\rho_A(t_0) - \lambda N_A^j \quad . \tag{6.36}$$

In analogy to equation (6.33), the predicted phase range correction at station B is:

$$\lambda\Phi_B^j(t)_{corr} = \rho_B^j(t) + \Delta\rho_{AB}(t) + \lambda N_{AB}^j \tag{6.37}$$

In equation 6.27 above, $\Delta\rho_{AB}(t) = \Delta\rho_A(t) - \Delta\rho_B(t)$ and $N_{AB}^j = N_B^j - N_A^j$ is the single difference of the phase ambiguities. If multipath is neglected, the pseudo phase range corrections are converted to a combined clock bias. That is:

$$\Delta\rho_{AB}(t) = c\delta_{AB}(t) = c\delta_B(t) - c\delta_A(t) \quad . \tag{6.38}$$

6.3.2 Real Time Kinematics positioning (RTK)

This is a real time differential GPS positioning that utilizes carrier-phase measurements to achieve a millimeter level positional accuracy. In practice, RTK systems use a single base station receiver at a known reference station and a number of mobile units at new points to be fixed. The basic principle is such that, the base station re-broadcasts the phase of the carrier that has measured along with its position to the mobile units also referred to as rovers via a communication link such as radio or internet. The rover receivers process the received phase along with their own phase measurements and compute their relative position to millimeters accuracy.

In principle, the carrier-phase observable is the total number of full carrier cycles and fractional cycles between the satellite antenna and the GPS receivers at any instant (Langley [1998, pp.71]). Position estimation with carrier phase GPS positioning is done through measuring the fractional cycles and track its changes while estimating the unknown integer number of complete cycles (also known as ambiguity) along with other unknowns (receiver coordinates). When the processing software can only estimate the ambiguity as real values (floating point numbers) the resulting solution is called a float-solution with a positional accuracy of up to 1 meter depending on how long the rover has been tracking the GPS signals. For more accurate applications, double and triple difference approaches are used to minimize the satellite and receiver clock errors and then process using least square filters of some kind to estimate the relative receiver position more accurately.

6.3.3 Real time positioning case study

A case study for DGPS positioning has been done using the NTRIP data protocol, though the initial intention was to test the application with UDP data protocol as provided by the RTIGS service that is meant for public use (see section 5.2 for details). This is due to the fact that, the RTIGS is still under development and the pilot study has fallen behind schedule. To facilitate access of real time GNSS data and products, the NTRIP service has developed/provided a separate caster (Figure 6.4) to broadcast data streams from the GNSS network.
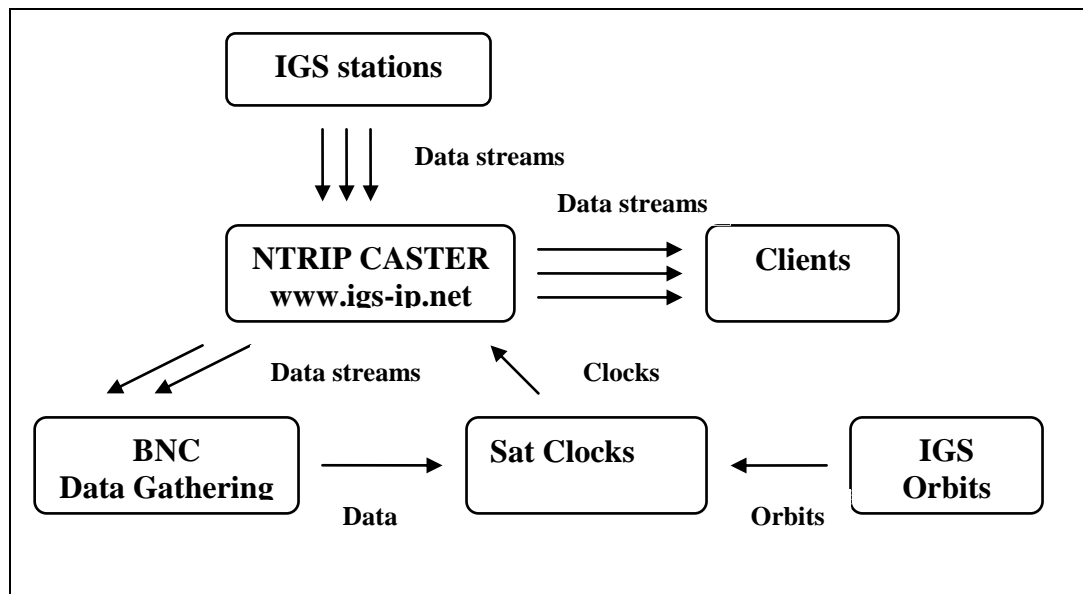
Figure 6.4 RT- IGS data flow via NTRIP (http://igs.bkg.bund.de/index_ntrip.htm)

In Figure 6.4, GNSS data is collected from the IGS stations and sent processing to the BKG NTRIP Client (BNC) data gathering centre for processing via

the IGS-NRIP Caster using the internet protocol. The processed data is refined with satellite clock corrections using predicted the IGS orbits to refine the DGPS corrections which are sent back to the IGS-NTRIP Caster to allow different users have access to the corrected data streams for different applications.

The overall procedure that has been adopted for the implementation of the real time positioning case study is explained in next sections.

6.3.3.1 Installation of GNSS internet radio

GNSS Internet Radio has to be installed to establish real time data communications between the reference station and the case study area. GNSS Internet Radio has been developed by the IGS in collaboration with the BKG for retrieving GNSS data streams from any NTRIP supporting broadcaster. It can be installed and accessed through personal computers, laptop, PDA, GPS receiver or a mobile phone depending on the user requirements. The GNSS radio is available in different versions to suit different application systems in handling the HTTP communication and transfer of the received GNSS data to a serial or IP port feeding networking software or a DGPS/RTK application. In the data collection GNSS internet radio version 1.4.11 was used and its main interface is shown in Figure 6.5.
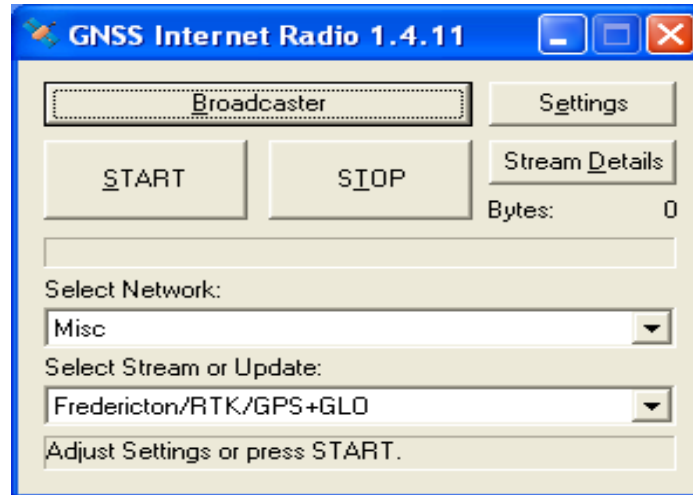
Figure 6.5 GNSS internet radio version 1.4.11 main menu

6.3.3.2 Installation of the receiver communication software

The second step in the implementation of the case study is to establish the receiver and computer communication and there are different ways of doing it depending on which type of the GNSS receiver is being used. The Novatel receiver families like the ProPak-V3 available at UNB use the Command Display Utility software (Figure 6.6) that has to be installed and then after extract, install and configure the USB drivers. Recommended settings are 38400/57600 for the baud rate with the handshaking option disabled and they have to be saved if the system has to remember the configuration.

Figure 6.6 CDU-the receiver computer communication software display

When working with the Trimble family receivers such as the Trimble R7 or 5700 that have been used in the case study, one needs to establish communication using two different software. The first software is the Trimble GPS Configurator software (Figure 6.7) for configuring the receiver and computer communication and type of the data to be collected.
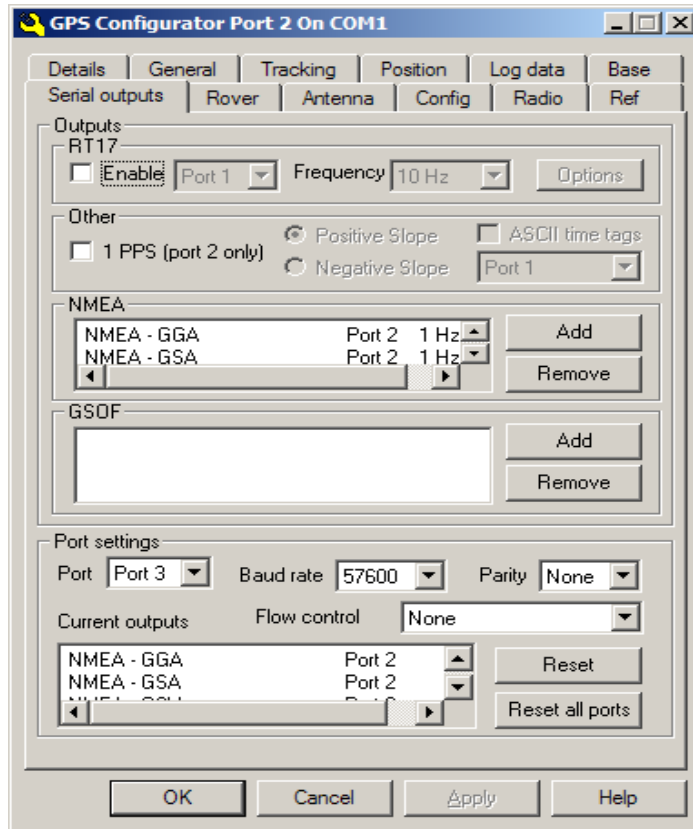
Figure 6.7 Display of the GPS Configurator software main menu

With proper configuration one can possibly view the position as illustrated in

Figure 6.8 but cannot record the information for further processing.
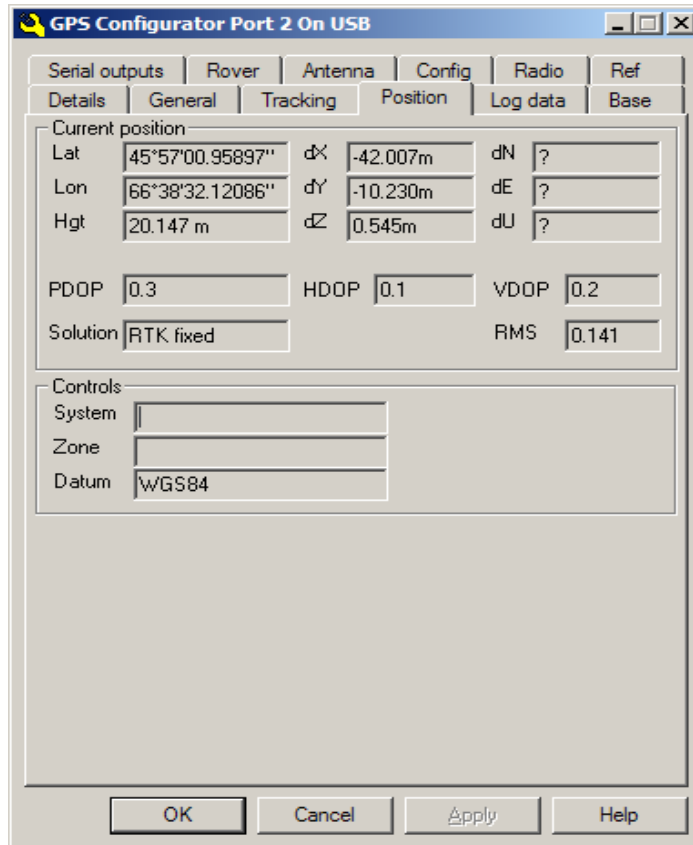
Figure 6.8 Display of the position fix with GPS Configurator software

To facilitate the data recording, the DGPS listener communication software (Figure 6.9) has to be installed and linked to the computer with the GPS configurator disabled before being initialized. As with the CDU, the DGPS listener needs to be well configured and the appropriate baud rate is either 38400 or 57600.

6.3.3.3 Real time data collection

A reference point was fixed on top of Gillin Hall at the University of New Brunswick by collecting data for 6 hours and then after post processed using the Way Point incorporated software Graf-Nav as fixed from UNB3 (processing results are in appendix V). Having known the position of the point to be used for the case study evaluations, communication between the computer and the GPS receiver was established via communication port 2. The reference point was then fixed by DGPS positioning using points from the Cancel Network for position fix evaluation.
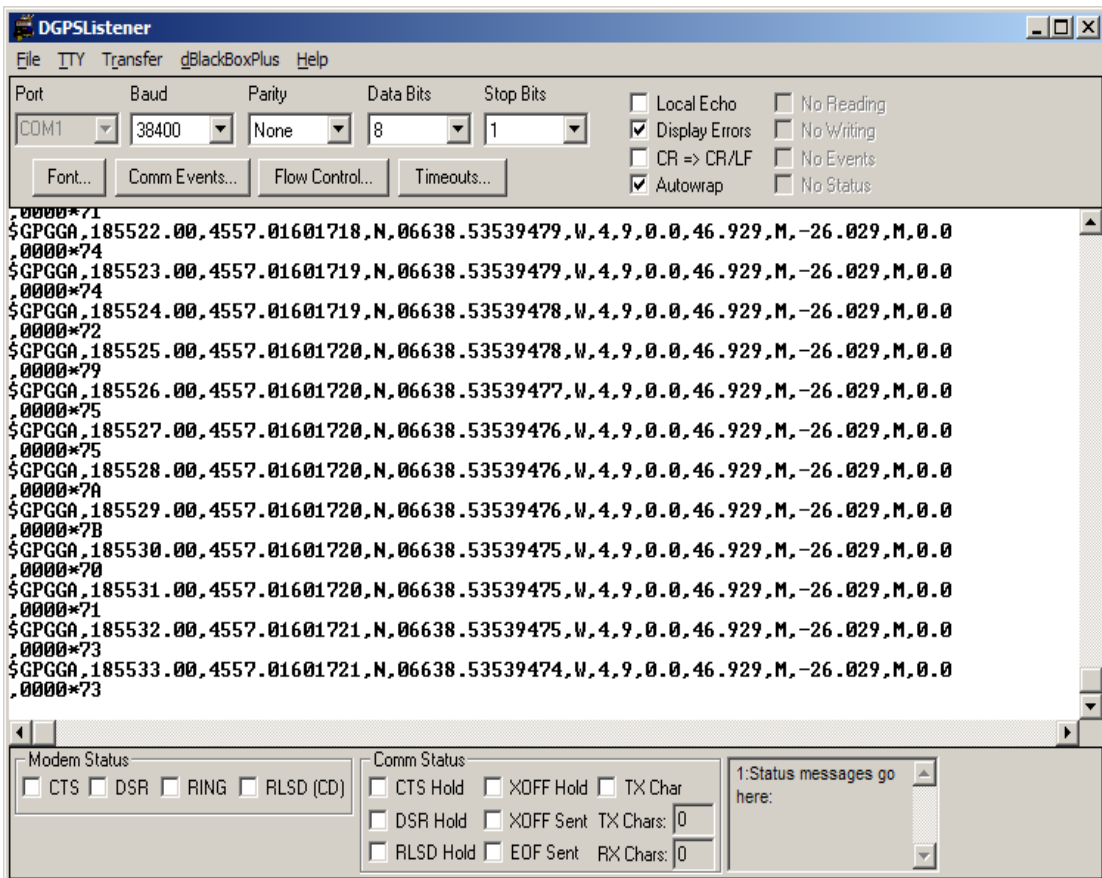
Figure 6.9 DGPS listener-the receiver computer

7. RESULTS AND ANALYSIS

This chapter gives the results of different case studies and their respective assessment and the concluding remarks as discussed in three different sections. Section one contains the results of the covariance analysis in terms of plots of the error ellipses of the adjusted network points. Error ellipses provide a graphical means of viewing the results of a network adjustment in terms of orientation and scale. Section two gives the results and analysis of the reference frame maintenance from the Bernese software v5.0. Section three gives the results and the assessment of the case study of real time GPS positioning using the differential.

7.1 Results and assessment of the covariance analysis case study

With reference to the discussions in section 6.1.1, GPS observations were simulated for different epochs of 8 February, 2008 and then adjusted to produce the final coordinates, the covariance matrices and the parameters of the respective error ellipses. Error ellipses are derived from the covariance matrix and the results of the three different scenarios of the adjusted networks and the error ellipses and their assessment are as follows:

7.1.1 Results of the covariance analysis TZRF10 scenario 1

TZRF10 Scenario 1 consists of ten permanent stations with point MCS as the reference station. It is on top of the Surveys and Mapping headquarters.
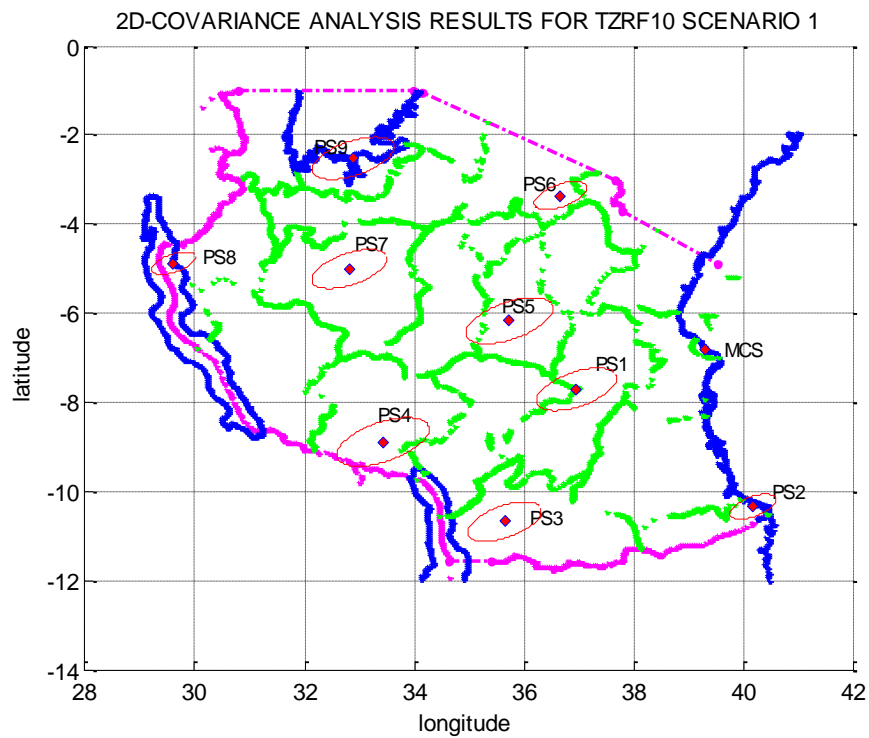
Figure 7.1 Standard ellipses at 95 % confidence level for TZR10 Scenario 1

Table 7.1 -The error ellipse parameters for TZR10 Scenario 1

Station	Semi axes (m)		Orientation		
ID	major	minor	degrees	minutes	seconds
PS1	0.7855	0.3791	25	11	58.42
PS2	0.4492	0.2191	26	5	51.50
PS3	0.7304	0.3508	25	0	15.07
PS4	0.9082	0.4328	24	23	37.85
PS5	0.8524	0.4097	24	50	35.09
PS6	0.5183	0.2499	24	58	51.55
PS7	0.7333	0.3488	24	5	45.72
PS8	0.4307	0.2024	23	20	14.93
PS9	0.7955	0.3784	24	1	58.38

Table 7.2- The final adjusted coordinates of TZRF10 Scenario 1

STN	Coordinate difference (m)			Final coordinates		
ID	DX	DY	DZ	X (m)	Y(m)	Z(m)
MCS	Reference station			4901315.404	4011134.984	-751902.559
PS1	0.089	1.213	0.635	5050948.956	3800636.229	-850047.126
PS2	0.219	0.518	0.356	4794390.931	4048946.229	-1137193.907
PS3	1.776	2.920	0.160	5094578.684	3654090.562	-1174460.852
PS4	1.582	4.135	0.237	5260861.295	3472855.555	-979416.010
PS5	2.604	2.773	0.229	5148120.718	3704753.498	-681075.476
PS6	1.341	0.672	0.173	5108008.724	3803233.169	-371387.912
PS7	1.422	2.102	0.236	5340706.717	3444490.917	-553390.603
PS8	0.132	0.943	0.211	5525900.857	3140425.280	-539028.392
PS9	0.390	0.260	0.692	5351828.378	3460927.691	-278620.516

Table 7.3- Statistical results for TZRF10 Scenario 1

STN ID	Standard Deviations (m)			Variance factors		
	X_STD	Y_STD	Z_STD	A-posteriori	Lower-bound	Upper-bound
MCS	0.05	0.05	0.08	Reference station		
PS1	1.082	1.645	0.352	2.8737	1.3598	9.5789
PS2	1.095	1.629	0.346	0.9496	0.4493	3.1654
PS3	1.086	1.662	0.348	2.4393	1.1542	8.1309
PS4	1.078	1.676	0.352	3.7346	1.7671	12.4485
PS5	1.076	1.652	0.355	3.3705	1.5949	11.2349
PS6	1.073	1.640	0.359	1.2618	0.5971	4.2060
PS7	1.069	1.674	0.359	2.4484	1.1585	8.1613
PS8	1.065	1.702	0.361	0.8227	0.3893	2.7423
PS9	1.065	1.670	0.363	2.8963	1.3705	9.6543

In the preceding Tables 7.2 and 7.3, DX, DY and DZ are the respective final differences in X, Y and Z between the approximate positions and the least square estimates with X_STD, Y_STD and Z_STD as the respective standard deviations.

7.1.2 Results of the covariance analysis TZRF10 Scenario 2

Figure 7.2, provides the results of the case study TZRF10 Scenario 2 with seven permanent stations. The simulated reference station is point PS5 that is on the top of the of regional government headquarters in central region of Dodoma.
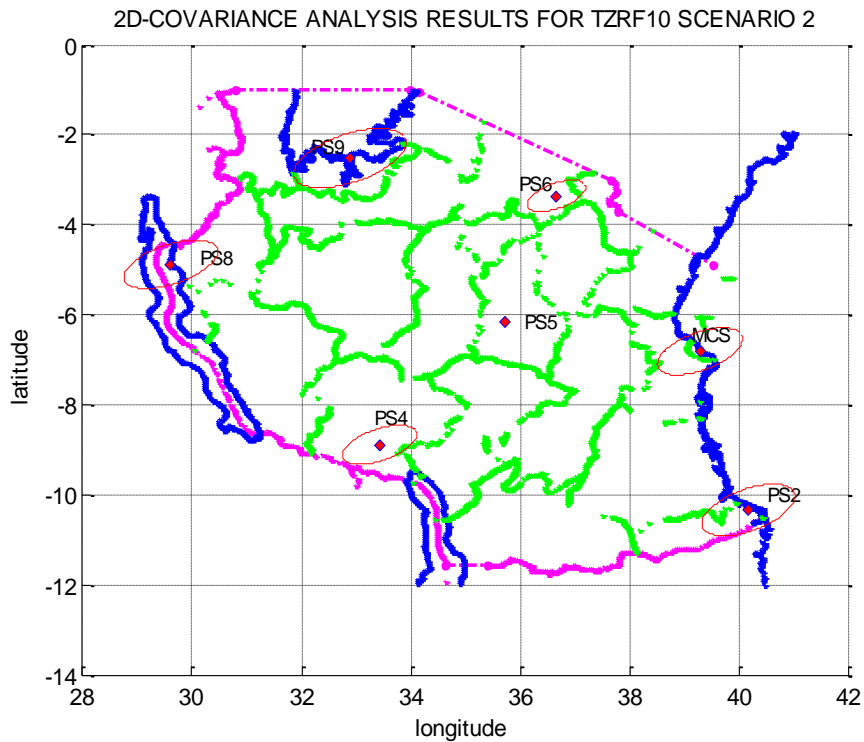
Figure 7.2 Standard ellipses at 95 % confidence level for TZR10 Scenario 2

Table 7.4- The error ellipse parameters for TZR10 Scenario 2

Station ID	Semi axes (m)		Orientation		
	major	minor	degrees	minutes	seconds
MCS	0.8439	0.4107	25	44	49.56
PS2	0.9253	0.4514	26	5	53.24
PS4	0.7283	0.3471	24	23	39.47
PS6	0.5714	0.2756	24	58	53.15
PS8	0.9182	0.4316	23	20	16.45
PS9	1.1036	0.5249	24	1	59.91

Table 7.5-The final adjusted coordinates of TZRF10 Scenario 2

STN ID	Coordinate Difference (m)			Final coordinates		
	DX	DY	DZ	X(m)	Y(m)	Z(m)
PS5	Reference station			5148118.114	3704750.725	-681075.247
MCS	2.633	2.709	0.222	4901312.771	4011132.275	-751902.337
PS2	2.870	2.186	0.534	4794388.280	4048943.525	-1137193.729
PS4	1.013	1.311	0.042	5260858.700	3472852.730	-979415.815
PS6	1.266	2.078	0.093	5108006.117	3803230.419	-371387.646
PS8	2.432	1.952	0.034	5525898.293	3140422.386	-539028.146
PS9	2.190	3.083	0.416	5351825.798	3460924.868	-278620.241

Table 7.6- Statistical results for TZRF10 Scenario 2

STN	Standard Deviations (m)			Variance factors		
ID	X_STD	Y_STD	Z_STD	A-posteriori	Lower-bound	Upper-bound
PS5	0.050	0.050	0.080	Reference station		
MCS	1.085	1.627	0.352	3.3736	1.5963	11.2453
PS2	1.095	1.629	0.346	4.0291	1.9065	13.4303
PS4	1.078	1.676	0.352	2.4017	1.1365	8.0057
PS6	1.073	1.640	0.359	1.5338	0.7258	5.1127
PS8	1.065	1.702	0.361	3.7392	1.7694	12.4642
PS9	1.065	1.670	0.363	5.5739	2.6375	18.5798

In the preceding Tables 7.5 and 7.6, DX, DY and DZ are the respective final differences in X, Y and Z between the approximate positions and the least square estimates with X_STD, Y_STD and Z_STD as the respective standard deviations.

7.1.3 Results of the covariance analysis TZRF10 Scenario 3

Figure 7.3, provides the results of the case TZRF10 Scenario 3 with four permanent stations. The simulated reference station is point PS9 that on top of the of regional government headquarters in north western region of Mwanza.
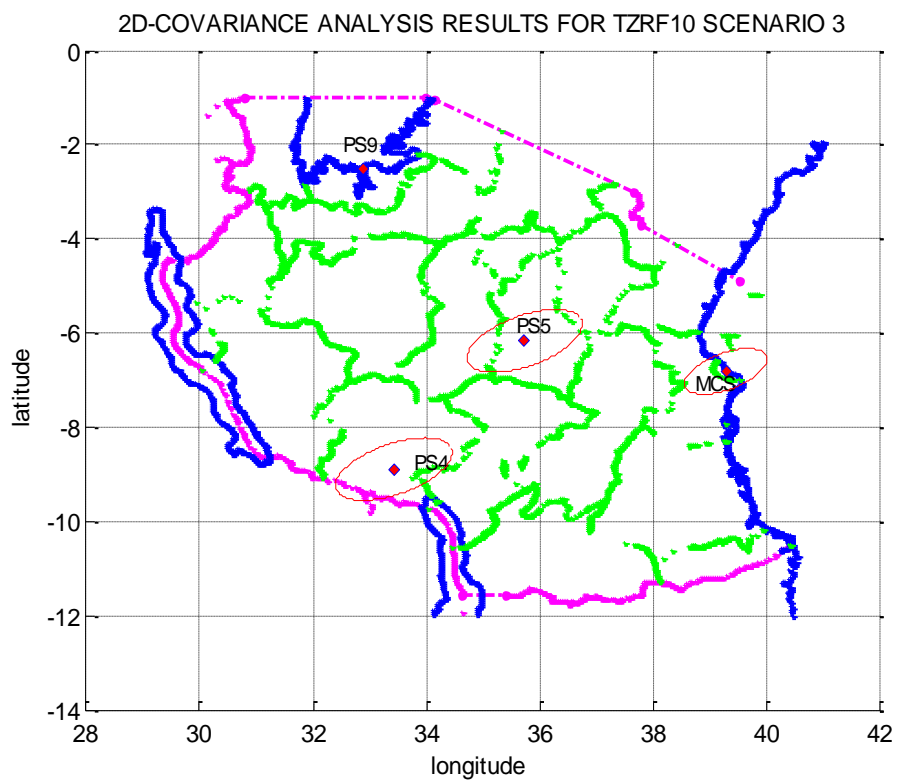
Figure 7.3 Standard ellipses at 95 % confidence level for TZR10 Scenario 3

Table 7.7- The error ellipse parameters for TZR10 Scenario 3

Station	Semi axes (m)		Orientation		
ID	major	minor	degrees	minutes	seconds
PS5	1.095	0.526	24	50	37.94
MCS	0.785	0.382	25	44	50.88
PS4	1.105	0.527	24	23	40.91

Table 7.8-The final adjusted coordinates of TZRF10 Scenario 3

STN	Station Coordinates (m)			Adjusted coordinates		
ID	DX	DY	DZ	X(m)	Y(m)	Z(m)
PS9	0.000	0.000	0.000	5351827.988	3460927.951	-278619.824
PS5	2.19	3.008	0.465	5148120.304	3704753.733	-681074.782
MCS	0.425	0.235	0.693	4901314.979	4011135.219	-751901.865
PS4	1.159	4.346	0.461	5260860.872	3472855.766	-979415.312

Table 7.9- Statistical results for TZRF10 Scenario 3

STN ID	Standard Deviations			Variance factors		
	X_STD	Y_STD	Z_STD	A-posteriori	Lower-bound	Upper-bound
PS9	0.050	0.050	0.080	Reference station		
PS5	1.076	1.652	0.355	5.5637	2.6327	18.5456
MCS	1.085	1.627	0.352	2.9205	1.3820	9.7351
PS4	1.078	1.676	0.352	5.5278	2.6157	18.4262

In the preceding Tables 7.8 and 7.9, DX, DY and DZ are the respective final differences in X, Y and Z between the approximate positions and the least square estimates with X_STD, Y_STD and Z_STD as the respective standard deviations.

7.1.4 Assessment of the covariance analysis case study

The assessment of the covariance analysis case study is based on three different criterions which are standard error ellipses, the network strength and standard deviations of the adjusted points as follows:

7.1.4.1 Standard error ellipses

With reference to illustration by Santos [2007], the standard error ellipses show the trace of standard errors in all directions using the parameters of the absolute error ellipses at that particular point. They show the region, if centered at the true point position, where the least squares estimate falls with respect to a required confidence region as well as the datum strength and weakness in orientation and scale of the adjusted points using the respective directions of the minor axes major axes towards the datum point. This is due to the fact that, the error ellipse parameters have the correlation between the positioning parameters unlike the pedal curves which are constructed from the locus of the end points of the standard deviations.

However, the error ellipse constructed from the standard deviations of the two dimensional quantities and the correlations between these two quantities (also known as 1-sigma" ellipse) contains only 39.4% of the position results. Therefore, the error ellipse's axes are generally inflated by an appropriate factor to create the standard

absolute error ellipse at a required confidence region such as 68.27 percent (1 sigma), 95.45 percent (2 sigma) and 99.73 percent (3sigma). In this case study, the standard absolute error ellipses of the adjusted points of the proposed networks were created using the multiplicative factors determined from the χ^2 distribution using the 95% confidence limits. The χ^2 distribution has been used because the a-priori variance factors are known from the computed covariance matrices and the resulting error ellipses were assessed as a basis of network selection.

In TZRF Scenario 1, furthest points PS3 (1,000km from datum point MCS), PS8 (1,200km from datum point MCS) and PS9 (1,200km from datum point MCS) have relatively smaller standard error ellipses as compared to such points in other networks. That is points PS2 (700km from datum point PS5), PS8 (800km from datum point PS5) and PS8 (800km from datum point PS5) in the TZRF10 scenario 2 and points PS4 (800km from datum point PS9) and MCS (1,200km from datum point PS9) in the TZRF10 scenario 3. Therefore, TZRF10 scenario 1 produced better results as compared to other networks in that perspective.

7.1.4.2 Strength of the proposed networks

The second assessment criteria is the network strength in terms of orientation (minor axes pointing to the datum point) and scale weakness (major axes pointing to the datum point). Regarding this assessment criteria, the adjusted results in all networks show no significant weakness in orientation and scale weakness and therefore they are comparatively similar in that perspective.

7.1.3.3 Standard deviations

The respective standard deviation in x, y, and z gives a guide to the precision of the least square approximation. With respect to this assessment criteria, the respective standard deviation in x, y, and z seems to have more or less the same precision in all points which are approximately 1.1m, 1.65m and 0.35m for each of the network scenario. This is due to the fact that, the same points has been used and the adjustment and has based on the same set of satellites on the same observation period resulting into more or less the same design matrix. Therefore, similar standard deviations should be expected and they are capable of producing reasonable results in any of the proposed network.

7.1.5 The proposed network

In view of the above observations, the TZRF scenario 1 would be preferred for the following reasons:

1)   It produces more accurate results at the network peripherals as compared to the other two networks.

2)   The present real time approach based on DGPS positioning approach and real time kinematics is based on the baseline length between the datum point and the fixed points. This network provides wide country coverage and thus more and extended applications are possible.

7.2 Results and analysis of the frame maintenance case study

This section presents the results and assessment of the modern reference frame maintenance case study as discussed in the following subsections.

7.2.1 Frame maintenance results

The most important results relevant to my frame maintenance case study are the weekly processing summary and the final coordinates and they are discussed in the following subsections.

7.2.1.1 The week processing summary

This is a weekly summary of the processed sessions comprising of a list of all processed stations for each day of the week and the root mean square error of the coordinate repeatability. Abbreviation "A" refers to the processed points whereas abbreviation "W" stands for the reference (control) station. A blank corresponds to no processing information on that day as illustrated in Table 7.10 through Tables 7.11a.

Table 7.10 List of processed stations GPS week 1368-1

NO.	STATION	FIL	GPS WEEK DAYS							Repeatability(mm)		
			0	1	2	3	4	5	6	N	E	U
1	ALBH 40129M003	7	A	A	A	A	A	A	A	0.9	1.2	4.5
2	ALGO 40104M002	7	W	W	W	W	W	W	W	1.4	0.7	3.4
3	ALRT 40162M001	7	A	A	A	A	A	A	A	1.2	0.8	3.1
4	AMC2 40472S004	7	A	A	A	A	A	A	A	0.9	0.8	3.2
5	BAIE 40151M001	7	A	A	A	A	A	A	A	1.3	0.7	3.5
6	BAKE 40152M001	7	A	A	A	A	A	A	A	1.1	0.4	2.9
7	BARH 49927S001	6	A	A	A	A		A	A	1.6	0.4	5.1
8	CAGS 40147M001	7	A	A	A	A	A	A	A	1.4	0.8	4.7
9	CHUR 40128M002	7	W	W	W	W	W	W	W	1.4	0.5	2.8
10	CHWK 40142M001	7	A	A	A	A	A	A	A	0.5	1.6	4.7
11	DRAO 40105M002	7	W	W	W	W	W	W	W	0.6	1.3	3.3
12	DUBO 40137M001	7	A	A	A	A	A	A	A	1.6	0.6	3.0
13	ESCU 40168M001	4				A	A	A	A	3.4	0.6	3.8
14	FLIN 40135M001	7	A	A	A	A	A	A	A	1.5	0.8	5.2
15	FRDN 40146M001	7	A	A	A	A	A	A	A	1.6	0.8	4.5
16	HLFX 40120M001	7	A	A	A	A	A	A	A	1.1	0.8	3.7
17	HOLB 40130M001	7	A	A	A	A	A	A	A	0.8	1.4	6.3
18	HOLM 40148M001	7	A	A	A	A	A	A	A	1.0	0.7	2.7

Table 7.11 List of processed stations GPS week 1368-2

NO.	STATION	FIL	GPS WEEK DAYS							Repeatability(mm)		
			0	1	2	3	4	5	6	N	E	U
19	KUUJ 40154M001	6		A	A	A	A	A	A	0.6	1.3	3.3
20	INVK 40150M001	7	A	A	A	A	A	A	A	1.4	1.0	2.7
21	LPOC 40170M001	7	A	A	A	A	A	A	A	1.1	0.8	3.9
22	NAIN 40164M001	7	A	A	A	A	A	A	A	1.1	0.6	2.8
23	NANO 40138M001	7	A	A	A	A	A	A	A	0.7	1.3	4.9
24	NLIB 40465M001	7	A	A	A	A	A	A	A	1.8	0.8	3.2
25	NRC1 40114M001	7	A	A	A	A	A	A	A	1.5	0.7	4.9
26	PICL 40155M001	7	A	A	A	A	A	A	A	0.9	0.8	4.4
27	PRDS 40124M001	7	A	A	A	A	A	A	A	0.9	1.4	5.3
28	QAQ1 43007M001	7	A	A	A	A	A	A	A	0.7	0.7	2.2
29	QIKI 40166M001	7	A	A	A	A	A	A	A	0.9	1.1	4.0
30	RESO 40149M001	7	A	A	A	A	A	A	A	2.9	1.2	3.9
31	SASK 40167M001	7	A	A	A	A	A	A	A	0.8	1.0	3.5
32	SCH2 40133M002	7	W	W	W	W	W	W	W	0.8	1.0	2.7
33	STJO 40101M001	7	A	A	A	A	A	A	A	2.1	2.9	7.7
34	THU3 43001M002	7	A	A	A	A	A	A	A	0.9	0.8	2.5
35	TUKT 40165M001	7	A	A	A	A	A	A	A	0.5	1.6	2.5
36	UCLU 40140M001	7	A	A	A	A	A	A	A	1.1	1.6	3.2

Table 7.11a List of processed stations GPS week 1368-3

NO.	STATION	FIL	GPS WEEK DAYS							Repeatability		
			0	1	2	3	4	5	6	N	E	U
37	USNO 40451S003	7	A	A	A	A	A	A	A	1.3	1.5	7.1
38	VALD 40156M001	7	A	A	A	A	A	A	A	1.4	0.7	3.7
39	WES2 40440S020	7	A	A	A	A	A	A	A	1.7	0.9	5.1
40	WHIT 40136M001	7	A	A	A	A	A	A	A	0.8	2.5	3.8
41	WILL 40134M001	7	A	A	A	A	A	A	A	0.6	1.4	4.8
42	WSLR 40141M001	7	A	A	A	A	A	A	A	0.6	1.5	3.7
43	YELL 40127M003	7	W	W	W	W	W	W	W	0.5	0.7	1.8

7.2.1.2 The processed in station coordinates

The second deliverable in the reference frame maintenance case study is the station coordinates and they are based on ITRF 05 as local geodetic datum. These are produced in SINEX format for each of the computation session (day). The daily solutions are then used to compute the weekly coordinate summary as provided in Table 7.13 through Table 7.15.

Table 7.13 -Weekly coordinate summary for GPS WEEK 1368-1

STATION NAME	X (M)	Y (M)	Z (M)
ALBH 40129M003	-2341332.9447	-3539049.4907	4745791.2852
ALGO 40104M002	918129.3755	-4346071.2385	4561977.8127
ALRT 40162M001	388042.6954	-740382.3715	6302001.8694
AMC2 40472S004	-1248596.1924	-4819428.1976	3976505.9572
BAIE 40151M001	1546823.3030	-3879765.1145	4804185.0252
BAKE 40152M001	-289833.9912	-2756501.0473	5725162.2272
BARH 49927S001	1693644.8458	-4239067.5434	4439567.1986
CAGS 40147M001	1096349.0554	-4335060.5823	4533255.1573
CHUR 40128M002	-236438.8556	-3307616.8301	5430049.2033
CHWK 40142M001	-2215259.8245	-3543996.8132	4802098.6866
DRAO 40105M002	-2059164.8022	-3621108.3758	4814432.2904
DUBO 40137M001	-417603.6875	-4064529.7763	4881432.1184
ESCU 40168M001	1852954.5308	-3937498.7380	4647314.6165
FLIN 40135M001	-766174.5605	-3611375.3018	5184056.1858
FRDN 40146M001	1760542.7624	-4080067.9622	4560178.5232
HLFX 40120M001	2018905.7783	-4069070.4772	4462415.3810
HOLB 40130M001	-2503040.5109	-3188233.2896	4908701.4495
HOLM 40148M001	-983071.9956	-1867623.6338	5998639.5211

Table 7.14 -Weekly coordinate summary for GPS WEEK 1368-2

STATION NAME	X (M)	Y (M)	Z (M)
INVK 40150M001	-1628432.1154	-1714393.0313	5903844.6598
KUUJ 40154M001	772857.5382	-3558198.7038	5219095.8737
LPOC 40170M001	1480313.1595	-4069017.6023	4667642.4853
NAIN 40164M001	1671836.6454	-3103473.2733	5297671.1790
NANO 40138M001	-2335726.8038	-3451608.3109	4812009.9083
NLIB 40465M001	-130934.6009	-4762291.7045	4226854.6156
NRC1 40114M001	1112777.1980	-4341475.8237	4522955.7738
PICL 40155M001	-11253.0652	-3980586.6730	4967210.2121
PRDS 40124M001	-1659602.9791	-3676725.7562	4925493.5024
QAQ1 43007M001	2170942.0982	-2251829.9392	5539988.3026
QIKI 40166M001	1069081.2724	-2195214.1711	5872518.9823
RESO 40149M001	-144107.5879	-1683119.7779	6129763.2559
SASK 40167M001	-1106129.6899	-3758704.8566	5016675.4623
SCH2 40133M002	1448636.7774	-3385243.6820	5191047.0097
STJO 40101M001	2612631.0930	-3426807.0119	4686757.8404
THU3 43001M002	538093.5438	-1389088.0253	6180979.2178
TUKT 40165M001	-1532091.3464	-1643291.6777	5949315.9185
UCLU 40140M001	-2440669.0651	-3416437.0546	4785136.7956
USNO 40451S003	1112189.7720	-4842954.9981	3985352.2227

Table 7.15 -Weekly coordinate summary for GPS WEEK 1368-3

STATION NAME	X (M)	Y (M)	Z (M)
VALD 40156M001	919075.8068	-4167766.2249	4724323.5031
WES2 40440S020	1492233.2489	-4458089.4622	4296045.9925
WHIT 40136M001	-2218337.9437	-2201205.0952	5543057.4993
WILL 40134M001	-2084258.1441	-3313872.9730	5019853.0140
WSLR 40141M001	-2227013.7083	-3439649.0830	4872522.1374
YELL 40127M003	-1224452.6648	-2689216.1199	5633638.2398

7.2.1.3 Computation of reference frame coordinates- NAD83 (CSRS)

The coordinates values presented in section 7.2.1.2 refers to the mid epoch of GPS week 1368, which is day 88.5 of the year 2006 (29 March 2006). These coordinates need to be reduced to the reference frame − NAD83 (CSRS) using the mathematical model provided in equation 5.1 in section 5.2. In those equations the time difference $\Delta t = t - t_o$ corresponds to the number of days between epoch 88.5 of 2006 and epoch 0 of 1997 at which the reference frame is defined.

7.2.2 Assessment of the reference frames maintenance results

The assessment of this case study is based on the baseline consistency, the RMS (mm) of the coordinate's repeatability and the difference between the computed and the published coordinate as provided in the following subsections.

7.2.2.1 Comparison of Baseline Differences

With reference to Dach at al. [2007, pp 113-115], the Bernese GPS Software uses double-differences as basic observables in the computation procedures. The double-differences for both phase and code measurements are created using the programs GPSEST and SNGDIF by adopting the maximum observation strategy and then stored in files for further processing computations and ambiguity resolution. For that reason, the predefined baselines have been assessed for consistency by comparing the baseline length between different permanent stations using the case study computed solutions and the NAREF published solutions.

With reference to the illustration on Figure 7.4, most of the differences in the baseline lengths between the NAREF solutions and the weekly computed solutions are showing a close agreement. 75.2 percent of them are less than 6 mm, 20 percent are between 6 and 10 mm and the remaining 4.5 percent are within 10 mm.
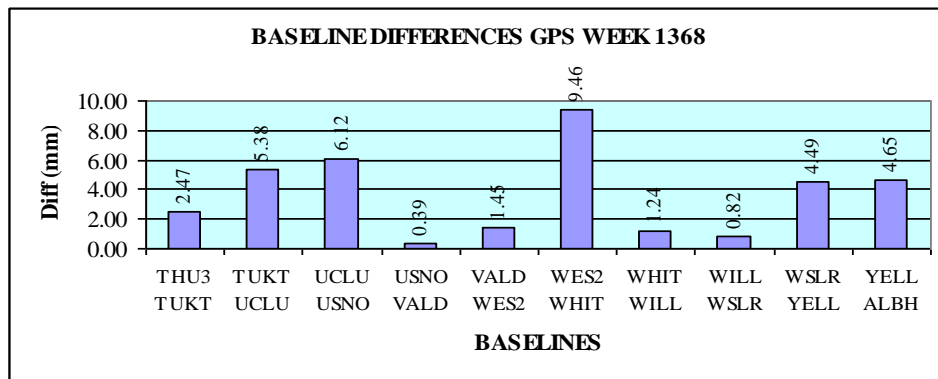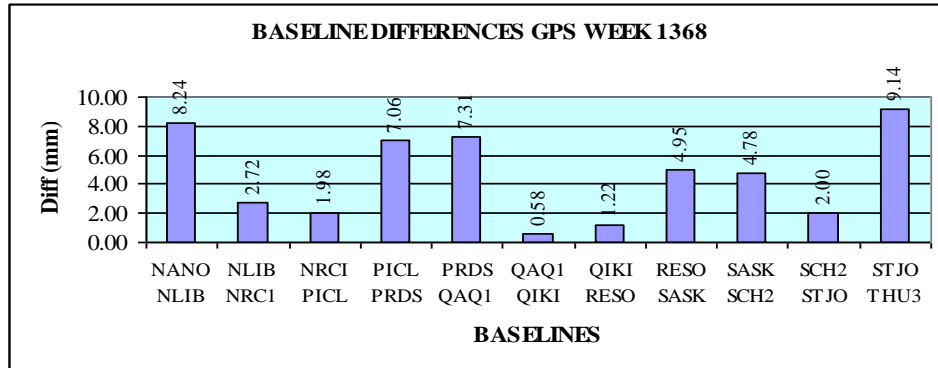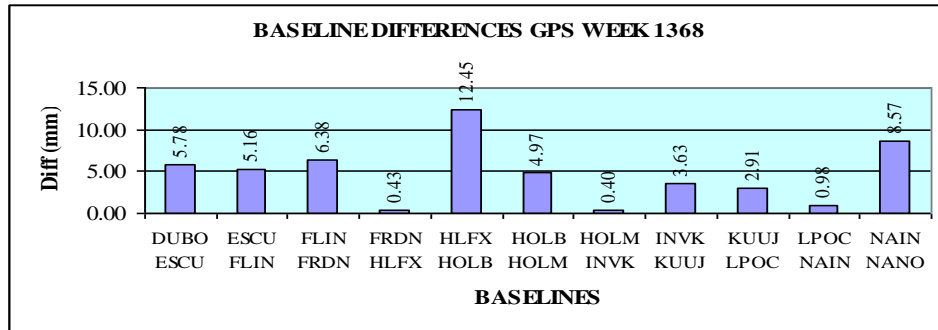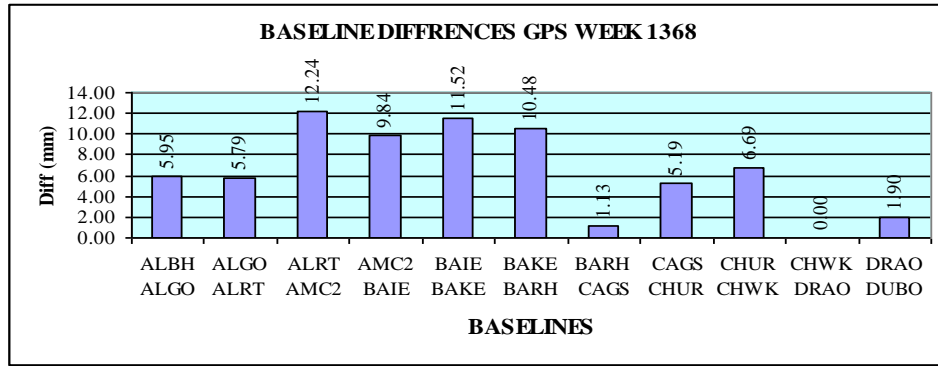
Figure 7.4 Graphical presentations of the baseline differences

7.2.2.2 The RMS (mm) of the daily coordinates repeatability

With reference to Dach at al. [2007, pp 221-235], the normal equation systems from subsequent sessions have to be combined in a multi-session solution using the ADDNEQ2 program to produce a weekly solution. When combining several normal equation systems, consistency is of utmost importance and for that reason coordinate residuals of the individual solutions in north, east and up, have to be computed with respect to the combined solution and reported in the output. These deliverables are vital to detect any station equipment inconsistencies and jumps or outliers that will most certainly degrade the quality of the results.

The computed results were therefore assessed for the consistency based on the information of the daily repeatability of the results as they would give the indication of any of the above named anomalies. From the computed results as have been illustrated in upper part of Figure 7.5, most of the weekly RMS values in the north and east components are less than 3 mm and values for the up component are below 5 mm as an indication of consistency. The computed RMS values show a close agreement with the NAREF solution values as shown on Figure 7.5 and Figure 7.6.
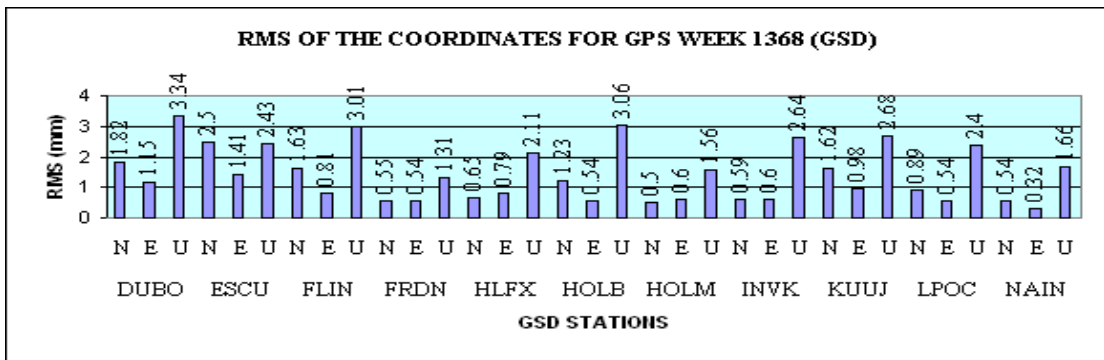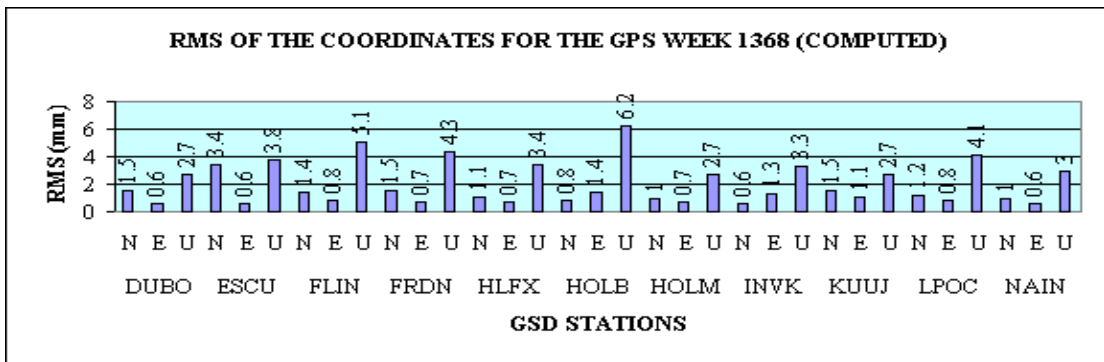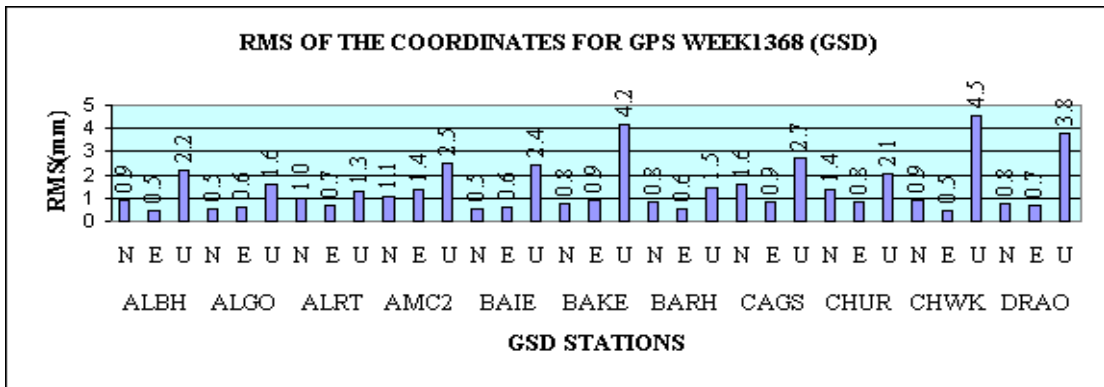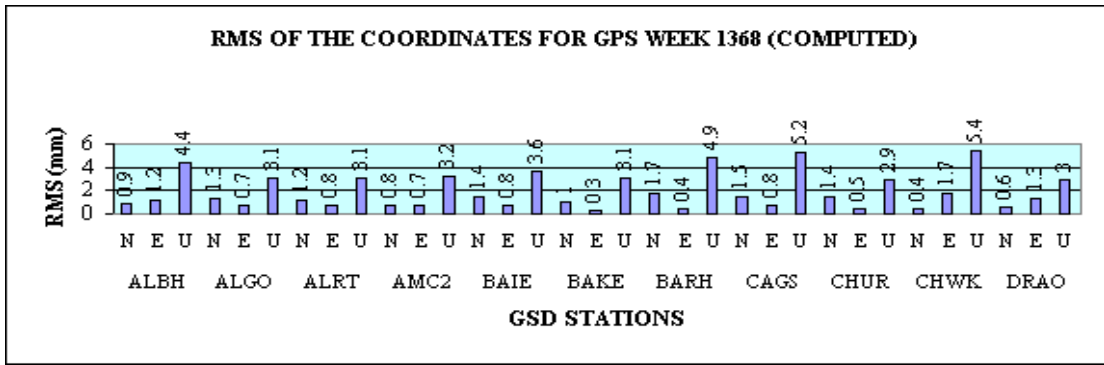
Figure 7.5 RMS of the daily coordinates repeatability-1
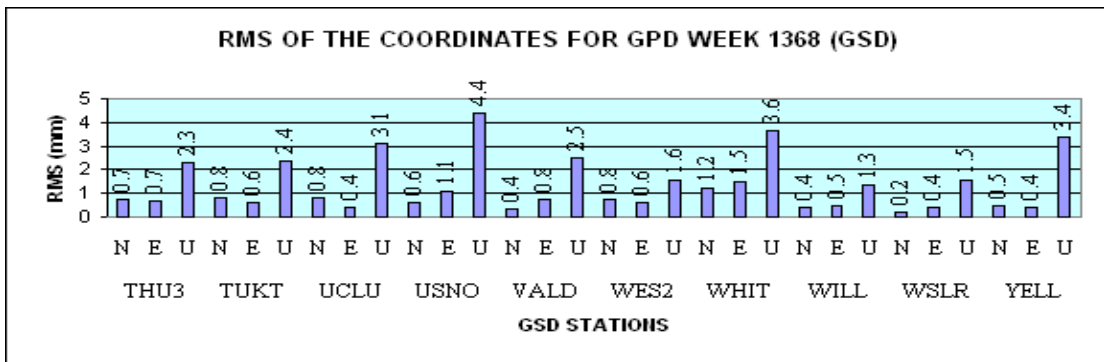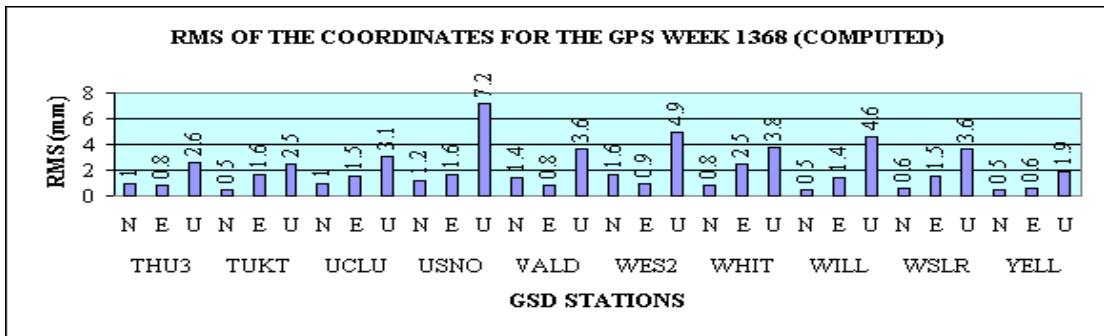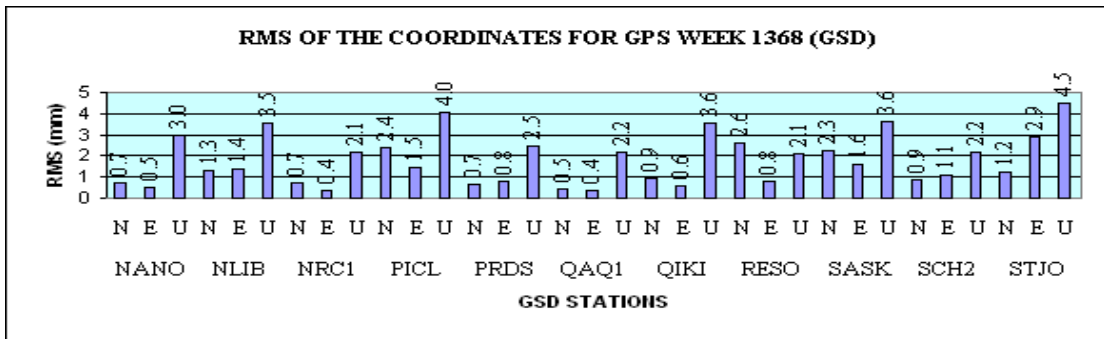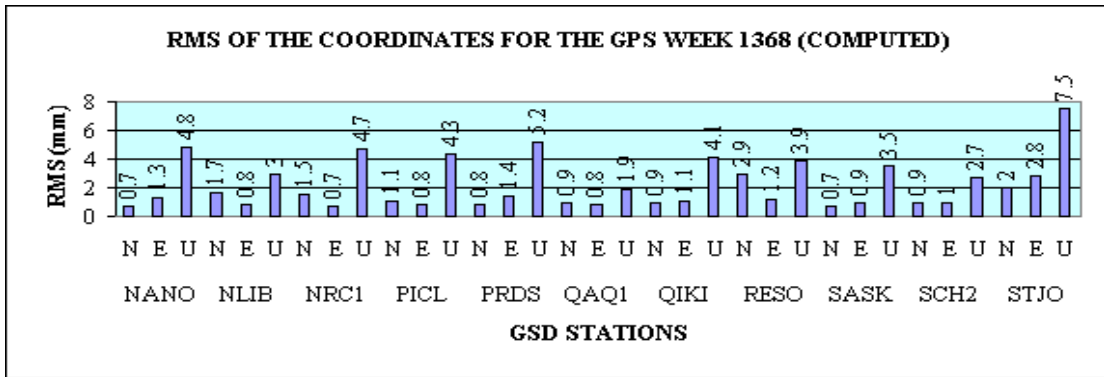
Figure 7.6 RMS of the daily coordinates repeatability-2

7.2.2.3 Differences of the computed coordinate values

The results were also assessed for the differences between the computed values from the published NAREF values. Illustrations from Figure 7.7 show that, about 90 percent of the coordinate components are well below 1 centimeter and the remaining 10 percent are less than 3 centimeter. This can discrepancy can be expected due to the fact that the data processing has done been using the Bernese v5.0 software version released on February 18, 2005. Since then there has been seven different releases to improve the software's processing capabilities and the Geodetic Survey Division of Canada is always adopting the improved versions.

With reference to the Bernese GPS Software Support centre, the Bernese V5.0 software version of the 18-February-2005 release has some errors. From the support centre it has been known that, the relative coordinate velocities constraint in the ADDNEQ2 file, used to combine the normal equations is wrong. As for that, the relative constraining of station positions or velocities in the station information file delivered with the BPE is not correct. It also known that there some errors in the program CODSPP when computing corrections for synchronizing the receiver clocks with respect to the GPS time. Some of these errors have corrected for better performance by releasing new files/programs [Walser, 2008]. Users need to have a username and a password to access these files to update their software using the update facility that has been offered by the support centre. In my processing, I did not update the problematic files as I had no access to Bernese system.
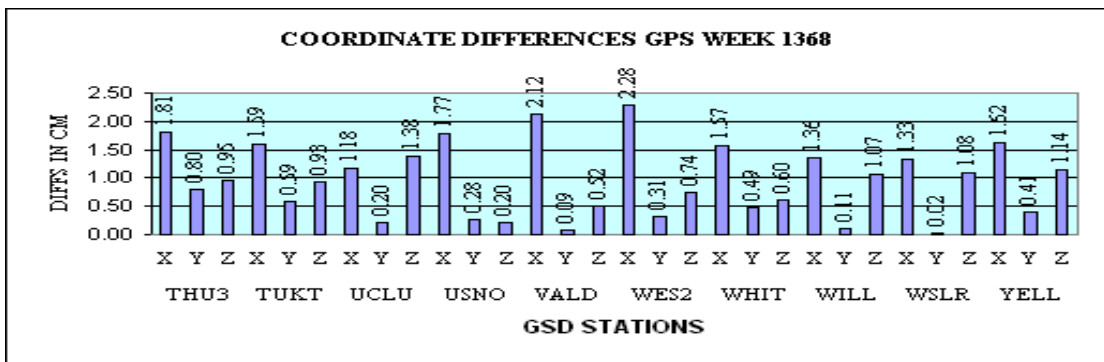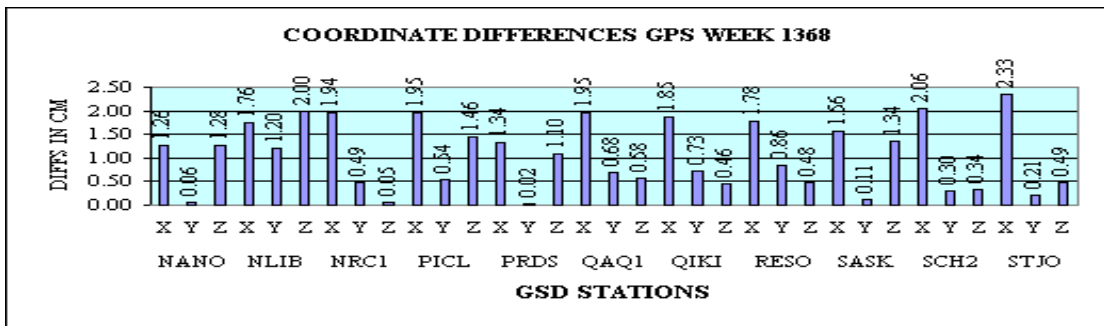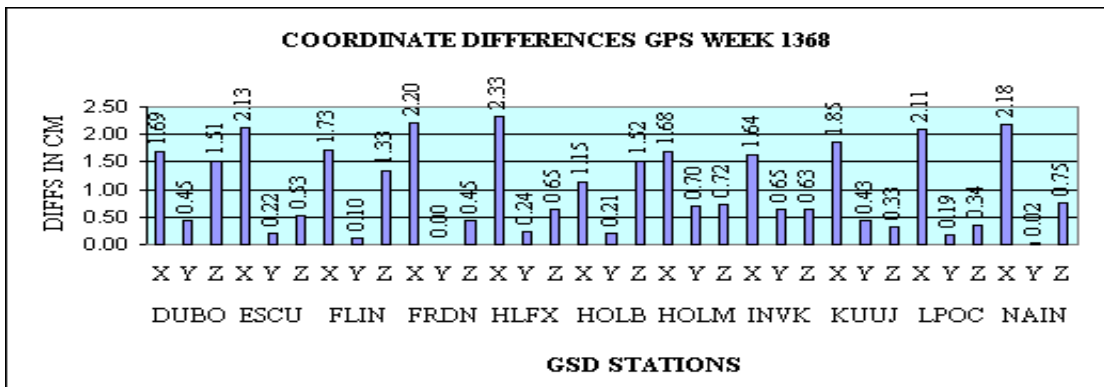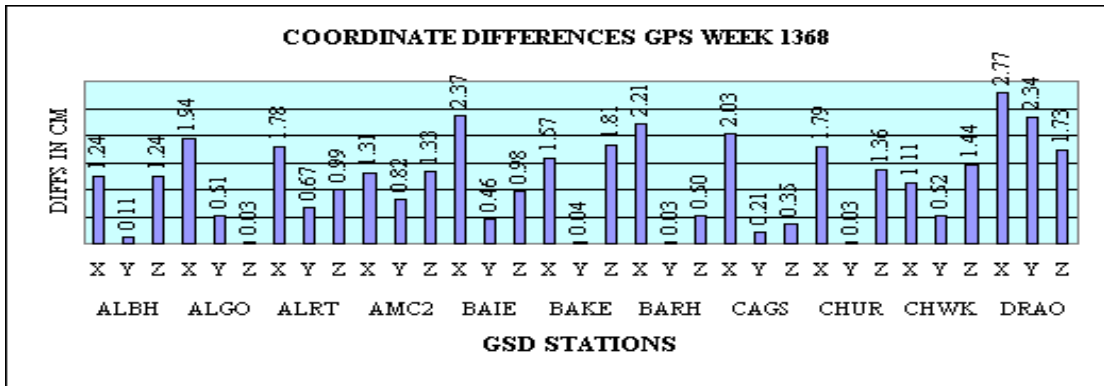
Figure 7.7 Differences in the computed solutions

7.3 Results and analysis of the Real time GPS positioning

Previous discussions by Bisnath and Langley [2002], Hofmann-Wellenhof et al. [2000] and Karen et al. [2003], has shown that, there are several factors limiting the accuracy of the RTK and DGPS position fixes. Most of them are beyond the control of the base station, rover and the operator and they include the following:

- The quality of the code measurements collected at the base stations.

- The compatibility of the base station within the NAD83 framework.

- The quality of the code measurement collected at the rover.

- The software and algorithms used to correct the rover.

- Satellite visibility at the rover and base stations.

- Multipath influence at the rover and base stations; and

- The relative distance between the rover and the base stations.

With reference to the discussion in section 6.3, the objective of this part of research was to establish how well can a particular point be positioned as compared to its true position (positional accuracy) using data transmitted over internet protocol. The test methodology was to occupy unknown reference point on top of a Gillin Hall (hereinafter referred to as 'RP') using the Trimble R7 receiver and observe for eight hours. RP was then after fixed from the point UNBJ by post processing using the Gravnav software so as to have the best position of the point. The point RP was then

fixed using the RTK and DGPS positioning methodology from four (4) different GPS points part of the CANSEL network for three different days of June, 2008. Table 7.16 gives the summary of the details of the datum points. The positioning exercise for the 10 June, 2008 and 24 June, 2008 was done using Trimble R7 receiver where as the positioning for the last day (that is 25 June, 2008) was done using the ProPak-V3 Novatel receiver.

Table 7.16 Details of the datum points used in the case study

Point	Latitude(N)			Longitude(W)			Height(m)	Distance(km)
RP	45	57	0.900	66	38	32.115	19.636	0
FEDERICTON	45	57	0.717	66	38	30.133	23.428	0.043
MILIFORD	45	0	48.903	63	25	54.172	8.042	240.028
TRURO	45	21	49.109	63	16	36.498	11.808	214.418
WINDSOR	42	19	26.284	83	0	46.805	153.262	1425.034

The RTK and DGPS position fixes were assessed for the position reliability to illustrate the degree of the expected positional accuracy which can be achieved or degraded given a good quality receivers and proper software algorithms. The assessment has been done using the R95 (horizontal 95 percent) scatter plots, time series of the metrics latitude and longitude differences as well as the histograms of positional differences. The output of the results and analysis was done using a Matlab code developed by the author.

7.3.1 The R95 (horizontal 95 percent) scatter plots

It is known that the position coordinates determined using GNSS system varies statistically due to positional errors. Graphic presentation of such results yields a scatter plot that forms one way of analysis to quantify position accuracy using error ellipses that have been determined using different approaches such as the root mean square (RMS), twice the distance root mean square (2drms), horizontal 95 percent accuracy, circular error probable (CEP) and spherical error probable (SEP).

This research has adopted the R95 (horizontal 95 percent) approach using the error ellipses that has been scaled using the Fisher distribution. With reference to previous illustrations by Langley [1991] and Strang et al., [1997], the chosen approach provides an ellipse, centered at the true antenna position, containing 95 percent of the points in the horizontal scatter plot. Assuming that, the error distribution along any axis (east, north, or up) is normal or Gaussian, the chosen approach can easily derive probabilities from other error analysis approaches.

The plotting of the R95 (horizontal 95 percent) scatter plots has been done using the Matlab software code developed by the author. The code computes the eigenvalues for each position fix as the basis of evaluating the parameters of the error ellipse and scaling them using the Fisher distribution to get the appropriate multiplication factors for the R95 for reasons that has been explained in section 6.1.1. Figure 7.8 to Figure 7.10 shows the RTK position fix of the point RP from point Fredericton and the numerical values of the error ellipse parameters in Table 7.17.

With reference to the plots, most of the positions are with the error ellipse as an illustration of the reliability of the internet protocol in real time GPS positioning.

Table 7.17 Values of the error ellipse parameters from Fredericton (RTK)

Date	Figure	Semi axes (cm)		Orientation		
		major	minor	deg	min	sec
10 June 2008	7.8	0.19	0.11	292	36	40.18
24 June 2008	7.9	4.47	3.86	176	0	45.65
25 June 2008	7.10	21.60	4.62	30	33	42.38
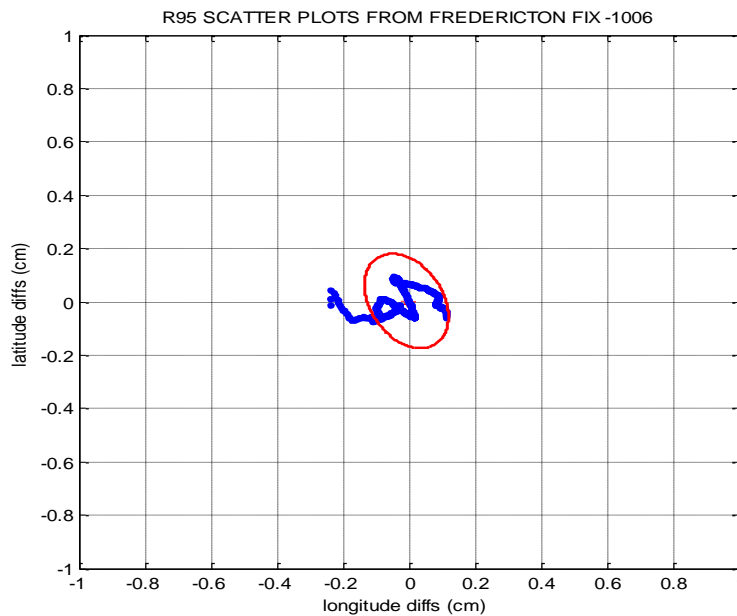
Figure 7.8 R95 scatter plot from Fredericton fix of 10, June 2008
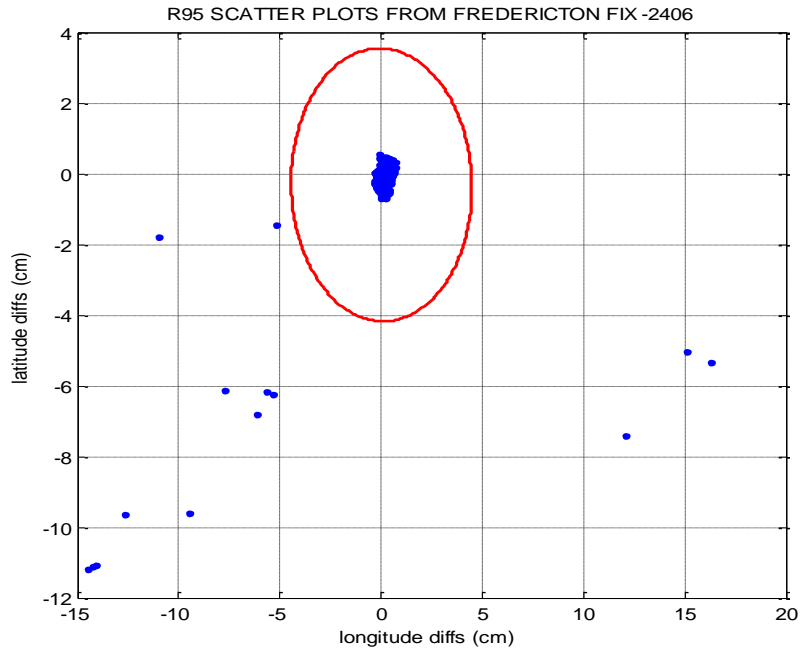
Figure 7.9 R95 scatter plot from Fredericton fix of 24, June 2008
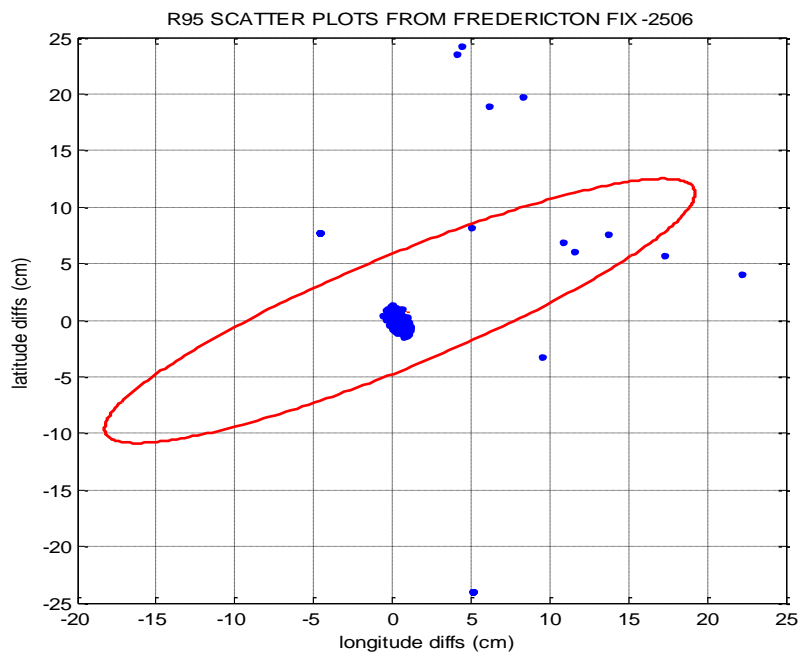
Figure 7.10 R95 scatter plot from Fredericton 25, June 08 (semi axes scaled by 0.5)

Figure 7.11 show the DGPS position fix of the test point from point Milford and the numerical values of the error ellipse parameters in Table 7.18. With reference to the plot, most of the positions are with the error ellipse as an illustration of the reliability of the internet protocol in real time GPS positioning.

Table 7.18 Values of the error ellipse parameters from Milford fix (DGPS)

Date	Figure	Semi axes (cm)		Orientation		
		major	minor	deg	min	sec
25 June 2008	7.11	21.60	4.62	30	33	42.38
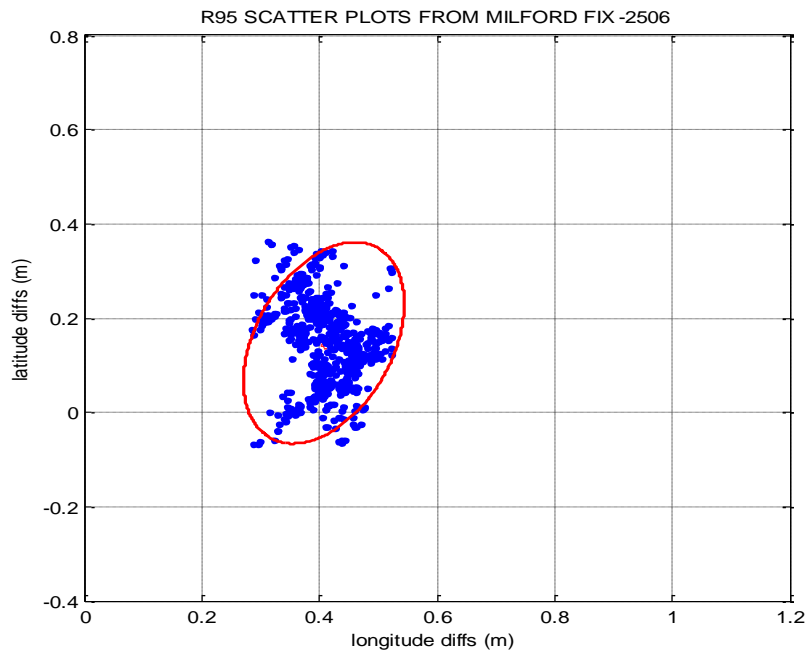
Figure 7.11 - R95 scatter plot from Milford fix of 25, June 2008

Figure 7.12 to Figure 7.14 shows the DGPS position fix of the test point from point Windsor and the numerical values of the error ellipse parameters in Table 7.19. With reference to the plots, most of the positions are with the error ellipse as an illustration of the reliability of the internet protocol in real time GPS positioning.

Table 7.19 Values of the error ellipse parameters from Windsor (DGPS)

Date	Figure	Semi axes (cm)		Orientation		
		major	minor	deg	min	sec
10 June 2008	7.12	0.451	0.246	55	46	56.23
24 June,2008	7.13	0.318	0.315	90	39	42.96
25 June 2008	7.14	0.338	0.209	58	17	43.45
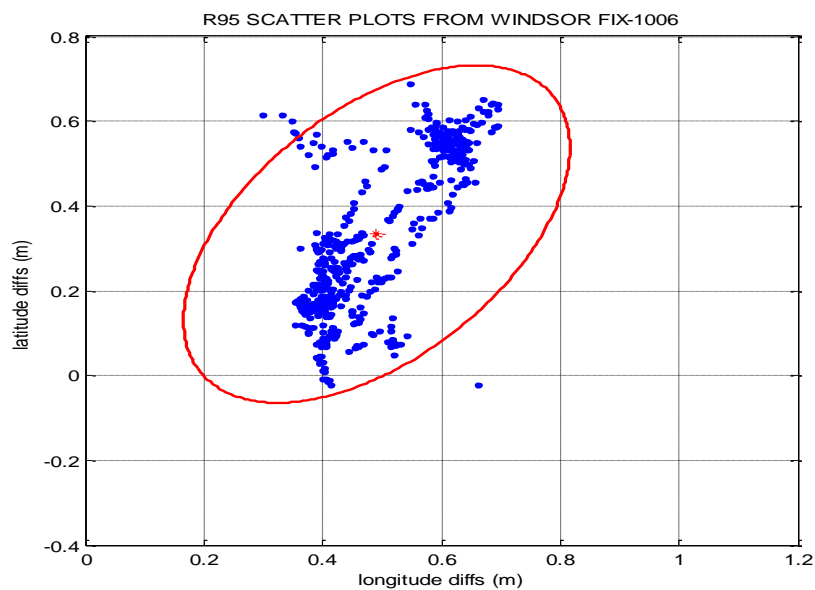
Figure 7.12 R95 scatter plot from Windsor fix of 10, June 2008
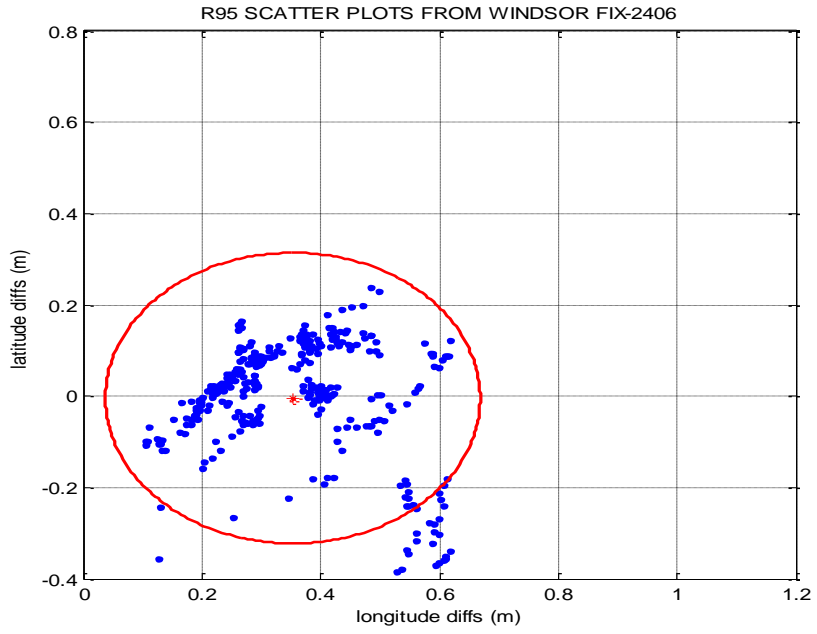
Figure 7.13 R95 scatter plot from Windsor fix of 24, June 2008
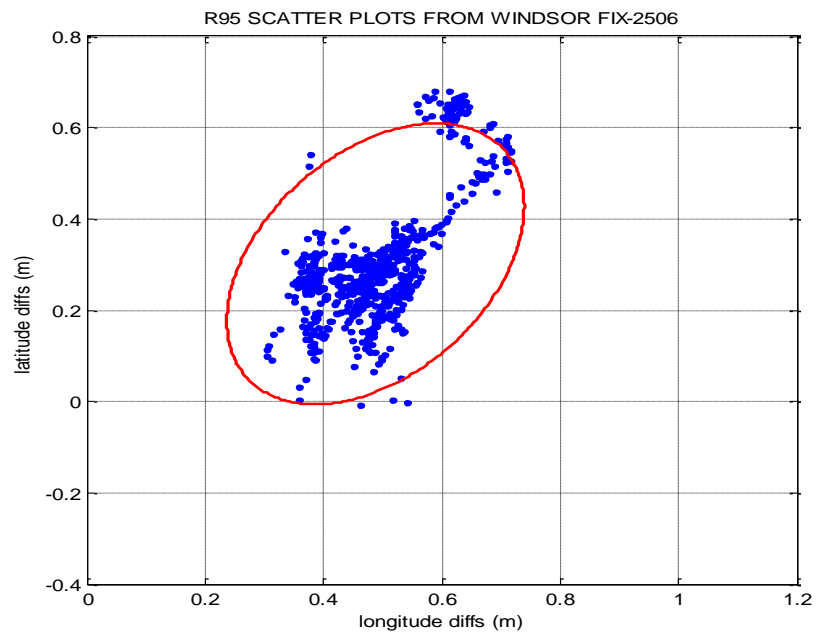
Figure 7.14 R95 scatter plot from Windsor fix of 25, June 2008

Figure 7.15 and Figure 7.16 shows the DGPS position fix from point Truro and the numerical values of the error ellipse parameters in Table 7.20.

Table 7.20 -Values of the error ellipse parameters from Truro (DGPS)

Date	Figure	Semi axes (cm)		Orientation		
		major	minor	deg	min	sec
10 June 2008	7.15	0.256	0.121	76	27	12.90
24 June 2008	7.16	0.400	0.331	70	20	53.11
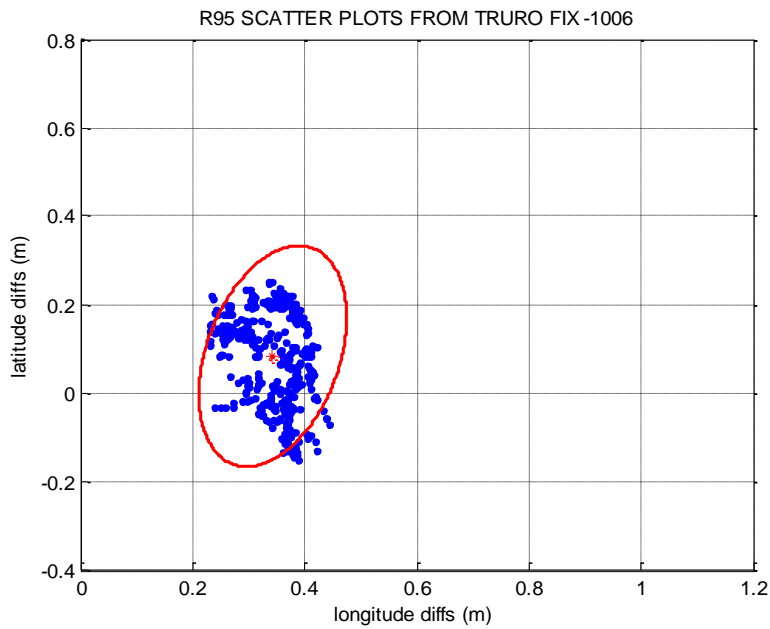
Figure 7.15 R95 scatter plot from Truro fix of 10, June 2008
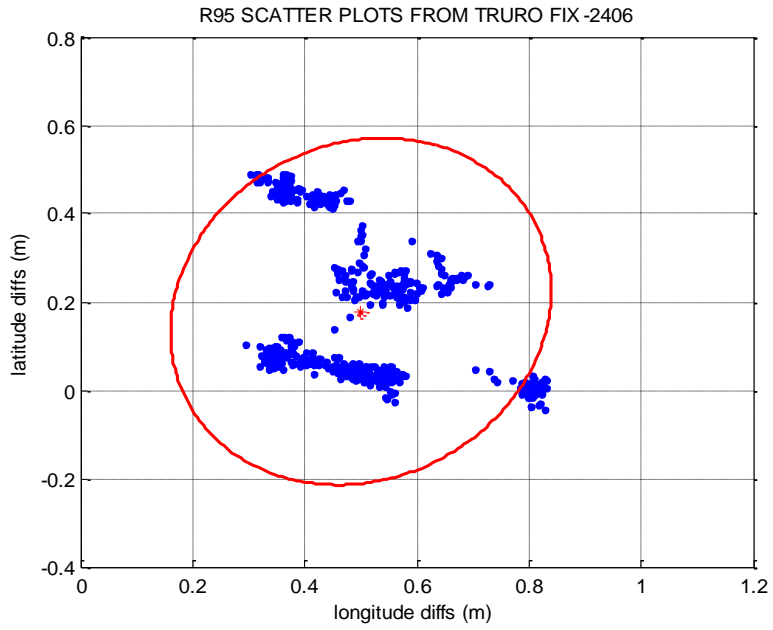
Figure 7.16 R95 scatter plot from Truro fix of 24, June 2008

179

7.3.2 Time series of the latitude and longitude differences

Time Series is an ordered sequence of observed values of a variable at equally spaced time intervals and RTK/DGPS solutions is an example of them. Time series are used to make analysis of such data pattern with two main goals as follows:

(a) Identifying the nature of the phenomenon represented by the sequence of observations usually referred to as trend.

(b) Prediction of the future values of the time series.

The trend represents a general systematic linear or (most often) nonlinear component that changes over time and does not repeat or at least does not repeat within the time range captured by our data. Sometimes it is common in practice to model trends using straight lines and polynomials for better analysis of the results. The prediction part depends on the formal similarity of the display of the time series and usually repeats itself in systematic intervals over time. Therefore, regardless of the depth of our understanding and the validity of our interpretation (theory) of the phenomenon fit is useful for extrapolating the data pattern to predict future events.

For that reasons, the time series of the RTK position fixes (Figures 7.17 to Figure 7.19) and that of the DGPS position fixes (Figures 7.20 to Figure 7.26) for different dates were prepared and plotted using the developed matlab code.
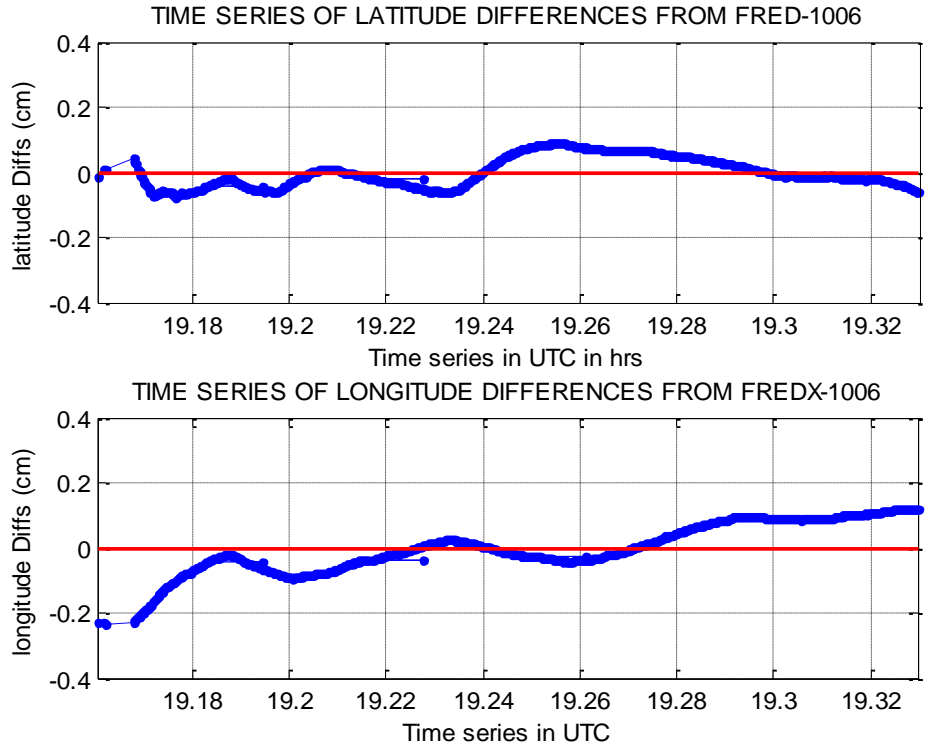
Figure 7.17-Time series of the from Fredericton fix-10 June 2008
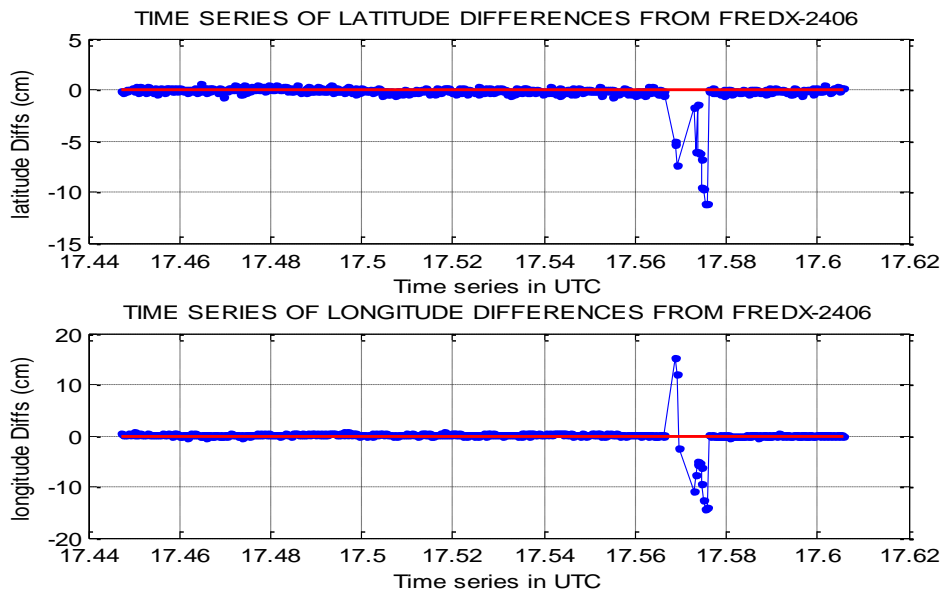
Figure 7.18- Time series of the from Fredericton fix-24 June 2008
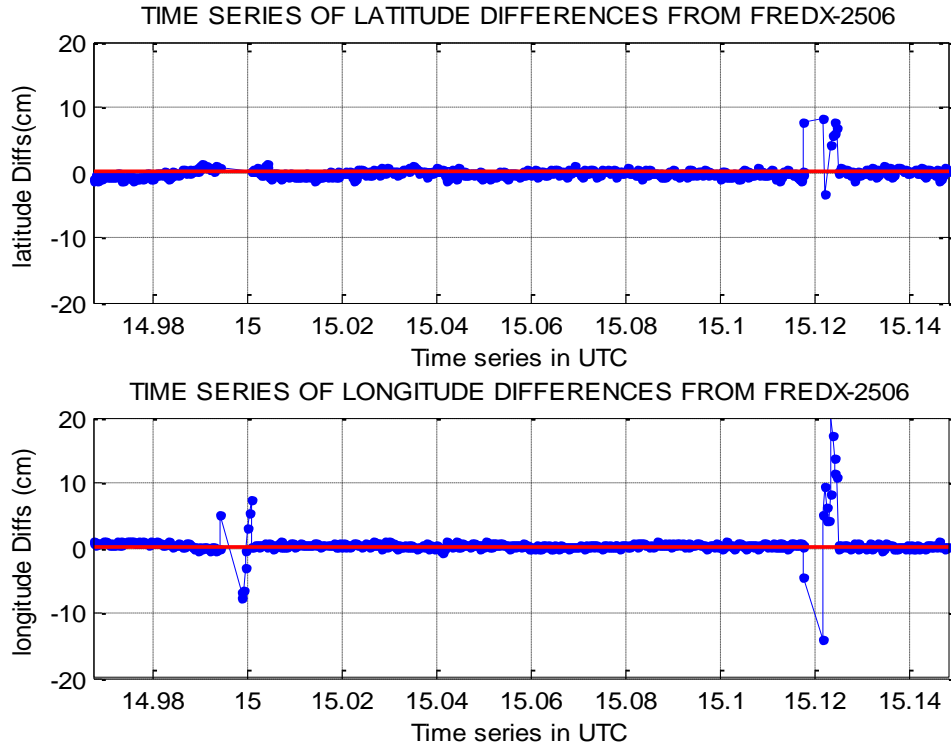
Figure 7.19 Time series of the from Fredericton fix-25 June 2008
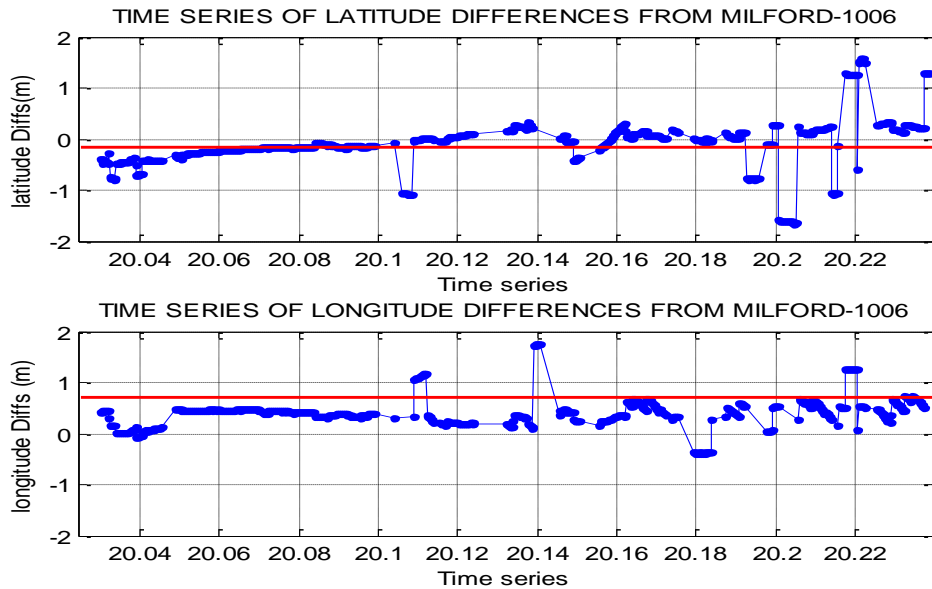
Figure 7.20 Time series of the from Milford fix-10 June, 2008
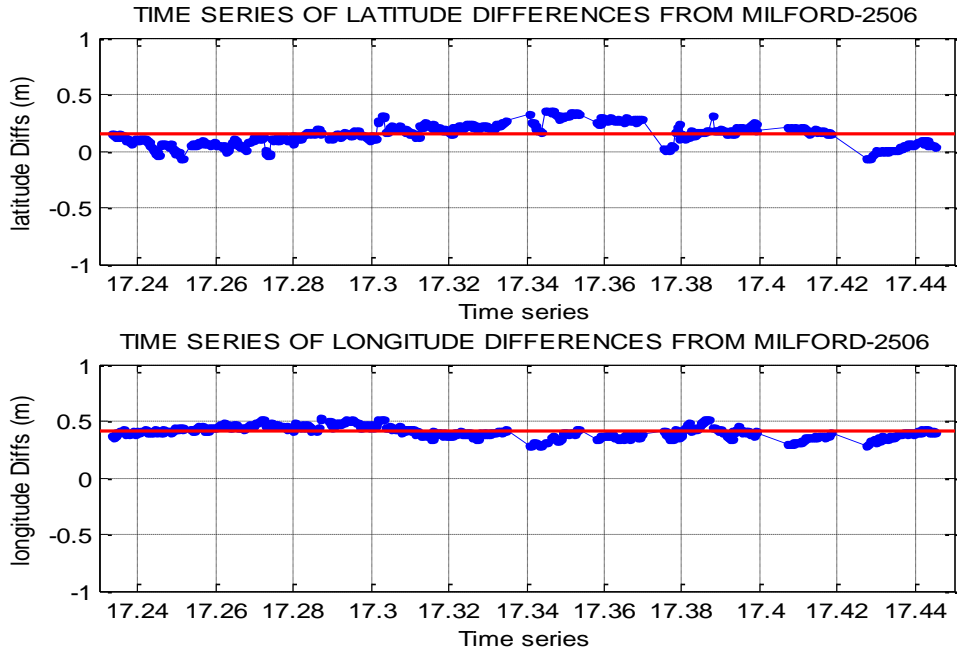
Figure 7.21 Time series of the from Milford fix-25 June, 2008
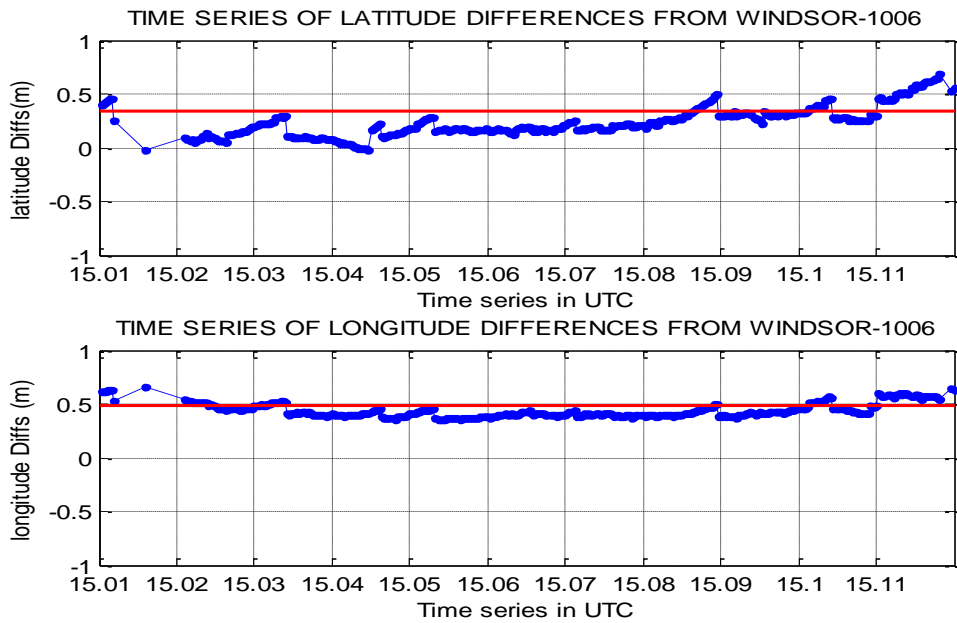
Figure 7.22 Time series of the from Windsor fix-10 June, 2008
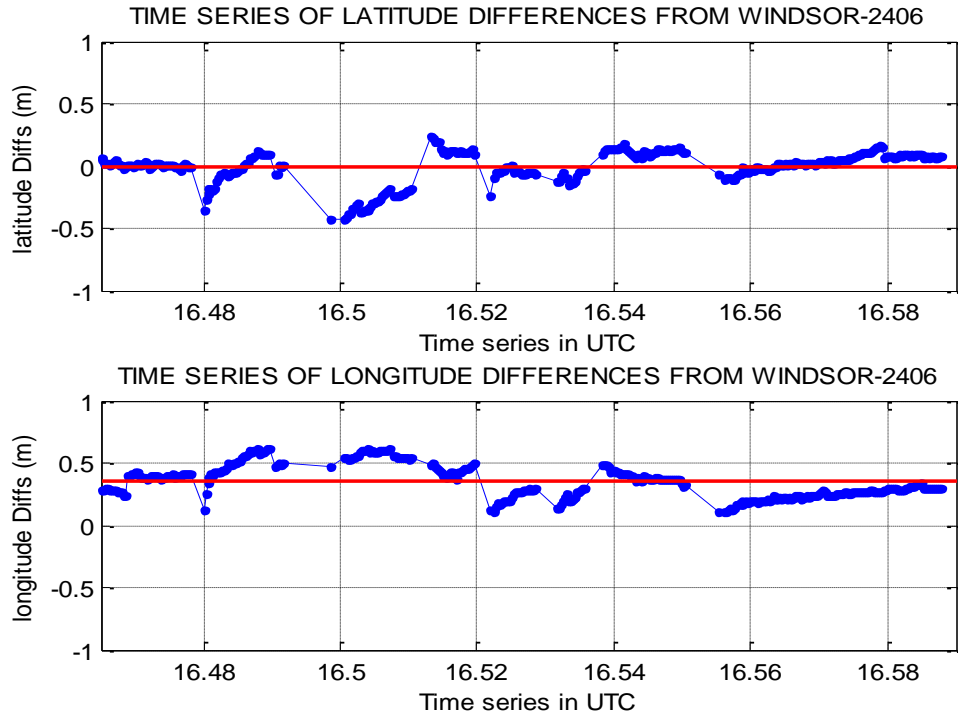
Figure 7.23 Time series of the from Windsor fix-24 June, 2008
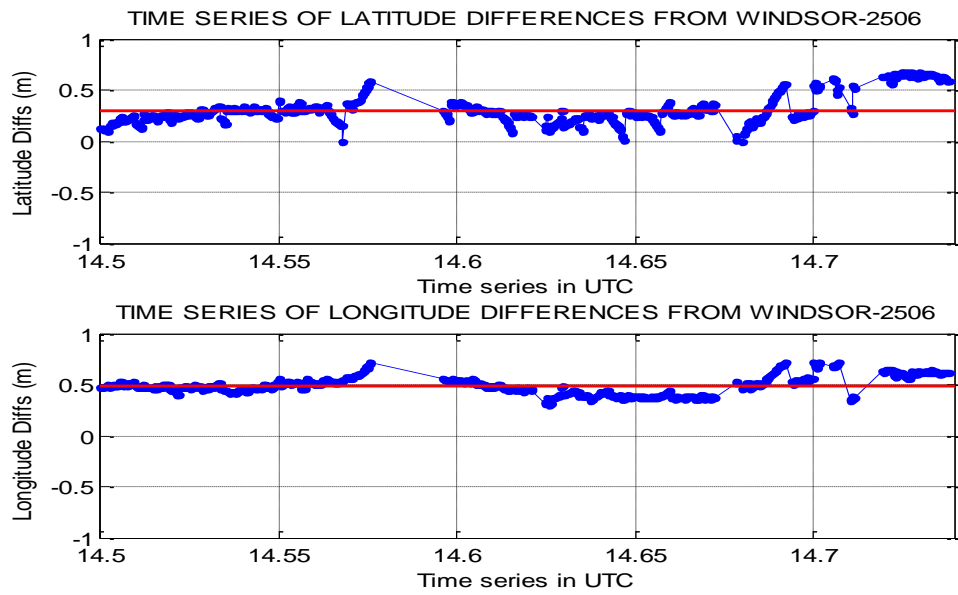
Figure 7.24 Time series of the from Windsor fix-25 June, 2008
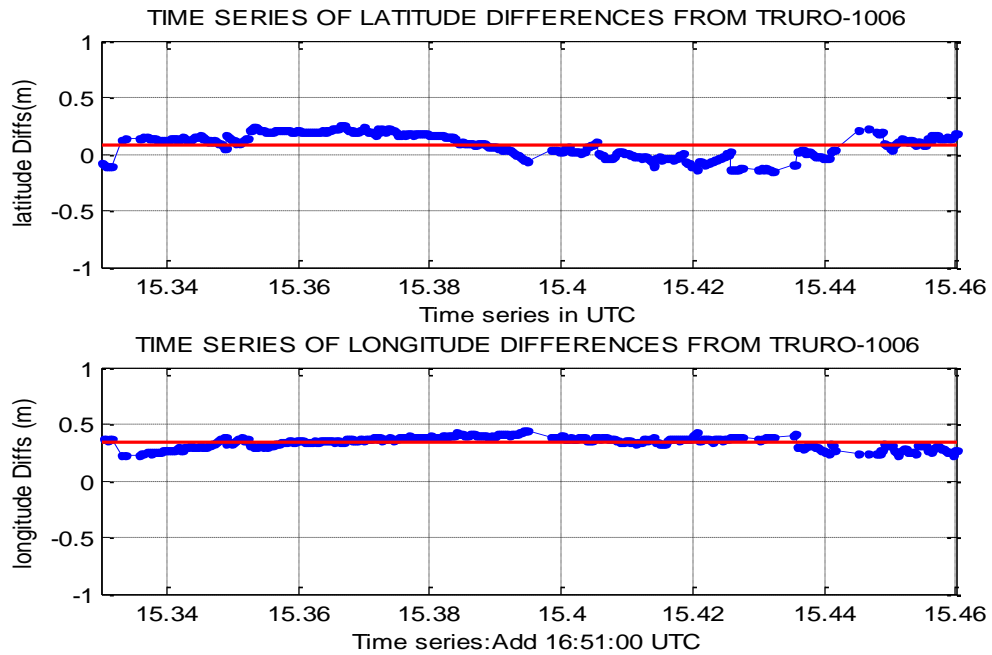
Figure 7.25 Time series of the from Truro fix-10 June, 2008
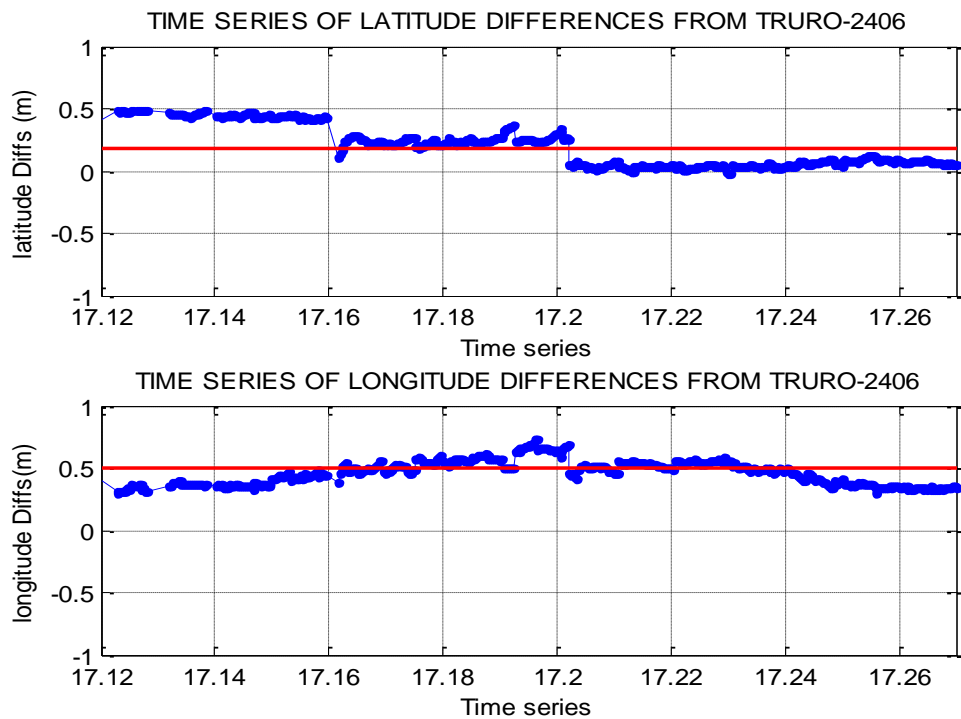
Figure 7.26 Time series of the from Truro fix-24 June, 2008

185

7.3.2.1 Assessment of the RTK time series

With reference to Figures 7.16 to 7.18, the general trends in the latitude differences time series and longitude differences time series in RTK are more or less straight lines or a well-defined low order polynomial with values that are within 2 centimetres for most of the positional fixes for all observational dates with few data breaks. Despite the inconsistency in the time of data capture one can easily predict that this trend can repeat over several days given a reliable internet connection.

7.3.2.2 Assessment of the DGPS time series

With reference to Figures 7.19 to 7.26, the DGPS positions have non-linear trend with latitude and longitude differences that are within decimetre levels with many data breaks. The data breaks (straight lines) are due to the loss of internet communication between the reference stations and the fixed position.

Moreover, it has been realized that the positional fixes show no similar pattern that can be useful to make any prediction based on them despite that no serious attempt has been made to collect data for that purpose.

7.3.3 The histograms of the positional differences

The positional differences between the fixed positions and the true position (also known as positional accuracy) were evaluated using the matlab software code developed for this research. The code computes differences in latitude and longitude between the two positions and then computes the metric differences plotted in histograms, as illustrated in Figures 7.27 to 7.34.
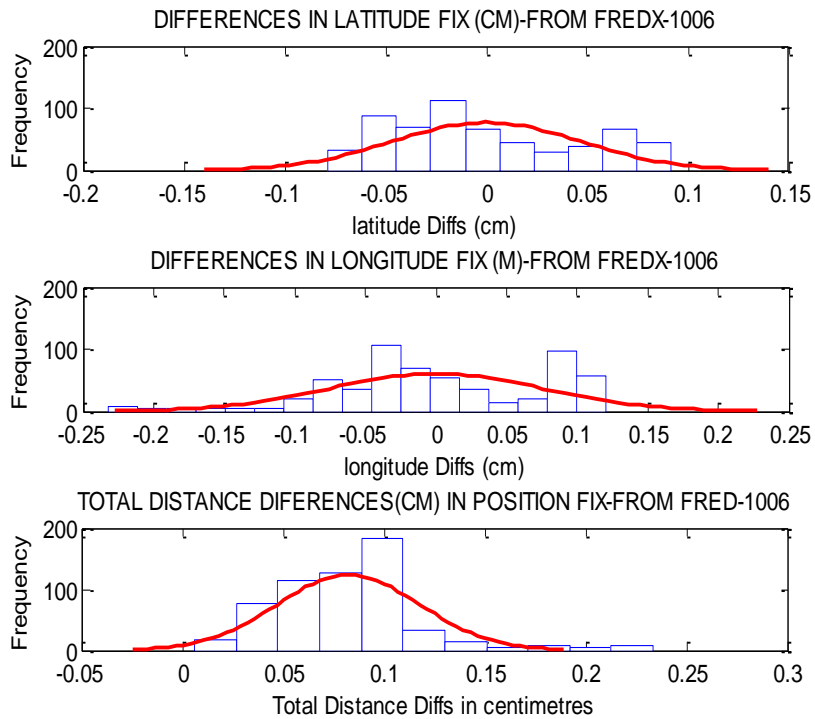
Figure 7.27- PDF test on Fredericton (RTK) positioning of 10 June 2008
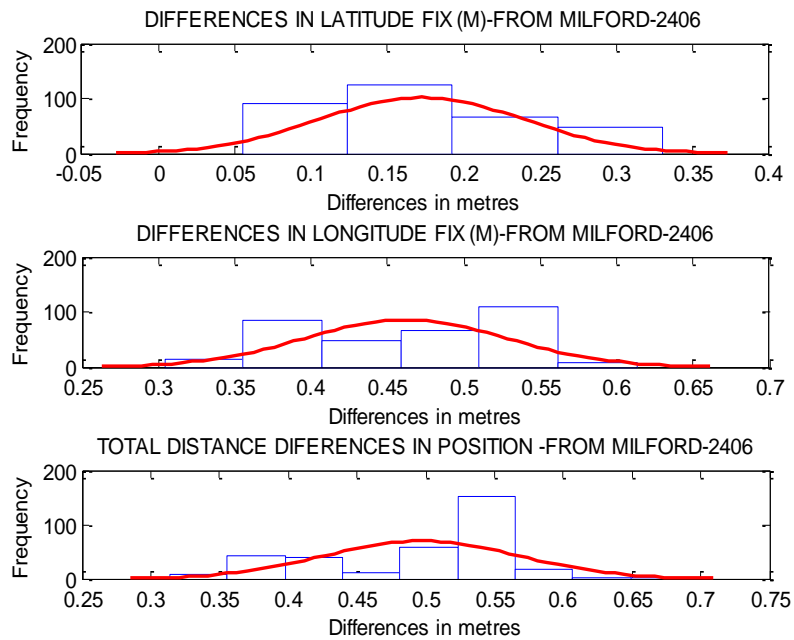
Figure 7.28 PDF test on Milford (DGPS) positioning of 24 June 2008
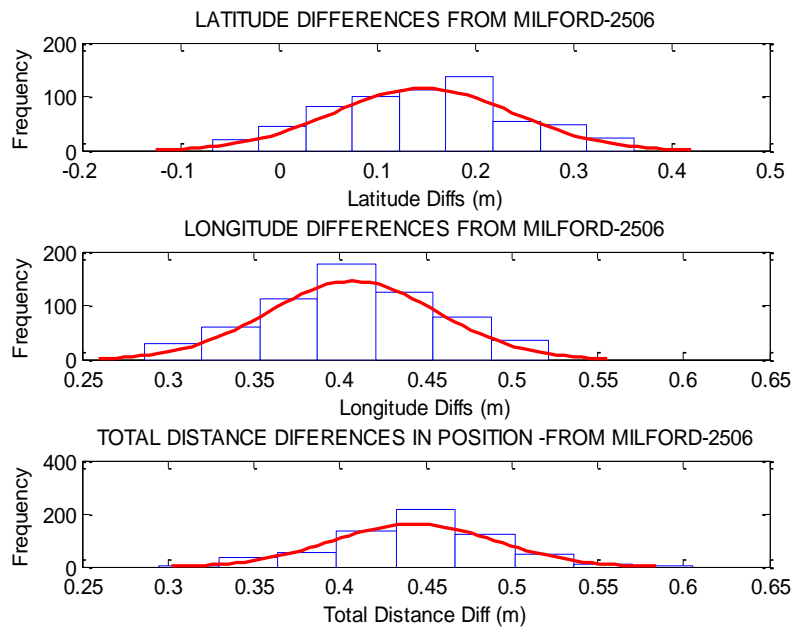
Figure 7.29 PDF test on Milford (DGPS) positioning of 25 June 2008
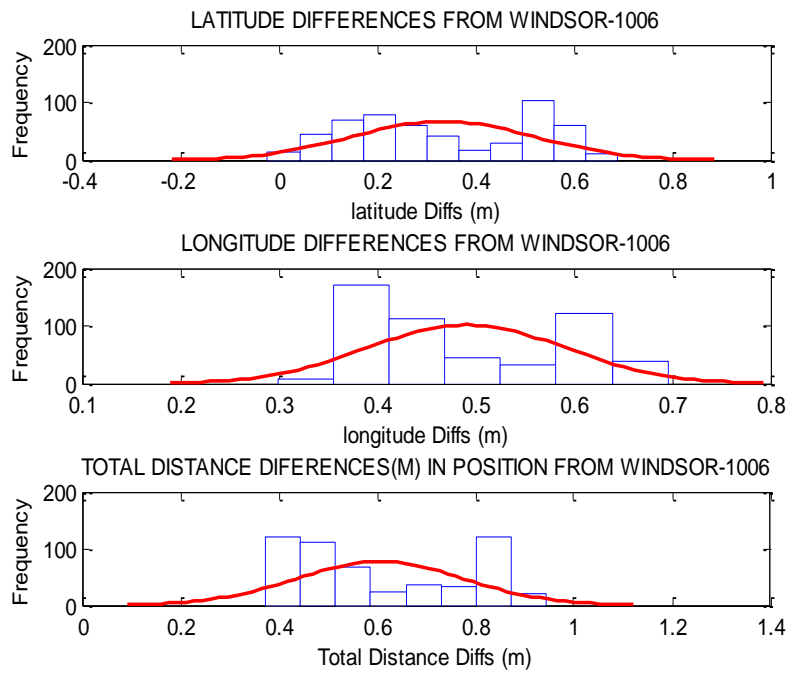
Figure 7.30- PDF test on Windsor (DGPS) positioning of 10 June 2008
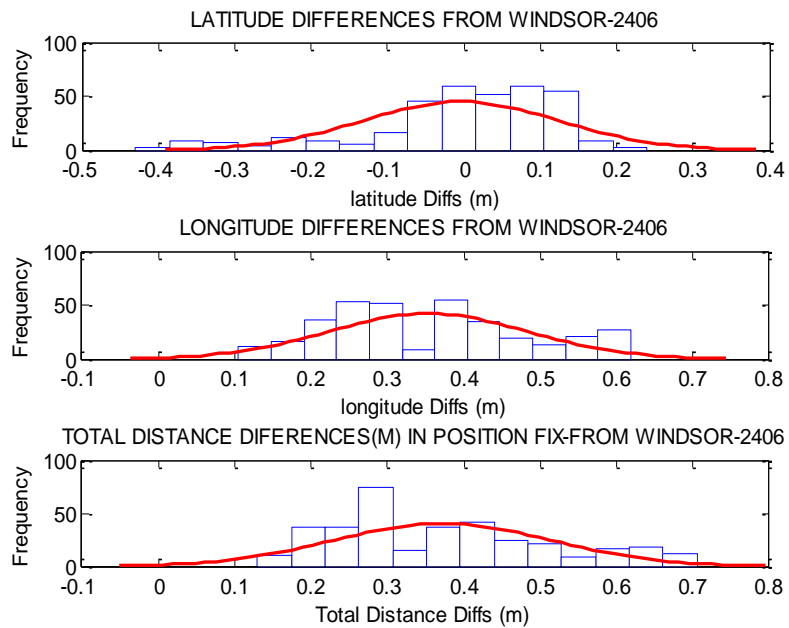
Figure 7.31- PDF test on Windsor (DGPS) positioning of 24 June 2008
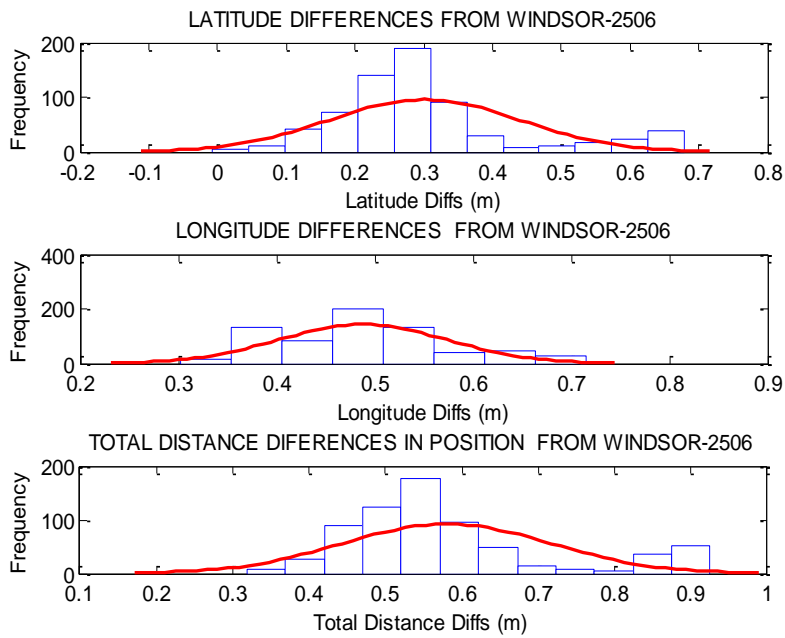
Figure 7.32- PDF test on Windsor (DGPS) positioning of 25 June 2008
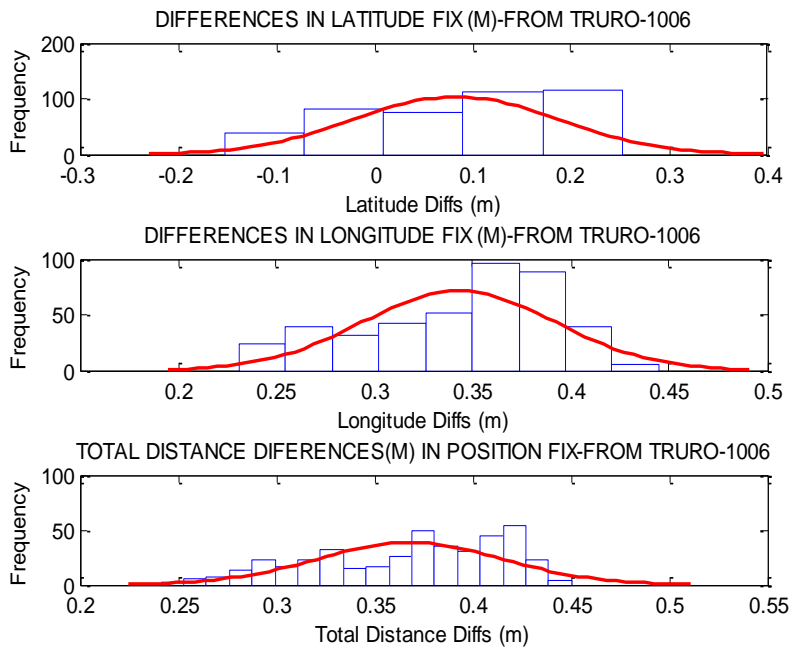
Figure 7.33- PDF test on Truro (DGPS) positioning of 10 June 2008
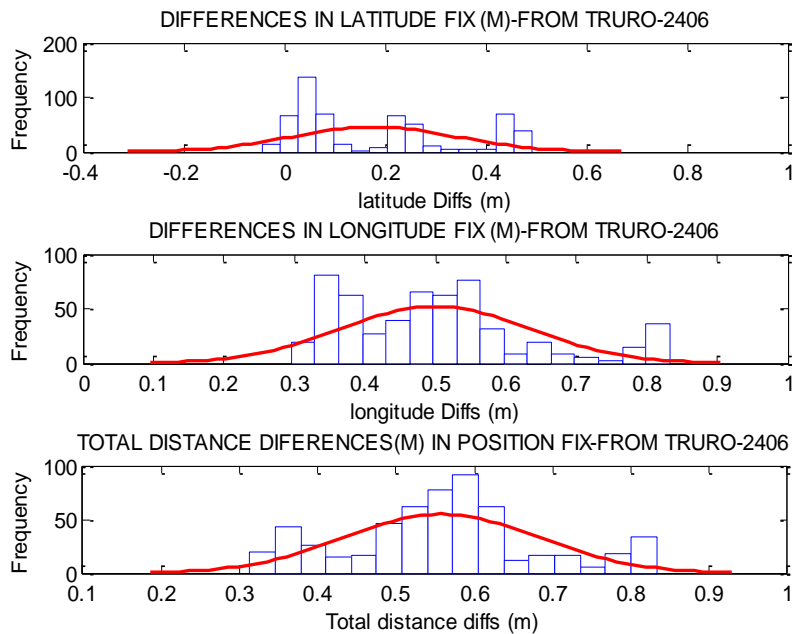
Figure 7.34- PDF test on Windsor (DGPS) positioning of 24 June 2008

Based on Figures 7.27 through 7.34, few observations can be made.

- The positional differences evaluated from the differences in latitudes and longitudes were found within the decimeter range from the "truth" solution with DGPS fixes. This performance evaluation has confirmed previous illustrations by Weber [2002] and Weber et al. [2003], that real time DGPS correction can economically deliver horizontal position accuracies better than 1m reliably using the internet protocol. These positions can be consistent on state-wide basis within areas of good internet coverage for geodetic applications.

- The positional differences evaluated using RTK measurements were consistently reliable to centimeter level accuracy with an average connection-initialization time of 5 to 10 seconds.

- In most cases, the histogram plots formed a typical Gaussian distribution as they were symmetrically distributed around a central point such that the farther from that point, the sparser the distribution. In other cases, as shown in some of the previous plots, they do not.

However, despite of the above observations, care should be taken when exercising DGPS positioning that, proper and satisfactory results can only be achieved if the receivers are high quality and have appropriate DGPS software.

8.0 CONCLUSION AND FUTURE WORK

8.1 Conclusion

The present Tanzania geodetic network is conventional and therefore not compatible with the current satellite positioning techniques. As such, it does not satisfy the growing mapping requirements of the country as well the requirements of other geo-related information applications. Examples of such applications include homogeneous cross border mapping activities, homogenous spatial mapping in urban areas, production and update of large-scale topographical maps in urban areas, prediction of weather, geophysical exploration surveys and information about station motions and their respective velocities.

For these reasons and many others, Tanzania has tried to establish a modern geocentric frame compatible with space positioning techniques in collaboration with other African countries to establish a unified African Geodetic Reference Frame (AFREF). However, the lack of appropriate expertise, proper awareness of the concepts amongst most of the national mapping organizations and differences in economic levels in the African countries has always been major limiting factors.

In view of such problems and many others associated with the present Tanzania conventional network and the major limiting factors towards the establishment of AFREF, the primary objective of this research is to provide the basis

of establishing and the maintaining a modern geodetic frame in Tanzania (TZRF10) in the ITRF system compatible to satellite position techniques.

The implementation of such a big project is costly in terms of money, time and personnel. This can lead to misconceptions and the poor quantification of the value of such investment to most users of the information system and especially decision makers. This is despite the high risk associated with wrong decision making on land related matters because of an un-reliable geo spatial frame. It can be negatively perceived as a sunk cost and therefore not a preference since most of the traditional ways of assessment failed to focus on the value the magnitude of the benefits resulting from a modern geodetic frame. Philip [1972], Duane [1977] and Epstein [1984] have also previously observed this problem. To make the research objectives more realistic to the case study area, the benefits of deploying a modern spatial frame have been addressed followed by a general review of different reference frame transformation strategies as the basis for selection of the best approach to suit the Tanzania environment.

There are available planning tools such as GeoLab simulation software and simulated least square covariance analysis for planning geometrically strong networks by making design tradeoffs of the factors affecting the network performance as previously illustrated by Pullen and Parkinson [1995], Wolf and Ghilani [1997] and Raquet et al.[1998]. Risk has therefore been avoided in the implementation strategies by making use of these tools for better implementation.

There is also considerable advancement in communication technologies with the increased capacity of the internet and applications that allows the transfer of continuous data streams by IP-packages, such as GNSS Internet Radio in a more reliable and economical manner. Previous discussion by Weber [2002] and Weber et al.[2003] has shown that those services have become well-established such that they enable real-time collection and exchange of GPS data (raw or RINEX) and broadcast the derived products to suit the geodetic application.

With the present geodetic requirements in parallel with the potentials of DGPS/RTK positioning using the internet protocol, three different case studies were developed and implemented to meet the research objectives:

1) A covariance analysis of the TZRF10 network for establishing the conceptual overview of the new frame with required geodetic strength.

2) The maintenance of a modern dynamic reference fame using scientific GPS processing software- Bernese v 5.0.

3) Real time positioning using the RTK and the DGPS approaches as the basis of future Kinematic and DGPS geodetic surveying in Tanzania.

With reference to the discussion in chapter six, the developed case studies were successfully implemented and then tested for their performance as elaborated in chapter seven. The covariance analysis indicates that, out of the three proposals the networks, the best results would come from the one consisting of 10 stations with the master control station MCS located in Dar es Salaam on top of the Survey and Mapping headquarters. The mathematical maintenance case study indicates that the weekly processed solutions can achieve a precision at the millimetrer level. The tests of the RTK and DGPS positioning using the internet protocol shows that the TZRF10 network can give support to meter-level geodetic applications around the country, satisfying all practical needs of the surveying community. In view of the implementation achievements and results of the performance evaluation, the research objectives have been met.

8.2 TZRF10 implementation and GNNS modernization

As has been previously discussed by Barker and Straton [2001] and Misra and Enge [2006, pp. 55-63], the Global Positioning System has embarked on an aggressive program of modernization of GPS signals from early spring of 2003. The present generation of modernized satellites is capable of transmitting seven different signals to improve positional accuracies with greater availability and integrity for different civilian and military applications. The seven signals are M1 and M2 for

military application, the two Code Access signals at L1 (1575.42 MHz) and L2C at L2 (1227.6 MHz), the two encrypted P(Y) signals transmitted at L1 and L2 and the L5 (1176.45 MHz) signal.

Therefore, despite the results discussed in chapter seven, care should be taken in the implementation strategy especially in the hardware and software selection. The GPS receivers must be of high geodetic quality with appropriate software that will be capable to match with the present development trends as discussed by Jovancevic et al. [2001] and Todd et al. [2008]. Modern geodetic receivers should be digital with modules that are easily configurable through internet with a user-friendly graphical interface for download converting and sampling of the new GPS signals. They should have software capability to track and process all possible open signal samples from healthy GNSS satellites in real time and store them for further processing. Other qualities include internal cycle slip mitigation and detection capabilities as well as compliance with the latest RINEX standards and low cost.

8.3 Future research

As part of future research, the Tanzania implementation strategy should consider working closely with RTIGS. The Real Time Working Group (RTWG) is currently developing real-time infrastructure to address the real-time delivery of raw data and the dissemination of products to real-time analysis centers and real-time users. With reference to Caissy [2008] and Broederbauer et al.[2007], a pilot project is underway for the implementation of a prototype infrastructure and processes system for the support of precise real-time positioning guided by the principles of robustness, sustainability and acceptance. The primary products of the proposed Tanzania system will be GPS/GNSS station data and satellite orbits and clocks, made available to the user by internet and other economical data streaming technologies available for all position applications. Users of other related applications such as natural hazards monitoring, atmospheric monitoring for weather prediction and real-time earthquake seismology will also be provided access to the frame products.

The successfully implementation RTIGS strategy, requires the global involvement of GPS tracking stations to provide data with reasonable quality, reliability and availability. Unfortunately, we have few IGS stations (less than five) south of the equator on the African continent. For this reason, the implementation strategy of the new frame needs to assist the IGS in achieving its objectives to support the near real time applications for the benefit of the global reference frame users including Tanzania.

References

Azevedo, J., A. Freitas, M. Augusto, L. Oliveira and M. C. Santos (2006). "Assessing Impacts of Adopting a New Geocentric Coordinate System in Brazil". *GSDI-9 Conference Proceedings, 6-10 November 2006, Santiago, Chile.*

Barker.B.,and J. Straton (2001)."GPS Military Signal Modernization Updates To Design And Characteristics"**.** *Proceedings of ION GPS 2001 program*

Beran, T., R. B. Langley, S. B. Bisnath and L. Serrano (2007). "High-Accuracy Point Positioning with Low-Cost GPS Receivers." *Navigation, Vol. 54, No. 1, Spring 2007, pp. 53-63.*

Broederbauer .V., M. Caissy, M. Opitz and R. Weber (2007)." Real Time GPS- Satellite- and Receiver Clock Estimation – An interactive RTIGS Web Service". *Geophysical Research Abstracts, Vol. 9, 06094, 2007.*

Bisnath, S.B. and R.B. Langley (2002). "High Precision, Kinematic Positioning with a Single GPS Receiver." *Journal of The Institute of Navigation*, Vol. 49, No. 3, *Fall 2002, pp. 161-169.*

Brunner, F. K. (1998). "Advances in Positioning and Reference Frames". Scientific Assembly, Rio de Janeiro, Brazil, September 3-9 International Association of Geodesy Symposia, Vol. 118, pp 8-17.

Boal, J.D. and J.P. Henderson (1988). "The NAD 83 Project - Status and Background". In *Papers for the CISM Seminars on the NAD'83 Redefinition in Canada and the Impact on Users*, The Canadian Institute of Surveying and Mapping, Ottawa, Canada.

Beutler, G., Rothacher, M., Schaer, S., Springer, T.A., Kouba, J., Neilan, R.E., (1999). "The International GPS Service (IGS): An interdisciplinary service in support of Earth sciences". Advanced Space Research, vol. 23, No. 4, pp. 631-635.

Boucher, C. and Z. Altamini (1996). "International Terrestrial Reference Frame". *GPS World*, 7 (9), pp.71-75.

Caissy, M. (2008)."Real time Pilot Project Overview and Status". *International GNSS Service Workshop, Miami, June 2008.*

Caissy, M. (2006) .*International GNSS Service -Call for participation.* International GNSS Service Real-Time Pilot Project. [On-line] 15 October 2007. http://www.rtigs.net/pilot/docs/IGS-RT-Pilot-Project-Call-For-Participation.pdf.

Craig, B.D. (1988). "NAD'83 Redefinition in Canada and the Impact on Users". *Papers for the Canadian Institute of Surveying and Mapping (CISM,) seminars, Ottawa, Ontario.*

Craymer, M., and M.Piraszewski. "The North American Reference Frame (NAREF): An Initiative to Densify the ITRF in North America." *Proceedings of KIS 2001: International Symposium on Kinematic Systems in Geodesy, Geomatics and Navigation,* Banff, Canada, June 5-8, 2001.

Craymer, M., and M. Piraszewski (2001). "The NAREF Initiative to Densify the ITRF in North America". *Proceedings of the EUREF Permanent Network Third Local Analysis Centres Workshop,* Warsaw University of Technology, Warsaw, Poland, May 31 - June 1, 2001.

Craymer, M., M. Piraszewski, C. Huot. and B.Donahue (2002). "Canadian Contributions to the NAREF Initiative to Densify the ITRF in North America." *Proceedings of AGU 2002 Fall Meeting*, San Francisco, December 6-10, 2002.

Craymer, M., and M.Piraszewski (2002). "Densification of ITRF: The NAFREF experience in North America". *IGS Network, Data and Analysis Center Workshop 2002,* Ottawa, Canada, April 8-11, 2002.

Craymer, M.R (2006). "The Evolution of NAD83 in Canada." GEOMATICA Vol. 60, No. 2, 2006 pp 151 to 164.

Craymer, M.R., M. Piraszewski, and J.A Henton (2007). "The North American Reference Frame (NAREF)". *Proceedings of ION GNSS 2007,* Texas, September, 25-28, 2007.

Craymer, M., R. Ferland and R. Snay (1999). "Realization and Unification of NAD83 in Canada and the U.S. via the ITRF". *Proceedings of the International Symposium of the International Association of Geodesy, Section II, Towards an Integrated Geodetic Observing System (IGGOS², Munich, October 5-9, 1998, pp. 118-121.*

Dach, R., U. Hugentobler, P. Fridez, and M. Meindl (2007). "User Manual Bernese GPS Software Version 5.0." Astronomical Institute University of Berne, January, 2007.

DeMets et al., (1994). "Effect of recent revisions to the geomagnetic reversal time scale on estimates of current plate motions". *Geophysical Research Lett. Vol. 21 No. 20, p. 2191-2194.*

Duane, C. B. (1977). "Densification of urban geodetic nets" *Photogrammetric and Remote sensing, 43,1977, pp.447-467.*

Elmar, L., "Networked Transport of RTCM via Internet Protocol (NTRIP) – Application and Benefit in Modern Surveying Systems" , FIG working week, Athens, Greece, 22-27 May 2004, [Online] 15 February 2007. http://www.fig.net/pub/athens/papers/ts03/ts03_2_lenz.pdf.

Epstein, E., (1994). "The Use and Value of Geodetic Coordinates Systems". *Research Performed Under Grant No. NA82AA-D-00016.*

Hofmann-Wellenhof, B., H. Lichtenegger and J.Collins (2000). GPS Theory and Practice, pp 186-267.

Hoyer, M., S. Arciniegas, K. Pereira, H. Fagard, R. Maturana, R. Torchetti, H.Drewes, M. Kumar, G. Seeber (1998). "The definition and realization of the reference system in the SIRGAS project". Springer, International Association of Geodesy Symposia Vol. 118, pp 167-173.

Junkins, D., and G. Gerrard (1998). "Demystifying Reference Systems". *GEOMATICA, Vol. 52, No. 4, 1998.*

Jovancevic.A., A. Brown, S. Ganguly, M. Kirchner, S. Zigic (2001). "Reconfigurable Dual Frequency Software GPS Receiver and Applications". *Proceedings of ION GPS 2001 program.*

Karen, C., M Santos, L., B.Remondi, and D Wells (2003). "Assessment of performance of ionospheric delay-free GPS carrier phase kinematic relative positioning with varying baseline lengths". *United States Hydrographic Conference 2003*, March, 25-27, Biloxi, Miss.

Kouba, J, Y. Mireault, G. Beutler, T. Springer, G. Gendt, (1998)."A Discussion of IGS Solutions and Their Impact on Geodetic and Geophysical Applications," GPS Solutions Vol.2, pp.3-15.

Klobuchar, J. A. (1991). "Ionospheric effects on GPS". *GPS World,* April, Vol. 2, No. 4, pp. 48-51.

Klous, W., and R. Tilling (1996). *This Dynamic Earth*.

Knight, M., M. Cervera and A. Finn, (1999). "A comparison of predicted and measured GPS performance in an ionospheric scintillation environment", *Proceedings of the ION GPS-99*, September 14-17, Nashville, Tennessee, 1437-1450, 1999.

Larson, K.M., J.T. Freymueller and S. Philipsen, (1997). "Global plate velocities from the Global Positioning System". *Journal of Geophysical Research*, *Vol. 102, No. B5, pp. 9961-9982.*

Langley, R., (1991). "The Mathematics of GPS." *GPS World,* July*/August 1991, pp. 4550.*

Langley, R., (1998). "RTK GPS." *GPS World, September, 1998, pp. 70-76.*

Leick, A. (2004). *GPS Satellite Surveying. (2nd edition).* John Wiley & Sons, Inc., New York, 435.

McCarthy, D. (1996). "IERS Technical Note 21". Observatoire de Paris, July 1996.

Mclintock, D.,G . Lesieur,J . Portsmouth, J. Brigoen,.R. Adams and J. Mclellansimpact (1989). "Impact Of The North American Datum (Nad83) Redefinition On The Petroleum Industry". *Canadian Journal Of Exploration Geophycs Vol. 25, No, 1,pp. 36~44*.

Misra, P., and P. Enge (2006). *Global Positioning System: Signals, Measurements and Performance*. Lincoln laboratory, Massachusetts Institute of Technology.

Moore, A.M., and R.E. Neilan (2005). "The International GPS Service Tracking Network: Enabling Diverse Studies And Projects Through International Cooperation," Journal of Geodynamics vol.40, pp. 461-469.

Moore, A. (2006). "IGS New Site Guidelines" International Global Navigation Satellite Systems Central Bureau. [On-line] 10 November 2007. http://igscb.jpl.nasa.gov/network/guidelines/checklist.html.

Moritz, H. (1979). "Report of Special Study Group N° 539 of I.A.G., Fundamental Geodetic Constants". *Proceeding for the at XVII General Assembly of I.U.G.G., Canberra. Australia.*

Mueller, I., R. Neilan and K.Gowey (1997) "International GPS Services for Geodynamics 1997 Technical Report- October, 1998*"*.

Parent, C. (1988). "NAD83 Secondary Integration". *CISM Journal ACSGC*, *Vol.42 (4), pp. 331-340*.

Philip, C.J (1972). *A measure of the Economic Impact of Urban Horizontal Geodetic Control Survey*. M.S thesis, Cornel University, New York, USA. 113pp.

Pullen,S, P. Enge, and B. Parkinson (1995). "A New Method for Coverage Prediction for the Wide Area Augmentation System (WAAS)". *Proceedings of the 51st AnnualMeeting of the Institute of Navigation*, pp. 501–513. Colorado Springs, Colorado, June 1995.

Raquet,J G.Lachapelle and L.P and L. Fortes (1998) . "Use of Covariance Analysis Technique for Predicting Performances of Regional Differential Code and Carrier-Phase Networks". *Proceeding of the meeting of The Institute of Navigation, pp25-34, Alexandria,V.A, 2001*.

Richard., A (2004). (NTRIP (http://igs.bkg.bund.de/index_ntrip.htm).: **euref-ip@bkg.bund.de** .

RTIGS (2002), "Prototype RT-IGS Archtecture". [Online] 15 March 2008. http://www.rtigs.net/architecture.php

Ruizhi, C., X. Li, and G. Weber, "Test Results of an Internet RTK System Based on the NTRIP Protocol". [Online] 15 March 2007. http://igs.ifag.de/pdf/Chen_GNSS2004.pdf.

Santos, M.C, P.Vani'cek and R.Langley (1996)." Principles of orbit improvement and generation of ephemerides for the Global Positioning Satellites". *Revista Brasileira de Geofisica, Vol.14(3),1996.*

Santos, M.C (2007)." Class notes for Advanced Adjustement Calculus-GGE3211". Department of Geodesy and Geomatics Engineering, University of New Brunswick.

Santos, M.C (2007)." Class notes for Geodesy II-GGE4211". Department of Geodesy and Geomatics Engineering, University of New Brunswick.

Santos, M.C, J. B. Azevedo, A. L. B. Freitas, M. J. C. Augusto and L. C. Oliveira. "Assessing Impacts of Adopting a New Geocentric Coordinate System in Brazil". *GSDI-9 Conference Proceedings, 6-10 November 2006, Santiago, Chile.*

Stamps, D., E. Calais, E. Saria, C. Hartnady, J. Nocquet,C. Ebinger and R. Fernandes (2007). "A kinematic model for the East African Rift". *Geophysical Research Letters, Vol. 35, L05304, Doi:10.1029/2007gl032781, 2008.*

Sella, G., S. Stein, T. Dixon, M. Craymer, T. James, S. Mazzotti, and R. Dokka (2006). "Observation of glacial isostatic adjustment in ''stable'' North America with GPS". *Geophysical Research Letters, Vol. 34, L02306, Doi:10.1029/2006gl027081, 2007.*

Seeber ,G.,(2003). "Satellite Geodesy" 2nd completely revised and extended edition pp10-30, 2003.

Snay, R., M.l Cline, W. Dillinger, R. Foote, S. Hilla, W. Kass, J. Ray, J. Rohde, G. Sella, and T . Soler (2006). "Using global positioning system-derived crustal velocities to estimate rates of absolute sea level change from North American tide gauge records". *Journal of Geophysical Research, Vol. 112, B04409, Doi:10.1029/2006jb004606, 2007.*

Strang,G., and K. Borre (1997)." Linear Algebra, Geodesy, and GPS"- *Random Variables and Covariance Matrices, pp.309-341.*

Teunissen, P.J.G., and A. Kleusberg, (1998). *GPS for Geodesy.* Springer-Verlag, Berlin Heidelberg New York, 650.

Teunissen, P. J. G., (1997). "GPS double difference statistics: with and without using satellite geometry". Journal of Geodesy, Vol. 71, No.3, pp.137-148.

Thilantha, D., P. Srinuandee, L. Samarakoon, J. Susaki, T. Srisahakit. "Potential Accuracy and Practical Benefits of NTRIP Protocol Over Conventional RTK and DGPS Observation Methods". [Online] 15 March 2007. http://www.gisdevelopment.net/technology/gps/ma06_102.htm.

Todd. H., L.Young and T.Panny (2008). "Consideration for Future IGS Receivers". *Proceedings of the IGS workshop, Miam Beach, FL.*

Walser Peter. "Bernese GPS Software Support for the 18-February-2005 release". [Online] 15 March 2008 [http://www.bernese.unibe.ch/Bugs18-FEB-05.html]

Wells, D.E et al., (1999). "Guide to GPS positioning". Department of Geodesy and Geomatics Engineering Lecture Notes No. 58, University of New Brunswick, Fredericton, N.B, Canada.

Weber,G.,(2002). "DGPS/RTK Over The Internet." *Proceedings of the EGS XXVII General Assembly, Nice, 21-26 April 2002.*

Weber,G., D. Dettmering and H. Gebhard (2003). "Networked Transport of RTCM via Internet Protocol (NTRIP)". *Proceedings of the International Association of Geodesy General Assembly Sapporo, Japan June 30 – July 11, 2003, Vol. 128,pp.60-64.*

Wolf, R.P and C.D.Ghilani (1997*).”Adjustment computations: Statistics and Least squares in Surveying and GIS”.* University of Wisconsin-Madison.

Wonnacott, R., (2005). “Background and Progress towards a Unified Reference Frame for Africa”. *Proceedings of the International Federation of Surveyors / GSDI-8 Conference in Cairo, Egypt, April 16-21 2005.*

Reigber, C., M.Tomassini, G.Dick and G.Gendl (2002). “Water Vapor Monitoring for Weather Forecasts “

Zakiewicz , T., (2005). “The Cape Geodetic Standards and Their Impact on Africa”. *FIG Working Week 2005 and GSDI-8Cairo, Egypt April 16-21, 2005.*

Appendix I

Geodetic Reference System 1980 (GRS80)

This appendix provides a summary of the parameters of the Geodetic Reference System 1980 used to define the global reference frame to map the whole world. GRS80 is geocentric and it is such that, its rotational axis has the direction of the same direction as the Conventional International Origin for the Polar Motion (CIO), and the zero meridians as defined by the Bureau International de l'Heure (BIH). The GRS80 has been adopted by means of IUGG Resolution No. 7 at the XVII General Assembly of the IUGG, in Canberra, December 1979 [Moritz, 1979] and these parameters (relevant to the case studies) have been used in the implementation.

Appendix I Table1-GRS80 parameters

Defining geometrical constants		
Parameter	Symbol	Value
equatorial radius of the Earth	a	6378137 m
semi minor axis (polar radius)	b	6356752.3141 m
Aspect ratio	b / a	0.996647189318775
Reciprocal flattening	1/f	298.257222101

Derived geometrical parameters		
Quadratic mean radius		6,372,797.5559 m
Mean radius	R_1	6371008.7714 m
Authalic mean radius (radius of sphere with same surface)	R_2	6,371,007.1810 m
radius of sphere with same volume	R_3	6371000.7900 m
Linear eccentricity	$\sqrt{a^2 - b^2}$	521,854.0097 m
Polar radius of curvature	$=a^2 / b$	6,399,593.6259 m;
Meridian quadrant		10,001,965.7293 m
first eccentricity	e^2	0.00669438002290
Defining physical parameters		
geocentric gravitational constant (including the atmosphere)	GM	$3986005 \cdot 10^8$ m^{3}s^{-2}
dynamical form factor (excluding permanent tides)	J_2	$108263 \cdot 10^{-8}$
angular velocity of the Earth	ω	$7292115 \cdot 10^{-11}$ rad s^{-1}
Derived physical parameters		
normal potential at ellipsoid	U_0	62636860.850 m^{2}s^{-2}
Normal gravity at equator	g_e	9.7803267715 m s^{-2}
Normal gravity at pole	g_p	9.8321863685 m s^{-2}

Appendix II

Covariance analysis results

This appendix provides a few intermediate and final results that had been achieved in the covariance analysis case study and the results are divided into eight (8) different parts. They are Appendix IIA, Appendix IIB, Appendix IIC, Appendix IID, Appendix IIE, Appendix IIF and Appendix IIG as will be explained in the following sections.

Appendix IIA Simulated GPS observations

Appendix IIA is comprised of nine (9) different tables that give the simulated GPS observations from the permanent stations to a selected set of satellites. Section 6.1.2.2 provides the details of the simulation procedure.

Appendix IIA Table 1 Satellite positions for the selected epochs

Satellite positions on 8 February 2008 Epoch 8:30 am			
Sat	$X_{sat}(m)$	$Y_{sat}(m)$	$Z_{sat}(m)$
6	11770424.993	17713134.394	16078270.095
18	18644697.700	18260156.541	6022432.790
22	23402136.588	10318718.686	-7082210.893
30	15143549.104	18679692.733	-11718734.810
Satellite positions on 8 February 2008 Epoch 9:00 am			
6	11454223.631	20908478.753	11865025.658
18	16755638.962	17678159.213	11169811.929
22	23974158.868	11352711.944	-1558296.199
30	12196233.648	17668660.294	-16032767.310
Satellite positions on 8 February 2008 Epoch 9:30 am			
6	11262338.301	23099404.097	6844980.272
18	13842419.163	16846543.563	15571406.586
22	23500789.212	11787061.227	4072536.707
30	8373468.250	16668249.999	-19276430.384

Appendix IIA Table 2 Simulated GPS observations station for PS1

Simulated codes epoch 8:30		
Sat _ ID	P_1 (*m*)	P_2 (*m*)
6	22918922.396	22918919.562
18	21002352.313	21002349.487
22	20447284.299	20447281.598
30	21008933.822	21008931.917
Simulated codes epoch 9:00		
6	22256535.160	22256532.789
18	21772976.804	21772974.155
22	20386843.761	20386841.716
30	21769065.372	21769063.434
Simulated codes epoch 9:30		
6	21684955.867	21684953.478
18	22740930.040	22740927.339
22	20698103.647	20698101.481
30	22718852.967	22718850.394

Appendix IIA Table 3 Simulated GPS observations station for PS2

Simulated codes epoch 8:30		
Sat _ ID	P_1 (m)	P_2 (m)
6	23059649.496	23059646.867
18	21096204.668	21096202.604
22	20515885.323	20515883.268
30	20811845.552	20811843.478
Simulated codes epoch 9:00		
6	22308183.626	22308181.144
18	21915505.942	21915503.903
22	20527686.497	20527684.179
30	21497955.984	21497953.253
Simulated codes epoch 9:30		
6	21644157.041	21644154.300
18	22909010.591	22909008.360
22	20903328.791	20903326.458
30	22385009.275	22385006.601

Appendix IIA Table 4 Simulated GPS observations station for PS3

Simulated codes epoch 8:30		
Sat _ ID	$P_1\ (m)$	$P_2\ (m)$
6	23235329.785	23235327.905
18	21183446.429	21183443.958
22	20358921.299	20358918.461
30	20926836.235	20926833.660
Simulated codes epoch 9:00		
6	22543012.625	22543010.521
18	22023535.402	22023533.282
22	20392519.175	20392517.275
30	21624319.034	21624316.188
Simulated codes epoch 9:30		
6	21919697.991	21919695.391
18	23043215.878	23043213.931
22	20795792.733	20795790.257
30	22534439.443	22534437.133

Appendix IIA Table 5 Simulated GPS observations station for PS4

Simulated codes epoch 8:30		
Sat _ ID	P_1 (*m*)	P_2 (*m*)
6	23154369.647	23154367.763
18	21138057.695	21138055.618
22	20327715.367	20327713.439
30	21077207.126	21077204.405
Simulated codes epoch 9:00		
6	22524178.919	22524176.629
18	21943668.235	21943665.447
22	20312925.998	20312923.711
30	21822554.870	21822552.411
Simulated codes epoch 9:30		
6	21964530.735	21964527.965
18	22944032.131	22944030.267
22	20672286.670	20672284.265
30	22772521.438	22772518.946

Appendix IIA Table 6 Simulated GPS observations station for PS5

Simulated codes epoch 8:30		
Sat _ ID	P_1 (m)	P_2 (m)
6	22824668.753	22824666.870
18	20951243.933	20951241.466
22	20443297.461	20443294.752
30	21118417.141	21118415.123
Simulated codes epoch 9:00		
6	22206755.017	22206752.864
18	21689498.249	21689495.427
22	20339143.203	20339140.540
30	21916688.857	21916686.617
Simulated codes epoch 9:30		
6	21683585.998	21683583.182
18	22637156.373	22637154.314
22	20609250.037	20609248.072
30	22896343.023	22896340.963

Appendix IIA Table 7 Simulated GPS observations station for PS6

Simulated codes epoch 8:30		
Sat _ ID	P_1 (m)	P_2 (m)
6	22549158.523	22549155.684
18	20811671.699	20811669.286
22	20546580.750	20546578.088
30	21231664.048	21231661.550
Simulated codes epoch 9:00		
6	21968018.457	21968015.909
18	21479765.322	21479762.628
22	20355224.851	20355222.020
30	22085559.884	22085557.490
Simulated codes epoch 9:30		
6	21501025.365	21501023.109
18	22373884.539	22373882.175
22	20537393.026	20537390.513
30	23099191.191	23099189.321

Appendix IIA Table 8 Simulated GPS observations station for PS7

Simulated codes epoch 8:30		
Sat _ ID	P_1 (*m*)	P_2 (*m*)
6	22837420.900	22837418.238
18	20970021.136	20970018.461
22	20398429.255	20398427.249
30	21280794.575	21280791.844
Simulated codes epoch 9:00		
6	22284146.828	22284144.757
18	21687131.352	21687128.802
22	20267104.458	20267101.935
30	22111909.538	22111907.059
Simulated codes epoch 9:30		
6	21820115.052	21820112.747
18	22625282.407	22625279.820
22	20513080.535	20513077.868
30	23121804.163	23121802.229

Appendix IIA Table 9 Simulated GPS observations station for PS8

Simulated codes epoch 8:30		
Sat _ ID	P_1 (m)	P_2 (m)
6	22967208.950	22967206.267
18	21065659.055	21065657.028
22	20344558.706	20344555.991
30	21423211.085	21423208.508
Simulated codes epoch 9:00		
6	22465738.865	22465736.619
18	21784163.826	21784161.515
22	20219270.539	20219268.126
30	22262502.799	22262500.613
Simulated codes epoch 9:30		
6	22040673.130	22040670.814
18	22728140.737	22728138.761
22	20472605.557	20472603.067
30	23285210.883	23285208.806

Appendix IIA Table 10 Simulated GPS observations station for PS9

Simulated codes epoch 8:30		
Sat _ ID	P_1 (*m*)	P_2 (*m*)
6	22624582.189	22624580.081
18	20866741.618	20866739.469
22	20472710.957	20472708.317
30	21409458.601	21409456.663
Simulated codes epoch 9:00		
6	22116158.840	22116156.700
18	21523087.059	21523084.331
22	20265960.068	20265957.506
30	22291227.785	22291224.959
Simulated codes epoch 9:30		
6	21710588.392	21710586.262
18	22416250.610	22416248.148
22	20436289.228	20436287.628
30	23334107.326	23334105.329

Appendix IIB Ionosphere (IO) free delay observables

Appendix IIB provides two tables with GPS observations from the permanent station to the satellites that are free from the ionosphere bias. Appendix IIB Table 1 contains ionosphere free observables for epoch 9:00 where as Appendix IIB Table 2 contains ionosphere free observables for epoch 9:30. Details of the computation procedures have been given in section 6.1.2.3.

Appendix IIB Table 1 Ionosphere free observables (P3) epoch 9:00

P3 observables for epoch 9:00 am of 8 February, 2008				
Sat_{ID}	$P3_{MCS}(m)$	$P3_{PS1}(m)$	$P3_{PS2}(m)$	$P3_{PS3}(m)$
6	22082742.6767	22256529.1256	22308177.3078	22543007.2687
18	21666556.5254	21772970.0586	21915500.7516	22023530.0044
22	20452926.9270	20386838.5540	20527680.5965	20392514.3377
30	21754275.2108	21769060.4375	21497949.0315	21624311.7886
Sat_{ID}	$P3_{PS4}(m)$	$P3_{PS5}(m)$	$P3_{PS6}(m)$	$P3_{PS7}(m)$
6	22524173.0884	22206749.5369	21968011.9699	22284141.5564
18	21943661.1369	21689491.0644	21479758.4633	21687124.8612
22	20312920.1761	20339136.4232	20355217.6426	20267098.0355
30	21822548.6086	21916683.1534	22085553.7897	22111903.2272

Sat_{ID}	$P3_{PS8}(m)$	$P3_{PS9}(m)$
6	22465733.1471	22116153.3917
18	21784157.9429	21523080.1140
22	20219264.3963	20265953.5453
30	22262497.2328	22291220.5910

Appendix IIB Table 2 Ionosphere free observables (P3) epoch 9:30

	P3 observables for epoch 9:30 am of 8 February, 2008			
Sat_{ID}	Sat_{ID}	Sat_{ID}	Sat_{ID}	Sat_{ID}
6	21506675.6150	21684949.7845	21644150.0645	21919691.3710
18	22608435.0608	22740923.1644	22909004.9126	23043210.9213
22	20728737.2646	20698098.1328	20903322.8512	20795786.4311
30	22702783.1496	22718846.4177	22385002.4659	22534433.5614

Sat_{ID}	$P3_{PS4}(m)$	$P3_{PS5}(m)$	$P3_{PS6}(m)$	$P3_{PS7}(m)$
6	21964523.6820	21683578.8276	21501019.6229	21820109.1851
18	22944027.3867	22637151.1325	22373878.5215	22625275.8211
22	20672280.5469	20609245.0344	20537386.6283	20513073.7457
30	22772515.0923	22896337.7784	23099186.4302	23121799.2397

Sat_{ID}	$P3_{PS8}(m)$	$P3_{PS9}(m)$
6	22040667.2342	21710582.9695
18	22728135.7055	22416244.3429
22	20472599.2185	20436285.1540
30	23285205.5964	23334102.2404

Appendix IIC Troposphere free delay observables

Appendix IIC provide nine tables of the GPS observations from the permanent station to the satellites that are free from the troposphere bias. Each of the table in the Appendix IIB contains troposphere free observables for three different epochs that are 8:30, 9:00 and 9:30. Details of the computation procedures are in section 6.1.2.4.

Appendix IIC Table 1 Troposphere free observables from PS1

Satellite	Satellite elevation			Dry delay	Wet delay	Total delay
	deg	min	sec	(m)	(m)	(m)
6	29	39	10.107	4.654	0.404	5.058
18	61	30	0.618	2.627	0.228	2.855
22	70	18	7.723	2.453	0.212	2.665
30	60	39	55.641	2.648	0.229	2.878
Epoch :9:00:00am						
6	37	31	42.585	3.785	0.328	4.113
18	47	0	4.964	3.155	0.273	3.428
22	73	48	49.108	2.405	0.208	2.613
30	47	8	31.258	3.148	0.273	3.421
Epoch :9:30:00am						
6	45	11	28.086	3.252	0.282	3.534
18	33	26	19.868	4.182	0.363	4.544
22	64	39	50.772	2.555	0.221	2.776
30	34	11	58.469	4.100	0.356	4.456

The table is headed by "Epoch :8:30:00am" before the first data block.

Appendix IIC Table 2 Troposphere free observables from PS2

Epoch :8:30:00am						
Satellite	Satellite elevation			Dry delay	Wet delay	Total delay
	deg	min	sec	(m)	(m)	(m)
6	36	49	57.544	3.846	0.333	4.179
18	44	45	44.617	3.276	0.284	3.560
22	68	42	42.602	2.478	0.215	2.693
30	51	44	41.527	2.939	0.255	3.194
Epoch :9:00:00am						
6	36	49	57.544	3.846	0.333	4.179
18	44	45	44.617	3.276	0.284	3.560
22	68	42	42.602	2.478	0.215	2.693
30	51	44	41.527	2.939	0.255	3.194
Epoch :9:30:00am						
6	45	48	51.842	3.218	0.279	3.496
18	31	22	3.883	4.425	0.384	4.809
22	59	38	15.015	2.676	0.232	2.908
30	38	34	1.473	3.699	0.321	4.019

Appendix IIC Table 3 Troposphere free observables from PS3

Epoch :8:30:00am						
Satellite	Satellite elevation			Dry delay	Wet delay	Total delay
	deg	min	sec	(m)	(m)	(m)
6	25	59	58.653	5.247	0.456	5.703
18	57	25	41.617	2.739	0.237	2.977
22	73	36	7.612	2.407	0.208	2.616
30	62	37	45.322	2.600	0.225	2.825
Epoch :9:00:00am						
6	33	48	37.376	4.141	0.359	4.501
18	43	7	40.775	3.374	0.292	3.667
22	73	31	58.417	2.408	0.209	2.617
30	49	31	54.281	3.034	0.263	3.296
Epoch :9:30:00am						
6	41	40	47.632	3.469	0.301	3.769
18	29	45	33.664	4.639	0.402	5.042
22	62	7	39.947	2.612	0.226	2.838
30	36	34	18.101	3.869	0.335	4.205

Appendix IIC Table 4 Troposphere free observables from PS4

Epoch :8:30:00am						
Satellite	Satellite elevation			Dry delay	Wet delay	Total delay
	deg	min	sec	(m)	(m)	(m)
6	26	55	4.302	5.082	0.441	5.523
18	58	23	27.375	2.711	0.235	2.946
22	74	55	0.851	2.392	0.207	2.599
30	59	5	54.499	2.691	0.233	2.924
Epoch :9:00:00am						
6	34	3	2.627	4.116	0.357	4.473
18	44	19	24.975	3.302	0.286	3.588
22	77	12	3.539	2.368	0.205	2.574
30	46	16	45.430	3.193	0.277	3.469
Epoch :9:30:00am						
6	41	2	28.772	3.513	0.304	3.817
18	30	56	33.461	4.479	0.389	4.868
22	65	19	16.483	2.541	0.220	2.761
30	33	31	19.172	4.173	0.362	4.534

Appendix IIC Table 5 Troposphere free observables from PS5

Epoch :8:30:00am						
Satellite	Satellite elevation			Dry delay	Wet delay	Total delay
	deg	min	sec	(m)	(m)	(m)
6	30	46	20.699	4.502	0.390	4.892
18	62	44	7.859	2.598	0.225	2.823
22	70	24	19.357	2.451	0.212	2.664
30	58	12	5.530	2.716	0.235	2.952
Epoch :9:00:00am						
6	38	11	38.825	3.729	0.323	4.052
18	48	21	16.611	3.088	0.268	3.356
22	75	54	58.610	2.381	0.206	2.587
30	44	48	47.304	3.274	0.284	3.557
Epoch :9:30:00am						
6	45	12	27.551	3.251	0.282	3.533
18	34	44	37.108	4.044	0.351	4.395
22	67	9	22.829	2.506	0.217	2.723
30	31	59	21.657	4.349	0.377	4.726

Appendix IIC Table 6 Troposphere free observables from PS6

Epoch :8:30:00am						
Satellite	Satellite elevation			Dry delay	Wet delay	Total delay
	deg	min	sec	(m)	(m)	(m)
6	34	9	56.571	4.104	0.356	4.460
18	66	28	59.840	2.518	0.218	2.736
22	67	5	28.774	2.507	0.217	2.724
30	55	50	41.700	2.790	0.242	3.031
Epoch :9:00:00am						
6	41	31	10.742	3.480	0.302	3.781
18	51	58	51.367	2.930	0.254	3.184
22	75	9	53.499	2.389	0.207	2.596
30	42	17	8.634	3.428	0.297	3.726
Epoch :9:30:00am						
6	48	7	17.451	3.099	0.269	3.368
18	38	11	51.511	3.729	0.323	4.052
22	69	25	8.252	2.467	0.214	2.680
30	29	33	4.351	4.669	0.405	5.074

Appendix IIC Table 7 Troposphere free observables from PS7

Epoch :8:30:00am						
Satellite	Satellite elevation			Dry delay	Wet delay	Total delay
	deg	min	sec	(m)	(m)	(m)
6	30	37	36.567	4.521	0.392	4.913
18	62	16	37.757	2.608	0.226	2.834
22	72	1	10.102	2.428	0.210	2.638
30	54	53	5.449	2.822	0.244	3.066
Epoch :9:00:00am						
6	37	10	2.796	3.816	0.331	4.147
18	48	24	0.356	3.086	0.267	3.353
22	79	57	49.001	2.346	0.203	2.549
30	41	54	50.716	3.453	0.299	3.752
Epoch :9:30:00am						
6	43	9	7.570	3.373	0.292	3.665
18	34	54	4.475	4.028	0.349	4.378
22	70	13	31.790	2.454	0.213	2.667
30	29	17	44.826	4.705	0.408	5.114

Appendix IIC Table 8 Troposphere free observables from PS8

Epoch :8:30:00am						
Satellite	Satellite elevation			Dry delay	Wet delay	Total delay
	deg	min	sec	(m)	(m)	(m)
6	29	6	1.665	4.734	0.411	5.145
18	60	2	0.741	2.665	0.231	2.896
22	74	12	1.291	2.400	0.208	2.608
30	52	13	14.955	2.920	0.253	3.173
Epoch :9:00:00am						
6	34	49	7.182	4.037	0.350	4.387
18	46	50	1.396	3.164	0.274	3.438
22	84	3	22.868	2.322	0.201	2.523
30	39	47	37.178	3.603	0.312	3.916
Epoch :9:30:00am						
6	39	59	53.469	3.588	0.311	3.899
18	33	36	40.757	4.163	0.361	4.524
22	71	40	59.838	2.433	0.211	2.643
30	27	24	46.250	4.998	0.434	5.432

Appendix IIC Table 9 Troposphere free observables from PS9

Epoch :8:30:00am						
Satellite	Satellite elevation			Dry delay	Wet delay	Total delay
	deg	min	sec	(m)	(m)	(m)
6	33	13	36.649	4.205	0.365	4.570
18	64	56	36.989	2.549	0.221	2.770
22	69	23	11.002	2.467	0.214	2.681
30	52	26	54.287	2.911	0.252	3.164
Epoch :9:00:00am						
6	39	26	36.072	3.630	0.315	3.945
18	51	12	37.491	2.961	0.257	3.218
22	80	1	47.369	2.345	0.203	2.548
30	39	22	39.582	3.635	0.315	3.950
Epoch :9:30:00am						
6	44	48	13.882	3.274	0.284	3.558
18	37	38	1.406	3.776	0.327	4.103
22	73	4	20.473	2.414	0.209	2.623
30	26	50	22.083	5.096	0.442	5.538

Appendix IID Double difference (DD) ionosphere free observables for TZRF10 Scenario 2

Appendix IID provides double difference ionosphere free observables between the reference stations and the adjusted station for the selected pairs of satellites for the TZRF10 Scenario 2. Details of the computation procedure has been discussed in section 6.1.2.5

Appendix IID Table 1 Double difference IO observables (m) PRN 6-18

Epoch	$DDI_{PS5-MCS}$	$DDI_{PS5-PS2}$	$DDI_{PS5-PS4}$	$DDI_{PS5-PS6}$
8:30	33601.196	-90017.084	-142886.139	-28121.920
9:00	101072.321	124581.916	-63253.479	-164316.732
9:30	148187.141	311282.543	25931.400	-266103.834

Epoch	$DDI_{PS5-PS8}$	$DDI_{PS5-PS9}$		
8:30	115585.630	135940.568		
9:00	-75814.805	29004.966		
9:30	-247910.931	-80713.406		

Appendix IID Table 2 Double difference IO observables (m) PRN 6-30

Epoch	$DDI_{PS5-MCS}$	$DDI_{PS5-PS2}$	$DDI_{PS5-PS4}$	$DDI_{PS5-PS6}$
8:30	-73094.073	-541550.576	-370912.695	162254.358
9:00	-38401.082	-520161.893	-411558.096	86830.469
9:30	-16651.416	-471906.549	-404767.541	31779.411

Epoch	$DDI_{PS5-PS8}$	$DDI_{PS5-PS9}$
8:30	491128.801	388758.349
9:00	465133.583	407608.203
9:30	410760.320	385407.856

Appendix IID Table 3 Double difference IO observables (m) PRN 30-18

Epoch	$DDI_{PS5-MCS}$	$DDI_{PS5-PS2}$	$DDI_{PS5-PS4}$	$DDI_{PS5-PS6}$
8:30	106695.269	451533.492	228026.556	-190376.279
9:00	139473.404	644743.809	348304.617	-251147.201
9:30	164838.557	783189.093	430698.940	-297883.245

Epoch	$DDI_{PS5-PS8}$	$DDI_{PS5-PS9}$
8:30	-375543.171	-252817.780
9:00	-540948.388	-378603.237
9:30	-658671.252	-466121.263

Appendix IID Table 4 Double difference IO observables PRN (m) 22-30

Epoch	$DDI_{PS5-MCS}$	$DDI_{PS5-PS2}$	$DDI_{PS5-PS4}$	$DDI_{PS5-PS6}$
8:30	-236825.136	-379161.258	74368.302	403531.289
9:00	-276198.446	-607278.295	-67918.298	465686.106
9:30	-313046.859	-805413.129	-186858.199	525513.634

Epoch	$DDI_{PS5-PS8}$	$DDI_{PS5-PS9}$
8:30	261627.993	9962.276
9:00	447720.315	152789.417
9:30	610724.342	274707.058

Appendix IIE Double difference (DD) ionosphere free observables for TZRF10 Scenario 3

Appendix IIE provides double difference ionosphere free observables between the reference stations and the adjusted station for the selected pairs of satellites for the TZRF10 Scenario 3. Details of the computation procedure have been discussed in section 6.1.2.5

Appendix IIE Table 1- PRN 6-18 double difference IO observables (m)

Epoch	$DDI_{PS9-PS5}$	$DDI_{PS9-MCS}$	$DDI_{PS9-PS4}$
8:30	-115585.630	-81984.434	-258471.769
9:00	75814.805	176887.126	12561.326
9:30	247910.931	396098.072	273842.331

Appendix IIE Table 2- PRN 6-30 double difference IO observables (m)

Epoch	$DDI_{PS9-PS5}$	$DDI_{PS9-MCS}$	$DDI_{PS9-PS4}$
8:30	-491128.801	-564222.874	-862041.496
9:00	-465133.583	-503534.665	-876691.679
9:30	-410760.320	-427411.736	-815527.861

Appendix IIE Table 3 - PRN 30-18 double difference IO observables (m)

Epoch	$DDI_{PS9-PS5}$	$DDI_{PS9-MCS}$	$DDI_{PS9-PS4}$
8:30	375543.171	482238.440	603569.727
9:00	540948.388	680421.792	889253.005
9:30	658671.252	823509.809	1089370.192

Appendix IIE Table 4 - PRN 22-30 double difference IO observables (m)

Epoch	$DDI_{PS9-PS5}$	$DDI_{PS9-MCS}$	$DDI_{PS9-PS4}$
8:30	-261627.993	-498453.129	-187259.691
9:00	-447720.315	-723918.762	-515638.613
9:30	-610724.342	-923771.201	-797582.541

Appendix IIF Double difference troposphere (DDT) free observables (m) for TZRF10 Scenario 2

Appendix IIF provides double difference troposphere (DDT) free observables between the reference stations and the adjusted station for the selected pairs of satellites for the TZRF10 Scenario 2. Details of the computation procedure have been discussed in section 6.1.2.6

Appendix IIF Table 1- DDT free observables (m) for PRN 6-18

Epoch	$DDT_{PS5-MCS}$	$DDT_{PS5-PS2}$	$DDT_{PS5-PS4}$	$DDT_{PS5-PS6}$
8:30	0.0848	-0.3413	-0.5083	-0.1791
9:00	0.1250	0.0779	-0.1880	-0.2522
9:30	0.1198	0.4506	0.1889	-0.2371
Epoch	$DDT_{PS5-PS8}$	$DDT_{PS5-PS9}$		
8:30	0.2695	0.3465		
9:00	-0.0302	0.0991		
9.30	-0.3164	-0.1778		

Appendix IIF Table 2- DDT free observables (m) for PRN 6-30

Epoch	$DDT_{PS5-MCS}$	$DDT_{PS5-PS2}$	$DDT_{PS5-PS4}$	$DDT_{PS5-PS6}$
8:30	0.0127	-0.6336	-0.6593	-0.0308
9:00	-0.0044	-0.4901	-0.5082	0.0242
9:30	-0.1324	-0.6700	-0.4756	0.3402

Epoch	$DDT_{PS5-PS8}$	$DDT_{PS5-PS9}$
8:30	0.5342	0.5122
9:00	0.5007	0.4395
9:30	0.7876	0.5128

Appendix IIF Table 3- DDT free observables (m) for PRN 30-18

Epoch	$DDT_{PS5-MCS}$	$DDT_{PS5-PS2}$	$DDT_{PS5-PS4}$	$DDT_{PS5-PS6}$
8:30	0.0721	0.2923	0.1511	-0.1483
9:00	0.1294	0.5680	0.3202	-0.2764
9:30	0.2522	1.1206	0.6645	-0.5773

Epoch	$DDT_{PS5-PS8}$	$DDT_{PS5-PS9}$
8:30	-0.2647	-0.1657
9:00	-0.5309	-0.3404
9:30	-1.1040	-0.6906

Appendix IIF Table 4-DDT free observables (m) for PRN 22-30

Epoch	$DDT_{PS5-MCS}$	$DDT_{PS5-PS2}$	$DDT_{PS5-PS4}$	$DDT_{PS5-PS6}$
8:30	-0.1490	-0.2393	0.0366	0.2772
9:00	-0.2121	-0.4690	-0.0741	0.4224
9:30	-0.3646	-0.8912	-0.2299	0.7857

Epoch	$DDT_{PS5-PS8}$	$DDT_{PS5-PS9}$
8:30	0.1946	0.0192
9:00	0.4320	0.1596
9:30	0.9122	0.3902

Appendix IIG Double difference troposphere (DDT) free observables for TZRF10 Scenario 3

Appendix IIG provides double difference troposphere (DDT) free observables between the reference stations and the adjusted station for the selected pairs of satellites for the TZRF10 Scenario 3. Details of the computation procedure have been discussed in section 6.1.2.6

Appendix IIG Table 1- DDT free observables (m) for PRN 6-18

Epoch	$DDT_{PS9-PS5}$	$DDT_{PS9-MCS}$	$DDT_{PS9-PS4}$
8:30	-0.2695	-0.1847	-0.7778
9:00	0.0302	0.1553	-0.1577
9:30	0.3164	0.4362	0.5053

Appendix IIG Table 2- DDT free observables (m) for PRN 6-30

Epoch	$DDT_{PS9-PS5}$	$DDT_{PS9-MCS}$	$DDT_{PS9-PS4}$
8:30	-0.5342	-0.5215	-1.1935
9:00	-0.5007	-0.5050	-1.0089
9:30	-0.7876	-0.9201	-1.2633

Appendix IIG Table 3- DDT free observables (m) for PRN 30-18

Epoch	$DDT_{PS9-PS5}$	$DDT_{PS9-MCS}$	$DDT_{PS9-PS4}$
8:30	0.2647	0.3368	0.4158
9:00	0.5309	0.6603	0.8511
9:30	1.1040	1.3562	1.7685

Appendix IIG Table 4- DDT free observables (m) for PRN 22-30

Epoch	$DDT_{PS9-PS5}$	$DDT_{PS9-MCS}$	$DDT_{PS9-PS4}$
8:30	-0.1946	-0.3436	-0.1580
9:00	-0.4320	-0.6440	-0.5061
9:30	-0.9122	-1.2768	-1.1420

Appendix III System maintenance results

Appendix III contains the results of a case study on frame maintenance in. Details of the results and the computation procedures are in sections 6.2 and 7.2.

Appendix III Table 1 Differences in the computed results -1

Station-ID		GSB Values	Computed values	Differences
ALBH	STAX	-2341332.9570	-2341332.9446	-0.0124
	STAY	-3539049.4896	-3539049.4907	0.0011
	STAZ	4745791.2729	4745791.2853	-0.0124
ALGO	STAX	918129.3561	918129.3755	-0.0194
	STAY	-4346071.2433	-4346071.2382	-0.0051
	STAZ	4561977.8122	4561977.8125	-0.0003
ALRT	STAX	388042.6777	388042.6955	-0.0178
	STAY	-740382.3782	-740382.3715	-0.0067
	STAZ	6302001.8595	6302001.8694	-0.0099
AMC2	STAX	-1248596.2053	-1248596.1922	-0.0131
	STAY	-4819428.1893	-4819428.1975	0.0082
	STAZ	3976505.9441	3976505.9574	-0.0133
BAIE	STAX	1546823.2793	1546823.3030	-0.0237
	STAY	-3879765.1099	-3879765.1145	0.0046
	STAZ	4804185.0152	4804185.0250	-0.0098

Appendix III Table 2 Differences in the computed results-2

Station-ID		GSB Values	Computed values	Differences
BAKE	STAX	-289834.0069	-289833.9912	-0.0157
	STAY	-2756501.0472	-2756501.0476	0.0004
	STAZ	5725162.2094	5725162.2275	-0.0181
BARH	STAX	1693644.8236	1693644.846	-0.0221
	STAY	-4239067.5430	-4239067.543	0.0003
	STAZ	4439567.1932	4439567.198	-0.0050
CAGS	STAX	1096349.0350	1096349.0553	-0.0203
	STAY	-4335060.5841	-4335060.5820	-0.0021
	STAZ	4533255.1533	4533255.1568	-0.0035
CHUR	STAX	-236438.8735	-236438.8556	-0.0179
	STAY	-3307616.8299	-3307616.8302	0.0003
	STAZ	5430049.1899	5430049.2035	-0.0136
CHWK	STAX	-2215259.8358	-2215259.8247	-0.0111
	STAY	-3543996.8084	-3543996.8136	0.0052
	STAZ	4802098.6726	4802098.6870	-0.0144
DRAO	STAX	-2059164.8299	-2059164.8022	-0.0277
	STAY	-3621108.3993	-3621108.3759	-0.0234
	STAZ	4814432.3079	4814432.2906	0.0173

Appendix III Table 3 Differences in the computed results-3

Station-ID		GSB Values	Computed values	Differences
DUBO	STAX	-417603.7043	-417603.6874	-0.0169
	STAY	-4064529.7719	-4064529.7764	0.0045
	STAZ	4881432.1035	4881432.1186	-0.0151
ESCU	STAX	1852954.5095	1852954.5308	-0.0213
	STAY	-3937498.7402	-3937498.7380	-0.0022
	STAZ	4647314.6112	4647314.6165	-0.0053
FLIN	STAX	-766174.5778	-766174.5605	-0.0173
	STAY	-3611375.3008	-3611375.3018	0.0010
	STAZ	5184056.1726	5184056.1859	-0.0133
FRDN	STAX	1760542.7404	1760542.7624	-0.0220
	STAY	-4080067.9620	-4080067.9620	0.0000
	STAZ	4560178.5186	4560178.5231	-0.0045
HLFX	STAX	2018905.7550	2018905.7783	-0.0233
	STAY	-4069070.4746	-4069070.4770	0.0024
	STAZ	4462415.3744	4462415.3809	-0.0065
HOLB	STAX	-2503040.5225	-2503040.5110	-0.0115
	STAY	-3188233.2876	-3188233.2897	0.0021
	STAZ	4908701.4344	4908701.4496	-0.0152

Appendix III Table 4 Differences in the computed results-4

Station-ID		GSB Values	Computed values	Differences
HOLM	STAX	-983072.0124	-983071.9956	-0.0168
	STAY	-1867623.6408	-1867623.6338	-0.0070
	STAZ	5998639.5140	5998639.5212	-0.0072
INVK	STAX	-1628432.1318	-1628432.1154	-0.0164
	STAY	-1714393.0378	-1714393.0313	-0.0065
	STAZ	5903844.6536	5903844.6599	-0.0063
KUUJ	STAX	772857.5197	772857.5382	-0.0185
	STAY	-3558198.7081	-3558198.7038	-0.0043
	STAZ	5219095.8704	5219095.8737	-0.0033
LPOC	STAX	1480313.1383	1480313.1594	-0.0211
	STAY	-4069017.6041	-4069017.6022	-0.0019
	STAZ	4667642.4816	4667642.4850	-0.0034
NAIN	STAX	1671836.6236	1671836.6454	-0.0218
	STAY	-3103473.2735	-3103473.2733	-0.0002
	STAZ	5297671.1713	5297671.1788	-0.0075
NANO	STAX	-2335726.8164	-2335726.8038	-0.0126
	STAY	-3451608.3104	-3451608.3110	0.0006
	STAZ	4812009.8956	4812009.9084	-0.0128

Appendix III Table 5 Differences in the computed results-5

Station-ID		GSB Values	Computed values	Differences
NLIB	STAX	-130934.6185	-130934.6009	-0.0176
	STAY	-4762291.6926	-4762291.7046	0.0120
	STAZ	4226854.5959	4226854.6159	-0.0200
NRC1	STAX	1112777.1786	1112777.1980	-0.0194
	STAY	-4341475.8283	-4341475.8234	-0.0049
	STAZ	4522955.7731	4522955.7736	-0.0005
PICL	STAX	-11253.0847	-11253.0652	-0.0195
	STAY	-3980586.6678	-3980586.6732	0.0054
	STAZ	4967210.1975	4967210.2121	-0.0146
PRDS	STAX	-1659602.9925	-1659602.9791	-0.0134
	STAY	-3676725.7560	-3676725.7562	0.0002
	STAZ	4925493.4914	4925493.5024	-0.0110
QAQ1	STAX	2170942.0788	2170942.0983	-0.0195
	STAY	-2251829.9461	-2251829.9393	-0.0068
	STAZ	5539988.2967	5539988.3025	-0.0058
QIKI	STAX	1069081.2539	1069081.2724	-0.0185
	STAY	-2195214.1784	-2195214.1711	-0.0073
	STAZ	5872518.9774	5872518.9820	-0.0046

Appendix III Table 6 Differences in the computed results-6

Station-ID		GSB Values	Computed values	Differences
RESO	STAX	-144107.6057	-144107.5879	-0.0178
	STAY	-1683119.7865	-1683119.7779	-0.0086
	STAZ	6129763.2511	6129763.2559	-0.0048
SASK	STAX	-1106129.7054	-1106129.6898	-0.0156
	STAY	-3758704.8556	-3758704.8567	0.0011
	STAZ	5016675.4491	5016675.4625	-0.0134
SCH2	STAX	1448636.7569	1448636.7775	-0.0206
	STAY	-3385243.6850	-3385243.6820	-0.0030
	STAZ	5191047.0061	5191047.0095	-0.0034
STJO	STAX	2612631.0697	2612631.0930	-0.0233
	STAY	-3426807.0138	-3426807.0117	-0.0021
	STAZ	4686757.8354	4686757.8403	-0.0049
THU3	STAX	538093.5258	538093.5439	-0.0181
	STAY	-1389088.0333	-1389088.0253	-0.0080
	STAZ	6180979.2084	6180979.2179	-0.0095
TUKT	STAX	-1532091.3622	-1532091.3463	-0.0159
	STAY	-1643291.6837	-1643291.6778	-0.0059
	STAZ	5949315.9093	5949315.9186	-0.0093

Appendix III Table 7 Differences in the computed results-7

UCLU	STAX	-2440669.0769	-2440669.0651	-0.0118
	STAY	-3416437.0527	-3416437.0547	0.0020
	STAZ	4785136.7819	4785136.7957	-0.0138
USNO	STAX	1112189.7540	1112189.7717	-0.0177
	STAY	-4842955.0006	-4842954.9978	-0.0028
	STAZ	3985352.2203	3985352.2223	-0.0020
VALD	STAX	919075.7857	919075.8069	-0.0212
	STAY	-4167766.2258	-4167766.2249	-0.0009
	STAZ	4724323.4979	4724323.5031	-0.0052
WES2	STAX	1492233.2261	1492233.2489	-0.0228
	STAY	-4458089.4588	-4458089.4619	0.0031
	STAZ	4296045.9849	4296045.9923	-0.0074
WHIT	STAX	-2218337.9594	-2218337.9437	-0.0157
	STAY	-2201205.1002	-2201205.0953	-0.0049
WILL	STAX	-2084258.1577	-2084258.1441	-0.0136
	STAY	-3313872.9741	-3313872.9730	-0.0011
	STAZ	4872522.1267	4872522.1375	-0.0108
YELL	STAX	-1224452.6809	-1224452.6647	-0.0162
	STAY	-2689216.1240	-2689216.1199	-0.0041
	STAZ	5633638.2284	5633638.2398	-0.0114

Appendix IV Matlab codes

Appendix IV provides different matlab software codes developed by the author as part of the three case studies as follows.

Appendix IV.1 Covariance analysis matlab code

This matlab software code has two main parts, which are network adjustment and determination of the error ellipses. With reference to the discussions in section 6.1, the first part of the program inputs the precise satellites position for three different epochs along with the approximate position of the network points to be analyzed and the pseudorange observations from those stations. The input observations are corrected for ionosphere delays and troposphere delay and then used to form ionosphere and troposphere double differences in the due cause of adjustment of the approximate positions.

The second part uses the covariance matrices of the adjusted positions to determine the a-priori variance factor and the parameters of the standard error ellipse at 95 percent confidence level using the expansion factors from χ^2 distribution. The outputs are plotted along with the map of the case study area- Tanzania.

```
%JAMES MTAMAKAYA S#3206337
%COVARIANCE ANALYSIS PART I-"RELATIVE POSITIONING USING GPS"
%---------------STEP (1) and its INPUTS:   ------------------------
%1- Initial values for the Station Coordinates.
%2- Satellite Coordinates
%3- Pseudorange range observations (P1 and P2)
%4- Map of Tanzania
% 1- APPROXIMATE COORDINATES OF THE SATIONS********************
 format long g
SMD=load('covsmd_ps.txt'); ps=SMD
% ---------Loading the map of Tanzania----------------
it_B=load('covTz_itB.txt');
is_B=load('covTz_isB.txt');
cl_B=load('covTz_clB.txt');
rg_B=load('covTz_rgB.txt');
itb=load('tzitb.txt');
ib_l1=load('itbl1.txt');
ib_l2=load('itbl2.txt');
ib_l3=load('itbl3.txt');
ib_l4=load('itbl4.txt');
ib_l5=load('covTz_nyasa.txt');
ib_l6=load('covTz_nyika.txt');  ib_l7=load('covTz_nyaza4.txt');
 %------------Redefining Tanzania map boundary for plotting
purposes-----------------
it_B1=it_B(:,1);it_B2=it_B(:,2);
is_B1=is_B(:,1);is_B2=is_B(:,2);
cl_B1=cl_B(:,1);cl_B2=cl_B(:,2);
rg_B1=rg_B(:,1);rg_B2=rg_B(:,2);
q1=itb(:,1);q2=itb(:,2);
k1=ib_l1(:,1);k2=ib_l1(:,2);
l1=ib_l2(:,1);l2=ib_l2(:,2);
m1=ib_l3(:,1);m2=ib_l3(:,2);
n1=ib_l4(:,1);n2=ib_l4(:,2);
z11=ib_l5(:,1);z12=ib_l5(:,2);
z21=ib_l6(:,1);z22=ib_l6(:,2);
z31=ib_l7(:,1);z32=ib_l7(:,2);

% establishing the earth centered matrix for each of the permanent
stations
ecf_ps1=zeros(12,3); ecf_ps2=zeros(12,3); ecf_ps3=zeros(12,3);
ecf_ps4=zeros(12,3) ; ecf_ps5=zeros(12,3);ecf_ps6=zeros(12,3);
ecf_ps7=zeros(12,3); ecf_ps8=zeros(12,3); ecf_ps9=zeros(12,3);
ecf_ps10=zeros(12,3);
ecf_ps1(:,1)=ps(1,1);ecf_ps1(:,2)=ps(1,2);ecf_ps1(:,3)=ps(1,3);
ecf_ps2(:,1)=ps(2,1);ecf_ps2(:,2)=ps(2,2);ecf_ps2(:,3)=ps(2,3);
ecf_ps3(:,1)=ps(3,1);ecf_ps3(:,2)=ps(3,2);ecf_ps3(:,3)=ps(3,3);
ecf_ps4(:,1)=ps(4,1);ecf_ps4(:,2)=ps(4,2);ecf_ps4(:,3)=ps(4,3);
ecf_ps5(:,1)=ps(5,1);ecf_ps5(:,2)=ps(5,2);ecf_ps5(:,3)=ps(5,3);
ecf_ps6(:,1)=ps(6,1);ecf_ps6(:,2)=ps(6,2);ecf_ps6(:,3)=ps(6,3);
ecf_ps7(:,1)=ps(7,1);ecf_ps7(:,2)=ps(7,2);ecf_ps7(:,3)=ps(7,3);
ecf_ps8(:,1)=ps(8,1);ecf_ps8(:,2)=ps(8,2);ecf_ps8(:,3)=ps(8,3);
ecf_ps9(:,1)=ps(9,1);ecf_ps9(:,2)=ps(9,2);ecf_ps9(:,3)=ps(9,3);
ecf_ps10(:,1)=ps(10,1);ecf_ps10(:,2)=ps(10,2);ecf_ps10(:,3)=ps(10,3)
```

```
%2- input coordinates (m) for satellite 6, 18, 22 and 30 from sp3
file *****
satcor_s1 = load('covsmd_sat1.txt'); % coordinates for epoch 8.30
satcor_s2 = load('covsmd_sat2.txt'); % coordinates for epoch 9.00
satcor_s3 = load('covsmd_sat3.txt'); % coordinates for epoch 9.30
satcord = [satcor_s1;satcor_s2;satcor_s3];
Xsat=satcord(:,1);Ysat=satcord(:,2);Zsat=satcord(:,3);
 %Relative Earth-Centered Cartesian Coordinates that is differences
%between satellite position and the permanent stations points
 dps1_Sat=satcord-ecf_ps1; dps2_Sat=satcord-ecf_ps2;
dps3_Sat=satcord-ecf_ps3;
dps4_Sat=satcord-ecf_ps4; dps5_Sat=satcord-ecf_ps5;
dps6_Sat=satcord-ecf_ps6; dps7_Sat=satcord-ecf_ps7;
dps8_Sat=satcord-ecf_ps8; dps9_Sat=satcord-ecf_ps9;
dps10_Sat=satcord-ecf_ps10;

% Rearranging Relative Earth-Centered Cartesian Coordinates for
% elevation computations

dX_ps1=dps1_Sat(:,1);dY_ps1=dps1_Sat(:,2);dZ_ps1=dps1_Sat(:,3);
dX_ps2=dps2_Sat(:,1);dY_ps2=dps2_Sat(:,2);dZ_ps2=dps2_Sat(:,3);
dX_ps3=dps3_Sat(:,1);dY_ps3=dps3_Sat(:,2);dZ_ps3=dps3_Sat(:,3);
dX_ps4=dps4_Sat(:,1);dY_ps4=dps4_Sat(:,2);dZ_ps4=dps4_Sat(:,3);
dX_ps5=dps5_Sat(:,1);dY_ps5=dps5_Sat(:,2);dZ_ps5=dps5_Sat(:,3);
dX_ps6=dps6_Sat(:,1);dY_ps6=dps6_Sat(:,2);dZ_ps6=dps6_Sat(:,3);
dX_ps7=dps7_Sat(:,1);dY_ps7=dps7_Sat(:,2);dZ_ps7=dps7_Sat(:,3);
dX_ps8=dps8_Sat(:,1);dY_ps8=dps8_Sat(:,2);dZ_ps8=dps8_Sat(:,3);
dX_ps9=dps9_Sat(:,1);dY_ps9=dps9_Sat(:,2);dZ_ps9=dps9_Sat(:,3);
dX_ps10=dps10_Sat(:,1);dY_ps10=dps10_Sat(:,2);dZ_ps10=dps10_Sat(:,3)

dX_ps=[dX_ps1,dX_ps2,dX_ps3,dX_ps4,dX_ps5,dX_ps6,dX_ps7,dX_ps8,dX_ps
9,dX_ps10];
dY_ps=[dY_ps1,dY_ps2,dY_ps3,dY_ps4,dY_ps5,dY_ps6,dY_ps7,dY_ps8,dY_ps
9,dY_ps10];
dZ_ps=[dZ_ps1,dZ_ps2,dZ_ps3,dZ_ps4,dZ_ps5,dZ_ps6,dZ_ps7,dZ_ps8,dZ_ps
9,dZ_ps10];
%*****************************************************************

%STEP (2) COMPUTATION OF TROPOSPHERE DELAY AT EACH STATION%Reference
Vanicek & Krakiwsky [1986, pp.316] for further reading
% inputs 1 are the semi major and semi minor axes of the ellipsoid:
a = 6378137; b = 6356752.3142; % these are for the GRS 80 ellipsoid.
  % inputs 2 are the constants to compute the troposphere delays
Kdry=2.31; Kwet = 0.20;
theta_dry = deg2rad(2.5); theta_wet = deg2rad(1.5);
 % 2.1- Compute the latitude, longitude and height from the geodetic
coordinates of
 % the stations using a function covcart2geod
X=ps(:,1);Y= ps(:,2);Z=ps(:,3);
[fi,h] = covsmdct2geod(X,Y,Z,a,b);
 for i=1:10;
    ps_x=ps(i,1); ps_y=ps(i,2);
    lbd3= covget_lambda(ps_x, ps_y); lbd4(i,:)=lbd3;
end
```

```
lbd=lbd4;
 lat_deci = fi.*180./pi;long_deci = lbd.*180./pi;ht_ps=h;
g_crd=[fi,lbd,h];




 % 2.3 Compute the elevation angles from permanent stations to the 4
% satellites at 3 epochs using the covelev_angle function
 ps_elv1=zeros(12,10);
j=1;
for i=1:10;
    fi1=g_crd(i,1);lbd1=g_crd(i,2); dX= dX_ps(:,j); dY=
dY_ps(:,j);dZ= dZ_ps(:,j);
    [Elv,Tp_crd] = covelev_angle(fi1,lbd1,dX,dY,dZ);
    Elv_ps=Elv;Tp_ps1=Tp_crd; ps_elv(:,i)=Elv_ps;
    j=j+1;
  end
ps_elv1=ps_elv;
 % 2.3 compute the troposphere delays at each station using the
satellite elevation angles from 2.2 above
ps_tpdly=zeros(12,10);
for i=1:10;
Td_ps = (Kdry./ (sin(sqrt((ps_elv(:,i).^2) + (theta_dry^2))))) +
(Kwet./ (sin(sqrt((ps_elv(:,i).^2) + (theta_wet^2)))));
ps_tpdly(:,i)=Td_ps;
end;
ps_tpdelay=ps_tpdly;



% ****STEP 3- REARRANGE THE SATELLITE COORDINATES ***
 Epoch1sat6  = satcor_s1(1,1:3); Epoch1sat18 = satcor_s1(2,1:3);
Epoch1sat22 = satcor_s1(3,1:3);Epoch1sat30 = satcor_s1(4,1:3);

Epoch2sat6  = satcor_s2(1,1:3);Epoch2sat18 = satcor_s2(2,1:3);
Epoch2sat22 = satcor_s2(3,1:3);Epoch2sat30 = satcor_s2(4,1:3);

 Epoch3sat6  = satcor_s3(1,1:3);Epoch3sat18 = satcor_s3(2,1:3);
Epoch3sat22 = satcor_s3(3,1:3);Epoch3sat30 = satcor_s3(4,1:3);

%*****************************************************************


%3.1- Load and rearrange pseudorange observations
% computed from the approximate positions of the permanent stations
 ps_p1p2 = load('covsmd_p1p2.txt');
ps_p3a=zeros(12,10);
for i=1:10;
    p=12*i; j=p-11; ps_p3a(:,i)=ps_p3b(j:p);
end;
ps_p3=ps_p3a;
****************************************************************
% 3.2 Compute the ionosphere free observables - p3 comps
%3.2.1- p3 comps for satellite 6
f1 = 1575.42; f2 = 1227.60; % all frequencies in MHz
```

```matlab
ps_p3b = ((ps_p1p2(:,2) * f1.^2) - (ps_p1p2(:,3) * f2.^2) )./(f1.^2
- f2.^2);
j=1;
psx_p3_st=zeros(3,2);
for k=1:10;
    for i=1:4:12;
    ps_p3_sa=ps_p3(:,k); ps_p3_sb(j,1) = ps_p3_sa(i);  j=j+1;
    end
 psx_p3_st(:,k)=ps_p3_sb((3*k-2):3*k);
end
ps_p3_s6=psx_p3_st;
 %3.2.2- p3 comps for satellite 18
 j=1; psx_p3_st=zeros(3,2);
for k=1:10;
    for i=2:4:12;
    ps_p3_sa=ps_p3(:,k);
    ps_p3_sb(j,1) = ps_p3_sa(i); j=j+1;
    end
    psx_p3_st(:,k)=ps_p3_sb((3*k-2):3*k);
end
ps_p3_s18=psx_p3_st;
%3.2.3- p3 comps for satellite 22
 j=1; psx_p3_st=zeros(3,2);
for k=1:10;
    for i=3:4:12;
    ps_p3_sa=ps_p3(:,k);
    ps_p3_sb(j,1) = ps_p3_sa(i);
    j=j+1;
    end
    psx_p3_st(:,k)=ps_p3_sb((3*k-2):3*k);
end
ps_p3_s22=psx_p3_st;
 %3.2.4- p3 comps for satellite 30
 j=1; psx_p3_st=zeros(3,2);
for k=1:10;
    for i=4:4:12;
    ps_p3_sa=ps_p3(:,k); ps_p3_sb(j,1) = ps_p3_sa(i); j=j+1;
    end
    psx_p3_st(:,k)=ps_p3_sb((3*k-2):3*k);
end
ps_p3_s30=psx_p3_st;
```

```
%3.3 Double differences of ionosphere free observables between
satellites from the
% reference stations MCS to all reference stations (PS1 to PS9) -
each  vector
 %contains IO free observables for satellite pairs: (6-18, 6-30, 30-
18, 22-30)
3.3.1 Double difference for satellite pair 6-18
 for k=2:10;
         for i=1:3;
         dd_sta(i,1)  = (ps_p3_s6(i,1)-ps_p3_s18(i,1))-
(ps_p3_s6(i,k)-ps_p3_s18(i,k));
      end
 dd_st(:,k-1)=  dd_sta;
       end
dd_ps6_18=dd_st;
% 3.3.2 Double difference ionosphere free observables for satellite
pair 6-30
 for k=2:10;
         for i=1:3;
         dd_sta(i,1)  = (ps_p3_s6(i,1)-ps_p3_s30(i,1))-
(ps_p3_s6(i,k)-ps_p3_s30(i,k));
      end
 dd_st(:,k-1)=  dd_sta;
   end
dd_ps6_30=dd_st;




% 3.3.4 Double difference ionosphere free observables for satellite
pair 30-18
 for k=2:10;
       for i=1:3;
        dd_sta(i,1)  = (ps_p3_s30(i,1)-ps_p3_s18(i,1))-
(ps_p3_s30(i,k)-ps_p3_s18(i,k));
      end
 dd_st(:,k-1)=  dd_sta;
 end
dd_ps30_18=dd_st;
  % 3.3.3 Double difference ionosphere free observables for
satellite pair 22-30
 for k=2:10;
     for i=1:3;
         dd_sta(i,1)  = (ps_p3_s22(i,1)-ps_p3_s30(i,1))-
         (ps_p3_s22(i,k)-ps_p3_s30(i,k));
     end
 dd_st(:,k-1)=  dd_sta;
end
dd_ps22_30=dd_st;
%*********************************************************
```

```matlab
% 4- Troposphere free observables derived from double differencing
between
% satellites from reference stations MCS to the permanent stations.
Each vector
% contains troposphere free observables for pairs: (6-18, 6-30, 30-
18, 22-30)

%4.1.1-Rearanging troposphere free observables for satellite 6
 j=1;
for k=1:10;
    for i=1:4:12;
    Td_sa=ps_tpdelay(:,k);  Td_sb(j,1) = Td_sa(i); j=j+1;
    end
    Td_st(:,k)=Td_sb((3*k-2):3*k);
end
Td_s6=Td_st;

% 4.1.2-Rearanging troposphere free observables for satellite 18
j=1;
for k=1:10;
    for i=2:4:12;
    Td_sa=ps_tpdelay(:,k);  Td_sb(j,1) = Td_sa(i);  j=j+1;
    end
    Td_st(:,k)=Td_sb((3*k-2):3*k);
end
Td_s18=Td_st;


% 4.1.3-Rearanging troposphere free observables for satellite 22
j=1;
for k=1:10;
    for i=3:4:12;
    Td_sa=ps_tpdelay(:,k);  Td_sb(j,1) = Td_sa(i); j=j+1;
    end
    Td_st(:,k)=Td_sb((3*k-2):3*k);
end
Td_s22=Td_st;

% 4.1.4-Rearanging troposphere free observables for satellite 30
j=1;
for k=1:10;
    for i=4:4:12;
    Td_sa=ps_tpdelay(:,k);  Td_sb(j,1) = Td_sa(i);  j=j+1;
    end
    Td_st(:,k)=Td_sb((3*k-2):3*k);
end
Td_s30=Td_st;
 %*********************************************

 % 4.2.1 troposphere free observables for satellite pair 6-18
for k=2:10;
    for i=1:3;   dd_sta(i,1)  = (Td_s6(i,1)-Td_s18(i,1))-
(Td_s6(i,k)-Td_s18(i,k));
      end
```

```
 dd_st(:,k-1)=  dd_sta;
end
ddT_ps6_18=dd_st;

% 4.2.2 troposphere free observations for satellite pair 6-30
for k=2:10;
    for i=1:3;   dd_sta(i,1)  = (Td_s6(i,1)-Td_s30(i,1))-
(Td_s6(i,k)-Td_s30(i,k));
      end
 dd_st(:,k-1)=  dd_sta;
end
ddT_ps6_30=dd_st;
 % 4.2.3 troposphere free observations for satellite pair 30-18
for k=2:10;
    for i=1:3;    dd_sta(i,1)  = (Td_s30(i,1)-Td_s18(i,1))-
(Td_s30(i,k)-  Td_s18(i,k));
      end
 dd_st(:,k-1)=  dd_sta;
end
ddT_ps30_18=dd_st;
 % 4.2.4 troposphere free observations for satellite pair 22-30
 for k=2:10;
    for i=1:3;  dd_sta(i,1)  = (Td_s22(i,1)-Td_s30(i,1))-
(Td_s22(i,k)-Td_s30(i,k));
      end
 dd_st(:,k-1)=  dd_sta;
end
ddT_ps22_30=dd_st;
  %***********************************************

 %5----STEP 5: Partial derivatives of equations for design matrix---
-
X1=ps(1,1);Y1=ps(1,2); Z1=ps(1,3);
j=2;ns=9;
Sp=zeros(ns+1,3);
 for p=2:ns+1;
X2=ps(p,1);Y2=ps(p,2); Z2=ps(p,3);
syms Xa Ya Za Xb Yb Zb XS1 YS1 ZS1 XS2 YS2 ZS2 real;
E1=(sqrt(((Xa-XS1)^2)+((Ya-YS1)^2)+((Za-ZS1)^2)))-(sqrt(((Xa-
XS2)^2)+((Ya-YS2)^2)+((Za-ZS2)^2)));
E2=(sqrt(((Xb-XS1)^2)+((Yb-YS1)^2)+((Zb-ZS1)^2)))-(sqrt(((Xb-
XS2)^2)+((Yb-YS2)^2)+((Zb-ZS2)^2)));

Equation=E1-E2;     % Differencing equation
Jacobian=jacobian(Equation,[Xa,Ya,Za,Xb,Yb,Zb]);
TRESHOLD=1000;
niterations=1;
 % set up counter to count the number of iterations required
 while TRESHOLD>10^-4 && niterations<2   % To avoid infinite loop

% linear combination 6-18
R1=subs(Jacobian,{Xa,Ya,Za,Xb,Yb,Zb,XS1,YS1,ZS1,XS2,YS2,ZS2},{X1,Y1,
Z1,X2,Y2,Z2,...
```

```
Epoch1sat6(1),Epoch1sat6(2),
Epoch1sat6(3),Epoch1sat18(1),Epoch1sat18(2), Epoch1sat18(3)});
R2=subs(Jacobian,{Xa,Ya,Za,Xb,Yb,Zb,XS1,YS1,ZS1,XS2,YS2,ZS2},{X1,Y1,
Z1,X2,Y2,Z2,...
Epoch2sat6(1),Epoch2sat6(2),Epoch2sat6(3),Epoch2sat18(1),Epoch2sat18
(2),Epoch2sat18(3)});
R3=subs(Jacobian,{Xa,Ya,Za,Xb,Yb,Zb,XS1,YS1,ZS1,XS2,YS2,ZS2},{X1,Y1,
Z1,X2,Y2,Z2,...
Epoch3sat6(1),Epoch3sat6(2),Epoch3sat6(3),Epoch3sat18(1),Epoch3sat18
(2),Epoch3sat18(3)});


 % linear combination 6-30
R4=subs(Jacobian,{Xa,Ya,Za,Xb,Yb,Zb,XS1,YS1,ZS1,XS2,YS2,ZS2},{X1,Y1,
Z1,X2,Y2,Z2,...
Epoch1sat6(1),Epoch1sat6(2),
Epoch1sat6(3),Epoch1sat30(1),Epoch1sat30(2),Epoch1sat30(3)});
R5=subs(Jacobian,{Xa,Ya,Za,Xb,Yb,Zb,XS1,YS1,ZS1,XS2,YS2,ZS2},{X1,Y1,
Z1,X2,Y2,Z2,...
Epoch2sat6(1),Epoch2sat6(2),Epoch2sat6(3),Epoch2sat30(1),Epoch2sat30
(2),Epoch2sat30(3)});
R6=subs(Jacobian,{Xa,Ya,Za,Xb,Yb,Zb,XS1,YS1,ZS1,XS2,YS2,ZS2},{X1,Y1,
Z1,X2,Y2,Z2,...
Epoch3sat6(1),Epoch3sat6(2),Epoch3sat6(3),Epoch3sat30(1),Epoch3sat30
(2),Epoch3sat30(3)});

% linear combination 30-18

R7=subs(Jacobian,{Xa,Ya,Za,Xb,Yb,Zb,XS1,YS1,ZS1,XS2,YS2,ZS2},{X1,Y1,
Z1,X2,Y2,Z2,...
Epoch1sat30(1),Epoch1sat30(2),
Epoch1sat30(3),Epoch1sat18(1),Epoch1sat18(2), Epoch1sat18(3)});
R8=subs(Jacobian,{Xa,Ya,Za,Xb,Yb,Zb,XS1,YS1,ZS1,XS2,YS2,ZS2},{X1,Y1,
Z1,X2,Y2,Z2,...
Epoch2sat30(1),Epoch2sat30(2),Epoch2sat30(3),Epoch2sat18(1),Epoch2sa
t18(2),Epoch2sat18(3)});
R9=subs(Jacobian,{Xa,Ya,Za,Xb,Yb,Zb,XS1,YS1,ZS1,XS2,YS2,ZS2},{X1,Y1,
Z1,X2,Y2,Z2,...
Epoch3sat30(1),Epoch3sat30(2),Epoch3sat30(3),Epoch3sat18(1),Epoch3sa
t18(2),
Epoch3sat18(3)});

% linear combination 22-30
R10=subs(Jacobian,{Xa,Ya,Za,Xb,Yb,Zb,XS1,YS1,ZS1,XS2,YS2,ZS2},{X1,Y1
,Z1,X2,Y2,Z2,...
Epoch1sat22(1),Epoch1sat22(2),Epoch1sat22(3),Epoch1sat30(1),Epoch1sa
t30(2), Epoch1sat30(3)});
R11=subs(Jacobian,{Xa,Ya,Za,Xb,Yb,Zb,XS1,YS1,ZS1,XS2,YS2,ZS2},{X1,Y1
,Z1,X2,Y2,Z2,...
Epoch2sat22(1),Epoch2sat22(2),Epoch2sat22(3),Epoch2sat30(1),Epoch2sa
t30(2),
Epoch2sat30(3)});
```

```
R12=subs(Jacobian,{Xa,Ya,Za,Xb,Yb,Zb,XS1,YS1,ZS1,XS2,YS2,ZS2},{X1,Y1
,Z1,X2,Y2,Z2,...
Epoch3sat22(1),Epoch3sat22(2),Epoch3sat22(3),Epoch3sat30(1),Epoch3sa
t30(2),Epoch3sat30(3)});


% design matrix
A=[R1;R2;R3;R4;R5;R6;R7;R8;R9;R10;R11;R12];

%compute the geometric double differences
GEO1_6_18_s1=subs(Equation,{Xa,Ya,Za,Xb,Yb,Zb,XS1,YS1,ZS1,XS2,YS2,ZS
2},{X1,Y1,Z1,X2,Y2,Z2,...
Epoch1sat6(1),Epoch1sat6(2),
Epoch1sat6(3),Epoch1sat18(1),Epoch1sat18(2), Epoch1sat18(3)});
GEO2_6_18_s2=subs(Equation,{Xa,Ya,Za,Xb,Yb,Zb,XS1,YS1,ZS1,XS2,YS2,ZS
2},{X1,Y1,Z1,X2,Y2,Z2,...
Epoch2sat6(1),Epoch2sat6(2),Epoch2sat6(3),Epoch2sat18(1),Epoch2sat18
(2),Epoch2sat18(3)});
GEO3_6_18_s3=subs(Equation,{Xa,Ya,Za,Xb,Yb,Zb,XS1,YS1,ZS1,XS2,YS2,ZS
2},{X1,Y1,Z1,X2,Y2,Z2,...
Epoch3sat6(1),Epoch3sat6(2),Epoch3sat6(3),Epoch3sat18(1),Epoch3sat18
(2),Epoch3sat18(3)});
GEO4_6_30_s1=subs(Equation,{Xa,Ya,Za,Xb,Yb,Zb,XS1,YS1,ZS1,XS2,YS2,ZS
2},{X1,Y1,Z1,X2,Y2,Z2,...
Epoch1sat6(1),Epoch1sat6(2),
Epoch1sat6(3),Epoch1sat30(1),Epoch1sat30(2), Epoch1sat30(3)});
GEO5_6_30_s2=subs(Equation,{Xa,Ya,Za,Xb,Yb,Zb,XS1,YS1,ZS1,XS2,YS2,ZS
2},{X1,Y1,Z1,X2,Y2,Z2,...

Epoch2sat6(1),Epoch2sat6(2),Epoch2sat6(3),Epoch2sat30(1),Epoch2sat30
(2),Epoch2sat30(3)});
GEO6_6_30_s3=subs(Equation,{Xa,Ya,Za,Xb,Yb,Zb,XS1,YS1,ZS1,XS2,YS2,ZS
2},{X1,Y1,Z1,X2,Y2,Z2,...
Epoch3sat6(1),Epoch3sat6(2),Epoch3sat6(3),Epoch3sat30(1),Epoch3sat30
(2),Epoch3sat30(3)});
GEO7_30_18_s1=subs(Equation,{Xa,Ya,Za,Xb,Yb,Zb,XS1,YS1,ZS1,XS2,YS2,Z
S2},{X1,Y1,Z1,X2,Y2,Z2,...
 Epoch1sat30(1),Epoch1sat30(2),
Epoch1sat30(3),Epoch1sat18(1),Epoch1sat18(2), Epoch1sat18(3)});
GEO8_30_18_s2=subs(Equation,{Xa,Ya,Za,Xb,Yb,Zb,XS1,YS1,ZS1,XS2,YS2,Z
S2},{X1,Y1,Z1,X2,Y2,Z2,...
Epoch2sat30(1),Epoch2sat30(2),Epoch2sat30(3),Epoch2sat18(1),Epoch2sa
t18(2),Epoch2sat18(3)});
GEO9_30_18_s3=subs(Equation,{Xa,Ya,Za,Xb,Yb,Zb,XS1,YS1,ZS1,XS2,YS2,Z
S2},{X1,Y1,Z1,X2,Y2,Z2,...
Epoch3sat30(1),Epoch3sat30(2),Epoch3sat30(3),Epoch3sat18(1),Epoch3sa
t18(2),Epoch3sat18(3)});
GEO10_22_30_s1=subs(Equation,{Xa,Ya,Za,Xb,Yb,Zb,XS1,YS1,ZS1,XS2,YS2,
ZS2},{X1,Y1,Z1,X2,Y2,Z2,...
Epoch1sat22 (1), Epoch1sat22(2),
Epoch1sat22(3),Epoch1sat30(1),Epoch1sat30(2), Epoch1sat30(3)});
GEO11_22_30_s2=subs(Equation,{Xa,Ya,Za,Xb,Yb,Zb,XS1,YS1,ZS1,XS2,YS2,
ZS2},{X1,Y1,Z1,X2,Y2,Z2,...
```

```
Epoch2sat22(1),Epoch2sat22(2),Epoch2sat22(3),Epoch2sat30(1),Epoch2sa
t30(2),Epoch2sat30(3)});
GEO12_22_30_s3=subs(Equation,{Xa,Ya,Za,Xb,Yb,Zb,XS1,YS1,ZS1,XS2,YS2,
ZS2},{X1,Y1,Z1,X2,Y2,Z2,...
Epoch3sat22(1),Epoch3sat22(2),Epoch3sat22(3),Epoch3sat30(1),Epoch3sa
t30(2),Epoch3sat30(3)});

%5.1 Form the misclosure vector for the linear satellite combination
n=p-1;
w1=dd_ps6_18(1,n) - GEO1_6_18_s1 - ddT_ps6_18(1,n);
w2=dd_ps6_18(2,n) - GEO2_6_18_s2 - ddT_ps6_18(2,n);
w3=dd_ps6_18(3,n) - GEO3_6_18_s3 - ddT_ps6_18(3,n);
w4=dd_ps6_30(1,n) - GEO4_6_30_s1 - ddT_ps6_30(1,n);
w5=dd_ps6_30(2,n) - GEO5_6_30_s2 - ddT_ps6_30(2,n);
w6=dd_ps6_30(3,n) - GEO6_6_30_s3 - ddT_ps6_30(3,n);
w7=dd_ps30_18(1,n) - GEO7_30_18_s1 - ddT_ps30_18(1,n);
w8=dd_ps30_18(2,n) - GEO8_30_18_s2 - ddT_ps30_18(2,n);
w9=dd_ps30_18(3,n) - GEO9_30_18_s3 - ddT_ps30_18(3,n);
w10=dd_ps22_30(1,n) - GEO10_22_30_s1 - ddT_ps22_30(1,n);
w11=dd_ps22_30(2,n) - GEO11_22_30_s2 - ddT_ps22_30(2,n);
w12=dd_ps22_30(3,n) - GEO12_22_30_s3 - ddT_ps22_30(3,n);
 w=[w1;w2;w3;w4;w5;w6;w7;w8;w9;w10;w11;w12];

%5.2 Form the covariance matrix, weight matrix and the identity
matrix
Cl=diag(ones(12,1));
 %5.3 Form the weight matrix Pl and the noise vector Pxo
Pl=inv(Cl);
 Pxo=[1/(0.050^2)       0        0               0    0    0
             0      1/(0.050^2) 0               0    0    0
             0          0      1/(0.080^2)   0    0    0
             0          0        0               0    0    0
             0          0        0               0    0    0
             0          0        0               0    0    0];

%5.4 calculate the delta vector
N=(A'*Pl*A+Pxo); u=(A'*Pl*w);   delta=(inv(N))*u;
TRESHOLD=sqrt(delta(1)^2+delta(2)^2+delta(3)^2+delta(4)^2+delta(5)^2
+ delta(6)^2);

 %increasing the number of Iterations
 niterations=niterations+1;

 %5.6 Update the X,Y,Z coordinates of points A and B

X1=X1+delta(1); Y1=Y1+delta(2); Z1=Z1+delta(3);
X2=X2+delta(4); Y2=Y2+delta(5); Z2=Z2+delta(6);
 niter=niterations;

 %5.7 xhat - estimated station coordinates
xhat=[X1,Y1,Z1;X2,Y2,Z2];

%*************************************************************
```

```
%---- STEP 6: STATISTICS AND STATISTICAL TEST ----------
%6.1 covariance of the parameters
Cx=inv(N);
for i=1:6
    sigmaXYZ_AB(i,1) = sqrt(Cx(i,i));
end
%6.2 Compute the residuals
r=A*delta+w;
%6.3 degrees of freedom (six parameters and 3 constrains/unknowns)
dof=6+3;
 %6.4 compute the a-priori variance factor
sigma_not_hat_squared=(r'*Pl*r)/dof
 %6.5 Chi-Squared value for dof=9 (95%)
chi_sq_975=19.02; chi_sq_025=2.70;
 %bounds
lower_bound=dof*sigma_not_hat_squared/chi_sq_975;
upper_bound=dof*sigma_not_hat_squared/chi_sq_025;


%7-------STEP 7: COMPUTE THE ERROR ELLIPSE PARAMETERS --------------
 %7.1 Compute the orientation angle t of the error ellipse axes
N=2*Cx(4,5);D=Cx(5,5)-Cx(4,4);
if N>0&D>0; ag_t=0.5*atan(N/D);
end
if N>0&D<0; ag_t=0.5*(2*pi-atan(abs(N/D)));
end
if N<0&D>0; ag_t=0.5*(pi - atan(abs(N/D)));
end
if N<0&D<0; ag_t=0.5*(pi/2 + atan(abs(N/D)));
end
 %7.2 Compute the semi major-(Su) and semi minor axes-(Sv) of the
```

error ellipse at 95% confidence level using χ^2 test.

```
sig_ref=sqrt (.050^2 + .050^2 + .080^2)
sig=sig_ref*sqrt(5.99*sigma_not_hat_squared)
Su=sig*sqrt(Cx(4,4)*(sin(ag_t))^2+2*Cx(4,5)*cos(ag_t)*sin(ag_t)+
Cx(5,5)*(cos(ag_t))^2);
Sv=sig*sqrt(Cx(4,4)*(cos(ag_t))^2-2*Cx(4,5)*cos(ag_t)*sin(ag_t)+
Cx(5,5)*(sin(ag_t))^2);
Sp(j,1)=Su;Sp(j,2)=Sv;Sp(j,3)=ag_t; el_p=Sp
lat_deci = fi.*180./pi;lon_deci = lbd.*180./pi;ht_ps=h;
g_crd=[lat_deci,lon_deci,h]

%----------------------- STEP (8): PRINT RESULTS ------------------
fprintf('\nFINAL RESULTS\n');
fprintf('\nPrinted:%s \n',datestr(now));
fprintf('\nNumber of iterations: %i\n',niterations);
fprintf('\tX1\t%8.4f\t\t%8.4f\t\t%8.4f\t\t%8.4f\n',xhat(1,1),
abs(ps(1,1)-xhat(1,1)),sqrt(Cx(1,1)));
fprintf('\n\tY1\t%8.4f\t\t%8.4f\t\t%8.4f\t\t%8.4f\n',xhat(1,2),abs(p
s(1,2)-xhat(1,2)),sqrt(Cx(2,2)));
fprintf('\n\tZ1\t%8.4f\t\t%8.4f\t\t%8.4f\t\t%8.4f\n',xhat(1,3),abs(p
s(1,3)-xhat(1,3)),sqrt(Cx(3,3)));
fprintf('\n\tX2\t%8.4f\t\t%8.4f\t\t%8.4f\t\t%8.4f\n',xhat(2,1),abs(p
```

```
s(p,1)-xhat(2,1)),sqrt(Cx(4,4)));
fprintf('\n\tY2\t%8.4f\t\t%8.4f\t\t%8.4f\t\t%8.4f\n',xhat(2,2),abs(p
s(p,2)-xhat(2,2)),sqrt(Cx(5,5)));
fprintf('\n\tZ2\t%8.4f\t\t%8.4f\t\t%8.4f\t\t%8.4f\n',xhat(2,3),abs(p
s(p,3)-xhat(2,3)),sqrt(Cx(6,6)));
fprintf('\n The a posteriori variance: %f\n',sigma_not_hat_squared);
fprintf('\n Lower boundary for Chi-square test on a priori variance:
%f\n',lower_bound);
fprintf('\n Upper boundary for Chi-square test on a priori variance:
%f\n',upper_bound);
   j=j+1;
end
end   % end of "while" loop
 %plotting the results
figure
 hold on; plot
(q2,q1,'magenta.','marker','*','markersize',2,'linestyle','none');
plot (k2,k1,'-.magenta.','LineWidth',2); plot (l2,l1,'-
.magenta.','LineWidth',2);
plot (m2,m1,'-.magenta.','LineWidth',2); plot (n2,n1,'-
.magenta.','LineWidth',2);
plot
(z12,z11,.b.','marker','*','markerfacecolor','r','markersize',2,
'linestyle','none');
plot (z22,z21,'-.b.','marker','*','markerfacecolor','r','markersize'
,2,'linestyle','none');
plot (z32,z31,'-.b.','marker','*','markerfacecolor','r','markersize'
,2,'linestyle','none');
plot (cl_B2,cl_B1,'-.b.','marker','*','markerfacecolor','r',
'markersize',2,'linestyle','none');
plot (rg_B2,rg_B1,'-.green.','marker','*','markerfacecolor','r',
'markersize',2,'linestyle','none');
plot(
lon_deci,lat_deci,'marker','d','markerfacecolor','r','markersize',5,
'linestyle','none')
text(g_crd(1,2)+.35,g_crd(1,1)+.01,'MCS','FontSize',8);
text(g_crd(2,2)+.35,g_crd(2,1)+.55,'PS1','FontSize',8);
text(g_crd(3,2)+.35,g_crd(3,1)+.35,'PS2','FontSize',8);
text(g_crd(4,2)+.45,g_crd(4,1)+.08,'PS3','FontSize',8);
text(g_crd(5,2)-.09,g_crd(5,1)+.60,'PS4','FontSize',8);
text(g_crd(6,2)-.15,g_crd(6,1)+.35,'PS5','FontSize',8);
text(g_crd(7,2)-.68,g_crd(7,1)+.25,'PS6','FontSize',8);
text(g_crd(8,2)+.10,g_crd(8,1)+.55,'PS7','FontSize',8);
text(g_crd(9,2)+.55,g_crd(9,1)+.15,'PS8','FontSize',8);
text(g_crd(10,2)-.72,g_crd(10,1)+.25,'PS9','FontSize',8)
title('2D-COVARIANCE ANALYSIS RESULTS FOR TZRF10 SCENARIO 1')
xlabel('longitude ');ylabel('latitude ')
 for i=2:ns+1;
h=ellipse(el_p(i,1),el_p(i,2),el_p(i,3),g_crd(i,2),g_crd(i,1), 'r');
end
grid on; hold off
```

Appendix IV.2 Reference frame matlab code

This matlab software code with six different functions as part of the reference frame case study and the first version of the code was created by fellow graduate student, Landon Urquhart and was later improved by myself.

With reference to the discussions on section 6.2.2, the first function of the code creates a new Bernese campaign and the program would skip this part if the campaign exists within the specified path. The remaining functions, access different sites as explained in the comment lines and download different files that are necessary for the Bernese v5.0 processing. The files are then unzipped and renamed in the Bernese processing format before being copied to the appropriate directories.

```
function getfiles(varargin).
%DOWNLOADS FILES FOR PROCESSING USING BERNESE SOFTWARE
% Created by: Landon Urquhart; Date: August 2007
% Input:  userdate --> string containing the date of required
% download. Format is 'dd.mm.yyyy'
% campaign name--> Name of campaign in Bernese program
% station names--> list of the station names which observation
% files are required. Format is 'unbj','ganp',...
% Note(1): Date must be less than current date
%   Example: getfiles('14.07.2007','tryone','unbj','alrt')
% Step 1 Creation of Bernese campaign and subdirectories
    clc

  if isequal(cell2str(varargin(1)),'-?');
        helpfile;
        return;
     elseif size(varargin,2)>1
        userDate=cell2str(varargin(1));
        campaign=cell2str(varargin(2));
        for i=1:size(varargin,2)-2
            stations(i)=varargin(i+2);
        end
     end
    warning('off', 'MATLAB:MKDIR:DirectoryExists');
     warning('off', 'MATLAB:DELETE:FileNotFound');
```

```matlab
        finaldir=['C:\GPSDATA\' campaign];
        if ~exist(finaldir,'dir')
            mkdir(finaldir)
        end
        mkdir([finaldir '\ATM\']);mkdir([finaldir '\BPE\']);
mkdir([finaldir '\OBS\']);
        mkdir([finaldir '\ORB\']); mkdir([finaldir '\ORX\']);
mkdir([finaldir '\OUT\']);
        mkdir([finaldir '\RAW\']); mkdir([finaldir '\SOL\']);
mkdir([finaldir '\STA\']);
            % end of subdirectories and campaign creation

%Step 2.1 converting the input date to correct date format
date=datestr(datenum(userDate, 'dd.mm.yyyy'), 'ddmmyyyy');
        today=datestr(now,'ddmmyyyy');
%Step2.2 converts both dates to Julian day
        jd=cal2jd(str2num(date(5:8)), str2num(date(3:4)),
str2num(date(1:2)));%converts from calendar to Julian date
        jdnow=cal2jd(str2num(today(5:8)), str2num(today(3:4)),
str2num(today(1:2)));
%Step 2.3 check input
        if jd>jdnow
            error('Date must be less then current date')
        end
 D=dateConversions(jd);%convert Julian date to all necessary dates
 fprintf(1,'\ndownloading for: %d-%d-%d\n\n',D.day,D.month,D.year);
%Step 2.4 Deal with cddis FTP server
        yearstr=num2str(D.year);
        fprintf(1,'Logging into cddis ftp server for SP3, CLK, EORP
& OBS files....\n');
cddis_ftp=ftp('cddis.gsfc.nasa.gov');
dirname=['/gps/data/daily/'yearstr'/'D.strdoy '/' yearstr(3:4)'o'];
        cd(cddis_ftp,dirname);
        cddisfiles=dir(cddis_ftp);
        ndpfiles(1)=
get_obsfiles(cddisfiles,cddis_ftp,finaldir,D,stations);%get obsfiles
cd(cddis_ftp,'..');cd(cddis_ftp,'..');cd(cddis_ftp,'..');cd(cddis_ft
p,'..');cd(cddis_ftp,'..');
dirname=['products/' num2str(D.week) '/'];% DIR of cddis server
        cd(cddis_ftp,dirname);%change directory on ftp site
        cddisfiles=dir(cddis_ftp);
        ndpfiles(2)=
get_sp3files(cddisfiles,cddis_ftp,finaldir,D,'igs');%get sp3files
ndpfiles(3)=get_clkfiles(cddisfiles,cddis_ftp,finaldir,D,'igs');%get
clkfiles
ndpfiles(4)=get_eopfiles(cddisfiles,cddis_ftp,finaldir,D,'igs');%get
Earth orientation parameters files
close(cddis_ftp);

%Deal with BERNE FTP server
fprintf(1,'Logging into berne ftp server for the DCB, CRX & CODE
files...\n'); berne_ftp=ftp('ftp.unibe.ch'); %get DCB files
        dirname=['aiub/CODE/' num2str(D.year)];
        cd(berne_ftp,dirname);%change directory
```

```
        bernefiles=dir(berne_ftp);%list all files in directory
ndpfiles(5)=get_DCBfiles(bernefiles,berne_ftp,finaldir,D,'igs');
        cd(berne_ftp,'..');%go up one directoy
        cd(berne_ftp,'..');
        dirname=['BSWUSER50/GEN/'];
        cd(berne_ftp,dirname);%change directory
        bernefiles=dir(berne_ftp);%list all files in directory
        CRXDIR='C:\BERN50\GPS\GEN\';
        if ~exist(CRXDIR,'dir')
            mkdir(CRXDIR);
        end
ndpfiles(6)= get_CRXfiles(bernefiles,berne_ftp,CRXDIR,D,'igs');%get
CRX files
        cd(berne_ftp,'..');%go up one directoy
        cd(berne_ftp,'..');
        dirname=['CODE/' num2str(D.year)];
        cd(berne_ftp,dirname);%change directory
        bernefiles=dir(berne_ftp);%list all files in directory
ndpfiles(7)=get_IONfiles(bernefiles,berne_ftp,finaldir,D,'igs');%get
IONfiles
        close(berne_ftp);

        %decide if it was successful
        if find(ndpfiles<1)%Then download was not successful
            fprintf(1,'Error in download. Please try again.\n');
        else
            fprintf(1,'All files downloaded.\n');
        end

%%%%%%%%%%%%%%%%%%%%%%%%%%%%%%%%%%%%%%%%%
function
ndpfiles=get_sp3files(cddisfiles,cddis_ftp,directory,D,typesp3)
% Downloads sp3 files from cddis server
 ndpfiles=0;%to count number of obs files downloaded
 for ifile=1:size(cddisfiles,1 % Download if match exists.
        if strcmpi(cddisfiles(ifile).name(10:end),'sp3.Z')...
                && strcmpi(cddisfiles(ifile).name(1:3),typesp3)&&
strcmpi(cddisfiles(ifile).name(8),num2str(D.dayOfWeek))
      mget(cddis_ftp,cddisfiles(ifile).name);
      copyfile(cddisfiles(ifile).name,'temp.sp3.Z');
      !gunzip temp.sp3.Z
      dfile=upper(cddisfiles(ifile).name);
      movefile('temp.sp3',[directory '\ORB\' dfile(1:end-5) 'PRE']);
      delete temp.sp3
            delete temp.sp3.Z;delete(dfile);
            delete(cddisfiles(ifile).name);ndpfiles=1;
            return;
        end%if
    end%for
%%%%%%%%%%%%%%%%%%%%%%%%%%%%%%%%%%%%%%%%%%


Function ndpfiles=get_obsfiles(cddisfiles,cddis_ftp,directory,D,
stations) % Downloads observation files from cddis server
```

```
D.year=num2str(D.year);
ndpfiles=0;%to count number of observation files downloaded
for j=1:size(stations,2)
    for ifile=1:size(cddisfiles,1) % Download if match exis.
      if strcmpi(cddisfiles(ifile).name(1:4),stations(j))
      mget(cddis_ftp,cddisfiles(ifile).name);
      copyfile(cddisfiles(ifile).name,['temp.07o.Z']);
      !gunzip temp.07o.Z
      dfile=upper(cddisfiles(ifile).name);
      copyfile('temp.07o',[directory '\RAW\' dfile(1:end-2)]);
      movefile('temp.07o',[directory '\ORX\' dfile(1:end-2)]);
      delete temp.07o; delete(dfile); delete(cddisfiles(ifile).name);
      ndpfiles=1;
      end%if
    end%for
end

%%%%%%%%%%%%%%%%%%%%%%%%%%%%%%%%%%%%%%%%
Function ndpfiles=get_DCBfiles(cddisfiles,cddis_ftp,directory,D,
typesp3); % Download code differential files from ftpBERNE server
if (D.month) <10
    D.month=['0' num2str(D.month)];
 else
    D.month=num2str(D.month);
end
D.year=num2str(D.year);
ndpfiles=0;%to count number of obs files downloaded
filename1=['P1P2' D.year(3:4) D.month '.DCB.Z'];
filename2=['P1C1' D.year(3:4) D.month '.DCB.Z'];
    for ifile=1:size(cddisfiles,1)  % Check for download match.
    if strcmpi(cddisfiles(ifile).name(9:end),filename1(9:end)) &&
strcmpi(cddisfiles(ifile).name(5:8),filename1(5:8))...
              ||
strcmpi(cddisfiles(ifile).name(9:end),filename2(9:end)) &&
strcmpi(cddisfiles(ifile).name(5:8),filename2(5:8))
            mget(cddis_ftp,cddisfiles(ifile).name);
            copyfile(cddisfiles(ifile).name,'temp.DCB.Z');
            !gunzip temp.DCB.Z
            dfile=upper(cddisfiles(ifile).name);
       movefile('temp.DCB',[directory '\ORB\' dfile(1:end-5) 'DCB']);
            delete temp.DCB; delete temp.DCB.Z
            delete(dfile); delete(cddisfiles(ifile).name);
ndpfiles=1;
        end%if
    end%for

function ndpfiles=get_clkfiles(cddisfiles,cddis_ftp,directory,D
,typesp3) % Downloads ERP files from cddis server
ndpfiles=0;%to count number of observations files downloaded
    for ifile=1:size(cddisfiles,1) % Check for download match.
        if strcmpi(cddisfiles(ifile).name(10:end),'erp.Z')...
              && strcmpi(cddisfiles(ifile).name(1:3),'igs')
            mget(cddis_ftp,cddisfiles(ifile).name);
      ndpfiles=ndpfiles+1;
```

```
        copyfile(cddisfiles(ifile).name,'temp.erp.Z');
        !gunzip temp.erp.Z
        dfile=upper(cddisfiles(ifile).name);
        movefile('temp.erp',[directory '\ORB\' dfile(1:end-5) 'IEP']);
            delete temp.erp;delete temp.erp.Z
            delete(dfile);delete(cddisfiles(ifile).name);
            ndpfiles=1;
            return;
        end%if
    end%for
function ndpfiles=get_IONfiles(cddisfiles,cddis_ftp,directory,D,
typesp3) % Downloads ION files from cddis server
D.year=num2str(D.year);
ndpfiles=0;%to count number of obs files downloaded
filename1=['COD' num2str(D.week) num2str(D.dayOfWeek) '.ION.Z'];
for ifile=1:size(cddisfiles,1)  % Check for download match.
if strcmpi(cddisfiles(ifile).name(9:end),filename1(9:end)) &&
strcmpi(cddisfiles(ifile).name(4:8),filename1(4:8))
     mget(cddis_ftp,cddisfiles(ifile).name);
     copyfile(cddisfiles(ifile).name,'temp.ion.Z');
     !gunzip temp.ion.Z
     dfile=upper(cddisfiles(ifile).name);
     movefile('temp.ion',[directory '\ATM\' dfile(1:end-5) 'ION']);
     delete temp.ion;
     delete temp.ion.Z;
       delete(dfile);
       delete(cddisfiles(ifile).name);
       ndpfiles=1;
      end%if
    end%for


function [week, day_of_week] = gps_time(jul)
%GPS_TIME  Conversion of Julian Day number to GPS week and
% Seconds of Week reckoned from Saturday midnight
%Kai Borre 05-20-96
%Copyright (c) by Kai Borre
%$Revision: 1.1 $  $Date: 1998/01/23  $
%*********************************
%     tested for following dates
%        January 15th, 1980;  October 28th, 2000; August 17th, 2050;
April 4th, 2099
%      Websites used in test
% SOPAC GPS DATE CONVERTER-
http://sopac.ucsd.edu/scripts/convertDate.cgi
%*****************************************
a = floor(jul+.5); b = a+1537; c = floor((b-122.1)/365.25); e =
floor(365.25*c);
f = floor((b-e)/30.6001); d = b-e-floor(30.6001*f)+rem(jul+.5,1);
day_of_week = rem(floor(jul+.5),7)+1;%LU
if day_of_week==7%LU
    day_of_week=0;%LU
end%LU
week = floor((jul-2444244.5)/7);
%%%%%%% end gps_time.m  %%%%%%%%%%%%
```

```
function [doy,yr]=jd2doy(jd)
% JD2DOY  Converts Julian date to year and day of year.
% . Non-vectorized version. See also CAL2JD, DOY2JD,
%   GPS2JD, JD2CAL, JD2DOW, JD2GPS, JD2YR, YR2JD.
% Version: 24 Apr 99
% Usage:   [doy,yr]=jd2doy(jd)
% Input:   jd  - Julian date
% Output:  doy - day of year;   yr  - year
%    tested for following dates
%  January 15th, 1980;   October 28th, 2000;  August 17th, 2050;
April 4th, 2099
%     Websites used in test
% SOPAC GPS DATE CONVERTER-
http://sopac.ucsd.edu/scripts/convertDate.cgi
if nargin ~= 1
  warning('Incorrect number of arguments');
  return;
end
if jd < 0
  warning('Julian date must be greater than or equal to zero');
  return;
end
 [yr,mn,dy] = jd2cal(jd); doy = jd - cal2jd(yr,1,0);
%%%%%%%%%%%%%%%%%%%%%%%%%%%%%%%%%%%%%%%%

function [yr,mn,dy]=jd2cal(jd)
% JD2CAL  Converts Julian date to calendar date using algorithm
%   from "Practical Ephemeris Calculations" by Oliver Montenbruck
%   (Springer-Verlag, 1989). Must use astronomical year for B.C.
%   dates (2 BC = -1 yr). Non-vectorized version. See also CAL2JD,
%   DOY2JD, GPS2JD, JD2DOW, JD2DOY, JD2GPS, JD2YR, YR2JD.
% Version: 24 Apr 99
% Usage:   [yr, mn, dy]=jd2cal(jd)
% Input:   jd - Julian date
% Output:  yr - year of calendar date;   mn - month of calendar date
%  dy - day of calendar date (including decimal)
%************************************
%    tested for following dates
%   January 15th, 1980; October 28th, 2000;August 17th, 2050;  April
4th, 2099
%     Websites used in test
%American Ass. Of Var. Star
%Observers-http://www.aavso.org/observing/aids/jdcalendar.shtml
%US Naval Observatory-
http://aa.usno.navy.mil/data/docs/JulianDate.html
 %************************************


if nargin ~= 1
  warning('Incorrect number of arguments');
  return;
end
if jd < 0
  warning('Julian date must be greater than or equal to zero');
```

```
  return;
end
 a = fix(jd+0.5);
if a < 2299161
  c = a + 1524;
else
  b = fix( (a-1867216.25) / 36524.25 );  c = a + b - fix(b/4) +
1525;
end
d = fix( (c-122.1)/365.25 );
e = fix(365.25*d);
f = fix( (c-e) / 30.6001 );
dy = c - e - fix(30.6001*f) + rem((jd+0.5),a);
mn = f - 1 - 12*fix(f/14);
yr = d - 4715 - fix( (7+mn)/10 );
```

Appendix IV.3 Real time positioning analysis matlab code

This is a matlab software code developed by the author for the analysis of the real time positioning case study. With reference to the discussions on section 6.3.3, the code inputs real time GPS positions (from DGPS and real time kinematics and tests them for any possible outliers before they use.

The code compares the observed positions with the true value computed from relative positioning as base of analysis in terms the R95 (horizontal 95 percent) scatter plots using the expansion factors that using the Fisher distribution. The second part of the computes and plot the time series of the latitude and the longitude differences whereas the last part plots the histograms of the latitude and longitude differences as detailed in sections 7.3.2, 7.3.3 and 7.3.4.

```
%JAMES MTAMAKAYA S#3206337
%REAL TIME DGPS POSITIONING ANALYSISS"
%1.0---------------STEP (1) and its INPUTS:   ---------------------
------
%1- Input the values for the Station Coordinates from static
observation.
%2- Input the Real Time positions from the NMEA data
%3- Compute minimum, maximum and average values
format long g;
st_p1  = load('100608_FR_ed.txt');
st_p2  = load('240608_FR_ed.txt');
st_p3  = load('250608_FR_ed.txt');

% 1.1 TRACING AND REMOVING OUTLIERS USING FUNCTION "outlier"
lat=st_p1(:,4)+st_p1(:,5)./60;lon=st_p1(:,6)+st_p1(:,7)./60;
ht1=st_p1(:,8);t_s=st_p1(:,1)+st_p1(:,2)./60+st_p1(:,3)./3600;
 [pos_FR_1006, nout, lv] = outlier (lat,lon,t_s);
lat1=pos_FR_1006(:,1);lon1=pos_FR_1006(:,2);t_s1=pos_FR_1006(:,3);
 lat=st_p2(:,4)+st_p2(:,5)./60;lon=st_p2(:,6)+st_p2(:,7)./60;
ht2=st_p2(:,8);t_s=st_p2(:,1)+st_p2(:,2)./60+st_p2(:,3)./3600;
 [pos_FR_2406,nout,lv] = outlier(lat,lon,t_s);

lat2=pos_FR_2406(:,1);lon2=pos_FR_2406(:,2);t_s2=pos_FR_2406(:,3);
```

```
  lat=st_p3(:,4)+st_p3(:,5)./60,lon=st_p3(:,6)+st_p3(:,7)./60;
ht3=st_p3(:,8);t_s=st_p3(:,1)+st_p3(:,2)./60+st_p3(:,3)./3600;
  [pos_FR_2506,nout,lv] = outlier(lat,lon,t_s);
lat3=pos_FR_2506(:,1);lon3=pos_FR_2506(:,2);t_s3=pos_FR_2506(:,3);

% 1.2 Initial data statistics for the maximum and minimum inputs
latmin1=min(lat1); latmax1=max(lat1),lonmin1=min(lon1);
lonmax1=max(lon1);
latmin2=min(lat2); latmax2=max(lat2);lonmin2=min(lon2);
lonmax2=max(lon2);
latmin3=min(lat3); latmax3=max(lat3);lonmin3=min(lon3);
lonmax3=max(lon3);

 av_lt=mean(lat1);av_ln =mean(lon1); av_h= mean(ht1);
av_lt1 = 45.9502500976034;av_ln1 = 66.6422541913277; av_ht1 =
19.6357581395352;

%2.--------------STEP 2 INITIAL COMPUTATIONS----------------------
----
 %2.1-Compute differences of the DGPS positions from the reference
positions first %  in degrees and then in metres
%2.2.1 Differences in degrees
dlt_ltd1=lat1-av_lt;dlt_lnd1=lon1-av_ln;
dlt_ltd2=lat2-av_lt;dlt_lnd2=lon2-av_ln;
dlt_ltd3=lat3-av_lt;dlt_lnd3=lon3-av_ln;
%2.2-computation of mean radius of curvature of the reference
position
 fi=av_lt*pi/180; lbd=av_ln*pi/180;
a = 6378137; b = 6356752.3142; es = 1-b^2/a^2;
Mp=a*(1-es)/((1-es*(sin(fi))^2)^1.5)
Np=a^2/(sqrt(a^2*((cos(fi))^2) + b^2*((sin(fi))^2)))
Re = sqrt(Mp*Np);

%2.2.2 Differences in metres
kost=pi/180;
d_lt1m=kost.*dlt_ltd1.*Mp;
d_ln1m=kost.*dlt_lnd1.*Np*cos(fi);dlt_ht1=ht1-av_ht;
d_lt2m=kost.*dlt_ltd2.*Mp;
d_ln2m=kost.*dlt_lnd2.*Np*cos(fi);dlt_ht2=ht2-av_ht;
d_lt3m=kost.*dlt_ltd3.*Mp;
d_ln3m=kost.*dlt_lnd3.*Np*cos(fi);dlt_ht3=ht3-av_ht;

%2.2.2 Total distance
d_ds1=sqrt(d_lt1m.^2+d_ln1m.^2); d_ds2=sqrt(d_lt2m.^2+d_ln2m.^2);
d_ds3=sqrt(d_lt3m.^2+d_ln3m.^2);

 %2.2.3 Maximum and minimum differences in latitude and longitude
d_lt1L=min(d_lt1m); d_lt1U=max(d_lt1m);d_ln1L=min(d_ln1m);
d_ln1U=max(d_ln1m);
d_lt2L=min(d_lt2m); d_lt2U=max(d_lt2m);d_ln2L=min(d_ln2m);
d_ln2U=max(d_ln2m);
d_lt3L=min(d_lt3m); d_lt3U=max(d_lt3m);d_ln3L=min(d_ln3m);
d_ln3U=max(d_ln3m);
```

```
 %2.2.4 Maximum and minimum values of total distance
d_ds1L=min(d_ds1),d_ds1U=max(d_ds1)
d_ds2L=min(d_ds2),d_ds2U=max(d_ds2)
d_ds3L=min(d_ds3),d_ds3U=max(d_ds3)

%2.2.5 Standard deviations
std_dlt1=std(d_lt1m),std_dln1=std(d_ln1m),std_ds1=std(d_ds1);
std_dlt2=std(d_lt2m);std_dln2=std(d_ln2m);std_ds2=std(d_ds2);
std_dlt3=std(d_lt3m);std_dln3=std(d_ln3m);std_ds3=std(d_ds3);

 %  Step 3 printing summary of the computation results

fprintf('\n');
fprintf('\tFREDX_1006Fix\t%4.8f\t\t%4.8f\t\t%4.8f\t\t%4.8f\n',latmin
1,latmax1,lonmin1,lonmax1);
fprintf('\tFREDX_2406Fix\t%4.8f\t\t%4.8f\t\t%4.8f\t\t%4.8f\n',latmin
2,latmax2,lonmin2,lonmax2);
fprintf('\tFREDX_2506Fix\t%4.8f\t\t%4.8f\t\t%4.8f\t\t%4.8f\n',latmin
3,latmax3,lonmin3,lonmax3);
fprintf('\n');
fprintf('\n');
fprintf('\tFREDX_1006Fix\t%4.4f\t\t%4.4f\t\t%4.4f\n',std_dlt1,std_dl
n1,std_ds1);
fprintf('\tFREDX_2406Fix\t%4.4f\t\t%4.4f\t\t%4.4f\n',std_dlt2,std_dl
n2,std_ds2);
fprintf('\tFREDX_2506Fix\t%4.4f\t\t%4.4f\t\t%4.4f\n',std_dlt3,std_dl
n3,std_ds3);




% 4 ---------------STEP PLOT GENERATION-----------------------
 %STATION - FREDERICTON
%-------------------Observation date 1-100608--------------------
-------------------------
%4.1.1-PLOTTING OF THE TIME SERIES FROM REFEENCE STATIONS
 dof=2; fisher_value_inf=3; tf=sqrt(dof*fisher_value_inf);
% ------Eigen values and Eigen vectors-----
v1=[std_dlt1^2,0;0,std_dln1^2]
[V,D] = eig(v1);
rv=sqrt(diag(D)); ra=100*tf*max(rv),rb=100*tf*min(rv);
temp=v1(1,:)*sqrt(D(1,1));
angle=atan2(mean(d_ln1m),mean(d_lt1m));

figure
hold on
plot(100*mean(d_ln1m),100*mean(d_lt1m),'-r*')
scatter(100*d_ln1m, 100*d_lt1m,'.','b')
dr=ellipse(ra,rb,angle,100*mean(d_ln1m),100*mean(d_lt1m),'r');
set(dr, 'linewidth',2)
title('2DRMS SCATTER PLOTS FROM FREDERICTON FIX -1006')
xlabel('longitude diffs (cm) ')
ylabel('latitude diffs (cm)')
grid on; hold off
```

```
 rl=0;
figure
subplot(2,1,1)
hold on; plot( t_s1,d_lt1m*100,'marker','.','linestyle','-')
title('TIME SERIES OF LATITUDE DIFFERENCES FROM FRED-1006')
xlabel('Time series in UTC in hrs'),ylabel('latitude Diffs (cm)')
avl= line([min(t_s1) max(t_s1)],[mean(d_lt1m)
mean(d_lt1m)],'LineWidth',2,'Color','r')
grid on
 subplot(2,1,2)
plot( t_s1,d_ln1m*100,'.','linestyle','-')
title('TIME SERIES OF LONGITUDE DIFFERENCES FROM FREDX-1006')
xlabel('Time series in UTC'),ylabel('longitude Diffs (cm)')
avl= line([min(t_s1) max(t_s1)],[mean(d_lt1m)
mean(d_lt1m)],'LineWidth',2,'Color','r')
grid on; hold off
%4.1.2-a Plotting of the histograms of the latitude differences
figure
subplot(3,1,1)
x1=100*(d_lt1L:0.00018:d_lt1U);
y1=100*d_lt1m;
n=length(x1);
histfit(y1,n)
h = findobj(gca,'Type','patch');
set(h,'FaceColor','w','EdgeColor','b')
title('DIFFERENCES IN LATITUDE FIX (CM)-FROM FREDX-1006')
xlabel('latitude Diffs (cm)'),ylabel('Frequency')

%4.1.2-b Plotting of the histograms of the longitude  differences
 subplot(3,1,2)
x1=100*(d_ln1L:0.00022:d_ln1U); y1=100*d_ln1m;
n=length(x1);
histfit(y1,n)
h = findobj(gca,'Type','patch');
set(h,'FaceColor','w','EdgeColor','b')
title('DIFFERENCES IN LONGITUDE FIX (M)-FROM FREDX-1006')
xlabel('longitude Diffs (cm)'),ylabel('Frequency')

%4.1.2-c Plotting of the histograms of the distance differences
 subplot(3,1,3)
x3=d_ds1L:0.00022:d_ds1U; d_ds1=d_ds1*100;
y3=d_ds1;
n=length(x3);
histfit(y3,n)
h = findobj(gca,'Type','patch');
set(h,'FaceColor','w','EdgeColor','b')
title('TOTAL DISTANCE DIFERENCES(CM) IN POSITION FIX-FROM FRED-
1006')
xlabel('Total Distance Diffs in centimetres');ylabel('Frequency')
```

```
 %---------- Observation date 2-240608-----------------------------
------------------
%4.2.1-Plotting of the time series from reference stations
 v1=[std_dlt2^2,0;0,std_dln2^2]
[V,D] = eig(v1);
rv=sqrt(diag(D)); ra=100*tf*max(rv),rb=100*tf*min(rv)
temp=v1(1,:)*sqrt(D(1,1))
angle=atan2(mean(d_ln2m),mean(d_lt2m))
figure
hold on; plot(100*mean(d_ln2m),100*mean(d_lt2m),'-r*')
scatter(100*d_ln2m, 100*d_lt2m,'.','b')
dr=ellipse(ra,rb,angle,100*mean(d_ln2m),100*mean(d_lt2m),'r');
set(dr, 'linewidth',2)
title('2DRMS SCATTER PLOTS FROM FREDERICTON FIX -2406')
xlabel('longitude diffs (cm) '); ylabel('latitude diffs (cm)')
grid on; hold off


figure
hold on; subplot(2,1,1)
plot(
t_s2,d_lt2m*100,'marker','.','markerfacecolor','r','linestyle','-')
title('TIME SERIES OF LATITUDE DIFFERENCES FROM FREDX-2406')
xlabel('Time series in UTC'),ylabel('latitude Diffs (cm)')
avl= line([min(t_s2) max(t_s2)],[mean(d_lt2m)
mean(d_lt2m)],'LineWidth',2,'Color','r')
grid on; hold off

 subplot(2,1,2)
plot(
t_s2,d_ln2m*100,'marker','.','markerfacecolor','r','linestyle','-')
title('TIME SERIES OF LONGITUDE DIFFERENCES FROM FREDX-2406')
xlabel('Time series in UTC');ylabel('longitude Diffs (cm)')
avl= line([min(t_s2) max(t_s2)],[mean(d_lt2m)
mean(d_lt2m)],'LineWidth',2,'Color','r')
grid on; hold off

 %4.1.1-a Plotting of the histograms of the latitude differences
figure
subplot(3,1,1)
x1=100*(d_lt2L:0.0097:d_lt2U); y1=100*d_lt2m;
n=length(x1);
histfit(y1,n)
h = findobj(gca,'Type','patch');
set(h,'FaceColor','w','EdgeColor','b')
title('DIFFERENCES IN LATITUDE FIX (CM)-FROM FRED-2406')
xlabel('latitude Diffs (cm)'),ylabel('Frequency')

%4.1.2-b Plotting of the histograms of the longitude differences
 subplot(3,1,2)
x1=100*(d_ln2L:0.0097:d_ln2U); y1=100*d_ln2m;
n=length(x1);
histfit(y1,n)
```

274

```matlab
h = findobj(gca,'Type','patch');
set(h,'FaceColor','w','EdgeColor','b')
title('DIFFERENCES IN LONGITUDE FIX (M)-FROM FRED-2406')
xlabel('longitude Diffs (cm)'),ylabel('Frequency')

%4.1.2-c Plotting of the histograms of the distance differences
 subplot(3,1,3)
x3=d_ds2L:0.0099:d_ds2U;d_ds2=d_ds2*100; y3=d_ds2;
n=length(x3); histfit(y3,n)
h = findobj(gca,'Type','patch');
set(h,'FaceColor','w','EdgeColor','b')
title('TOTAL DISTANCE DIFERENCES(CM) IN POSITION FIX-FROM FRED-
2406')
xlabel('Total Distance Diffs in centimetres'); ylabel('Frequency')

 %------------- Observation date 3-250608-------------------------
-------------------
%4.2.1-Plotting of the time series from reference stations
 v1=[std_dlt3^2,0;0,std_dln3^2]
[V,D] = eig(v1);
rv=sqrt(diag(D)); ra=100*tf*max(rv),rb=100*tf*min(rv)
temp=v1(1,:)*sqrt(D(1,1))
angle=atan2(mean(d_ln3m),mean(d_lt3m))
 figure
hold on; plot(100*mean(d_ln3m),100*mean(d_lt3m),'-r*')
scatter(100*d_ln3m, 100*d_lt3m,'.','b')
dr=ellipse(ra,rb,angle,100*mean(d_ln3m),100*mean(d_lt3m),'r');
set(dr, 'linewidth',2)
title('2DRMS SCATTER PLOTS FROM FREDERICTON FIX -2506')
xlabel('longitude diffs (cm) ')
ylabel('latitude diffs (cm)')
grid on; hold off

figure
hold on; subplot(2,1,1)
plot(
t_s3,d_lt3m*100,'marker','.','markerfacecolor','r','linestyle','-')
title('TIME SERIES OF LATITUDE DIFFERENCES FROM FRED-2506')
xlabel('Time series in UTC'),ylabel('latitude Diffs(cm)')
avl= line([min(t_s3) max(t_s3)],[mean(d_lt3m)
mean(d_lt3m)],'LineWidth',2,'Color','r')
grid on; hold off

subplot(2,1,2)
hold on; plot(
t_s3,d_ln3m*100,'marker','.','markerfacecolor','r','linestyle','-')
title('TIME SERIES OF LONGITUDE DIFFERENCES FROM FRED-2506')
xlabel('Time series in UTC'),ylabel('longitude Diffs (cm)')
avl= line([min(t_s3) max(t_s3)],[mean(d_lt3m)
mean(d_lt3m)],'LineWidth',2,'Color','r')
grid on
hold off

%4.2.2-a Plotting of the histograms of the latitude differences
```

275

```
figure
subplot(3,1,1)
x1=100*(d_lt3L:0.0012:d_lt3U);y1=100*d_lt3m;
n=length(x1); histfit(y1,n)
h = findobj(gca,'Type','patch');
set(h,'FaceColor','w','EdgeColor','b')
title('DIFFERENCES IN LATITUDE FIX (CM)-FROM FREDX-2506')
xlabel('latitude Diffs (cm)'),ylabel('Frequency')

%4.2.2-b Plotting of the histograms of the longitude differences
 subplot(3,1,2)
x1=100*(d_ln3L:0.0012:d_ln3U); y1=100*d_ln3m;
n=length(x1);
histfit(y1,n)
h = findobj(gca,'Type','patch');
set(h,'FaceColor','w','EdgeColor','b')
title('DIFFERENCES IN LONGITUDE FIX (CM)-FROM FREDX-2506')
xlabel('longitude Diffs (cm)'),ylabel('Frequency')
%4.2.2-c plotting of the histograms of the distance differences
 subplot(3,1,3)
x1=100*(d_ds3L:0.0012:d_ds3U); y1=100*d_ds3;
n=length(x1);
histfit(y1,n)
h = findobj(gca,'Type','patch');
set(h,'FaceColor','w','EdgeColor','b')
title('TOTAL DISTANCE DIFERENCES(M) IN POSITION FIX-FROM FREDX-
2506')
```
xlabel('Total Distance Diffs in centimetres'),ylabel('Frequency')

VITA

Candidate's Full Name	James Daniel Mtamakaya
Place and Date of Birth	Songea, Tanzania 8th February 1960
Permanent address	Survey and Mapping Division
	Ardhi House Kivukoni Front,
	P.O Box 9201,
	Dar Es Salaam, Tanzania .
Marital status	Married
Nationality	Tanzanian
Profession	Land Surveyor

EDUCATION BACKGROUND

2006-2008	Master of Science degree Course in Geodesy and Geomatics Engineering (UNB, Canada).
1989-1990	Post-Graduate Diploma in Geographic Information Systems for Cadastral Applications [ITC Enschede, The Netherlands].
1980-1983	Advanced Diploma in Land Surveying University College of Lands and Architectural Studies [then Ardhi Institute].
Professional Affiliation	Full Registered Surveyor of the National Council of Professional Surveyors of Tanzania (NCPS)